UNIVERSITÉ DE STRASBOURG

ÉCOLE DOCTORALE des Sciences de la Vie et de la Santé

Centre de Biologie Intégrative, IGBMC, UMR7104, Illkirch

THÈSE présentée par :

Vladimir ROUDKO

Soutenue le : **19 Septembre 2014**

pour obtenir le grade de : **Docteur de l'université de Strasbourg**

Discipline/ Spécialité : Aspects moléculaires et cellulaires de la biologie

(Molecular and Cellular Biology)

Structural and functional characterisation of the CCR4-NOT deadenylation complex

Caractérisation fonctionnelle et structurale du complexe de déadénylation CCR4-NOT

THÈSE dirigée par :

Dr. SERAPHIN Bertrand	DR, CNRS, IGBMC, Illkirch.

RAPPORTEURS :

Dr. CHARPENTIER Bruno	PR2, CNRS, IMoPA, Nanc
Dr. ALAIN Jacquier	Chargé de recherche, Institut Pasteur, Paris.

AUTRES MEMBRES DU JURY :

Dr. GAGLIARDI Dominique	Chargé de recherche, CNRS, IBMP, Strasbourg.
Dr. IZAURRALDE Elisa	Scientific Director, MPI, Tübingen.
Dr. ROMBY Pascal	Chargé de recherche, CNRS, IBMC, Strasbourg.

Table of contents

Table of contents 2
List of figures 4
List of tables 6
Acknowledgements 7
Abstract 10
Resume 12
1. Introduction 15
1.1 Eukaryotic gene expression: all roads lead to the RNA. 15
1.2 Transcription, processing and mRNA export 16
1.3 Translation 18
1.3.1 Components of translation cycle 18
1.3.2 Translation Initiation 22
1.3.3 Translation Elongation 25
1.3.4 Termination and recycling 26
1.3.5 Polysome organization and genome wide translation profiles 27
1.3.6 Mechanisms of translation inhibition 28
1.4 mRNA degradation 32
1.4.1 Basic cytoplasmic mRNA decay pathway 33
1.5 Project outline 72
1.5.1 Structural and functional characterization of CCR4-NOT complex 72
1.5.2 Not1 essential function and structural heterogeneity of the CCR4-NOT complex *in vivo* 72
1.5.3 Mechanism of action of the CCR4-NOT complex: translation repression and recruitment by the Puf3 protein 73
2. Results 74
2.1 Study of the CCR4-NOT deadenylation complex function 74
2.1.1 Structural and functional characterization of the CCR4-NOT complex 74
2.1.2 The Not1 essential function(s) and potential structural heterogeneity of the CCR4-NOT complex *in vivo* 98
2.1.3 Translation repression by the CCR4-NOT complex 111
2.1.4 Genome-wide mRNA expression profiles of mRNA processing factors: Puf3-mediated CCR4-NOT complex recruitment 115
3. Discussion and Perspectives 132
3.1 Structural and functional characterization of the CCR4-NOT complex 132

3.2 Translation repression by CCR4-NOT complex. 137
3.3 Genome-wide mRNA expression profiles of mRNA processing factors: Puf3-mediated CCR4-NOT complex recruitment. 140
4. Materials and Methods 143
4.1 Strains and media 143
4.1.1 Bacterial media 143
4.1.2 Yeast media 143
4.1.3 Yeast strains and plasmids 143
4.2 Bacterial manipulations 146
4.2.1 Molecular cloning 146
4.3 Yeast manipulation 147
4.3.1 Yeast methods used for cloning and strain construction 147
4.3.2 Yeast phenotypic assays 149
4.4 Biochemical methods 150
4.4.1 RNA analysis methods 150
4.4.2 Protein analysis 152
4.5 List of Buffers 155
4.6 Bioinformatics 156
5. French introduciton. Introduction 157
5.1 L'expression des gènes eucaryotes: tous les chemins passent par l'ARN. 157
5.2 La transcription, la maturation et l'export des ARNm 157
5.3 Traduction 159
5.3.1 Composantes du cycle de traduction 160
5.4 La dégradation des ARNm. 164
5.4.1 Le mécanisme de la dégradation des ARNm dans le cytoplasme 165
5.4.1.1 Première étape de la dégradation des ARNm – la déadénylation. 166
5.4.1.7 Rôle particulier du complexe CCR4-NOT de levure dans la dégradation de l'ARNm induite par les protéines de liaison aux ARN: le cas de la protéine Puf 171
5.5 Aperçu du projet 174
5.5.1 Caractérisation structurale et fonctionnelle du complexe CCR4-NOT 175
5.5.2 Fonction essentielle de Not1 et l'hétérogénéité structurelle du complexe CCR4-NOT *in vivo* 175
5.5.3 Mécanisme d'action du complexe CCR4-NOT: répression de la traduction et recrutement par la protéine Puf3 175
6. References 177

List of figures

Figure 1. Gene expression in eukaryotes. 17
Figure 2. Protein translation. 18
Figure 3. The “standard” genetic code. 19
Figure 4. Typical eukaryotic mRNA organization. 19
Figure 5 Two representations of tRNA. 20
Figure 6. Composition of ribosomes from different kingdoms of life. 21
Figure 7. Aminoacil-tRNA binding sites within ribosome 21
Figure 8. Ribosome translation initiation. 24
Figure 9. Ribosome translation elongation. 26
Figure 10. Ribosome translation termination and recycling. 27
Figure 11. Polysome structures, revealed by electron tomography 28
Figure 12. Translation repression by eIF2 phosphorylation. 30
Figure 13. Translation repression by targeting eIF4E-eIF4G interaction. 31
Figure 14. Translation repression during mRNA transport by specific mRNA-binding proteins 32
Figure 15. The core pathway for eukaryotic mRNA degradation 34
Figure 16. Possible connection between translation and deadenylation through PABP. 35
Figure 17. Link between deadenylation and decapping 38
Figure 18. RNA exosome composition. 39
Figure 19. Mechanism of exosome priming mediated by Ski-complex. 41
Figure 20. Composition of mammalian P-bodies and stress granules. 42
Figure 21. mRNP transition between active translation pool in cytoplasm to P bodies and stress granules. 43
Figure 22. NMD pathway. 46
Figure 23. Examples of Dom34-Hbs1 dependent quality control mechanisms. 48
Figure 24. CCR4-NOT complex architecture. 50
Figure 25. Structure of a heterotrimeric complex containing associated fragments of Not1, Caf1, and Ccr4. 51
Figure 26. Structure of a complex containing the C-terminal domain of Not1 with Not2 and the N-terminal part of Not5. 52
Figure 27. Ccr4 structure 54
Figure 28. Structures of mammalian (A) and yeast (B) Caf1 proteins 56
Figure 29. Puf3 protein with cognate RNA structure. 59
Figure 30. Role of in mRNA localization and translation repression. 61
Figure 31. miRNA maturation process. 64
Figure 32. Model of miRNA mediated mRNA repression. 67
Figure 33. Pum1 controls access of miRISC to the p27 mRNA 3’-UTR by unfolding a stem-loop structure 69
Figure 34. TTP stimulated mRNA decay. 70

Figure 35. Roquin mediated TNF-α mRNA degradation 71
Figure 36. 13 different yeast Not1 deletion mutants. 99
Figure 37. Yeast FOA-based plasmid shuffling assay. 100
Figure 38. Result of the plasmid shuffling assay. 101
Figure 39. Protein expression analysis of Not1 deletion mutants 102
Figure 40. Analysis of Not1 alternative protein isoforms 103
Figure 41. Principle of the two-hybrid interaction assay in yeast 104
Figure 42. Interaction map of yeast CCR4-NOT complex. 107
Figure 43. Two step co-immunoprecipitation protocol. 108
Figure 44. Two-step co-immunoprecipitation purifications results 109
Figure 45. Co-immunoprecipitation from diploid yeast strains. 111
Figure 47. Structural alignment of the Not1(MIF4G-like)-Caf1 and eIF4G(MIF4G)-eIF4A complexes 112
Figure 48. Designed mutations in putative surface of interaction 113
Figure 49. Co-immunoprecipitation analyses with selected helicase targets. 115
Figure 50. Dynamic transcriptome analysis (DTA) experimental procedure. 116
Figure 51. Correlation plots based on cDTA measurements obtained by Sun et al. 2012 118
Figure 52. Pairwise log-scaled correlation plots 120
Figure 53. Enrichment analysis.. 122
Figure 54. A) GO-term analysis of significantly stabilized mRNAs 124
Figure 55. Interaction of Puf3 with the CCR4-NOT complex. 126
Figure 56. Features of Puf-family proteins and of its mRNA targets. 127
Figure 57. Proposed model of translationally-regulated Puf3-mediated mRNA decay 129
Figure 58. Experimental testing of the model presented in Figure 56. 135
Figure 60. How many CCR4-NOT complex(es) are recruited on a given mRNA? 136
Figure 61. Concomitant or mutually exclusive association of partners to Not1 could provide specific biological functions. 139
Figure 62. Hypothesis of Puf3-mediated mRNA localization and repression mediated by co-translational changes in targeted mRNA secondary structure. 142

List of tables

Table 1. Measurement of normalized β-galactosidase activity in two-hybrid assay for CCR4-NOT complex subunits. 105
Table 2. Assaying interaction between Caf40 subunit and Not1 mutants in two different orientations using the two-hybrid system. 106
Table 3. Yeast strains. 143
Table 4. Yeast plasmids. 144
Table 5. Antibodies used for western blot analyses. 154
Table 6. List of Buffers. 155

Acknowledgements

First of all, I would like to thank Bertrand, for giving me great opportunity to join your team and get taste of solid fundamental molecular biology. I appreciate how much I learnt from you, your great expertise in RNA and your professional vision of how to make robust and trustful science. You gave me opportunity to explore collaborative science, merging both functional and structural biology. Same time, you gave me freedom to pose scientific questions and to address them designing appropriate experiments. I am very grateful you gave me opportunity to drive my science basing on bioinformatical predictions: even though many ideas based on computational predictions I was not able to confirm, I kept in mind you were supporting me in these directions. I thank you for your mentorship and being open for questions, for giving advices and critical view during discussions. And of course for your temper – I pretty sure, it is hard to keep in hands when there is a guy laughing so loudly around!

I am also grateful to all members of Seraphin lab, with whom I had great pleasure to work with. When I just arrived, I and Benjamin were just two guys in the lab, it was amazing! Benjamin, who was research engineer at the moment, or simply “acta-man”, - we shared great fun working at the one bench next to each other, discussing ideas and joking in the CROUS during the lunches. I still remember how I was trying to learn French names for Zodiac signs, it was fun! And of course our plans to conquer the world, and your perfect pictures of two mice.,, I still keep them. I am very happy to meet so many nice girls! Tonnie, Delphine, Maria – I shared awesome moments in my life with you, both in the lab and out of it. I remember our walks in Strasbourg and around, Christmas markets and St. Nicolas games! And of course hard work in the lab, where we all were excited when someone was doing TAP purifications or dissecting yeast. Tonnie – you are admired great time eating in CROUS, and our discussions of science and things around, I got lots of inspiration from you. I always admired your clear vision, easy thinking and straight forward way of talking and doing what exactly you will. And I am very sure, great future in science is in front of you! I hope I would arrive to grow up same things in me. Delphine: when I arrived, you were almost finishing your thesis – but I remember how you were helping me with French language, thank you very much! I almost learnt it by the way. Maria – you are the one person once

met, I would never forget. You helped me a lot in the beginning, and then after your words of support and helpful hand and word. And your open heart and soul for everyone who is indeed. Thank you Maria, you are great!

Of course I want to mention our great Fabienne, Celine, Claudine, Natasha and Olga. Celine is one with strong character and your great way to organize things around you – that is amazing how you were ruling the lab, and by the way managing huge and growing family – that's awesome. Claudine and Natasha, I am very thankful for your help and assistance during my first steps in the lab, it was very important for me in the beginning. Olga – I am very grateful for your constant support, shared discussions during the work and your warming evening spent in your home! I will never forget you opened the door of your home for me, when I needed it very much. Fabienne, thank you very much for your advices and constructive remarks.

I am very grateful for people in the lab, who came later during my stay – Ola, Benjamin, Jordane, Eric, Valerio. Well, I think if I not mention Valerio, it would mean I have to delete everything I wrote before. Valerio – you are just fabulous. I have no other words – so energetic, so open-minded and open-hearted man I have never seen before. And by the same way very determined and clear vision. I am very happy to have shared with you so many activities and being passed so many adventures – it is just amazing. Of course our constant jokes about everything, shared food and your cooking. I will miss you!

I would like to thank people which I met during this amazing journey. People from Marat Yusupov lab: Iskander, Simone, Ira, Nicolas, Melanie, David, Justine, Lesha, Sergey and especially from structural department: Sasha, Heena, Anna, Karima and fabulous Alastair. I am very happy to share time with you. I am very happy to meet constantly Sergey during my life. Your wisdom and inspiring talks about science world are often helped me to push forward in science. Your rational way of life, intelligence and open-minded personality, constant willness to share it with everyone – you are a great teacher not just in the science, but mostly in leaving the life. I think, it was very important for me to keep constant discussions with you and it helped me a lot. And especially warm hugs to my friend Alastair who spent his sleepless nights correcting my thesis.

I would like the members of the jury Elisa Izaurralde, Pascal Romby, Bruno Charpentier and the rapporteurs Dr. Dominique Gagliardi, Dr. Jacquier Alain for reading my thesis and coming to my defence.

I would like to thank my family, my parents and my wonderful sister. I am very grateful for your constant support, for your warm words and strong believe in me. During all my journey, during all my ups and downs, you are with me and always ready to help. Thank you, I am very happy to have best family ever!

Abstract

mRNA degradation is a highly complex and versatile process. In a manner similar to polymerase complexes in transcription and ribosomes in translation, protein complexes mediating mRNA decay are tightly regulated. Eukaryotic mRNA decay follows a conserved pathway initiated by deadenylation that generates transcripts with short poly(A) tails. The latter intermediates are degraded either by decapping followed with 5'-3' trimming mediated by Xrn1, or by exosome-mediated digestion in the 3'-5' direction. In my thesis I present a functional dissection of the CCR4-NOT deadenylase complex based on its structural analysis. Essentially, I addressed five fundamental questions related to this complex:

- Is CCR4-NOT complex formation required for deadenylation activity?
- What is the molecular role of associated Not2/3/5 subunits?
- Why is the Not1 protein essential in yeast?
- Does the CCR4-NOT complex play a role in translation regulation?
- How is the CCR4-NOT complex targeted to its mRNA substrates?

The yeast CCR4-NOT complex contains at least 9 subunits. It can be subdivided into two modules: the Ccr4-Caf1(Pop2)-Not and the Not1-5-Caf40-Caf130. Both modules are assembled around the scaffold subunit Not1. Structural analyses revealed the details of two interactions within the catalytic module: Not1-Caf1 and Caf1-Ccr4 - Caf1 thus bridges Not1 and Ccr4. Functional analyses revealed that these interactions are required for deadenylation *in vivo*, demonstrating a direct implication of Not1 in mRNA decay control.

Determination of the structure of the Not1-2-5 complex revealed three binary interactions between these subunits. Interestingly, the Not5 surface of interaction with Not1 is conserved in Not3, supporting the hypothesis that Not3 or Not5 may associate with Not1 and that the subunit composition of the CCR4-NOT complex may be heterogeneous. Disrupting protein interactions resulted in Not2/3/5 subunit instability *in vivo* and reduced growth rates, but no evidence of mRNA decay alteration was detected.

Dissecting Not1 identified a truncated form of the protein sufficient to perform its essential function in yeast. Intriguingly, this minimal Not1 comprises only the middle and C-terminal

domains, required for interaction with the Caf1 and Ccr4 deadenylases and the Not2-3-5 subunits. These data give a perspective for structural studies on Not1.

The structure of the Not1-Caf1-Ccr4 module suggested a possible linkage between the mRNA deadenylation machinery and translation. Indeed, the Not1 domain that recruits Caf1 and Ccr4 resembles the fold of the middle domain of initiation factor 4G (MIF4G). We hypothesize that the Not1 MIF4G domain interacts with a specific helicase, possibly inhibiting new rounds of translation initiation on an mRNA targeted for degradation. Mutating this region impacted on yeast growth. However, we did not identify any helicase as a Not1 partner in contrast to results obtained in parallel systems showing that human Not1 engages the Dhh1 orthologue Ddx6 to targeted mRNA, thus repressing translation. In yeast, this putative translation repression role may be generally dispensable and affect only specific mRNAs.

Analyzing the principles of CCR4-NOT complex targeting to mRNA substrates, we identified an interaction between the Pumilio RNA-binding protein Puf3 and the CCR4-NOT complex. Puf3 is an armadillo-repeat domain containing protein involved in regulation of mRNAs encoding proteins targeted to mitochondria. We observed that this interaction is regulated by growth conditions, namely carbon source, suggesting an influence of the metabolic state on mRNA decay regulation.

Overall this study demonstrates the importance of the Ccr4-Caf1-Not1 module in mediating deadenylation, translation inhibition and importance the CCR4-NOT complex for cellular adaptation to specific growth conditions.

Resume

La dégradation des ARN messagers (ARNm) est un processus universel extrêmement complexe. D'une manière semblable aux polymerases pour la transcription et ribosomes pour la traduction, les complexes de protéines effectuant la dégradation des ARNm sont précisément régulés. La dégradation des ARNm eucaryotes s'effectue selon un schéma conservé évolutivement qui est initié par la déadénylation résultant dans la formation de transcrits avec des queues poly(A) courtes. De tels intermédiaires sont alors dégradés par le clivage de leur coiffe suivi par une digestion exonucléolytique 5'-3' effectuée par Xrn1, ou alternativement par une digestion 3 '-5' catalysée par l'exosome.

Dans ma thèse je présente une dissection fonctionnelle du complexe de déadénylation CCR4-NOT basée sur son analyse structurale. Je me suis essentiellement intéressé à cinq questions fondamentales concernant ce complexe :

- La formation du complexe CCR4-NOT complexe est-elle requise pour la déadénylation ?

- Quel est le rôle moléculaire de sous-unités Not2/3/5 du complexe ?

- Pourquoi la protéine Not1 est-elle essentielle chez la levure ?

- Le complexe CCR4-NOT joue-t-il un rôle dans la répression de la traduction ?

- Comment le complexe CCR4-NOT est-il ciblé sur ses substrats ARNm ?

Le complexe CCR4-NOT de levure contient au moins 9 sous-unités. Il peut être subdivisé en deux modules : Ccr4-Caf1(Pop2)-Not1 et Not1-5-Caf40-Caf130. Les deux modules sont assemblés autour de la sous-unité Not1 qui sert d'échafaudage. Les analyses structurales ont révélé les détails de deux interactions au sein du module catalytique : Not1-Caf1 et Caf1-Ccr4; Caf1 servant donc de lien entre Not1 et Ccr4. Les analyses fonctionnelles ont révélé que ces interactions sont requises pour déadénylation *in vivo*, mettant ainsi en évidence une implication directe de Not1 dans le contrôle de la dégradation des ARNm.

La détermination de la structure du complexe Not1-2-5 a révélé trois interactions binaires entre ces sous-unités. D'une façon intéressante, la surface de Not5 interagissant avec Not1 est conservée dans Not3, étayant l'hypothèse que Not3 ou Not5 peuvent s'associer exclusivement avec Not1 et que le complexe CCR4-NOT serait hétérogène dans la composition de ses sous-unités. Les mutations bloquant les interactions au sein de ce module conduisent à l'instabilité des sous-unités Not2/3/5 *in vivo* et à une croissance réduite, mais aucune évidence d'un changement de la dégradation des ARNm n'a été obtenue.

La dissection de Not1 nous a permis d'identifier une forme tronquée de la protéine suffisante pour remplir sa fonction essentielle chez la levure. De façon intéressante, cette forme minimale de Not1 comprend seulement les domaines centraux et C-terminaux requis pour interagir avec les déadénylases Caf1 et Ccr4 et les sous-unités Not2-3-5. Ces données donnent de nouvelles perspectives pour les études structurales de Not1.

La structure du module Not1-Caf1-Ccr4 a suggéré une association possible de la machinerie de déadénylation et celle impliquée dans la traduction. Effectivement, le domaine Not1 qui lie Caf1 et Ccr4 adopte le même repliement que le domaine central du facteur d'initiation de la traduction 4G (MIF4G). Cette observation suggérait l'hypothèse que, comme son homologue structural, le domaine MIF4G de Not1 s'associerait avec une hélicase spécifique qui lui permettrait peut-être d'inhiber de nouveaux cycle d'initiation de la traduction pour des ARNm engagés dans la dégradation. Des mutations de cette région conduisent à une croissance ralentie. Cependant, nous n'avons pas identifié d'hélicase partenaire de Not1 chez la levure au contraire des résultats obtenus dans le parallèle chez l'homme. En effet, la protéine Not1 humaine lie l'orthologue de Dhh1, nommément Ddx6, réprimant ainsi la traduction des ARNm ciblés. Dans la levure ce rôle potentiel de répression de traduction pourrait être superflu pour la majorité des ARNm et affecterai seulement des ARNm spécifiques.

En analysant les principes du ciblage du complexe CCR4-NOT sur des ARNm substrats, nous avons identifié une interaction entre la protéine Puf3 de la famille Pumilio et le complexe CCR4-NOT. Puf3 est une protéine de liaison à l'ARN contenant des répétitions Armadillo essentiellement impliquée dans la régulation des ARNm codant des protéines ciblées à la

mitochondrie. Nous avons remarqué que cette interaction est régulée en fonction des conditions de croissance, à savoir la source de carbone. Ceci suggère que l''état du métabolisme cellulaire sur la régulation de la dégradation des ARNm.

Globalement, cette étude démontre l'importance du module Ccr4-Caf1-Not1 pour l'activité de déadénylation et l'importance du complexe CCR4-NOT pour l'adaptation cellulaire aux différentes conditions de croissance.

Publications:

[1] Bhaskar V, **Roudko V**, Basquin J, Sharma K, Urlaub H, Séraphin B, Conti E., Structure and RNA-binding properties of the Not1-Not2-Not5 module of the yeast CCR4-NOT complex. Nature Structural and Molecular Biology (2013) 20(11):1281-8.

[2] Basquin J*, **Roudko VV***, Rode M, Basquin C, Séraphin B, Conti E "Architecture of the nuclease module of the yeast Ccr4-not complex: the Not1-Caf1-Ccr4 interaction," Molecular Cell (2012) 48(2):207-18.

* co-premier auteurs

[3] Khutornenko AA, **Roudko VV**, Chernyak BV, Vartapetian AB, Chumakov PM, Evstafieva AG. Pyrimidine biosynthesis links mitochondrial respiration to the p53 pathway. Proc Natl Acad Sci USA. (2010) 107(29):12828-33.

Note: travail effectué avant la thèse

Présentations à des conférences:

[1] Présentation orale 9th FASEB meeting on Post-transcriptional control of gene expression: Mechanisms of mRNA degradation. Big Sky, Montana (USA) 6-11 juillet 2014.

« Functional studies of the CCR4-NOT deadenylation complex» **Roudko, V**, Basquin, J., Bhaskar, V., Conti, E., Séraphin, B.

[2] Présentation orale, retraite du département Génomique Fonctionnelle et Cancer. Illkirch (France), 13 octobre 2012

« Recruitment of Ccr4-Caf1 in the Not complex is required for efficient mRNA deadenylation *in vivo* » **Roudko VV**, Basquin J, Rode M, Basquin C, Séraphin B, Conti E.

[3] Poster EMBO Symposia The Complex Life of mRNA – Heidelberg (Allemagne), 7-10, octobre 2012

« Structural and functional study of the CCR4-NOT complex » **Roudko VV**, Basquin J, Séraphin B, Conti E.

1. Introduction

1.1 Eukaryotic gene expression: all roads lead to the RNA.

The central molecular biology dogma of genetic information transition is based on three basic events: DNA is transcribed into messenger RNA (mRNA) that, after a sequence of events, is used as a template for protein translation. This is true for all kingdoms of life: prokaryotes, archaeans and eukaryotes. Importantly, in the case of eukaryotes this sequence of events is spatially and temporally divided due to the presence of a nuclear envelope. It is also tightly regulated at all levels. The precursor mRNA molecule resulting from transcription is also highly processed and passes through multiple maturation and quality control steps before being translated. The final products of gene expression – proteins themselves – undergo chaperone mediated folding and are sometimes targeted for posttranslational modifications (Madhani 2013).

Through gene expression regulation, each type of cell within a highly organized organism gets its own identity and specialization. Different RNAs are transcribed and then differently processed before being released from the nucleus. This influences their localization within the cell, their stability, the type and amount of protein being translated, and in some cases the cellular compartment where this protein is finally located. This complex gene expression pathway strongly underlines the central importance of RNA regulation within the cell.

This thesis work revolves around the functional dissection of the CCR4-NOT complex, a central protein assembly required for mRNA stability control. An important basis for this work is the structural analysis of the CCR4-NOT assembly. Due to the conservation of this complex throughout different eukaryotic species, the model yeast system, *Saccharomyces cerevisiae*, was used for our study. After a brief introduction to mRNA transcription, processing and export, this first part of the manuscript will focus on the diverse mechanisms employed in the mRNA degradation pathways. It will also cover connections of mRNA decay with other cellular processes, such as translation, localization and transcription.

1.2 Transcription, processing and mRNA export

Transcription can be defined as the synthesis of an RNA molecule using a DNA strand as a template. In eukaryotes transcription takes place in the nucleus of the cell, and is regulated by a plethora of different factors. This reaction is performed by the (DNA-dependent) RNA polymerases I, II and III, with each being required for the synthesis of a specific class of RNAs. RNA polymerase II is responsible for the synthesis of all cytoplasmic mRNAs in the cell. The process is initiated at the 5'-end of the gene, in the promoter region, and requires the recruitment and assembly of many transcription initiation factors. After this, the transcription machinery moves along the gene, elongating the growing mRNA and finally terminating at the 3'-end of the gene, after transcript cleavage and polyadenylation. Importantly, transcription can be affected at any step by protein factors and even by distant regions of the DNA, called enhancers.

Eukaryotic transcripts are heavily processed (Figure 1). This includes the introduction of cap structure to the 5'-end of mRNAs, alternative splicing of primary transcripts, introduction of nucleotide modifications, and polyadenylation at the 3'-end. The mRNA cap, a 7-methyl-guanine nucleotide attached to the mRNA sequence by a 5'-5' triphosphate linkage, together with the poly(A) tail, is required for efficient mRNA translation in the cytoplasm, and affects mRNA stability, protecting the mRNA body from degradation by exoribonucleases. Due to the continuous nature of transcription elongation, primary mRNA transcripts contains both exons, translatable afterwards into protein, and introns, noncoding sequences. In order to remove the latter, a highly organized molecular complex called the spliceosome will act upon the mRNA. It cuts the primary transcript at the exon-intron edges and ligates the exons to form the mature RNA. Importantly, some introns can be retained, some exons can be skipped, or optional splice sites can be used, generating a variety of alternative mRNAs from one gene. Methyl-6-adenine residues were long known to be present in mRNAs (Desrosiers et al. 1975; Wei et al. 1976). The precise molecular function of this post-transcriptional reaction still needs to be determined but recent experiments suggest that they affect mRNA stability. Following the maturation process, mRNA transcripts are targeted to the nuclear envelope with different structural and regulatory proteins being assembled around the

mRNA, forming an mRNP complex. This is then exported to the cytoplasm through nuclear pore (Figure 1).

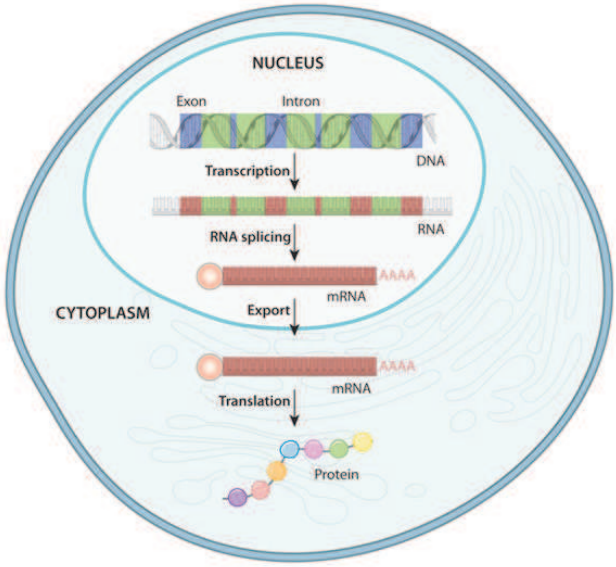

Figure 1. Gene expression in eukaryotes (Nature education 2010).

Once they reach the cytoplasm, newly transcribed RNA passes threw multiple steps of quality control, that will detect and destroy all improperly processed and spliced molecules (Madhani 2013). One of the determinants for a specific pathway of quality control, called nonsense-mediated decay (NMD), is the Exon Junction Complex (EJC). This complex is deposited in the vicinity of an exon-exon linkage, normally 20-24 nt upstream of the splice junction. The EJC is composed from several highly conserved subunits, eIF4III, Magoh, Y14 and MLN51 forming a core that associates with peripheral proteins. The EJC mark serves as a footprint of splicing events which happen on the mRNA. Interestingly, the EJC is functionally linked to mRNA translation. If a ribosome encounters a premature stop codon during translation, the downstream EJC plays a significant role in induction of the rescue mechanism, called nonsense-mediated decay NMD.

1.3 Translation

The information carried by mRNAs has to be decoded in order to produce protein – the final product of each mRNA. Translation of mRNA to protein is performed by ribosomes which are large conserved ribonucleoprotein complexes. Translation is a cyclic process, divided in 4 steps: initiation; elongation; termination; and recycling. During initiation ribosomes assemble onto mRNA and become activated; during elongation the ribosome incorporates amino acid residues into the growing polypeptide chain; at the termination step the ribosome encounters the termination signal, releasing the newly synthesized protein before being recycled to reinitiate another cycle of translation (Figure 2). In order to properly describe how the different steps occur during the of an mRNA molecule are linked together, I will enter into some detail of the eukaryotic mRNA translation process.

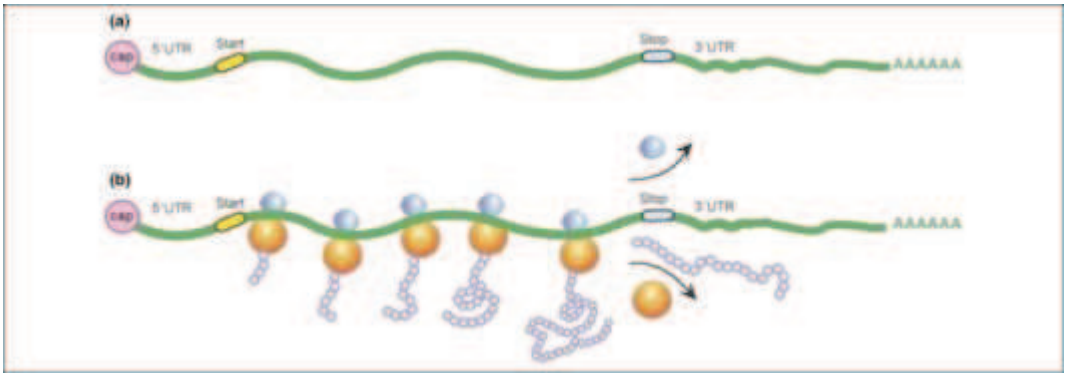

Figure 2. Protein translation (Lodish 2008).

1.3.1 Components of translation cycle

1.3.1.1 mRNAs

The eukaryotic mRNA sequence can be subdivided into: a cap; a 5'-untranslated region (5-UTR); an open reading frame (ORF); a 3'-untranslated region (3-UTR); and a poly(A) tail. The ORF by itself is divided in base triplets called codons, each corresponding to a specific amino acid residue or a stop signal (Figure 3).

1st letter	Second Letter: U	Second Letter: C	Second Letter: A	Second Letter: G	3rd letter
U	UUU Phe UUC UUA Leu UUG	UCU UCC Ser UCA UCG	UAU Tyr UAC UAA Stop UAG Stop	UGU Cys UGC UGA Stop UGG Trp	U C A G
C	CUU CUC Leu CUA CUG	CCU CCC Pro CCA CCG	CAU His CAC CAA Gln CAG	CGU CGC Arg CGA CGG	U C A G
A	AUU AUC Ile AUA AUG Met	ACU ACC Thr ACA ACG	AAU Asn AAC AAA Lys AAG	AGU Ser AGC AGA Arg AGG	U C A G
G	GUU GUC Val GUA GUG	GCU GCC Ala GCA GCG	GAU Asp GAC GAA Glu GAG	GGU GGC Gly GGA GGG	U C A G

Figure 3. The “standard” genetic code (Lodish 2008).

The ribosome, helped by initiation factors, binds to the cap, scans through the 5’-UTR, recognizes the AUG start codon through a methionine-loaded tRNA, and then elongates along the ORF, incorporating a new amino acid for each codon, until it reaches one of three stop codons. The mRNA 5’-UTR and 3’-UTR mostly serve for regulatory purposes: thus many RNA-binding protein sites are located in 3’-UTR(Figure 4) (Castello et al. 2013; Castello et al. 2012).

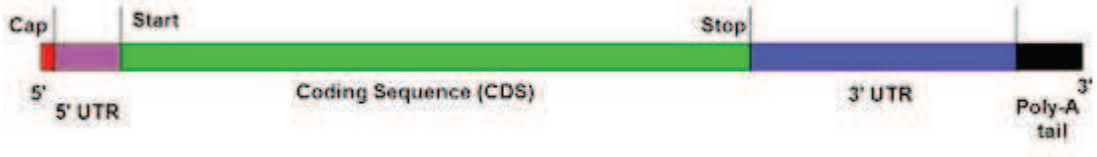

Figure 4. Typical eukaryotic mRNA organization (Lodish 2008).

1.3.1.2 Aminoacylated-transfer RNAs (aa-tRNAs)

In order to synthesize a protein that corresponds to the mRNA codon sequence, intermediate molecules are required. Aminoacyl-transfer RNAs (aa-tRNA) are these adaptors: they adopt a characteristic 4 stem-loop structure. One stem-loop, called the anticodon, recognizes the cognate codon in the mRNA by base pairing. Another stem-loop, called the acceptor stem, carries an amino acid residue specific for this tRNA (Figure 5). Therefore during translation the ribosome incorporates into the growing polypeptide chain,

amino acid residues, brought by tRNAs, according to the mRNA sequence through the base pairing of codons with anti-codons.

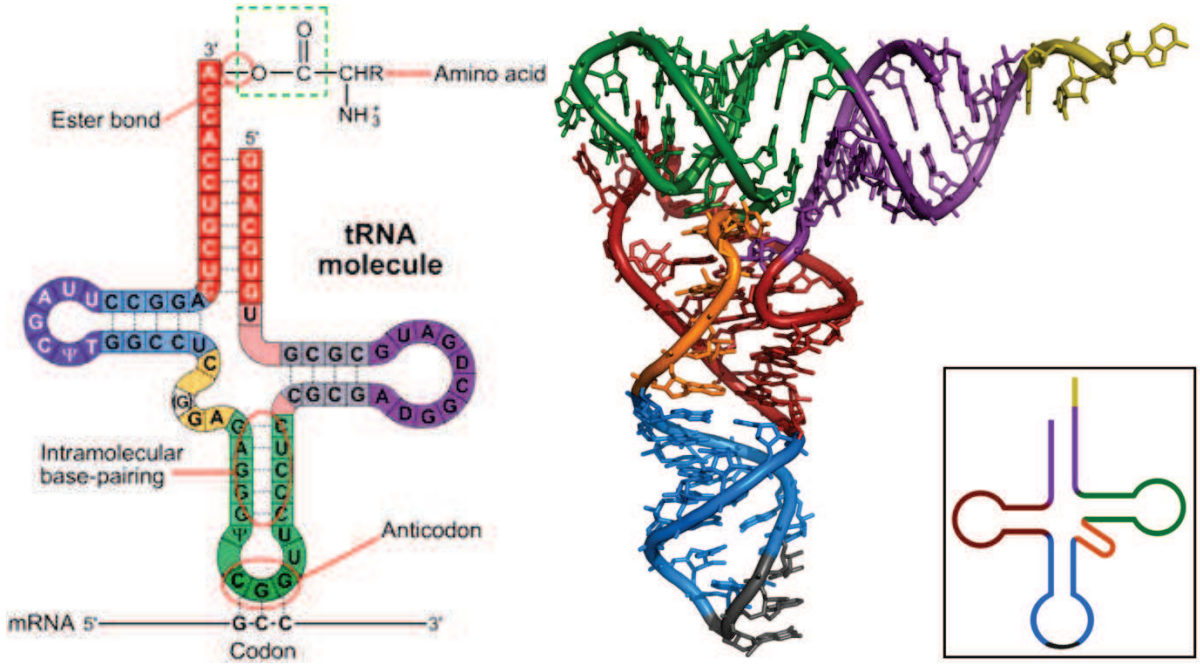

Figure 5 Two representations of tRNA: 2D map of the aminoacylated form (left) and 3D structure without the amino acid residue (right) (Lodish 2008).

1.3.1.3 Ribosome

The ribosome is a large protein complex catalysing protein synthesis. Eukaryotic ribosomes, referred to as 80S ribosomes, consist of two unequal subunits: a smaller 40S subunit and a larger 60S subunit. Each subunit is composed of many specific ribosomal proteins and of one or more ribosomal RNA(s) (rRNAs). In eukaryotes, the 40S subunit contains the 18S rRNA and 33 proteins while the 60S subunit is composed of the 28S, 5.8S and 5S rRNAs associated with 47 ribosomal proteins (Melnikov et al. 2012). Recent X-ray structures of full eukaryotic ribosomes from *S. cerevisiae* provided details of the 3D organization of this molecular machinery and of the molecular interactions that occur in this large assembly (Figure 6) (Jenner et al. 2012; Ben-Shem et al. 2011).

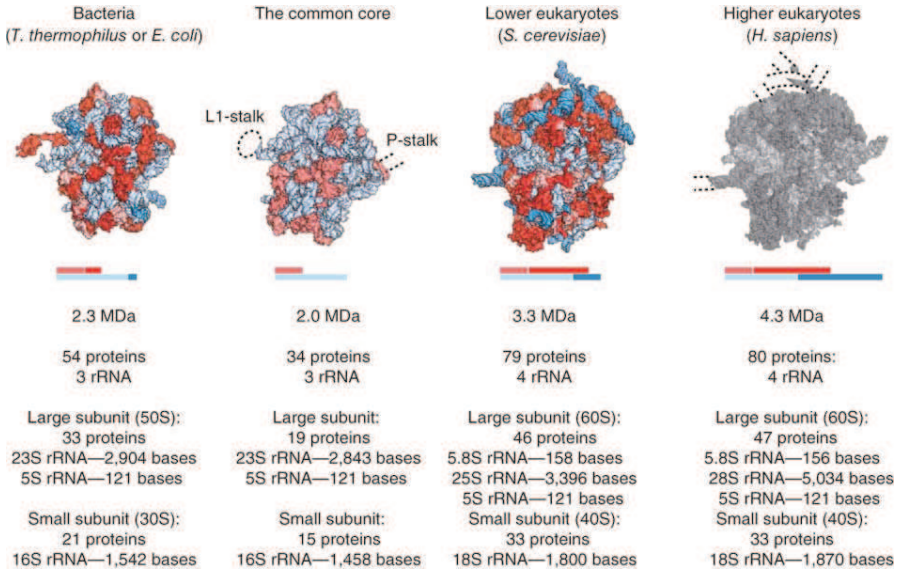

Figure 6. Composition of ribosomes from different kingdoms of life. rRNA is represented in blue, ribosomal proteins are in red. The crystal structure of the human ribosome is not yet known, hence the corresponding structural model is in grey (Melnikov et al. 2012).

A ribosome harbours three conserved functional regions, designed to accommodate tRNAs and mediate the proper amino acid residues in a growing polypeptide chain (Figure 7). These sites are called A – aminoacyl tRNA, P – peptidyl transferase and E – exit sites (Steitz 2008).

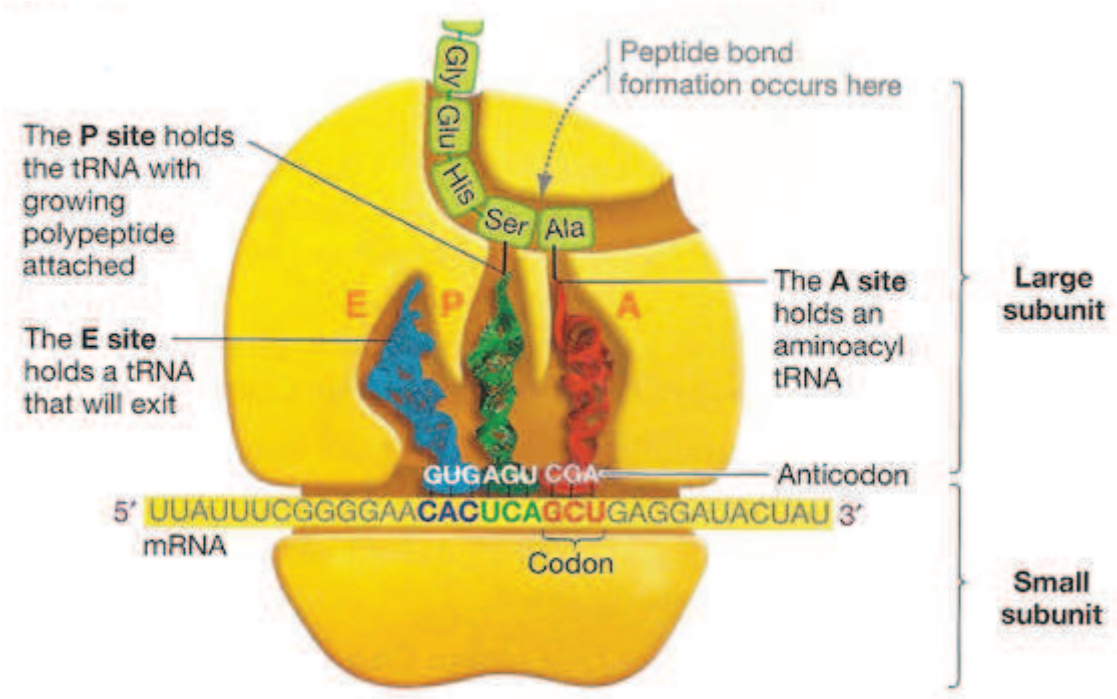

Figure 7. Aminoacil-tRNA binding sites within ribosome (discoveryandinnovation.com).

During each step of the translation cycle except initiation, the growing peptide is held by tRNA in the P-site. The incoming tRNA is introduced into the A-site. If codon-anticodon recognition successfully occurs, the tRNA will be stably bound to the ribosome and a peptide bond will be formed with the preceding amino acid residue carried by the tRNA in the P-site. With the help of additional factors, the new tRNA migrates from the A-site to the P-site, while the previous tRNA exits through the E-site (Rodnina et al. 2007; Beringer and Rodnina 2007a; Beringer and Rodnina 2007b). This cycle can be reiterated for each new codon of the mRNA. In the next paragraph, I will describe the essential steps of translation, initiation, elongation and termination in eukaryotes as details in this process provide clues on how translation is linked to mRNA life, and decay in particular.

1.3.2 Translation Initiation

Eukaryotic translation initiation is a highly complex and a deeply studied mechanism. It is considered to be the rate limiting step in protein production (Dever 1999; Jackson et al. 2010; Hinnebusch and Lorsch 2012; Aitken and Lorsch 2012; Groppo and Richter 2009). Indeed, many regulatory mechanisms affect translation initiation. Thus, many viruses inhibit host protein translation by scavenging or inhibiting translation initiation factors (Walsh and Mohr 2011). Also some mRNA degradation mechanisms are accompanied by inhibition of translation initiation allowing target mRNAs to exit from polysomes, while others can be degraded co-translationally (see mRNA decay part). Initiation starts by the formation of a 43S pre-initiation complex (43S-PIC). First, initiation Met-tRNAi, whose anticodon is complementary to the AUG initiation codon, interacts with initiation factors eIF2 bound to GTP, forming an assembly called the ternary complex (TC). Then the TC complex joins the 40S ribosomal subunit in association with other initiation factors: eIF1, eIF1A, eIF3 and eIF5. The resulting assembly is named the 43S pre-initiation complex (PIC). The PIC complex is recruited onto mRNAs bound by initiation factor eIF4F at their cap structure. The PIC then initiates scanning of the 5'-UTR of the mRNA until it reaches the start codon (Sonenberg and Hinnebusch 2009; Hershey et al. 2012; Parsyan et al. 2011).

The eIF4F complex, which "activates" mRNA translation by recruiting the PIC, comprises three factors: eIF4G, which acts as a scaffold protein; eIF4E, which binds the mRNA cap; and eIF4A, a protein endowed with RNA helicase activity. eIF4G also interacts with poly(A)

binding protein (PABP). Thus two interactions between the mRNA and translation initiation factors are formed: through eIF4E with the cap at the 5'-end of the mRNA and indirectly via eIF4G associated with PABP. With these interactions linking the mRNA 5' and 3' ends, the mRNA adopts a loop conformation. This "closed loop" model of translation initiation may also favour translation reinitiation on the same mRNA by a ribosome after termination (Jackson et al. 2010).

Recruitment of the PIC by eIF4F bound to an mRNA involves an interaction of eIF4G with eIF3. The 43S complex then starts unwinding the 5'-UTR with the help of the helicase activity of eIF4A and the accessory factor eIF4B until the AUG start codon is located. Additional factors, like Ded1, Dbp1 (in yeast) or Ddx3 (in humans), might play role in scanning through the highly complex 5'-UTR of some cellular mRNAs, or viral RNAs (Parsyan et al. 2011; Chuang et al. 1997; Tarn and Chang 2014; Berthelot et al. 2004; Hilliker et al. 2011).

As soon as start codon is recognized, hydrolysis of ATP by eIF2 occurs, and 48S complex is formed. This triggers binding to the 60S large ribosomal subunit, while several translation initiation factors that are bound to the 40S subunit are displaced. Thus eIF2-GDP, eIF3 and eIF5 are released, while the 60S subunit joins the complex following GTP hydrolysis by the eIF5B GTPase. This hydrolysis event is believed to stimulate the dissociation of the GTPase eIF5B and eIF1A, allowing the final assembly of the 80S ribosome on the start codon before the start of translation elongation (Figure 8) (Hinnebusch 2006; Groppo and Richter 2009).

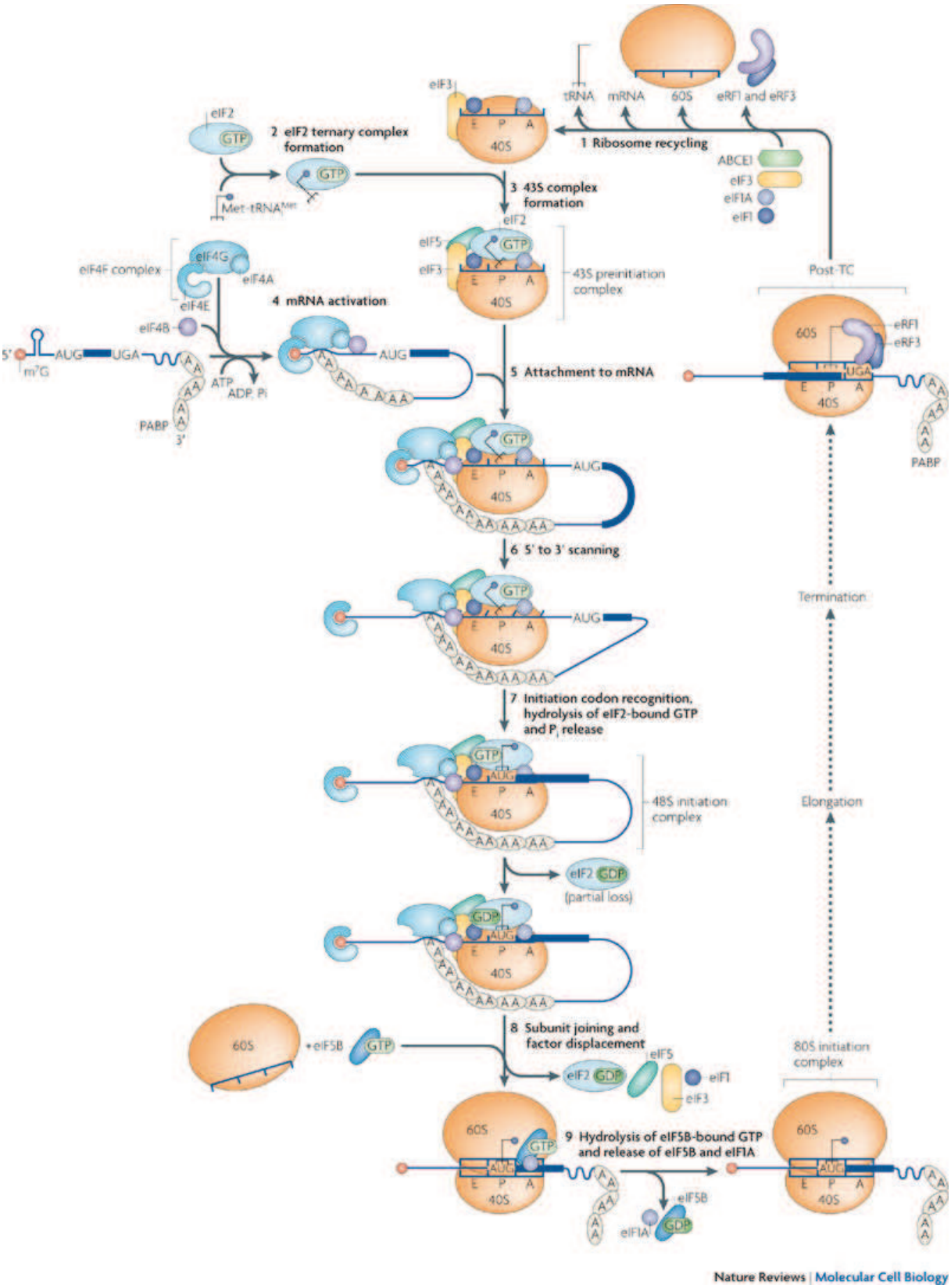

Figure 8. Ribosome translation initiation. The main events are reviewed in the above text (Jackson et al. 2010).

1.3.3 Translation Elongation

The initiating ribosome is localized on the start-codon with the Met-tRNA$_i$ located in its P-site, elongation starts by recruiting the next aa-tRNA according to the codon positioned in the A-site. Delivery of aa-tRNA happens through a complex formed of the aminoacyl-tRNA and elongation factor eEF1-alpha. Importantly, decoding happens in a GTP-dependent manner, and as soon as the correct aminoacyl-tRNA is accepted in the A-site it becomes fixed in the 60S ribosome subunit by GTP hydrolysis. The peptidyl-transferase centre in the large ribosome subunit then catalyses the formation of a peptide bond between the aminoacyl-tRNA in the P-site and the aminoacyl-tRNA in the A-site, transferring the growing polypeptide onto the tRNA in the A-site. This reaction happens right at the moment of translocation of the large ribosomal subunit relative to small one. Importantly, this reaction is strongly stimulated by elongation factor eEF2 bound to GTP. In the middle of the elongation cycle, the two tRNAs are localized in hybrid states: while in the 40S subunit deacetylated-tRNA and peptidyl-tRNA are located in the P- and A-sites, in the 60S subunit translocation induces their delocalization towards the E- and P-sites respectively. This conformational torsion induces the final translocation of the small ribosomal subunit. The former P-site tRNA is now fully localized in the E-site and can leave the ribosome. The former A-site tRNA is now located in the P-site. Hydrolysis of eEF2-bound GTP then stimulates the dissociation of the factor from the A-site, making it accessible for decoding of a new aminoacyl-tRNA (Figure 9). The cycle of elongation events repeats until the ribosome reaches the stop-codon, where the process of termination begins (Dever and Green 2012; Andersen et al. 2003; Petrov et al. 2012; Groppo and Richter 2009).

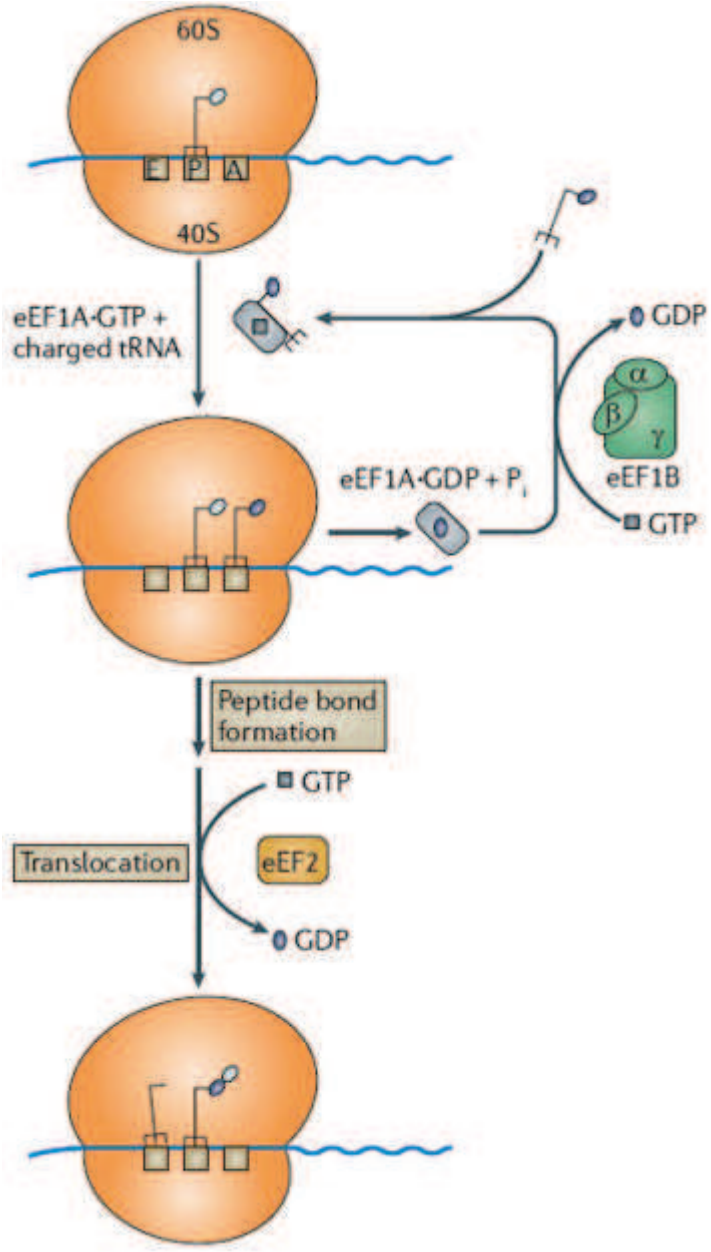

Figure 9. Ribosome translation elongation. Main events are reviewed above in the text (Walsh and Mohr 2011).

1.3.4 Termination and recycling

Translation termination occurs when a stop codon enters into the ribosome A-site. Three stop codons (UAA, UAG and UGA) are recognized by termination factor eRF1 leading to the hydrolysis of the peptidyl-tRNA located in the peptidyl-transferase center of the large ribosomal subunit. By itself eRF1 is strongly inefficient and requires association with eRF3 in complex with GTP (Salas-Marco and Bedwell 2004; Alkalaeva et al. 2006; Mitkevich et al. 2006; Inge-Vechtomov et al. 2014). This interaction stimulates eRF1-mediated peptide

release in a GTP dependent manner. Hydrolysis of GTP induces release of the eRF3 factor from the complex and eRF1 positioning in in peptidyl-transferase centre, thus the active site of eRF1 will be in a proper conformation to induce hydrolysis of the aminoacyl-tRNA bond. Importantly, the recycling factor Rli1 can modulate this process by facilitating eRF3 dissociation and fast eRF1 accommodation in an ATP-dependent manner (Dever and Green 2012).

As soon as the growing peptide, which is now a fully translated protein, is cleaved from the P-site tRNA, the post-termination ribosomal complex engages in recycling. The Rli1 iron-sulfur protein plays key role in this process. Interaction between Rli1 and eRF1 and subsequent ATP hydrolysis induces dissociation of the ribosomal subunits, leaving the mRNA and P-site tRNA associated with the 40S subunit. Termination and recycling factors are released. Curiously, dissociation of the mRNA and P-site tRNA is induced by initiation factors eIF1 and eIF3 (Figure 10). This might indicate a coupling mechanism between the termination/recycling and reinitiation steps of translation on particular mRNAs (Alkalaeva et al. 2006; Jackson et al. 2010; Groppo and Richter 2009).

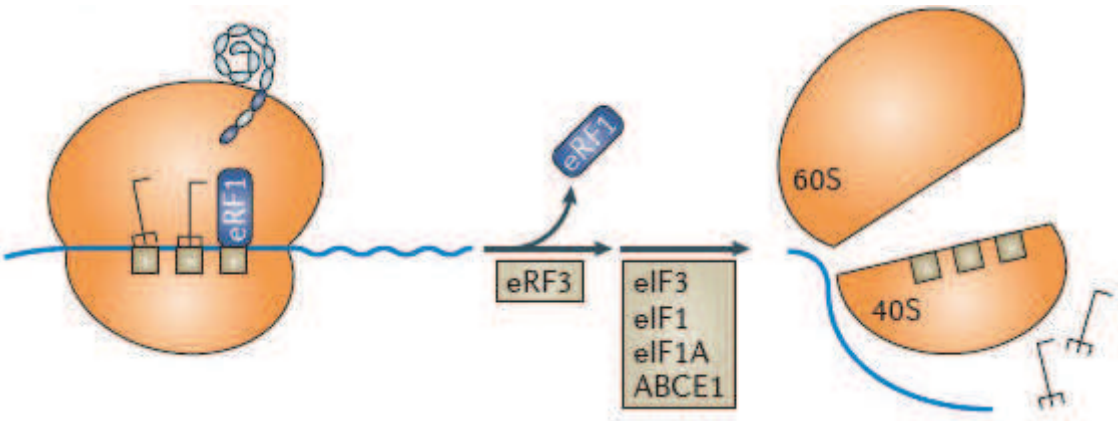

Figure 10. Ribosome translation termination and recycling. The main events are reviewed in the above text (Walsh and Mohr 2011).

1.3.5 Polysome organization and genome wide translation profiles

In *in vivo* and *in vitro* reconstituted translation, each mRNA that is long enough is bound by several ribosomes at each moment. Thus while one ribosome is engaged in the initiation or termination phase, several others are involved in elongation, and all ribosomes on the mRNA

form one huge mRNP particle called a polysome. With recently developed high-throughput techniques, it became possible to characterize all ribosome-bound mRNAs in a cell (Ingolia et al. 2009; Ingolia et al. 2012; Ingolia et al. 2013). This technique, called polysome profiling, allows one to gain deep insight into the "translatome" of a plethora of cell types and conditions. Such snapshots of translation have made it possible to identify many unknown upstream ORFs and decipher their impact on translation initiation. Additional techniques allowing the identification of mRNAs associated with ribosomes have recently been developed. For example, a strategy allowing the recovery of all mRNAs bound to ribosomes in a specific cell type present in a complex tissue or organism was developed (Heiman et al. 2014; Heiman et al. 2008). Such a strategy will provide us with informative pictures of translation in different environments and experimental conditions. These analyses, together with the deciphering of the 3D structural organization of single polysome particles (Figure 11) *in vitro* and *in vivo*, will allow a fine understanding of translation and its organization in cells (Brandt et al. 2009; Myasnikov et al. 2013).

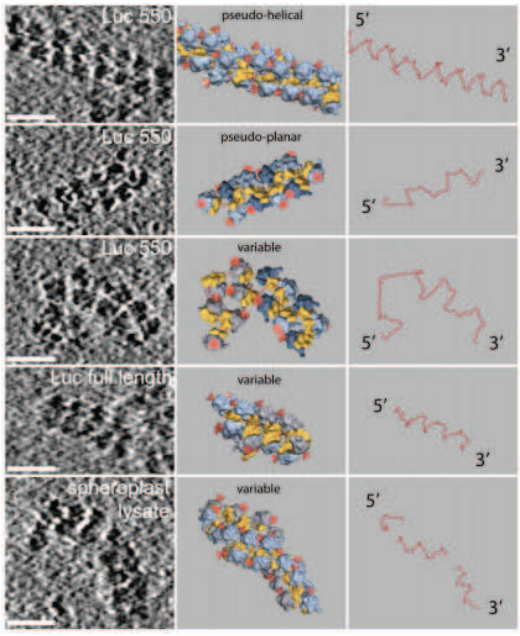

Figure 11. Polysome structures, revealed by electron tomography (Brandt et al. 2009).

1.3.6 Mechanisms of translation inhibition

Even though initiation is a critical step in the regulation of translation in the cellular context, one should not overlook the importance of protein synthesis inhibition in modulating

protein production. Translation inhibition may be triggered by an external input, may result from specific stress condition, may be due to viral factors or toxin, or may be mediated by cellular proteins. As polysomes have ultimately to exit the translation cycle when they are degraded, the existence of connections between translation inhibition and mRNA decay were expected. During my PhD research, I addressed among others a possible implication of the CCR4-NOT complex in translation inhibition; thus I will give a general view of possible routes mediating this process

1.3.6.1 Global mechanisms of translation control. Repressing translation initiation machinery

Among many repression mechanisms, there are two well described pathways that affect the general cellular rates of protein translation: specific phosphorylation of eIF2 and association of eIF4E with inhibitory proteins (Gebauer and Hentze 2004).

As it was mentioned above, eIF2 is a part of ternary complex, bound to Met-tRNA$_i$ and GTP, that is required for the delivery of the initation-tRNA and the formation of the 43S-PIC. Once the initiation reaction is complete, GTP is hydrolyzed into GDP. In order to be reactivated, eIF2:GDP must be converted into eIF2:GTP. This exchange is promoted by the multi-subunit GTP/GDP exchange factor eIF2B. Thus, association of eIF2 with eIF2B is essential to maintain the translation process. Specific phosphorylation of one subunit of eIF2 disrupts transformation of eIF2:GDP into eIF2:GTP by blocking dissociation of eIF2B from the ternary complex (Figure 12). Consistently, numerous translation inhibitors are kinases that regulate the eIF2 phosphorylation state:

- GCN2 (general control non-derepressible 2), activated by amino-acid starvation;
- Haem-regulated inhibitor, stimulated by haem depletion;
- PKR (protein kinase activated by double-stranded RNA), stimulated by viral infection;

and PERK, activated during endoplasmic reticulum (ER) stress conditions (Gebauer and Hentze 2004).

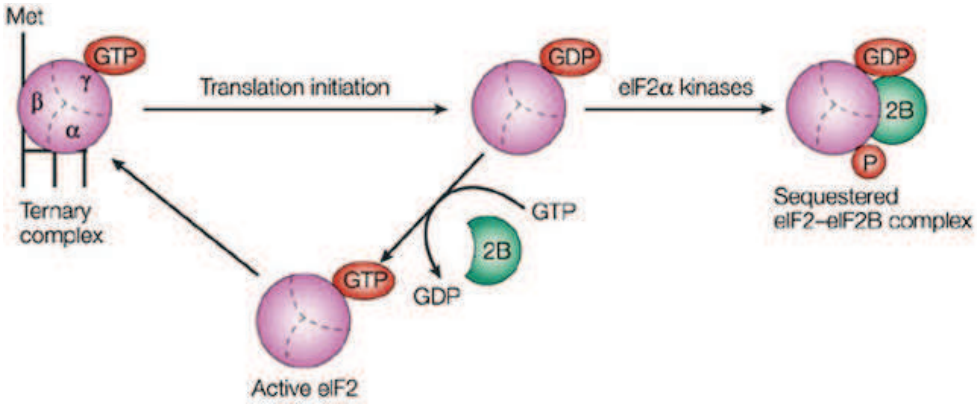

Figure 12. Translation repression by eIF2 phosphorylation (Gebauer and Hentze 2004).

Another route of translation inhibition is the targeting of the eIF4E cap-binding protein. As described above, eIF4E is a part of eIF4F initiation complex, which recruits the 43S PIC to the substrate mRNA promoting the initiation of scanning along the 5'-UTR. eIF4E is bound to the eIF4G scaffold protein in the eIF4F complex. But this interaction is competitively targeted by a variety of eIF4E interaction proteins (eIF4E-BP). Interestingly, under normal conditions eIF4E-BPs are highly phosphorylated and thus their association with eIF4E is inhibited. In these conditions, translation is not affected. With changing environmental cues, dephosphorylation of specific eIF4E-BPs occurs, inducing their association with eIF4E. This keeps the cap-binding protein away from eIF4G , thus repressing translation initiation by decreasing 43S PIC-mRNA interaction (Figure 13) (Youtani et al. 2000; Gingras et al. 2001; Gingras et al. 1999).

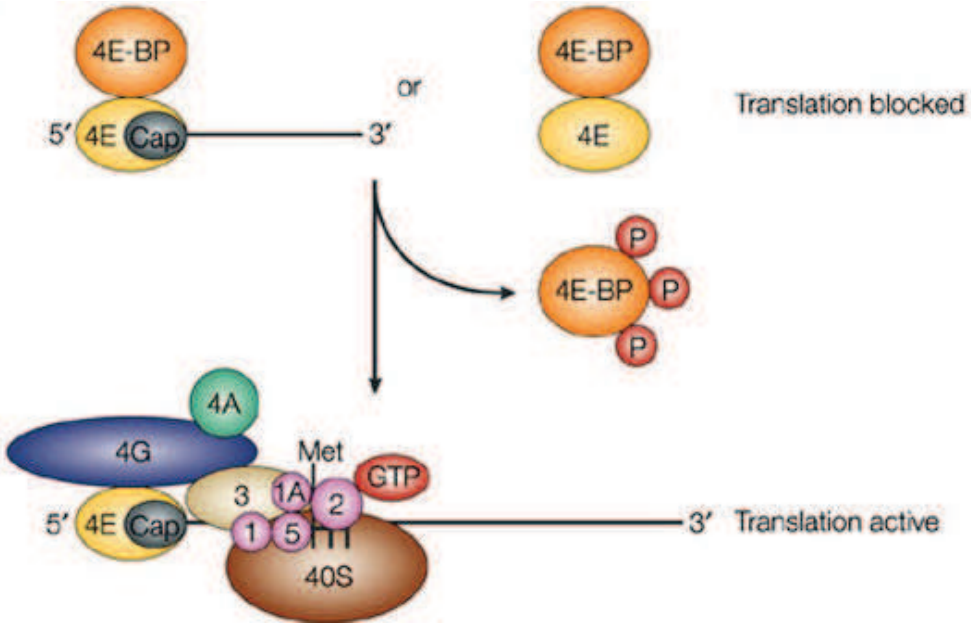

Figure 13. Translation repression by targeting eIF4E-eIF4G interaction (Gebauer and Hentze 2004).

Proteolysis can result in the same mode of protein inhibition by disrupting the cap-dependent ribosome scanning. Indeed, several viral proteases, as well as the cellular apoptotic caspase-3, were reported to cleave eIF4G. Such cleavages disrupt the eIF4F and PABP interaction, thus preventing mRNA circulation and interfering with mRNA translation initiation (Kempf and Barton 2008; Castelló et al. 2009).

1.3.6.2 mRNA localization coupled with translation inhibition

Many mRNAs are known to be localized in specific compartments before being translated. Such spatial control of mRNA translation provides an efficient mechanism to control protein delivery to the location of its future function. In some organisms, this coupled localization/translation mechanism of specific mRNAs plays a major role during embryonic differentiation. For example, during the anteroposterior axis formation in the early *drosophila* embryo, the mRNA encoding *nanos* becomes concentrated and translated in the posterior pole of the oocyte. The protein Smaug binds to the *nanos* mRNA 3'-UTR and recruits the eIF4E-BP repressor protein Cup (Igreja and Izaurralde 2011). This ensures that the *nanos* mRNA remains translationally silent during its transport. Another well-described example concerns the *oscar* mRNA. Interaction of the RNA-binding protein Bruno with the

Bruno responsive element in the 3'-UTR of the *oscar* mRNA allows the recruitment of the Cup protein, resulting in translation initiation inhibition (Gebauer and Hentze 2004). The same mechanism of translation repression is achieved by Biocoid and Mascin/CPEB RNA-binding proteins (Figure 14). Interestingly, components of the EJC complex located close to the first exon junction in the *oscar* mRNA also play an important role in controlling its localization (Jambor et al. 2014; Ghosh et al. 2012). Importantly, the mechanism described above relies on inhibition of translation initiation by blocking eIF4E but appears to happen on polysome-bound mRNAs. This suggests that at least the first round of translation initiation is completed. The spatial regulation of the mechanism mediating this translation inhibition also needs to be decoded.

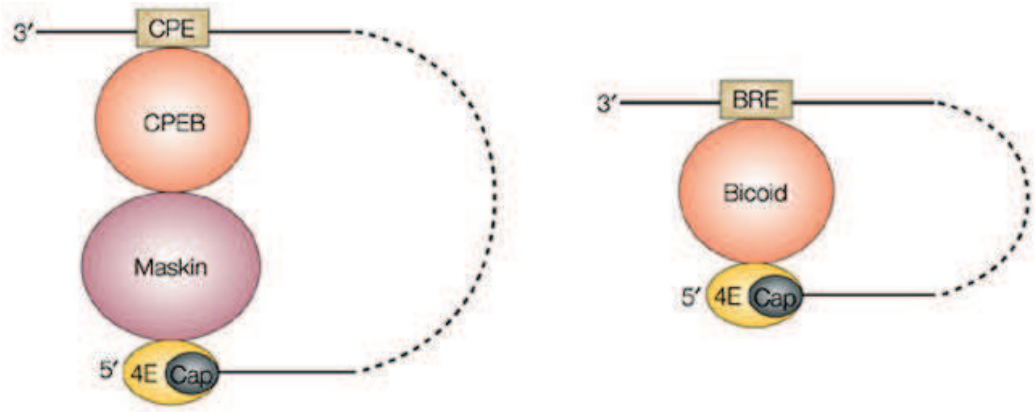

Figure 14. Translation repression during mRNA transport by specific mRNA-binding proteins (Gebauer and Hentze 2004).

1.4 mRNA degradation

All transcripts that have been synthesized must at some point be degraded. Eukaryotic RNA degradation is mediated by multiple protein complexes that are tightly regulated and tuned for specific cellular needs. Basic mRNA decay specifies the half-life of each transcript, which, together with the transcript transcription rate, determines the total level of this mRNA in a given cell (Garneau, Wilusz, and Wilusz 2007). Basic mRNA decay rates can be modulated in a transcript specific manner by RNA-binding proteins, microRNAs, or siRNAs. Moreover, specialized pathways that targets mRNAs with defects in the sequence or difficulties in being translated by ribosomes do exist. Translation of aberrant mRNA or abnormal translation could result in the production of non-functional proteins. Several processes, named

nonsense-mediated decay (NMD), no-stop decay (NSD), no-go decay (NGD) and non-functional ribosome decay (NRD), together referred to as the quality control system, eliminate aberrant mRNA and translation complexes (Behm-Ansmant et al. 2007; Chang et al. 2007).

The major eukaryotic mRNA decay pathways have been extensively analysed in different model systems, including yeast, human and *C. elegans*. As my PhD work focused on the yeast system, I will concentrate mainly on the mechanisms occurring in *S. cerevisiae* and I will briefly describe differences with the human system or other species. A special emphasis will be given to mRNA decay modulated by specific mRNA-binding proteins and by microRNA. The physiological importance of mRNA decay in different contexts will be also addressed. Finally, I will give a description of the basic molecular machineries involved in mRNA decay, concentrating on the CCR4-NOT assembly that was at the heart of my project.

1.4.1 Basic cytoplasmic mRNA decay pathway

Considering mRNA as a continuous ribonucleic sequence capped at its 5'-end and terminating with a poly(A) at its 3'-end, three major routes to initiate its decay can be imagined: exonucleolytically from the 3'-end by shortening the poly(A) tail; by removing the 5' protecting cap; or by internal endonucleolytic cleavage of the mRNA body. Indeed these three strategies are implemented in nature. For Basic mRNA decay, the poly(A) tail is essentially degraded leading to the formation of oligoadenylated mRNA. These are processed at their 5'-end by the decapping complex Dcp1/Dcp2, and finally degraded by the Xrn1 exonuclease in a 5'-3' direction. mRNA molecules resulting from deadenylation can also be degraded exonucleolytically by the exosome from their 3'-ends. While ribonucleotides resulting from mRNA decay can be recycled by entering the nucleotide salvage pathway, cap molecules have to be further processed. DcpS/Dcs1 appears to be the main scavenger enzyme involved in cap metabolism (Beelman and Parker 1995; Decker and Parker 1993). I will now give a detailed picture of mRNA decay, its regulation, and connections to other cellular processes (Figure 15).

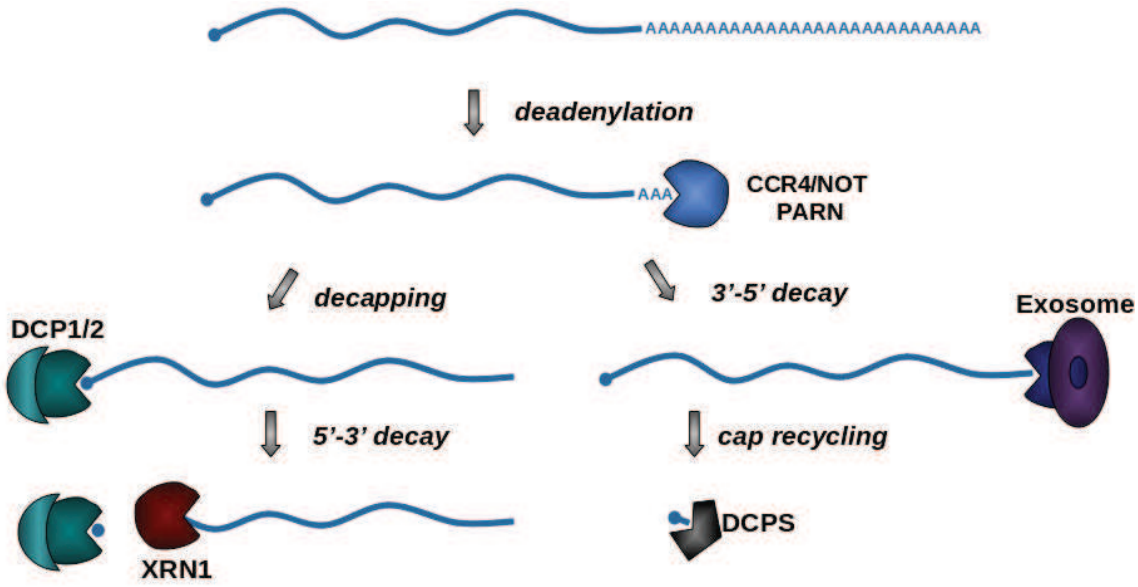

Figure 15. The core pathway for eukaryotic mRNA degradation (Beelman and Parker 1995).

1.4.1.1 Deadenylation and translation repression

Basic cytoplasmic mRNA decay is initiated by the 3'-5' directional elimination of adenine nucleotides constituting the 3' poly(A) tail, a process termed deadenylation. mRNA deadenylation can be catalysed by several protein complexes. It is believed that the Pan2-Pan3 complex performs the first trimming step while the CCR4-NOT complex takes over and performs most of the work degrading poly(A) tails until 10-20 adenine residues are left at the 3'-end (Funakoshi et al. 2007). Apart from these two complexes, the specific deadenylases PARN and Nocturnin have been described as being crucial for oocyte maturation or for circadian programs respectively (Baggs and Green 2003; Copeland and Wormington 2001). It is noteworthy that deadenylation is a reversible reaction that can be counteracted by cytoplasmic mRNA polyadenylation enzymes as has been shown for mRNAs targeted by the cytoplasmic polyadenylation element binding protein (CPEB) (Villalba et al. 2011).

Deadenylation is a highly regulated and rate-limiting step, and it is not surprising that most cellular regulation of mRNA decay happens at this level. Deadenylation affects proteins involved in mRNA activation during translation by preventing the binding of the cytoplasmic poly(A)-binding protein PABP. Thus deadenylation has an important impact on the transition of an mRNA between the active translatable state to the translationally silent mRNA pool

that is being degraded. Conversely, PABP was shown to stimulate deadenylation performed by Pan2-Pan3 while inhibiting degradation by the CCR4-NOT complex and PARN *in vitro*. Consistent with these *in vitro* findings, mutations affecting PABP release from mRNA poly(A) tails, have an inhibitory effect on mRNA decay *in vivo* (Simón and Séraphin 2007). This implies that a high rate of mRNP remodelling occurs during the initial steps of mRNA degradation. Not surprisingly, many specific mRNA binding proteins and PABP partners were shown to modulate mRNA decay. This includes the armadillo-repeat proteins (Puf family proteins), the zinc-finger protein nanos, and TOB/Btg factors. Their mode of their action is, however, different. Puf proteins and *nanos* bind to target mRNAs by recognizing specific sequences usually located within the 3'-UTR. They direct the degradation and/or translation repression of these RNAs in part by attracting deadenylation complexes. The TOB and Btg APRO-domains bind to the Caf1 subunit of CCR4-NOT complex. TOB also binds directly to PABP bridging the deadenylation complex and its substrate mRNA (Figure 16). Thus, while not binding the mRNA, TOB factors apparently still stimulate mRNA decay in a global manner (Horiuchi et al. 2009; Funakoshi et al. 2007). While the mechanism of action of Btg factors has not been elucidated, they also globally activate mRNA decay (Mauxion et al. 2008).

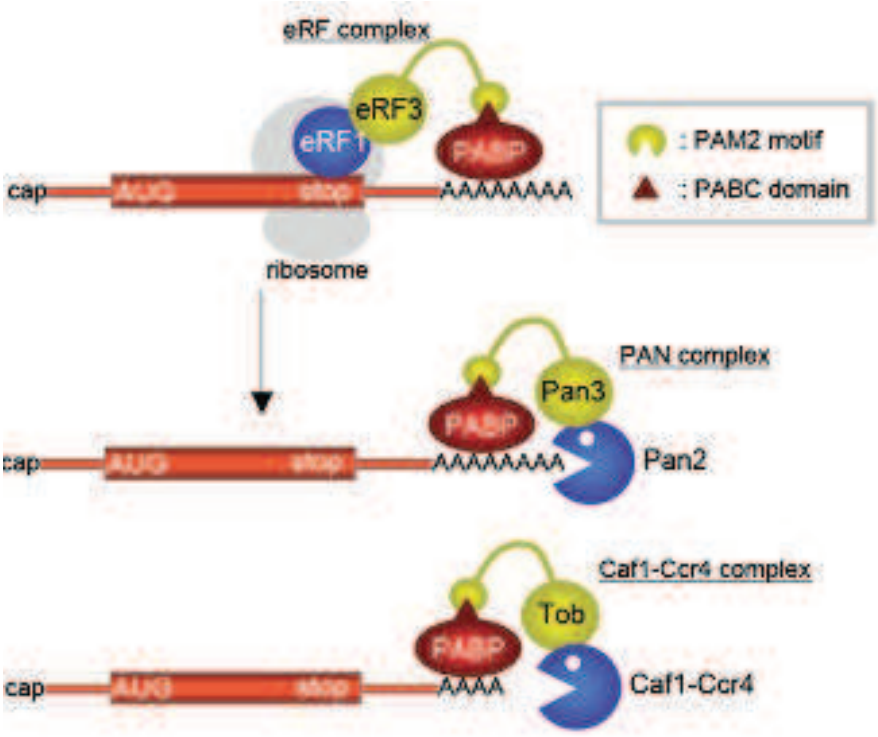

Figure 16. Possible connection between translation and deadenylation through PABP. The translation termination complex eRF1-eRF3 interacts with PABP and mediates translation termination. Afterwards, the Pan2-Pan3 complex is targeted to the mRNA through Pan3-

PABP interaction which involves a PAM motif. Subsequently, the CCR4-NOT complex can be targeted to the remaining poly(A) tail via a TOB factor. (REFERENCE)

It is generally thought that translation has somehow to be inhibited before an mRNA is degraded. Indeed, if the protein translation machinery moving from 5' to 3' would meet an mRNA degradation machinery approaching from 3'-end of the transcript, protein synthesis could not be completed. Also, the presence of eukaryotic initiation factor 4E bound to the 5' mRNA cap structure would prevent the mRNA decapping complex Dcp1/Dcp2 from initiating decay from the 5' end (Tharun and Parker 2001; Schwartz and Parker 2000). Indeed, these two systems were shown to compete *in vitro* and a temperature-sensitive allele of eIF4E suppressed the decapping defect of a partial loss-of-function allele of DCP1, thus suggesting that elimination of eIF4E from the cap occurs before Dcp1 action (Schwartz and Parker 2000). These observations argue for a mechanism where mRNAs are removed from the active translation pool prior to, or simultaneously with, mRNA deadenylation or other early steps of mRNA decay that precede decapping. Consistently, the human CCR4-NOT complex was reported to target Ddx6 mRNAs, a homologue of the yeast Dhh1, a factor that was shown to repress translation (Chen et al. 2014; Mathys et al. 2014). However, the exact molecular mechanism linking translation initiation repression with mRNA decay is still poorly understood and needs further characterization. Moreover, the presence of decapped RNA in the polysome pool was also reported suggesting that the decay of a given mRNA could be initiated while this mRNA is still present in the translatable mRNA pool.

1.4.1.2 Decapping and 5'-3' mRNA decay

The 5'-3' decay mediated by mRNA decapping and Xrn1-mediated exonucleolytic degradation is a major mRNA turnover pathway *in vivo* (Decker and Parker 1993). Moreover, mRNA decapping is generally believed to be irreversible making this a critical step in the decay process. Decapping mediated by the Dcp2 enzyme appears to be under strong molecular control (van Dijk et al. 2002; LaGrandeur and Parker 1996). Indeed, in yeast the catalytic subunit Dcp2 is strongly associated with Dcp1, which stimulates Dcp2 activity *in vitro* (LaGrandeur and Parker 1998; Beelman et al. 1996). Once the transcript has been

decapped, the Xrn1 exoribonuclease totally degrades the mRNA body (Muhlrad et al. 1995; Muhlrad et al. 1994).

The handing-over of deadenylated molecules to the Dcp1/Dcp2 complex is mediated by the Pat1-Lsm complex, which preferentially binds oligoadenylated RNAs *in vitro* (Tharun 2014; Chowdhury et al. 2012; Tharun et al. 2000; Bouveret et al. 2000). Interactions between Pat1 and the Dcp1/Dcp2 complex directly, or mediated by decapping activator enzymes, have been described (Fourati et al. 2014; Haas et al. 2010). This provides a molecular link between deadenylation and decapping. Another potentially important interaction occurs between Pat1 and Dhh1 which could, perhaps, keep the still capped mRNA in a translationally repressed state (Sharif et al. 2013; Y. Chen et al. 2014). Several decapping enhancers have been described and may ensure maximal decapping activity. Thus it has been given the name “Edc” for Enhancer of DeCapping. Hence, direct evidence supports binding of Edc3 to Dcp2 which stimulates decapping (Figure 17) (Kshirsagar and Parker 2004; Fourati et al. 2014; Fromm et al. 2012). A specialized mRNA degradation pathway has been described for the Rps28B mRNA. In this case, Edc3 participates in the decapping of this particular mRNA, degradation of which is induced in the presence of an excess of Rps28. This specific pathway skips the initial deadenylation step and requires a direct interaction of Rps28 with Edc3 and recognition of a specific structure in the Rps28B mRNA (He et al. 2014; Kolesnikova et al. 2013; Badis et al. 2004).

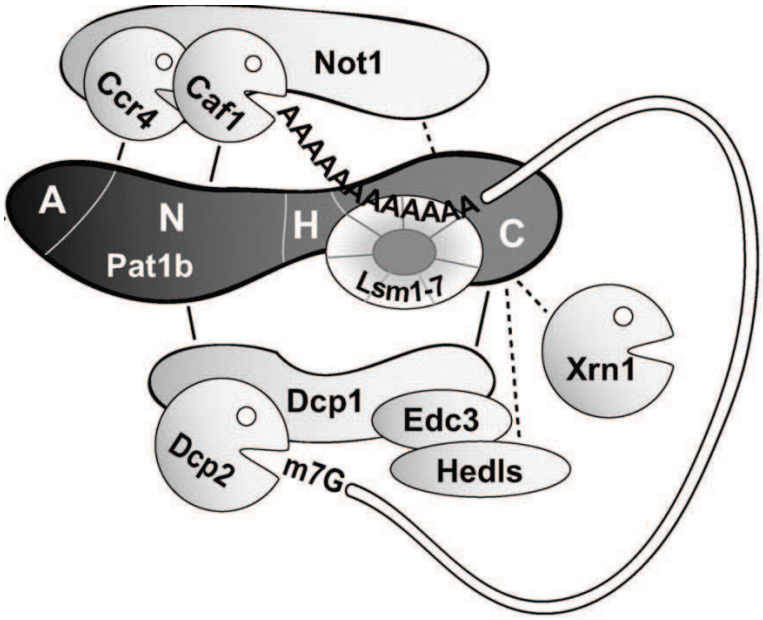

Figure 17. After deadenylation is completed by the CCR4-NOT complex, the Pat1-Lsm complex binds to oligoadenylated mRNAs and recruits the decapping machinery via interaction with Dcp1 and/or Dcp2. Different mRNA decapping enhancers, such as the Edc3 protein, participate in this process (Ozgur et al. 2010).

Indeed, whether mRNA degradation can skip the first deadenylation step and proceed directly to decapping, is still debatable question. Several cases have been described for particular mRNAs. But due to the fact that NMD does not require and initial deadenylation, and targets its substrates to be decapped directly, characterizes NMD decay as deadenylation-independent (Hu et al. 2010).

1.4.1.3 3'-5' decay by the exosome

After the initial deadenylation step, mRNA degradation intermediates can also be degraded in a3'-5' direction by a multisubunit 3'-5' exonuclease complex called the exosome. This assembly is not only involved in mRNA degradation in cytoplasm, but also highly required for RNA processing in the nucleus. The central core structure of the exosome, called exo-9, is composed from six protein subunits, named Rrp41-43, Rrp45, Rrp46, Mtr3, forming a barrel and three RNA-binding proteins called Rrp40, Csl4 and Rrp4 that bind on top of the barrel. Despite similarities with bacterial exonucleases, the exo-9 complex is enzymatically inactive (Figure 18). It associates with activity-harbouring subunits: in the cytoplasm there is only

one, Dis3 (Rrp44), while in nucleus exo-9 associates with both Dis3 and Rrp6 (Bonneau et al. 2009; Makino et al. 2013).

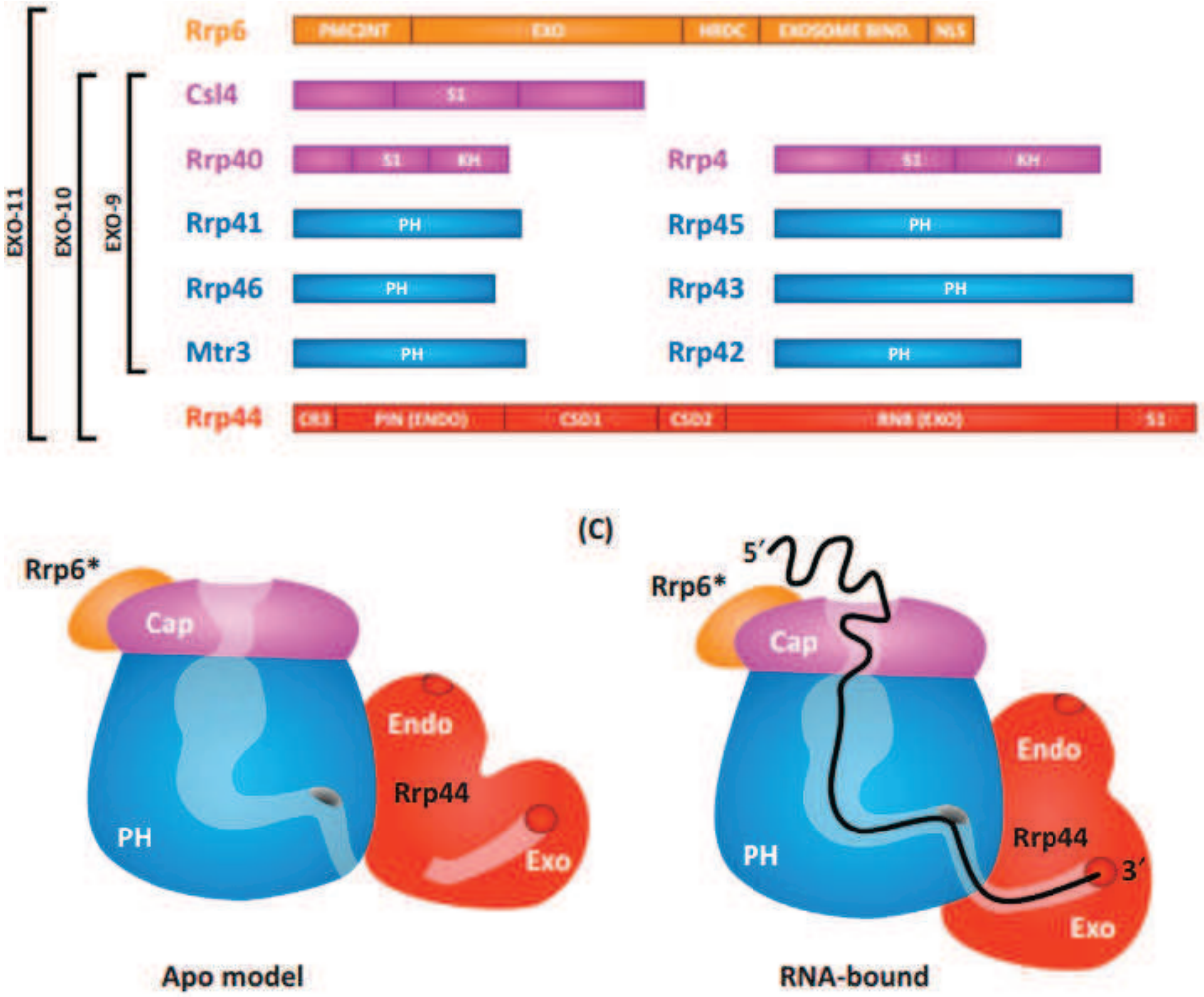

Figure 18. RNA exosome composition (Makino et al. 2013).

Interestingly, Dis3 possess both exo- and endoribonuclytic activities, located in its RNAse II-like and PIN domains (Dziembowski et al. 2007; Lebreton et al. 2008). These activities are partly redundant and inhibiting one or the other has a milder effect than simultaneous inactivation of both. Rrp6 is predominantly located in nucleus and carries only 3'-5' exoribonuclease activity. Evidence strongly supports the interplay of the two enzymatic subunits, Rrp6 and Dis3 (Wasmuth and Lima 2012; Schneider et al. 2009). Even though the exosome exo-9 core is enzymatically inactive, these subunits are required for threading the RNA substrate through the barrel towards Dis3 (Schneider et al. 2009; Dziembowski et al. 2007; Lorentzen et al. 2008). The function of the exosome in cellular RNA metabolisms is far

from restricted to mRNA degradation in the cytoplasm. The nuclear exo-11 complex (exo-9 associated with Dis3 and Rrp6) plays an important role in nucleolar rRNA maturation and in the processing of small nuclear and nucleolar RNAs (snRNAs and snoRNAs, respectively) (Houseley et al. 2006; Allmang et al. 1999; Allmang et al. 2000). Exo-11 also has a substantial role in scavenging aberrant mRNAs or non-coding RNAs that result from pervasive polymerase activity. The latter are polyadenylated by a non-canonical polyadenylation complex generally coined as TRAMP (LaCava et al. 2005; Wyers et al. 2005). Importantly, the TRAMP complex plays great role in loading the exosome onto its targeted transcripts.

The cytoplasmic form of the exosome, exo-10 (exo-9 plus Dis3) also requires cofactors for maximal performance. One of these cofactors is the Ski-complex. The Ski complex is composed from 3 subunits, unequally represented: a protein scaffold, Ski3; the Ski2 helicase; and two subunits of the accessory subunit Ski8 (Synowsky and Heck 2008; Halbach et al. 2013). Interestingly, when the Ski complex is positioned on the exosome lid it extends the threading RNA substrate that goes first through the RNA channel domain of Ski2 before continuing into the barrel of the exosome core. Thus the helicase activity of the Ski2 subunit could ensure the unfolding of the target transcript before it enters the exo-9 channel. Loading of the Ski complex onto the exosome is mediated by Ski7, an adaptor protein (Araki et al. 2001). Interestingly, mammalian cells lack an ortholog to Ski7 (Figure 19). Thus, the exact mechanism of recruitment of the exosome by the Ski complex in these species remains to be determined. The functional importance of exo-10 in cytoplasmic RNA decay was best revealed by its role in degrading RNA in xrn1 and decapping mutants as well as by its synthetic interactions with those genes (Houseley et al. 2006).

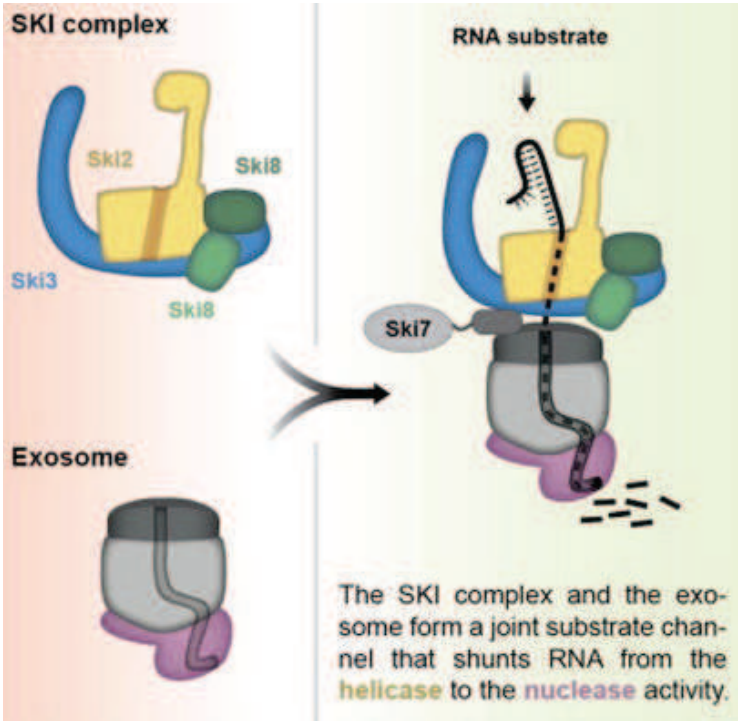

Figure 19. Mechanism of exosome priming mediated by Ski-complex. Threading of the RNA substrates through the RNA-exosome channel (Halbach et al. 2013).

1.4.1.4 Localisation of mRNA decay. P bodies and co-translational mRNA decay

The molecular processes of transcription and translation in eukaryotes are clearly compartmentalized and separated by the nuclear envelope. mRNA decay appears to happen in both the nuclear and cytoplasmic compartments. Moreover, in the cytoplasm a concentration of RNA turnover factors at specific locations was detected. Those sites were call Dcp-bodies or P-bodies (Figure 20). Decapping factors and many partners, like Dhh1, Edc3, the Pat1-Lsm complex subunits, tend to accumulate inside P bodies (Sheth and Parker 2003; Bloch et al. 2011; Cougot et al. 2004; van Dijk et al. 2002). P bodies are not, in general, the site of concentration of mRNA-associated factors as translation initiation factors are, for example, excluded from them. Several lines of evidence indicate that mRNA decay happens partly in this compartment. It is unclear however, how much of the decay process occurs elsewhere. Evidence that decapping and even NMD happens co-translationally, supports the idea that decapping and mRNA decay do not occur exclusively in P bodies (Hu et al. 2010; Hu et al. 2009). This conclusion is also supported by the presence of turnover factors diffusely located in the cytopasm. It is possible that these events are transcript-specific, P bodies targeting particular mRNAs while others are degraded in the cytoplasm.

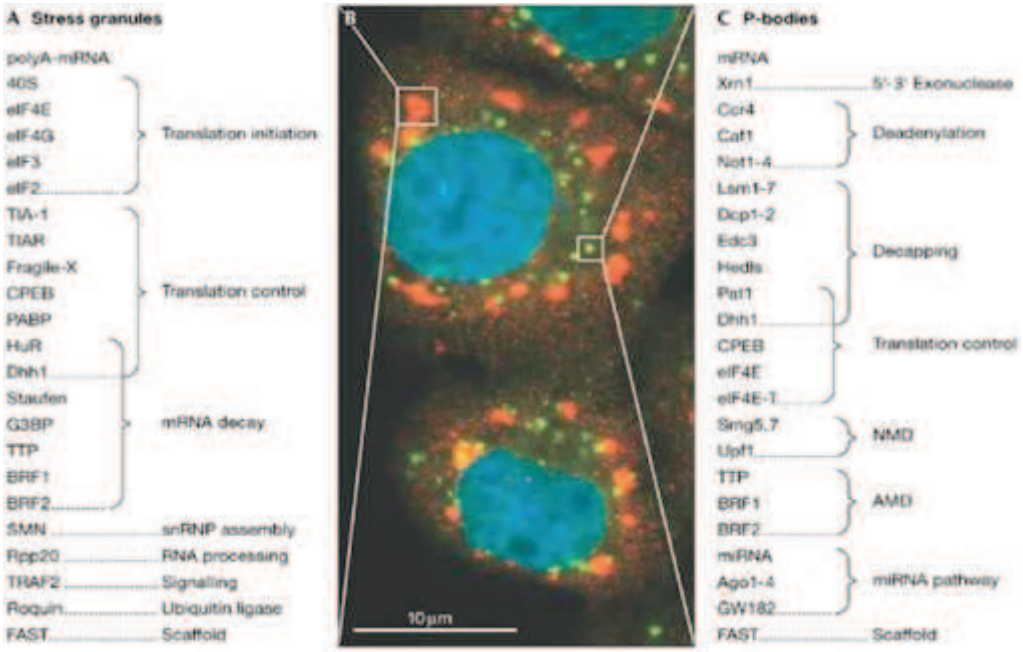

Figure 20. Composition of mammalian P-bodies and stress granules. A) List of factors detected in stress granules; B) Visualisation of P-bodies and stress granules; C) Mammalian P-bodies composition (M.J. Fritzler, Cell Signaling).

During stress conditions, P bodies tend to increase in size and number, thus suggesting increased mRNA decay under these conditions, or that P-bodies store mRNAs in a translationally repressed state. After stress removal these mRNAs could be reactivated and re-enter the translatable pool of mRNA substrates. Under stress conditions another type of cellular aggregate accumulates, called stress granules (Cougot et al. 2004; Thomas et al. 2011; Decker and Parker 2012). Many translation initiation factors have been shown to accumulate within stress granules, such as eIF4G, eIF4A, eIF4E, the 40S ribosomal subunit, PABP, eIF3, and other associated factors. Thus it is believed, that RNA is stored within 48S initiation complexes during stress conditions. This would allow for fast translation reactivation once the stress is removed. Observations that either P bodies or stress granules increase in size and quantity in stressed cells suggests the existence of crosstalk between the mechanisms localizing mRNAs in these compartments at the expense of the mRNAs in the active polysome pool. It has been hypothesized that mRNAs can exit the active translation pool upon remodelling of the RNP and can either be stored in P bodies in a translationally repressed state, or alternatively be degraded there. Alternatively, an mRNA engaged in a translation initiation cycle and bound to a 48S initiation complex would be targeted to stress

granules during the stress response and be stored there in order to be reactivated once the stress is alleviated (Figure 21).

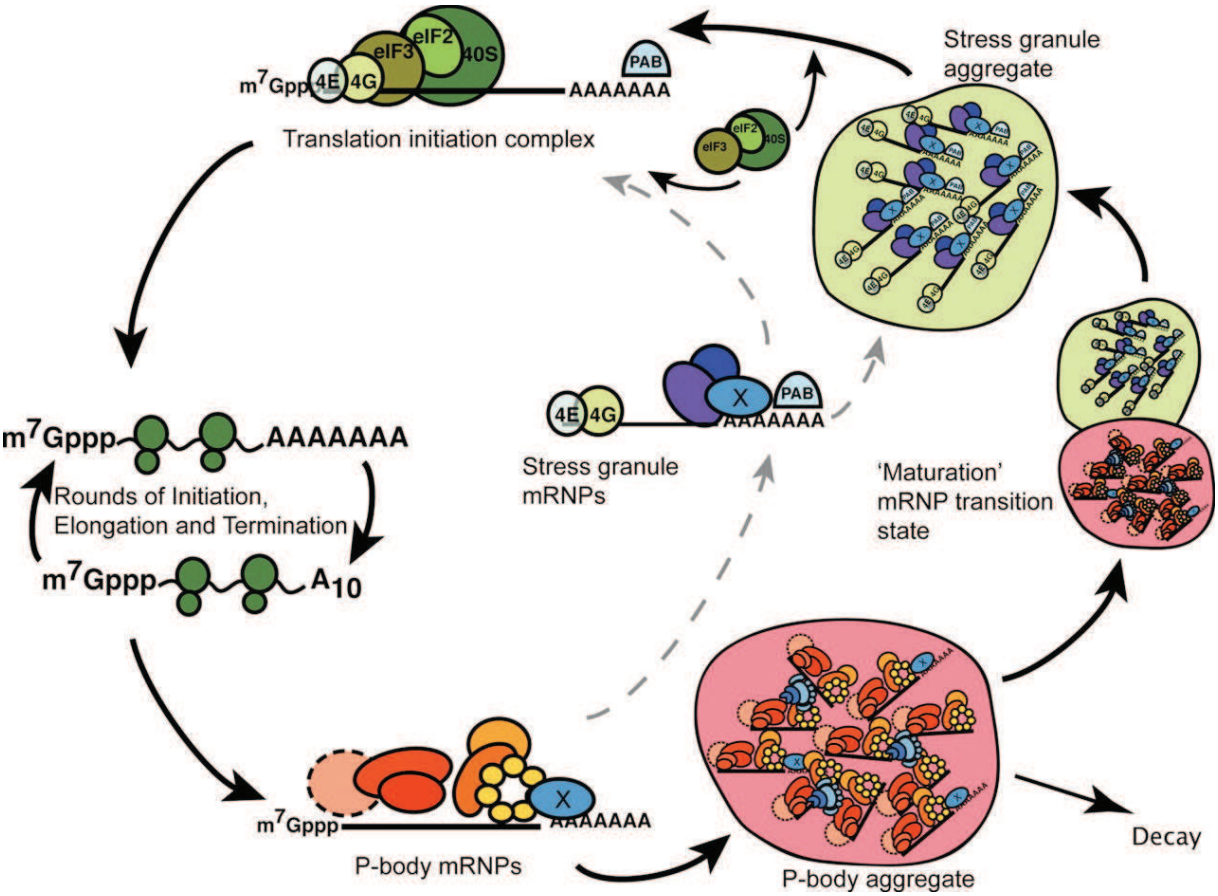

Figure 21. mRNP transition between active translation pool in cytoplasm to P bodies and stress granules. As far mRNA is decided to be degraded, it interacts with mRNA degradation factors and is targeted to P-bodies for subsequent degradation. Alternatively, mRNA associated with translation initiation factors can be stored in stress granules and subsequently reactivated for new translation cycles (Buchan et al. 2008).

1.4.1.5 Quality control mechanisms. NMD, NGD, NRD and NSD

All biosynthetic processes are imperfect and sometimes errors occur, although usually at a relatively low rate. Some mistakes, particularly in transcription or during RNA processing, can produce non-functional ribosomal RNA, the appearance of premature stop-codons, or the removal of a stop codon in an mRNA body. In order to avoid harmful consequences resulting from the translation of such mRNAs, or of the altered function of ribosomal RNAs, cells have evolved specific molecular machineries that are designed to target the

corresponding defective RNAs for rapid degradation. Indeed, all three situations targeting aberrant mRNAs have been extensively described at the molecular level. The respective pathways were named as Nonsense mediated decay (NMD), the surveillance mechanism for premature stop-codon containing mRNAs; Non-stop decay, for the elimination of mRNAs lacking a proper stop-codon; and No-Go decay, for mRNAs inducing ribosomal stalling through the presence of stem loops or other aberrant structures (Schweingruber et al. 2014; Inada 2014; van den Elzen et al. 2010; Graille and Séraphin 2012). In parallel, the Non-functional ribosomal decay pathway targets translation complexes stalled on mRNAs. The degradation machinery involved in quality control pathways is the same as the one used for basic and regulated mRNA decay. A specific overview of each of these surveillance pathways is presented below.

1.4.1.5.1 Nonsense mediated decay NMD

As presented above, after transcription each mRNA is exported from the nucleus as a huge mRNP complex composed of many different protein factors that will, in part, specifically differentiate the newly transcribed mRNA from old cytoplasmic mRNAs. Indeed, three main determinants exist: the nuclear cap-binding complex composed of CBP20/CBP80; the exon junction complex, EJC, in mammals; and the nuclear poly(A) binding protein PABPN/Nab2. The mRNA exported from the nucleus most likely remains coated by some of these factors. The particular protein composition of this new cytoplasmic mRNP will influence the first round of translation, because factors involved in recruiting the 40S subunit will be different, at least in part, and because the elongating ribosome will bump into unusual factors. During the first round of translation, the detection of possible premature termination codons (PTC) happens triggering the rapid and complete degradation of the corresponding mRNA.

A prerequisite for NMD is the progression of the first translating ribosome along the mRNA open reading frame. As soon as the ribosome reaches the PTC, a signalling mechanism is activated. Two complementary models exist to explain how this triggering happens. According to the first model, the EJC plays a critical role in PTC recognition. Normally, as a ribosome progresses along an mRNA open reading frame, it removes EJCs such that all EJC complexes have been evicted when it reaches the normal stop codon (consistently, normal

stop codons are nearly exclusively located in the terminal exon). When a PTC is present, the translating ribosome will reach it while a downstream EJC is still present on the mRNA. The EJC complex is composed of Y14, Magoh and eIF4AIII which interact with the classical NMD Upf factors, Upf2 and Upf3. The presence of downstream EJC bound to the mRNA when a PTC is present greatly facilitates interaction of these NMD factors with the ribosome terminating translation on the PTC. As during normal translation termination, the ribosome terminating on the PTC recruits the termination factors eRF1 and eRF3. It also interacts with Upf1, a critical factor for NMD initiation, and SMG1, a specific Upf1-kinase. The formation of this protein complex, called SURF (SMG1-Upf1-eRF1-eRF3), is strongly dependent on the presence of Upf2 and Upf3 which associate with the downstream EJC via direct interactions between Upf1-Upf2-Upf3, which in turn stimulates the ATPse and helicase activities of Upf1 (Chamieh et al. 2008). Interaction between SURF and Upf2/3 triggers the phosphorylation of Upf1 . This step ensures inhibition of further translation initiation rounds through direct interaction between eIF3 and phosphor-Upf1 (Isken et al. 2008), and is also crucial for the attraction of additional SMG factors, called SMG5, SMG6 and SMG7, which in turn will initiate the degradation of the PTC-containing mRNA. RNA decay may happen through two pathways: either by SMG6-mediated endonucleolytic cleavage of the mRNA followed by elimination of the resulting decay intermediates by the general RNA decay machinery; or by SMG5-SMG7 mediated induction of the basic mRNA decay pathway, involving decapping steps (Figure 22) (Conti and Izaurralde 2005; Schoenberg and Maquat 2012).

According to second model, which has been proposed both for metazoans and yeast, initiation of NMD is a 3'-UTR length dependent process, meaning that the distance between the PTC and the poly(A) tail plays a major role in differentiating the PTC from standard termination codons. Indeed, mRNA poly(A) tails are covered by PABP proteins, which in turn interact with the ribosome termination complex eRF1-eRF3 to facilitate normal ribosome termination. However, eRF1-eRF3 also interacts with Upf1. Thus there is a competition between Upf1, which is essential for triggering NMD, and PABP, which is important for normal translation termination. An mRNA with a long distance between the stop codon and the poly(A) tail will favour the interaction of eRF1-eRF3 with Upf1, thus favouring recognition of the stop codon as a PTC. In agreement with this model, artificial tethering of PABP close to a PTC suppresses NMD induction (Schweingruber et al. 2014; Behm-Ansmant

et al. 2007). The two models presented above are not mutually exclusive and a mixed mechanism of NMD induction might exist in mammalian cells (Decourty et al. 2014).

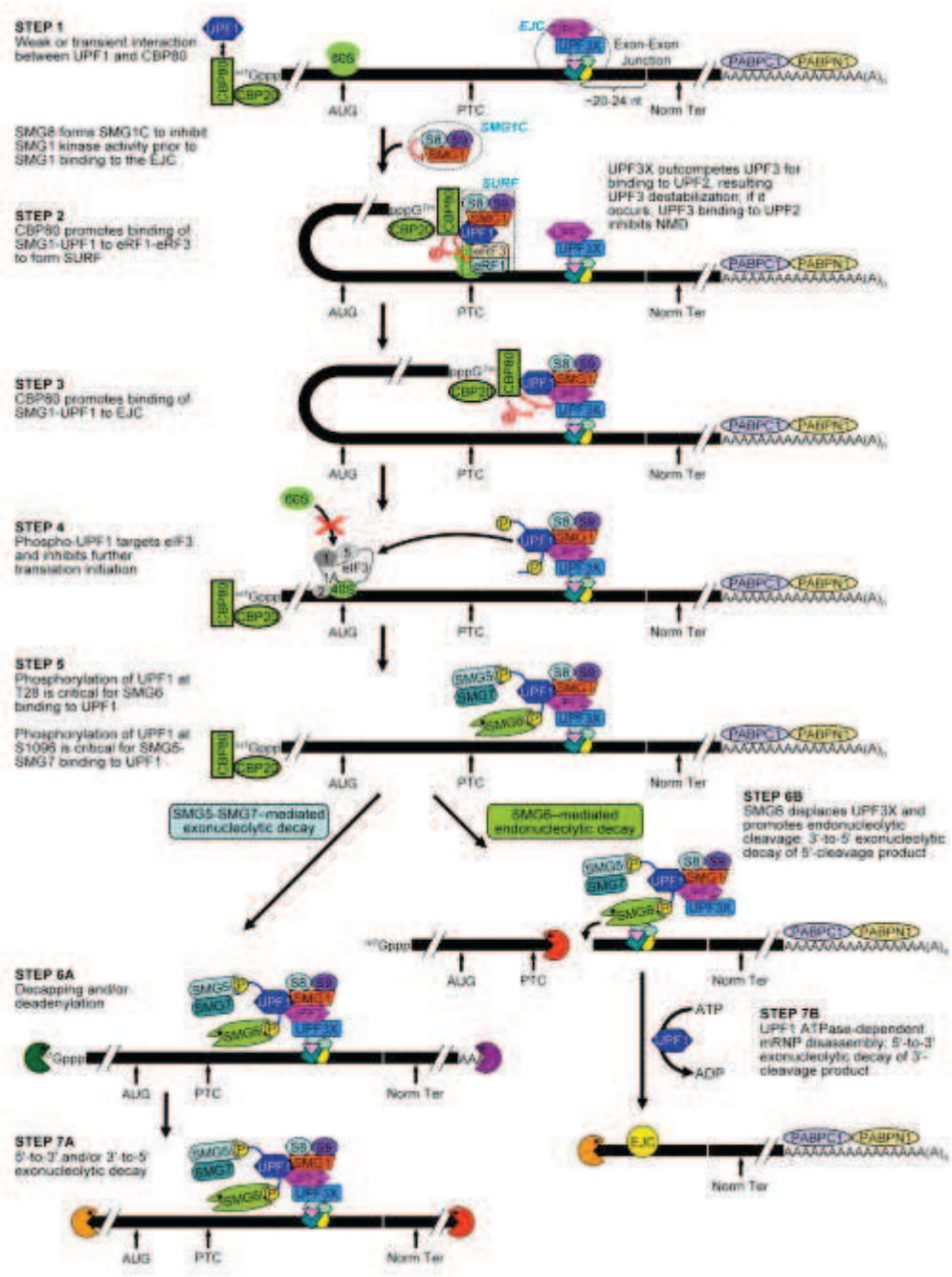

Figure 22. NMD pathway. Important steps and protein factors are presented. See text for details (Schoenberg and Maquat 2012).

Besides artificial mRNA reporters, which were used to discover and study the mechanism of NMD, multiple physiological examples of NMD have been reported. Many NMD-targeted transcripts result from alternative splicing which leads to the inclusion of a PTC in the final

mRNA. This process is called AS-NMD. Many splicing regulatory proteins of the SR family autoregulate their expression by AS-NMD, promoting the formation of an alternatively spliced mRNA containing a PTC when they are present at high concentration (Zhang and Krainer 2004; Isken and Maquat 2008). mRNAs that contain an intron interrupting their 3'-UTR are also likely to be natural targets of NMD. Some mRNAs with this peculiar structure are highly expressed in neuron cells and are targeted to the synaptic regions in dendrites. Upon synaptic activation, these mRNAs are expressed, but NMD activation allows the rapid inactivation of their translation. This particular mechanism plays a great role in the memory consolidation mechanism mediated by Arc protein expression and axon guidance mediated by Robo3.2 (Bramham et al. 2008; Giorgi et al. 2007; Colak et al. 2013).

1.4.1.5.2 No-go decay NGD, nonfunctional ribosome decay NRD and no-stop decay NSD

These quality control pathways were first observed by using an artificial mRNA with an inserted ribosome stall-site (NGD); an mRNA with a mutated stop codon allowing the ribosome to translate through 3'-poly(A) tail (NSD); or mutated 25S or 18S rRNAs defective in the peptidyl-transferase or decoding centres of the ribosome (NRD), respectively (Figure 23).

Generally all three mechanisms are variations of a similar event: triggered ribosome stalling which induces prolonged pausing on the mRNA. Ribosome blocking, resulting from an acquired stall-site or from translation of the poly(A) tail, is rescued by recruitment of a specific complex called Dom34-Hbs1. The 3D structure of this complex shows that its shape is similar to that of the classical termination complex eRF1-eRF3, or to the complex of the bacteria elongation factor EF-Tu with tRNA (van den Elzen et al. 2010; Becker et al. 2011). Indeed, the Hbs1-Dom34 complex binds to the vacant A-site in stalled ribosomes and then triggers RNA degradation. It was proposed that the mRNA undergoes endonucleolytic cleavage and that the intermediates produced are degraded by 5'-3' and 3'-5' mRNA decay pathways (Dever and Green 2012; Inada 2014; Graille and Séraphin 2012). Mutations in the endonucleolytic domain of the exosome and in the Ski-complex do not inhibit NGD, while degradation of NSD-derived mRNA intermediates is Ski7-dependent (van Hoof et al. 2002;

Frischmeyer et al. 2002). However, deletion of Xrn1 resulted in accumulation of NGD decay intermediates, suggesting that their decay is 5'-3' directed (Harigaya and Parker 2014; Doma and Parker 2006). The stalled ribosome complex is subsequently dissociated and recycled, as it was shown that Hbs1-Dom34 can efficiently induce Rli1-dependent ribosome recycling. The premature-terminated peptide is scavenged by ubiquitin-mediated proteasomal degradation mediated by the Ltn1 containing ribosome quality control complex (RQC) (Matsuda et al. 2014).

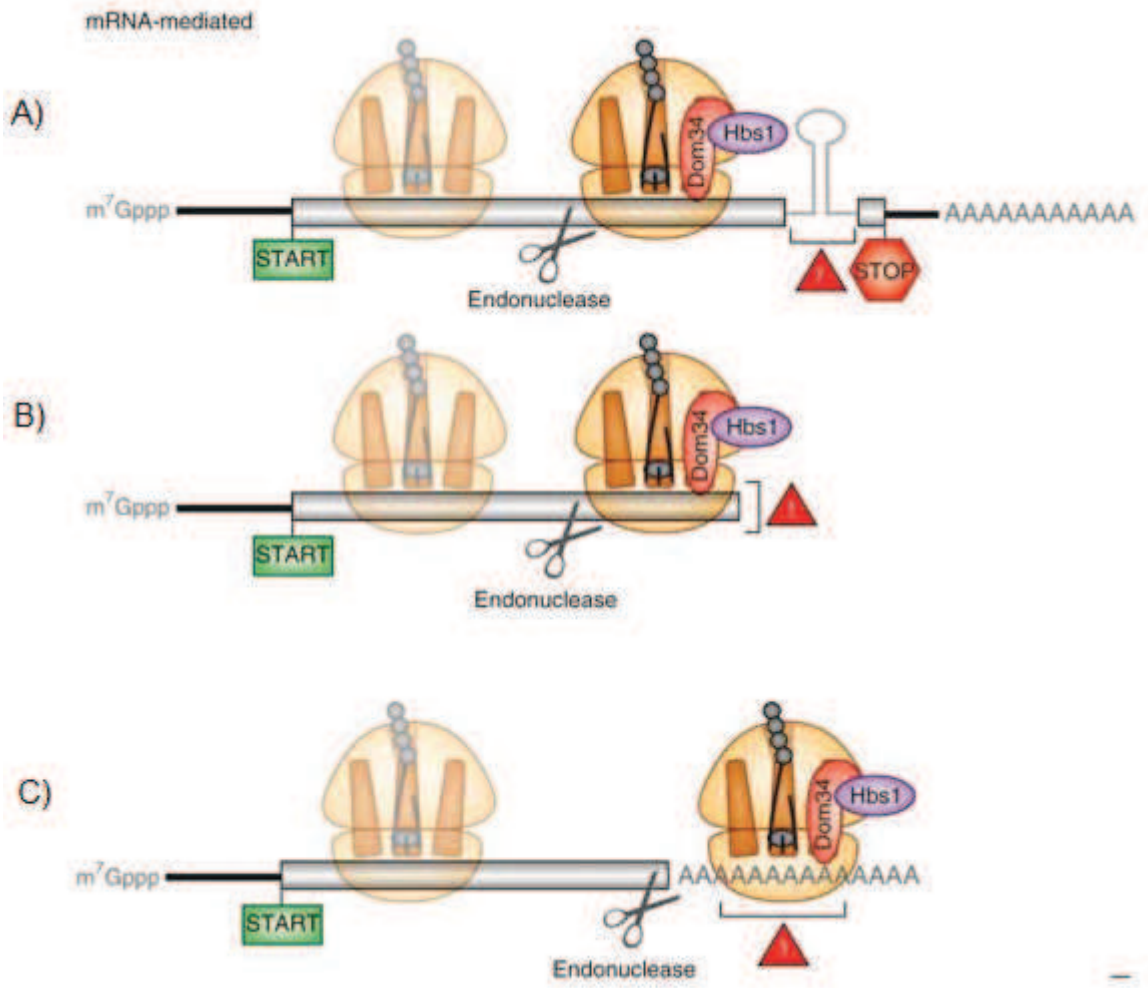

Figure 23. Examples of Dom34-Hbs1 dependent quality control mechanisms. A) - No-Go decay; B) and C) – No-stop decay pathways (Dever and Green 2012).

1.4.1.6 Initial step of mRNA degradation – deadenylation.

As described above, deadenylation is a key initial step in the degradation of most mRNAs. The CCR4-NOT complex contributes to the initial step of poly(A) tail shortening and translation inhibition. Interfering with initiation cap-binding complexes results in recruitment of decapping factors and subsequent mRNA degradation in the 5'-3' direction. In this chapter, I concentrate on factors mediating mRNA deadenylation with emphasis on the CCR4-NOT complex that was the subject of my studies.

Global architecture of yeast CCR4-NOT deadenylation complex

The CCR4-NOT complex is a highly conserved protein assembly in eukaryotes with an approximate mass of 1 MDa (Figure 24). The yeast complex is composed of 9 core subunits and other additional protein factors required for exerting its molecular function. CCR4-NOT was first described as a transcriptional complex negatively modulating mRNA levels and some genetic experiments linked it to transcription (Collart and Panasenko 2012; Collart and Struhl 1994). More recently it became widely accepted that the CCR4-NOT complex has a major role in mRNA deadenylation (Daugeron et al. 2001). The yeast CCR4-NOT complex contains two subunits with RNA nuclease activity, namely Caf1 and Ccr4; a subunit with an E3-ubiquitin ligase domain containing protein, namely Not4; the Not1 subunit, a mostly helical protein that basically forms the scaffold of the complex; and the Not2-3-5, Caf40 and Caf130 proteins (J Chen et al. 2001; Bai et al. 1999). Purification of the mammalian CCR4-NOT complex revealed several differences: Caf130 is not conserved in mammals while only one protein similar to both Not3 and Not5 is found in these species. It is also noteworthy that a Not4 subunit is encoded in mammalian genomes but that it was not reported to associate with the human CCR4-NOT assembly in contrast to yeast. Conversely, Cnot10 and Cnot11 are present in the human complex but absent in the fungal CCR4-NOT complex. (Ito et al. 2011; Collart and Timmers 2004; Mauxion et al. 2013). Additional complexity can be found in the human complex with, in some cases, two genes coding for alternative subunits of the CCR4-NOT complex (e.g., two "Caf1" subunits CNOT7 and CNOT8) and in other cases variants arising by alternative spicing. Looking at phylogenetically more distant organisms provides more surprises. For example, CCR4 homologues are absent from trypanosomas and plants. As my research was aimed at dissecting, both structurally and functionally, the CCR4-

NOT complex from yeast, each of the subunits of this assembly is presented below. This includes some data that were published when my project was ongoing.

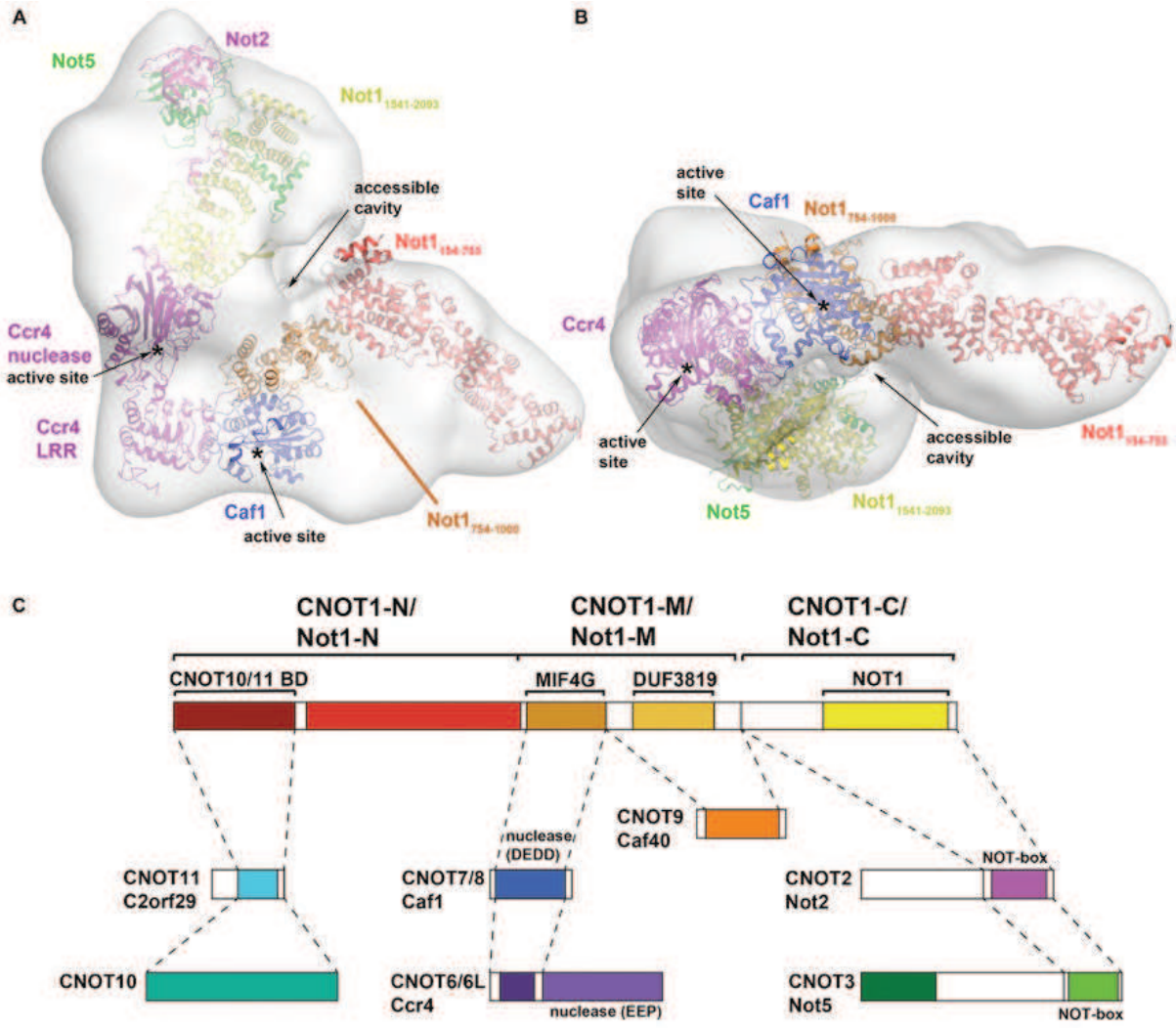

Figure 24. CCR4-NOT complex architecture. A) and B) Recent cryo-EM low-resolution CCR4-NOT structure reveals an L-shaped form of the complex. Solved X-ray structures of subcomplexes were fitted into this envelope. C) Schematic representation of known CCR4-NOT complex subunits indicating binding partners and interaction domains. Both the human (upper) and yeast (lower) names of proteins are indicated.(Basquin et al. 2012a).

Interaction studies have revealed that the 240 kDa Not1 protein forms the scaffold of the yeast CCR4-NOT complex (CNot1 in humans). Structural analyses demonstrated that it is mostly formed from HEAT-repeats, which are alpha-helical structures. This huge protein is

essential for yeast viability while its knock-down in human cells results in cell death through apoptosis (Ito et al. 2011).

Interaction analyses have revealed at least three binding domains within Not1 (Figure 25). Those are located mostly in its central and C-terminal parts: the surface interacting with the Caf1 deadenylase subunit is located in the central domain. It adopts a structure related to the MIF4G fold of the eIF4G initiation factor. This surface indirectly recruits the Ccr4 subunit that binds, through its leucine-rich repeat (LRR) domain, to Caf1 (Chen et al. 2002). Importantly, while in the human and *drosophila* complexes both subunits Caf1 and Ccr4 are actively involved in deadenylation, in yeast Ccr4 appears to be mediating most of the activity. In contrast, in plants and trypanosomes, the absence of a Ccr4 homologue suggests that Caf1 is entirely responsible for the nuclease activity of the complex.

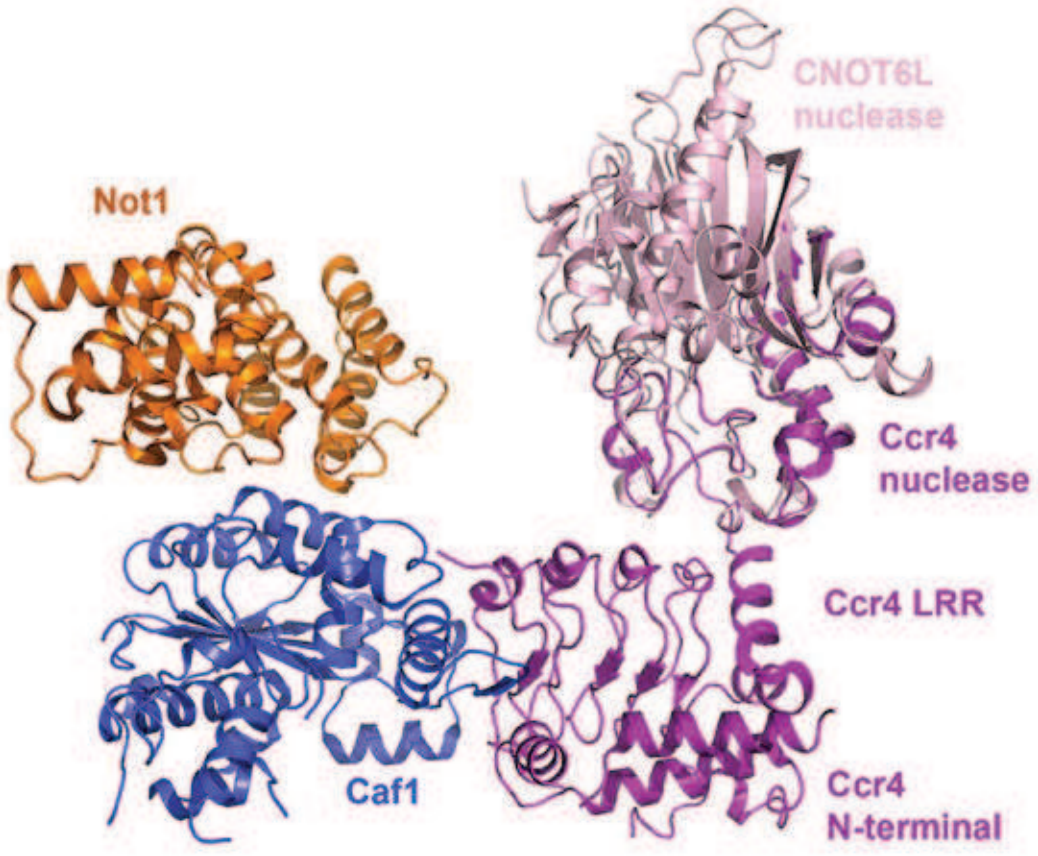

Figure 25. Structure of a heterotrimeric complex containing associated fragments of Not1, Caf1, and Ccr4. This structure reveals that Caf1 bridges the Not1 and Ccr4 subunits of the complex. (Basquin et al. 2012a).

The structure of C-terminal part of Not1 revealed two interaction surfaces for the Not2 and Not5 subunits of the CCR4-NOT complex (Figure 26). It is believed that Not3 can interact in a similar manner to Not5. Not1 forms a prolonged HEAT-repeat domain, around which the Not2 and Not5 subunits are assembled. Interestingly, these two subunits share the same N-terminal domain fold that mediates interaction with the C-terminal part of Not1 and as well as between each other. In yeast two paralogous proteins exist, Not3 and Not5. The idea that these two factors interact with Not1 and Not2 in a similar manner could suggest that the CCR4-NOT complex is heterogeneous, as Not3 and Not5 would be mutually exclusive: some entities would contain Not3 while others would contain Not5. However, given the sequence and structure similarity between the N-terminus of Not2, Not3 and Not5, one could also envisage that some complexes could contain Not3-Not5 heterodimers.-(Bhaskar et al. 2013; Boland et al. 2013).

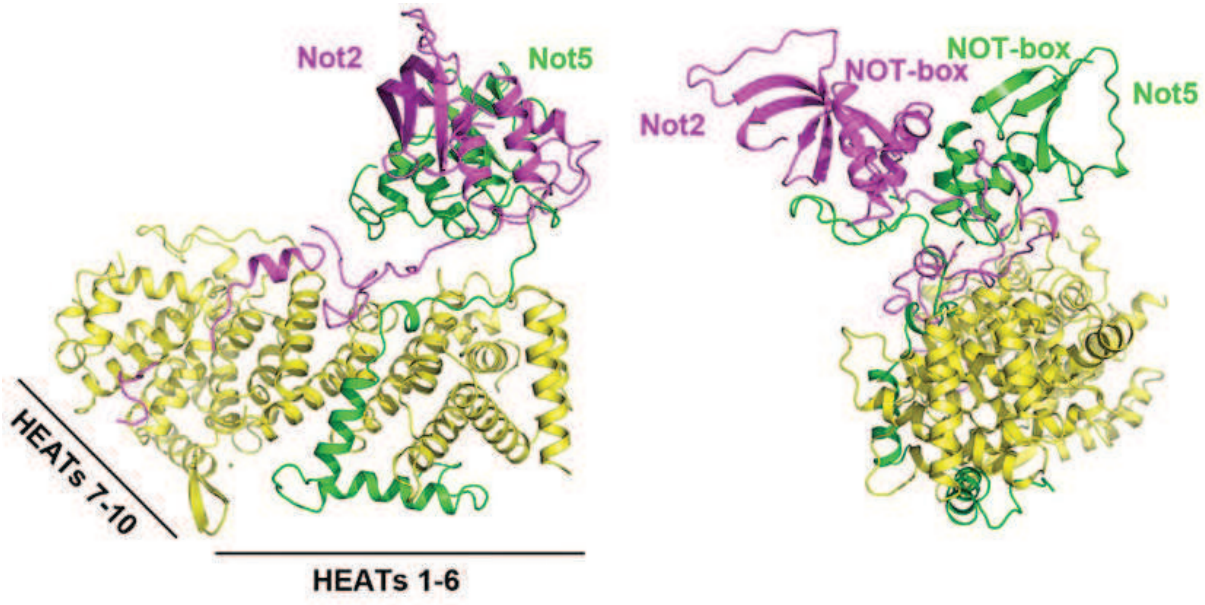

Figure 26. Structure of a complex containing the C-terminal domain of Not1 with Not2 and the N-terminal part of Not5. This structure reveals the regular HEAT-repeat organization of Not1. Not2 and Not5 interact with each other through their conserved NOT-box domain. Both subunits also interact directly with Not1 through a random coil regions.(Bhaskar et al. 2013).

Structural studies of the N-terminal part of Not1 reveal the same extensive HEAT-repeat, mostly helical fold (Basquin et al. 2012b). This region could bind multiple accessory proteins,

like RNA-binding proteins or other regulatory factors. Indeed, the Not1 mammalian counterpart interacts with the mammalian specific subunits of the complex, namely Cnot10 and Cnot11, through the N-terminal part of Not1 (Mauxion et al. 2013; Bawankar et al. 2013).

Other subunits of the yeast complex, named Not4, Caf40 and Caf130, and other binding partners seem to bind either to the central domain of Not1 or in its proximity. Determining the interaction pattern of all regulatory partners of the CCR4-NOT complex is currently an area of intensive research (Panasenko and Collart 2011; Azzouz et al. 2009).

1.4.1.6.1 Ccr4 and Nocturnin

Ccr4 is a protein subunit that contains an exonuclease-endonuclease-phosphatase (EEP) domain and exhibits catalytic 3'-5' exonuclease activity (Arraiano et al. 2014) (Figure 27). This activity is Mg^{2+}-dependent and poly(rA)-specific as shown by *in vitro* studies. However, evidence was presented that *in vivo*, Ccr4 was not restricted to the degradation of poly(rA) sequences as, when targeted to a specifc transcript, it was able to degrade its 3'UTR (Finoux and Séraphin 2006). Ccr4, as all EEP proteins, catalyzes phosphate ester bond hydrolysis with the help of two Mg^{2+} ions, which facilitate deprotonation of a water molecule for attack on the phosphorus, and stabilize the negative charges developing on the non-bridging oxygen and the leaving hydroxyl group. As expected, mutations affecting Mg^{2+} ion coordination or targeting residues involved in catalysis, abolish the Ccr4 deadenylation activity *in vivo* and *in vitro* (Chen et al. 2002; Wahle and Winkler 2014; H. Wang et al. 2010). In addition to its nuclease domain, Ccr4 contains a leucine-rich repeat (LRR) region. Such domains are usually responsible for protein binding, and, in the case of Ccr4, the LRR domain interacts with Caf1 which links it to Not1. In human, two Ccr4 orthologues named CNOT6 and CNOT6L have been shown to compete for interaction with two Caf1 homologues, CNOT7 and CNOT8. While these proteins may not all be expressed in the same cells, these observations suggest that up to 4 different CCR4-NOT complexes may be formed in mammals. Importantly, the presence of both a LRR and a EEP domain is required to define a protein as a Ccr4 "true" orthologue.

Another poly(A)-specific nuclease containing an EEP domain exists, called Nocturnin. It lacks, however, an LRR domain and is clearly not a CCR4 orthologue. Interestingly, even though Nocturnin lacks an LRR domain, it was reported to associate with a distant Caf1 family member named Caf1z (Wagner et al. 2007; Baggs and Green 2003). This heterodimeric complex is able to degrade poly(A) *in vitro.* Evidence for its involvement in mRNA degradation *in vivo* is limited. Most likely, the deadenylation function of Nocturnin is restricted to specific RNAs and Nocturnin would thus impact on particular biological functions, such as regulation of circadian rhythms (Godwin et al. 2014; Baggs and Green 2003).

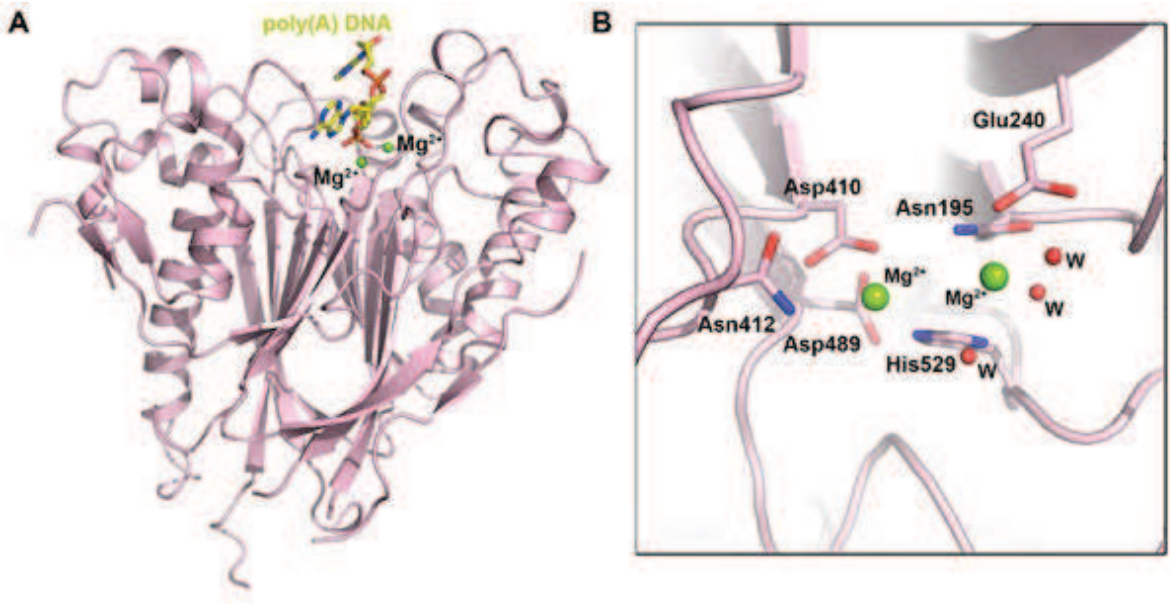

Figure 27. A) Structure of the Ccr4 catalytic domain reveals a conserved heart-shaped structure characteristic of the EEP family proteins. B) The Ccr4 active site contains two Mg^{2+} ions required for poly(A) tail hydrolysis(Wahle and Winkler 2014).

1.4.1.6.2 Caf1 and PARN

Another deadenylase subunit of the CCR4-NOT complex is Caf1 (Figure 28). It contains characteristic amino acid residues at diverse locations along its sequence. These amino acids, Asg-Glu-Asp-Asp or DEDD, have given the name of this specific family of nucleases: the DEDD-type nucleases. The nuclease activity of Caf1 is also divalent cation dependent, and requires two Mg^{2+} ions bound to the protein. Importantly, even though yeast Caf1 can hydrolyze RNA *in vitro*, acting preferentially on poly(A) compared to poly(G) and poly(C), it

seems to contribute very little nuclease activity to deadenylation *in vivo*. One could propose that in yeast cells the role of Caf1 is restricted to non-specific molecular interactions with RNA, thus helping to thread the substrate towards the enzymatically active subunit Ccr4. In contrast to the yeast situation, the CNOT7 and CNOT8 orthologous proteins in human, or the *drosophila* homologue are catalytically active *in vitro* and this activity appears to contribute significantly to poly(A) degradation *in vivo* (Daugeron et al. 2001; Aslam et al. 2009; Hata et al. 1998; Finoux and Séraphin 2006).

Another deadenylase, belonging to the DEDD-nuclease family, was identified and called poly(A)-specific ribonuclease (PARN). Interestingly, PARN can also simultaneously bind the 7-methyl-guanosine cap on mRNAs 5' end. This interaction influences the processivity of the enzyme and increases the rate of poly(A) tail removal. The cap-binding activity of PARN suggests that it could compete with cap-binding factors, such as eIF4E in the cytoplasm, or the CBC20/80 complex in nucleus, as PARN was shown to act in both of these compartments (Dehlin et al. 2000). Interestingly, the biological function of this enzyme extends from basic RNA poly(A) tail length control to more specific roles, especially for the nuclear fraction of the enzyme. Indeed, it was shown that PARN plays a role in the maturation of snoRNA tails and mRNA decay following DNA damage. PARN is likely to play a role in the NMD quality control mechanism, as it can be efficiently precipitated with the Upf1, Upf2 and Upf3 factors (Berndt et al. 2012; Lejeune et al. 2003). PARN is also an important factor in neuronal cell function and memory consolidation, as it was shown to act in association with the cytoplasmic polyadenylation complex (CPEB) (Lin et al. 2010). In neuronal cells, PARN was reported to keep target mRNAs translationally "silenced" by trimming their poly(A) tails. However, synaptic stimulation induces PARN dissociation from the complex. In such conditions, target mRNA poly(A) tails become extended, leading to a local induction of translation in dendrites. This mechanism suggests a significant importance of local mRNA degradation in controlling poly(A) tail length and gene expression (Udagawa et al. 2012).

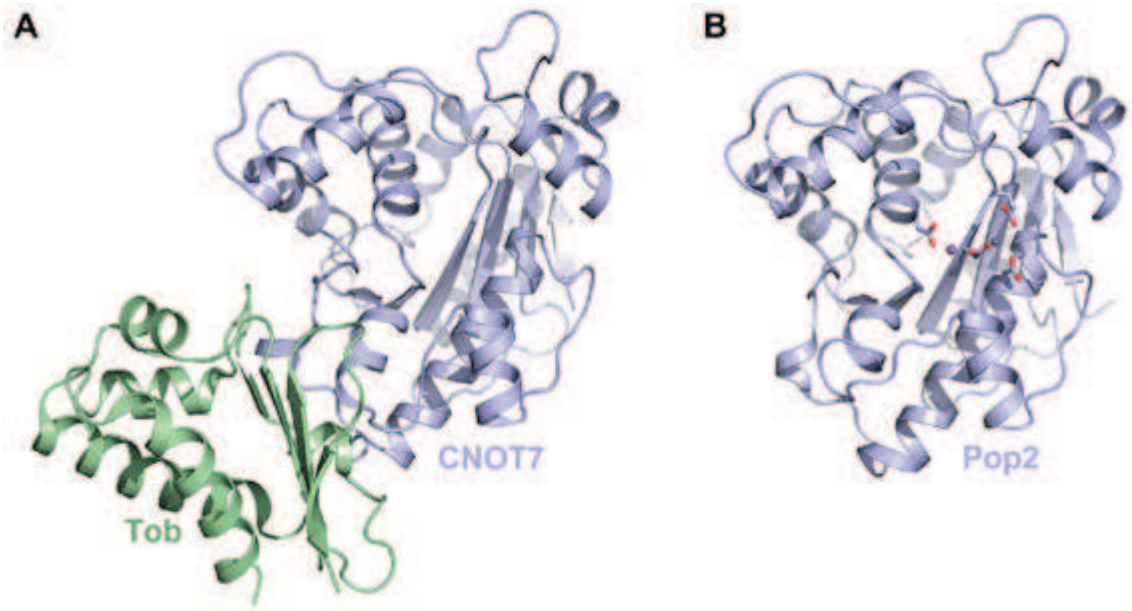

Figure 28. Structures of mammalian (A) and yeast (B) Caf1 proteins. Caf1 belongs to the conserved DEDD family of proteins. The mammalian protein is presented in complex with Tob1, a cofactor required for activation of deadenylation by exogenous stimulus. (Wahle and Winkler 2014).

1.4.1.6.3 The Not-module: Not2, Not3 and Not5 non-catalytic subunits of CCR4-NOT complex

As mentioned above, the C-terminal part of yeast Not1 interacts with the Not2, Not3 or Not5 proteins, and CNOT2 and CNOT3 interact with the corresponding region of CNOT1 in mammals. Not2 and Not3/5 are mysterious proteins in terms of molecular function. They share the same N-terminal motif, termed the Not-box. Not2 is essentially composed of a single Not-box domain. It is considerably shorter than Not3 and Not5. Not3 and Not5 contain a highly conserved C-terminal extension of unknown function that is called the Not3-domain. Not3 and Not5 seem to be paralogues and likely resulted from a gene duplication event in the fungal lineage. While their precise molecular function remains unclear, their implication in the structural integrity of the CCR4-NOT complex has been suggested (Ito et al. 2011; Collart and Struhl 1994).: disruption of Not2 resulted in complex instability. Loss of function mutations in Not3 and Not5 displayed different phenotypes. However, some of these differences may be due to the genetic backgrounds and not related to the protein identity. It has been described, for example, that deletion of Not5 is crucial for yeast vegetative growth while loss of Not3 had little, if any, effect on this process. An implication of Not2-3-5

proteins in mRNA decay has also been proposed, but their precise molecular function in this process remains to be deciphered (Muhlrad and Parker 2005; Boland et al. 2013). Specific mRNAs targeted by Not2-3-5 have been identified, as Not3 and Not5 have been shown to be involved in Edc1 mRNA degradation regulation. Similarly, decay of the *drosophila* hsp70 mRNA after heat shock recovery was shown to be largely dependent on the integrity of the Not-module. *In vitro* studies have revealed that these proteins can bind poly(U) RNA stretches. Such elements are indeed present in the 3'-UTR of multiple mRNAs and may thus be the targets for Not-protein mediated RNA decay regulation. Several CCR4-NOT complex subunits were observed to be present in P-bodies suggesting that they could act in these mRNA storage and decay centres (Muhlrad and Parker 2005). Altogether, while interaction data indicate a molecular link between Not proteins and deadenylases, functional experiments only hint to the function of this protein in RNA decay. These area needs to be investigated to clarify the molecular role of the Not-module of the CCR4-NOT complex.

1.4.1.6.4 Other CCR4-NOT complex subunits: Caf40, Caf130 and Not4

Another conserved subunit of the CCR4-NOT complex of unknown function is Caf40 (CNOT9 in mammals). It contains a highly conserved Rcd-1 domain. This subunit binds to the middle region of the Not1 scaffold subunit, just after the Caf1 subunit. The structure of the Rcd-1 domain from *H. sapiens* revealed a regular armadillo-repeat fold formed by alpha-helices arranged in a spiral (Garces et al. 2007). This protein motif is frequently found in many factors of diverse biological function where it usually serves as a platform for protein-protein interactions. CNOT9 was first described for its role in hormone-receptor transcription activation (Garapaty et al. 2008), but recent *in vivo* studies demonstrated the role of CNOT9 in binding to GW-repeats in GW182/TNRC6, thus providing a molecular link between miRNA mediated repression of gene expression and deadenylation mediated by the CCR4-NOT complex (Mathys et al. 2014; Chen et al. 2014). The CNOT9 interaction with GW-proteins observed in mammals cannot occur in yeast where no GW182 orthologue exists. This suggests the existence of another conserved function for Caf40 in the CCR4-NOT complex. One possibility is that Caf40 might directly bind, specifically or non-specifically, to RNA. In the latter scenario, Caf40 would provide a molecular link between the CCR4-NOT complex and the mRNA targeted for degradation. *In vitro* studies suggest that Caf40 binds

preferentially to poly(G), poly(C) and poly(T) oligonucleotides, and specific mutations in the highly positively charged pocket abolish these interactions (Garces et al. 2007). Nevertheless, the functional importance of these interactions remains to be determined.

Not4 (CNOT4 in mammals) has also been identified as a subunit of CCR4-NOT complex as it can be efficiently co-precipitated from yeast extracts with other subunits of this assembly (Chen et al. 2001). Even though this protein appears to be conserved in animals, it is absent from the complex pulled-down from human and *drosophila* (Lau et al. 2009). The Not4 function is likely to be conserved, however, as human CNOT4 can partially compensate for the absence of the yeast protein. Not4 has been shown to function as an E3-ubiquitin ligase due to the presence in the N-terminus of a conserved RING-domain, a domain characteristic of E3-ubiquitin ligases (Panasenko and Collart 2011; Mulder et al. 2007). The NMR structure of this domain has been determined, providing information about its organization. Functional studies of the yeast Not4 subunit revealed its involvement in ubiquitin-mediated degradation of nascent peptides, thus suggesting a possible role in polypeptide quality control (Dimitrova et al. 2009). Other substrates include the ribosomal protein rps7a and the Egd complex, a ribosomal chaperone involved in nascent peptide co-translational folding (Panasenko and Collart 2011). Thus, the biological function of this particular subunit of the CCR4-NOT complex appears to be distantly related, if at all, from deadenylation and mRNA degradation control. It can nevertheless be connected with the possible co-translational functions of the CCR4-NOT complex.

Finally, the yeast CCR4-NOT complex also contains the Caf130 protein. No clear homologue is present in the human complex even if some similarities with CNOT10 have been suggested. The function of this protein is elusive as deletion of the corresponding gene does not result in obvious growth defects.

1.4.1.7 Particular role of the yeast CCR4-NOT complex mRNA decay induced by specific RNA binding proteins: the case of Puf-protein regulated decay

After having presented the basic composition and structure of the yeast CCR4-NOT complex, I will describe how this protein machinery can be targeted to substrate mRNAs by accessory factors such as specific RNA-binding proteins. One well-described case is that of Puf-protein mediated RNA decay.

The Puf family of RNA-binding proteins has six well described members in yeast, called Puf1-6. In higher eukaryotes, the corresponding orthologous proteins are called FBF in *C. elegans*, Pum in *drosophila* and humans (in *H. sapiens* two orthologues have been identified: Pum1 and Pum2). Structurally these proteins adopt an armadillo-repeat fold, which in the case of Puf proteins is required for RNA binding (Jenkins et al. 2009; Caro et al. 2006). Interestingly, differences in amino acid residues of the RNA-binding surface dictate substrate preferences. Such preferences have been described for each yeast Puf protein (Figure 29). The corresponding motifs are frequently found in the 3' UTRs of mRNA with related functions. Thus, the yeast Puf3 protein binds mostly to mRNAs encoding mitochondrial targeted proteins, while Puf4 interacts with mRNAs encoding ribosome biogenesis factors (Galgano et al. 2008; Gerber, Herschlag, and Brown 2004; Kershner and Kimble 2010). Structurally, the complex made by Puf proteins with its RNA binding site involves stacking interactions between nucleotides and conserved aromatic amino acid residues (Figure 29). This network of interaction explains the strict specificities of each Puf-mRNA pair. The regulatory actions of Puf proteins use a variety of mechanisms to regulate expression of target mRNAs: depending on the mRNA and organism, Puf proteins can either repress mRNA expression or induce it. One general trend is that Puf proteins exert their function a defined location. These points will be discussed by focusing on yeast Puf protein functions.

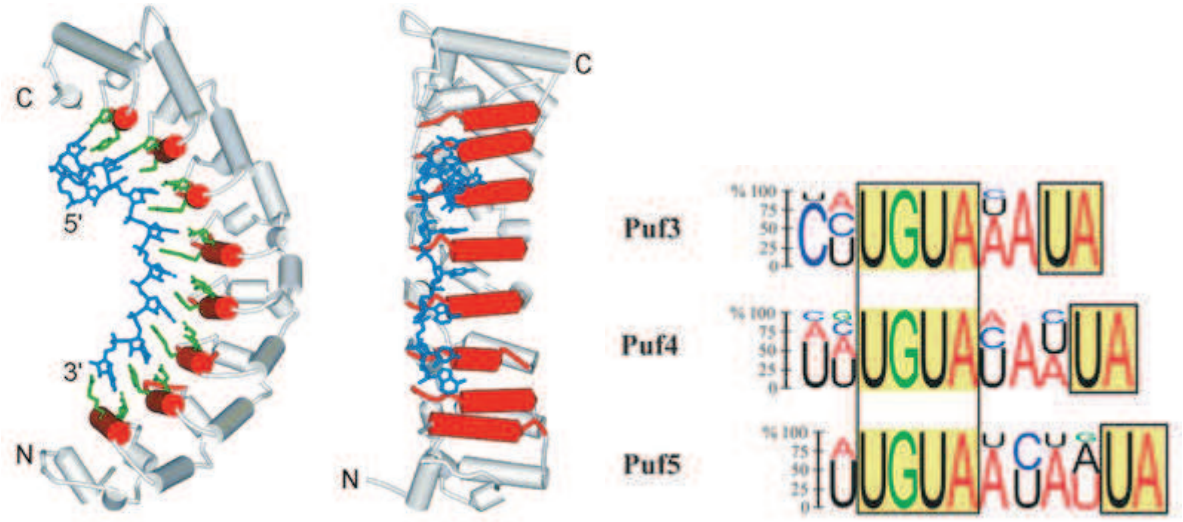

Figure 29. (Left) Scheme depicting the interaction of human Pumillio1 and its RNA binding motif. RNA binding α-helices are shown as red cylinders, RNA binding amino acid side chains are in green and RNA is in blue. (Right) Different Puf protein binding motifs. Conserved nucleotides are boxed (Jenkins, Baker-Wilding, and Edwards 2009).

As mentioned above, yeast has six different orthologous Puf proteins. The best studied of these factors are Puf3, Puf5 and Puf6. One of the functions of these proteins is mRNA localization. Several lines of evidence suggest that the Puf3 protein localizes its mRNA targets to the vicinity of mitochondria, thus facilitating import of mitochondria targeted proteins. Deletion of *puf3* resulted in delocalization of the Cox17 and Oxa1 proteins, both of which are puf3 mRNA substrates (Gadir et al. 2011; Eliyahu et al. 2010). Importantly, incubating cells with the translation inhibitor cycloheximide for a short period of time also abolished mRNA localization, suggesting that Puf3-mediated mRNA targeting is dependent upon active translation (Saint-Georges et al. 2008; Gadir et al. 2011). This observation also questions the mechanism associated with localization of Puf3 associated mRNAs: Is Puf3 the main targeting factor or is the protein mitochondrial import sequence the primary signal for mRNA localization? The combination of these two signals is certainly important as, in agreement with biochemical data, the simultaneous disruption of *puf3* and of the gene encoding the mitochondrial import receptor Tom20 resulted in a lethal genetic interaction, with yeast being unable to grown on media containing a non-fermentable carbon source, such as glycerol (Eliyahu et al. 2010).

A similar localization function was described for Puf6 (Figure 30). Indeed Puf6 is implicated in the regulation of the Ash1 mRNA by promoting its localization and translation in the yeast bud. Ash1 encodes a transcription factor active only in yeast daughter cells. This specific pattern of expression is achieved by the asymmetric localization of the Ash1 mRNA in the bud tip that represents the future daughter cell. Translation of this mRNA is also controlled and only occurs shortly before or soon after cell division, ensuring that only the daughter cell inherits the Ash1 protein. Puf6 is required for silencing mRNA translation during transport by binding to the response element located in the 3'-UTR of Ash1 mRNA and by interacting with initiation factor eIF5B preventing the joining of the 60S ribosomal subunit to the 48S initiation complex. Interestingly, localization of the Ash1 mRNA also involves interaction of the She2 protein subunit of the "locasome complex" with RNA elements present in the Ash1 open reading frame. Thus, inhibition of translation by Puf6 certainly facilitates this binding and travelling of mRNA to the bud. When the Ash1 mRNA reaches its destination, translation

activation occurs: Puf6 is phosphorylated and dissociates from the recognition motif (Gu et al. 2004; Quenault et al. 2011).

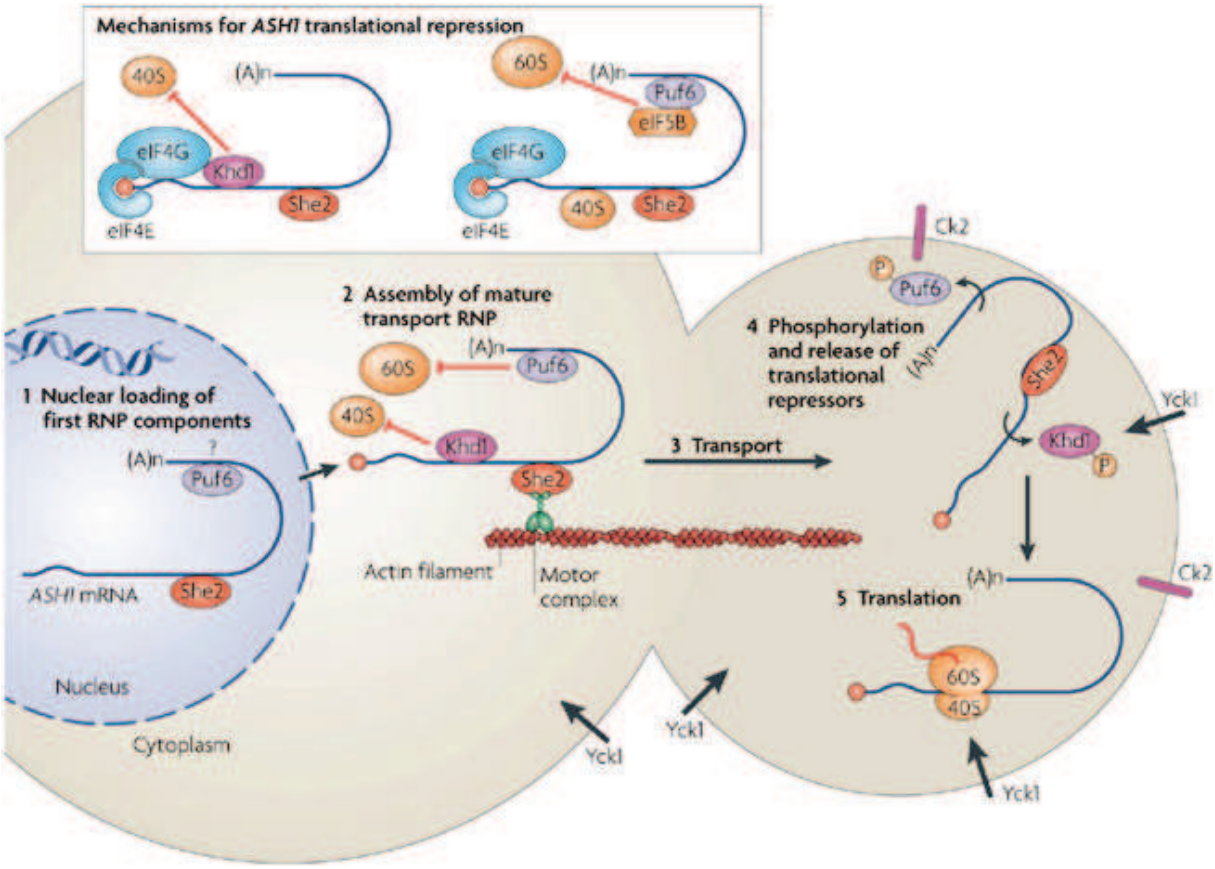

Figure 30. Role of in mRNA localization and translation repression. During Ash1 mRNA transport to the bud, Puf6 interacts with eIF5B, thus inhibiting joining of the 60S ribosome subunit. Translation repression is also achieved by the action of Khd1 protein, which inhibits 40S scanning. In the bud, Ash1 mRNA is translationally activated by phosphorylation of the inhibitory proteins Puf6 and Khd1 and their release from the mRNA (Besse and Ephrussi 2008).

The mechanism of translation repression mediated by Puf5 differs from those identified for Puf6. It has been shown that Puf5 precipitates with the Caf1 subunit of CCR4-NOT-Not complex, thus repressing target mRNA expression by inducing deadenylation (Goldstrohm et al. 2006; Chritton and Wickens 2010).

In conclusion, Puf proteins are versatile repressors. The recruitment of the CCR4-NOT complex and subsequent mRNA deadenylation and degradation appears to be a pathway conserved in yeast and metazoans (see also the description of the function of human and *drosophila* pumilio proteins below) and a prevalent mechanism of Puf-mediated mRNA

repression. At this stage, however, one cannnot exclude that other repression mechanisms might (co-)exist.

1.4.1.8 Characteristics of the mammalian CCR4-NOT complex. Involvement in RNA-binding protein mediated and miRNA-driven mRNA repression

As mentioned above, several structural and functional differences exist between the yeast and mammalian CCR4-NOT complexes. In this section, I would like to focus on the functional specificities of the mammalian assembly. Indeed, microRNA driven mRNA repression is perhaps the most important function of the mammalian CCR4-NOT complex. Small noncoding RNAs are important regulators of gene expression in higher eukaryotes that are absent from yeast. It has recently been described that miRNAs can bind their target mRNA, recruit the CCR4-NOT complex to their poly(A) tail and induce both translation repression and mRNA decay. Before describing the mechanism of miRNA-driven CCR4-NOT translation repression and deadenylation in detail, I would like first to briefly introduce miRNA biogenesis and processing. Connected to this topic, I also would also like to discuss the role of Pum1 (mammalian Puf protein orthologue) in miRNA driven decay. Finally, I will describe other important functional roles of the CCR4-NOT complex in the TTP-regulated and Roquin-mediated inflammation response.

1.4.1.8.1 Origins of miRNA, maturation process, function

MicroRNAs belong to the large class of small non-coding RNAs, known to affect gene expression (Du and Zamore 2007; Ghildiyal and Zamore 2009; Winter et al. 2009). The biological importance of these small RNAs is wide, and many important roles were described for them including in embryonic development, cancer propagation, immune response and even in light perception by retinal cells. Three major types of small non-coding RNAs have been distinguished: siRNAs, miRNAs and piRNAs. They differ from each other by their transcription, processing and target specificity. piRNAs are expressed in germ-line cells and suppress transposon-element expression. siRNAs and miRNAs differ from each other in functional output: while siRNAs usually induce endonucleatic cleavage of target mRNA, miRNAs can either destabilize mRNA by inducing deadenylation or repress translation.

Normally miRNA are transcribed by RNA polymerase II as mRNA like long primary pri-miRNAs. Each miRNA is contained within a stem-loop structure roughly 70 nt in size. Pri-miRNAs have the same characteristics as mRNAs: the presence of a cap structure at their 5'-end and of a poly(A) tail at their 3'-end. It is believed that these determinants ensure pri-miRNAs stability and also serve as quality control signals. pri-miRNA production is followed by processing in the nucleus by an RNAse III-like endonuclease called Drosha. Processing of pri-miRNA results in a 60 nucleotide-long pre-miRNA. This precursor still adopts a hairpin structure, but now lacks a 5' cap and a poly(A) extensions. Pre-miRNAs have a two-nucleotide overhang at their 3' ends and a 5' phosphate group, which are indicative of their production by an RNase III-like enzyme. In flies, mammals, and worms another source of pre-miRNAs has been described. Indeed, pre-miRNAs can result from pre-mRNA splicing events. These pre-miRNA-like introns, or pre-mitrons, are spliced from mRNA precursors. Debranching of lariat structures resulting from a normal splicing event yields pre-miRNAs that have no specific characteristic beside their peculiar history. Pre-miRNAs are then exported from the nucleus to the cytoplasm by a standard RNA export pathway that requires GTP-dependent exportins.

In the cytoplasm another enzyme of the RNase III family, called Dicer, cleaves pre-miRNAs. This cleavage event generates a duplex, called miRNA-miRNA*, corresponding to a part of the two strands of previously existing stem-loop. One of these strand will be true miRNA, called the guide strand, and the other, the passenger strand, will ultimately be degraded. This functional asymmetry depends on the thermodynamic stability of the base pairs at the two ends of the duplex: the miRNA strand with the less stable base pair at its 5´ end in the duplex is kept as the guide miRNA. Mature miRNAs are 20-22 nucleotide-long RNAs with a 5'-phosphate and a 3'-OH terminus. Finally, miRNA is loaded onto the effector Ago protein, thus generating the RNA-induced silencing complex RISC (Figure 31).

Importantly, this brief description is a simplified model of a generally more complex process. Indeed, pri-miRNA transcripts can be post-transcriptionally modified by ADARs (adenine deaminases acting on RNA), leading, in some cases, to adenosine conversion into to inosine. Such changes may increase the pool of targeted mRNAs, because inosine normally base pairs with cytosine, as does guanosine.

The effector factors of the RISC complex are the Ago proteins loaded with miRNAs. They mediate mRNA targeted translation repression and mRNA degradation. Importantly, in flies two Ago proteins exist: Ago1 and Ago2. miRNAs with full complementarity to the passenger strand are loaded onto Ago2-RISC, which harbours endonuclease activity. This RISC complex cleaves mRNA as when associated with siRNA. miRNAs with partial complementarity to the passenger strand are loaded onto Ago1-RISC, resulting in the miRNA effector complex, which represses mRNA with the help of the basic mRNA degradation machinery. The mechanism explaining the sorting of the different miRNA-miRNA* duplexes according to their complementarity in mammals remains to be deciphered (Winter et al. 2009).

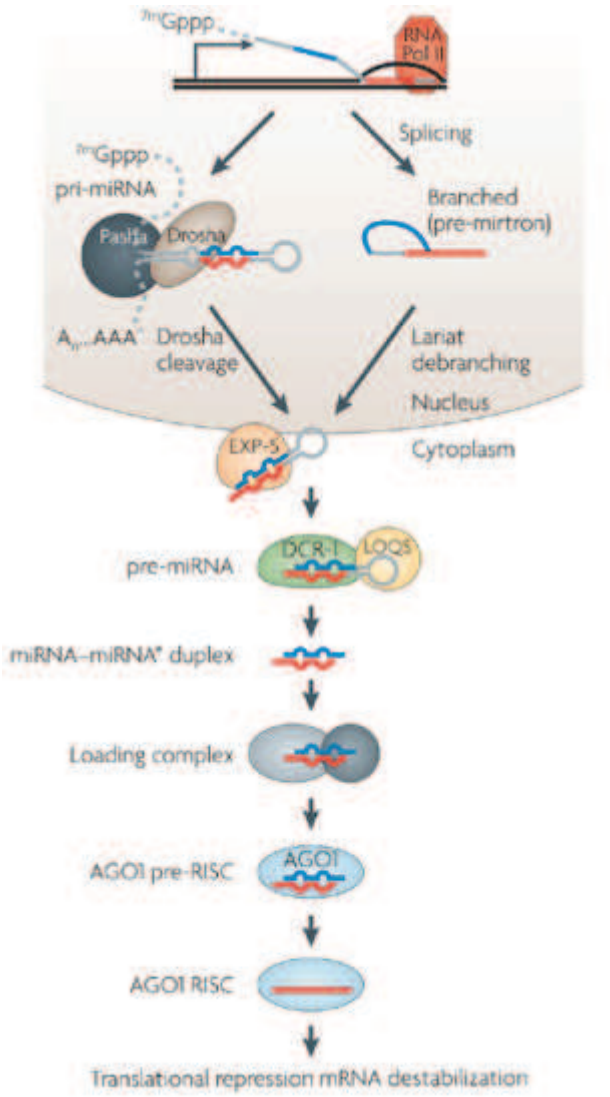

Figure 31. miRNA maturation process. A Description of the important steps is in the main text (Ghildiyal and Zamore 2009).

An important question is to understand how the miRNA-RISC assembly affects mRNA translation repression and degradation? Recently, it became evident, that miRISC interacts with the general CCR4-NOT deadenylation complex with the help of additional protein factors. These observations help explain how miRISC mediates both repressive activities.

1.4.1.8.2 Molecular function of the mammalian CCR4-NOT complex in miRISC mediated mRNA repression

Structurally the mammalian CCR4-NOT complex distinguishes itself from its yeast homologue by the presence of several additional subunits, such as CNOT10 and CNOT11, and the absence of others, such as Caf130 and Not4. Functionally the mammalian CCR4-NOT complex is involved in more pathways of gene expression repression. This includes pathways directed by miRNAs. This requires additional factors to associate with the CCR4-NOT complex.

Recently it became clear, that miRNA repression is achieved by two mechanistically seperate events: translational repression and deadenylation of the target mRNA. I will firstly describe and discuss the deadenylation step and then present the molecular basis for translation repression (Djuranovic et al. 2012; Bazzini et al. 2012).

To become repressed the target mRNA needs first to be recognized by the miRISC complex. This usually occur by interactions of the miRISC complex with sequences complementary to the miRNA which are generally located in the 3'-UTR of the target mRNA. Interaction of the first 2-7 nucleotides from the 5'-end of the miRNA, called the "seed" sequence, is usually sufficient to trigger mRNA silencing. The fact that the miRNA and the mRNA do not display a perfect complementarity is important for two reasons:

1) The requirement for a partial complementarity greatly increases the number of mRNAs that can be targeted by a given miRNA;

2) This feature also prevent cleavage of the target mRNA by Ago proteins. The presence of a bulge between nucleotides 9-12 is particularly important in such cases.

Once the RISC complex is bound to its target mRNA, its Ago subunit can recruit GW-repeat proteins that will establish a link with repression complexes. GW-repeat proteins, named

TNRC6 in human and TNRC6 and GW182 in *drosophila*, contain two well-defined functional domains: an N-terminal Ago-binding domain and a C-terminal domain required for silencing. Within the silencing domain interaction surfaces for two deadenylase complexes, the CCR4-NOT and the Pan2-Pan3 complexes, have been described (Braun et al. 2011). Analysis of the Pan2-Pan3 complex revealed that the stimulatory Pan3 subunit is present in two copies, and that its dimerization forms a W-repeat binding pocket, required for direct interaction with the GW-protein. In the CCR4-NOT complex, the CNOT9 protein is responsible for binding to the GW-repeat proteins, ensuring the recruitment of the main deadenylase to the target mRNA (Y. Chen et al. 2014). Thus, the GW182 protein is able to stimulate the rapid and efficient deadenylation of the substrate RNA by using the two catalytic activities of the CCR4-NOT and/or the Pan2-Pan3 complexes. However, many Interesting questions remain to be answered. Thus, it is unclear whether a single GW-protein can recruit both deadenylases or whether two GW-proteins are required to attract these two complexes. One can also wonder whether these two deadenylation events always occur for each mRNA and if so whether they are temporally resolved, or if they can happen in a non-defined order. It would also be interesting to know if the CCR4-NOT and the Pan2-Pan3 complexes compete for binding with a GW-repeat protein.

Recruitment of the CCR4-NOT complex also provides a mean to mediate translational repression. This process involves the central domain of the Not1 subunit . As is presented above, this region adopts a MIF4G-fold. Such a domain is present in the eIF4G translation initiation factor and was shown to interact with the eIF4A helicase. The MIF4G-fold present in Not1 and CNOT1 shares conserved residues with eIF4G at the location of the eIF4G-eIF4A interface. This suggests that it could interact similarly with an RNA helicase. This putative Not1-associated helicase was identified as the DEAD-box ATPase DDX6, the human orthologue of the yeast Dhh1 helicase, which was known to have a repressive effect on translation (Figure 32). Structure-based mutations showed that the CNOT1 MIF4G-DDX6 interaction is important for miRNA-mediated translational repression, as disruption of the interaction resulted in a decreased repression activity on a luciferase reporter. CNOT1 also has a stimulatory effect on the DDX6 ATPase activity, which is most likely required to reach full translation repression *in vivo* (Chen et al. 2014; Mathys et al. 2014).

Analysis of the translation step being affected by miRNA revealed that both initiation and elongation were impacted in different systems. Thus, in worms, several miRNA were detected in polysomes, suggesting that repression happens at a post-initiation step. Further support came from the observation that these miRNAs can repress IRES-initiated translation which bypasses the requirement for a cap structure. In parallel to these observations, studies using cell-free extracts revealed that miRNAs act mostly by repressing translation initiation (Mathonnet et al. 2007). Thus, miRNAs silenced mRNAs containing a m^7Gppp cap but not transcripts harbouring an artificial Appp-terminal structure. Additional data argues that miRNAs most probably interfere with the function of the eIF4F complex by modulating the interaction of inhibitory eIF4E-binding proteins (Igreja and Izaurralde 2011; Mathonnet et al. 2007; Pillai et al. 2005).

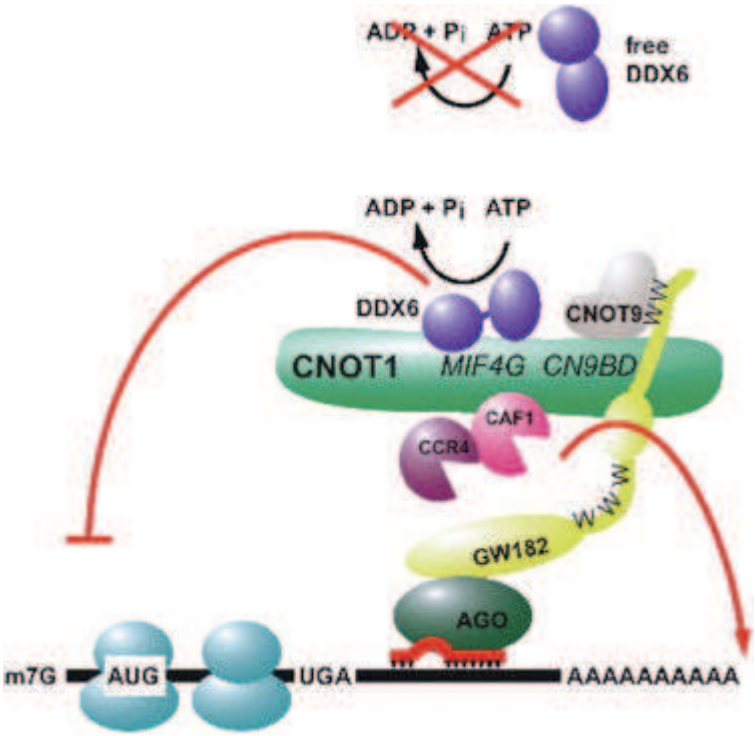

Figure 32. Model of miRNA mediated mRNA repression. Two activities performed by CCR4-NOT complex: translation repression by its DDX6 component (Dhh1 yeast orthologue) and deadenylation activity by the Ccr4 and Caf1 subunits (Mathys et al. 2014).

1.4.1.8.3 Pum1 and Pum2 pumilio proteins: cooperative mechanism for miRNA-mediated repression.

Pum1 and Pum2 are two human orthologues of the yeast Puf proteins. As their yeast counterparts, both proteins bind to specific motif, named the pumilio response element (PRE). PREs are most often located within the mRNA 3'-UTR and Pumilio proteins repress the expression of target mRNAs. Interestingly, studies on the p27 mRNA revealed a crosstalk between pumilio and miRNA-mediated mRNA repression. The p27 mRNA encodes a tumour suppressor factor with cyclin-dependent kinase inhibitory activity: p27 is highly expressed in quiescent cells, while its expression is inhibited in cycling cells. Expression of p27 is regulated by Pum1 and miRNA-221/222 (Figure 33). Interestingly, the Pum1 and miRNA-221/222 binding sites form a stem-loop structure. Moreover during the transition from quiescent to growing state, Pum1 becomes highly expressed and phosphorylated. The latter modification indirectly affects the ability of Pum1 to bind to target mRNAs. The loading of Pum1 onto its binding site unwinds the stem-loop structures allowing the miRISC complex loaded with miRNA-221/222 access to its target site which represses p27 expression. Altogether, by stimulating miRNA-221/222 loading, Pum1 indirectly reduces p27 expression and allows cells to transit from the quiescent to the cycling state (Kedde et al. 2010; Triboulet and Gregory 2010). Interestingly, a similar cooperation between pumilio proteins and miRNA was described in worms for the let-7 miRNA, suggesting an evolutionary conservation of this mechanism (Nolde et al. 2007).

Computational and genome-wide studies have revealed that this Pum-miRISC cooperation might be a fairly general phenomena (Jiang et al. 2013; Incarnato et al. 2013; Galgano et al. 2008). Indeed, genome-wide studies observed high level of co-occurrence of Pum binding sites with miRNA binding sites, while computational work predicts that these sites are present in ordered mRNA secondary structure (Incarnato et al. 2013; Jiang et al. 2013).

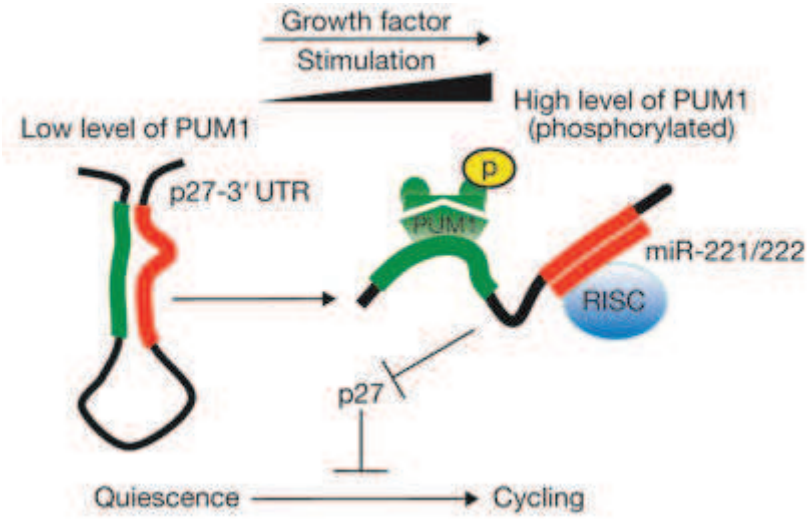

Figure 33. Pum1 controls access of miRISC to the p27 mRNA 3'-UTR by unfolding a stem-loop structure (Kedde et al. 2010).

Further mechanistic studies in worms and human cells revealed the presence of Pum-Ago-eEF1A complexes by both co-immunoprecipitation and recombinant protein binding assays. This complex was shown to block translation elongation by inhibiting the GTPase activityof the elongation factor eEF1A *in vitro*. Under these conditions, ribosome accumulation upon the open reading frame of reporter mRNAs was detected (Friend et al. 2012).

Altogether, these findings directly implicated Pum factors in translation repression and provided a molecular base for a miRISC and Pumilio crosstalk..

1.4.1.8.4 Association of the mammalian RNA decay regulators TTP and Roquin with the CCR4-NOT complex

Tumour necrosis factor-α (TNF-α) is one of the central cytokines involved in the proinflammatory response. The local production of TNF-α at sites of injury or infection is important in triggering an immune response, yet its systemic or chronic release has detrimental consequences by causing septic shock and chronic inflammatory diseases. Expression of TNF-α is highly regulated at the level of mRNA stability. TNF-α mRNA contains several sequence elements which are required for mRNA stability control. One of them is a AU-rich element (ARE) which is required for rapid mRNA translation suppression and mRNA decay. It is recognized by the Zn-finger of the ARE-binding protein Tristetraprolin (TTP),

which promotes mRNA degradation by recruiting the CCR4-NOT complex (Figure 34). A recent crystal structure of a TTP peptide interacting with a fragment of CNOT1 revealed the structural basis of this ARE-mediated mRNA decay. Mutations disrupting this interaction stabilize the TNF-α mRNA stabilization by slowing its deadenylation step (Fabian et al. 2013).

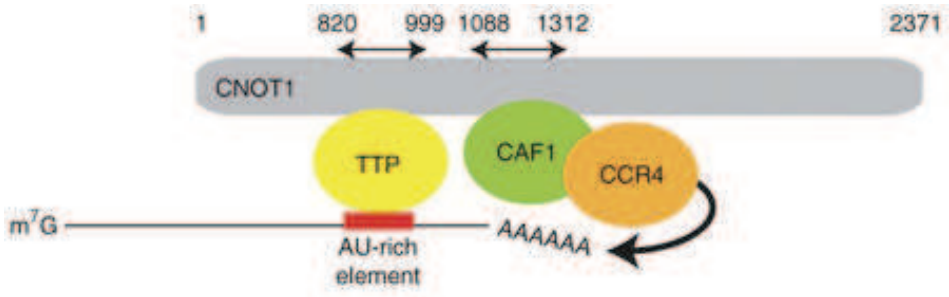

Figure 34. TTP stimulate target mRNA decay by recruiting the CCR4-NOT complex. (Fabian et al. 2013).

Interestingly, the same TNF-α mRNA contains an additional element which also regulates its stability (Stoecklin et al. 2003). This element was identified in conditions where ARE-mediated degradation was blocked. (Macrophage stimulation in a cell line deficient in TTP resulted in transiently inhibited ARE-mediated decay.) In these conditions the TNF-α mRNA was still rapidly degraded. A second element called the constitutive decay element (CDE) was identified and mapped to a 80 nucleotide-long mRNA segment downstream of the ARE. It was proposed that the CDE represses TNF-α expression by ensuring that the mRNA is short-lived, thereby preventing excessive induction of TNF-α after macrophage stimulation.

Recently, the CDE element was determined to be a conserved stem-loop structure, actively folded in the 3'-UTR of the TNF-α mRNA. It was shown that two RNA-binding proteins, called Roquin1/2, are the binding partners for this stem-loop structure. Furthermore these factors were shown to trigger the rapid decay of the TNF-α mRNA by recruiting the CCR4-NOT complex. These proteins contain an N-terminal ROQ domain, required for binding to the stem, and an unstructured C-terminal domain essential for binding to CNOT1 and CAF1 (Figure 35). Supporting evidence for this mechanism comes from experiments where either disruption of the CDE stem-loop structure by a specific morpholino, or deletion of Roquin1/2 interaction domains with the stem, or inactivation of the CCR4-NOT complex resulted in a strong stabilization of the TNF-α mRNA (Leppek et al. 2013; Stoecklin et al. 2003).

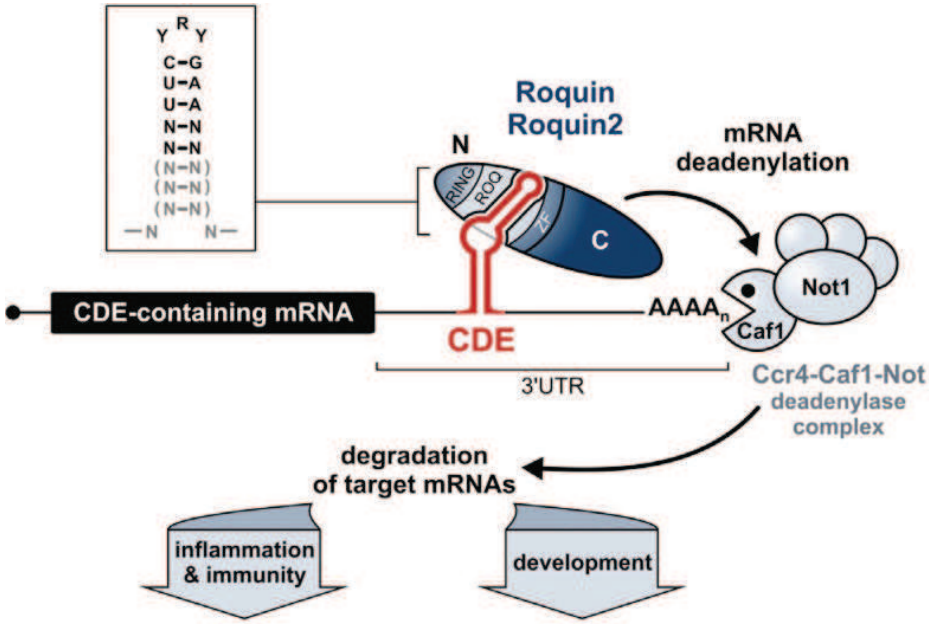

Figure 35. Roquin mediated TNF-α mRNA degradation requires a conserved RNA stem-loop structure in the TNF-α mRNA 3'-UTR and the CCR4-NOT complex (Leppek et al. 2013).

1.4.1.8.5 The CCR4-NOT complex: a master regulator of the posttranscriptional fate of mRNA

Our ever increasingknowledge about CCR4-NOT structure and function provides growing evidence for its importance in cell physiology, embryonic development, immune response, neuron function, and yeast homoeostasis. Multiple roles in mRNA regulation and mRNA quality control have been proposed, either through mRNA decay regulation or through mRNA translation repression. These functional steps require many additional factors that often bind transiently to the CCR4-NOT complex core. The CCR4-NOT complex is thus at the heart of an extensive protein-protein interaction network of which it is a major effector. These facts make it important to understand the structural organization of this complex, the function of its subunits and associated proteins, and the mechanisms by which it affects mRNA translation and decay.

Below, I would like to briefly outline my PhD project objectives and, in particular, the questions that I addressed to understand function of the CCR4-NOT complex in the yeast *S. cerevisiae*.

1.5 Project outline

During my PhD work I studied the function of the CCR4-Not complex of the yeast *S. cerevisiae*. I addressed several questions related to this assembly. The first part of my work was to decipher the role of protein-protein interactions occurring within the CCR4-Not complex in relation to deadenylation *in vivo*. These functional studies were based on the determination of the structure of CCR4-NOT subcomplexes by our collaborators. I also addressed the nature of the essential function of Not1 and the question of structural heterogeneity of subunit composition in the yeast complex. Finally, I analysed the mechanism of translation repression by the CCR4-NOT complex and the mechanism of its targeting to mRNAs by the Puf3 RNA-binding protein

1.5.1 Structural and functional characterization of CCR4-NOT complex

When I started working on this project, very limited information on the structural organization of the CCR4-NOT complex was available. Several models of complex composition had been proposed based on *in vivo* and *in vitro* binding assays. The importance of each subunit of the complex in deadenylation was also poorly defined. In collaboration with the lab of Elena Conti, the structure of two yeast subcomplexes were solved, namely fragments of Not1-Caf1-Ccr4 and a fragment of Not1 with Not2 and the N-terminus of Not5. Based on this structural information I performed functional characterization of the interaction between these subunits. In particularly, I asked:

- Are interactions between Not1-Caf1, Caf1-Ccr4, or within Not module, important for deadenylation *in vivo*?
- Are interactions within these modules physiologically important and required for cell growth?

1.5.2 Not1 essential function and structural heterogeneity of the CCR4-NOT complex *in vivo*

- It is surprising that Not1 is the only essential subunit of the CCR4-NOT complex. Therefore, I tried to uncover why. By protein deletion analysis, I tried to determine the minimal Not1 sequence required to perform its essential function.

- In parallel, due to the paralogous nature of the Not3 and Not5 subunits that are found in yeast but not in mammals, I tried to understand whether the CCR4-NOT complex has a unique protein composition or whether it is an heterogeneous assembly.

1.5.3 Mechanism of action of the CCR4-NOT complex: translation repression and recruitment by the Puf3 protein

mRNA decay is associated with the exit of the target mRNA from active translation. Therefore the translation repression mechanisms may be intimately linked to mRNA decay. The structure of the Not1-Caf1-Ccr4 interaction module suggested a possible mechanism for translation repression by the CCR4-NOT complex. Genetic suppression screens that I performed also identified several candidate proteins mediating translation repression as functional partner of the CCR4-NOT complex. Based on these observations, I hypothesize the existence of a Not1-specific helicase partner responsible for the translational repression of the complex. I performed binding assays with several putative partners and also developed a tethering luciferase-based assay to quantitatively measure translation repression activities and assayed the effect of different CCR4-NOT complex subunits on the reporter construct.

Genome-wide analyses of mRNA expression revealed a significant enrichment of mRNAS targeted by the Puf3 factors in transcripts affected in CCR4-NOT mutant strains. To understand the molecular basis of this effect, I performed binding studies between the Puf3 protein and the CCR4-NOT complex in different conditions. This project gave interesting preliminary results that will need to be investigated more thoroughly in the future.

The results of my work are presented in the following sections and include two papers published in Molecular Cell in 2012, and Nature Structural and Molecular Biology in 2013 and of which I am a co-author.

2. Results

2.1 Study of the CCR4-NOT deadenylation complex function

2.1.1 Structural and functional characterization of the CCR4-NOT complex

In eukaryotes, mRNA deadenylation is catalysed predominantly by the Pan2-Pan3 and CCR4-NOT complexes. The deadenylation step is the first step of mRNA decay that is also a reversible reaction as cytoplasmic polyadenylation enzymes can re-extend the poly(A) tail. As deadenylation is usually rate-limiting for mRNA degradation, it is a highly regulated step that is targeted by multiple stimulators and repressors. Many regulators of mRNA decay were described as binding to the CCR4-NOT complex. These include:

- miRNA that recruit the CCR4-NOT complex to target mRNAs through GW182 family members;
- RNA decay stimulated by a variety of RNA-binding proteins such as Pumilio family members, TTP, and Roquin1/2.

There is therefore a growing need to understand the global organization and function of CCR4-NOT as well as a detailed knowledge of the structure of each subunit of the complex. Based on this observation, we undertook a structure-function analysis of CCR4-NOT subcomplexes, namely fragments of Ccr4-Caf1-Not1 and fragments of Not5-Not1 with Not2. Our collaborators Dr. J. Basquin and Dr. E. Conti obtained high-resolution crystal structures of these two modules. To understand the biological function of these protein-protein interactions, I designed and constructed point mutants specifically disrupting these molecular interfaces. In the case of the Ccr4-Caf1-Not1 subcomplex, which demonstrated structurally how Caf1 bridges Ccr4 and Not1, I prepared:

- Ccr4 substitution mutants disrupting interaction with Caf1;
- Caf1 substitution mutants disrupting interactions with either with Ccr4 or Not1;
- Not1 substitution mutants disrupting interactions with Caf1.

In the structure-function study of the Not1-Not2-Not5 subcomplex, which revealed that each protein contacts the two other subunits, I was confronted with a problem, however, given the difficulty in analysing phenotypes resulting from Not5 mutation. As Not3 was hypothesized to adopt a structure similar to Not5 and the *not3* mutant produce a scorable phenotype, Not3 was used as a surrogate model of Not5. Therefore, I constructed:

- Not1 mutants disrupting interactions with either Not2 or Not3/5, as well as a double mutant, disrupting both interaction interfaces;

- Not2 mutants disrupting interactions with either Not1 or Not3/5, as well as a double mutant, disrupting both interaction interfaces;

- Not3 mutants disrupting putative interactions with either Not1 or Not2, as well as a double mutant, disrupting both interaction interfaces.

These mutants were assayed in cell growth assays revealing the functional importance of interaction interfaces internal to the CCR4-NOT complex. The impact of these mutations on mRNA decay regulation was also investigated by performing deadenylation assays and half-life measurements *in vivo*. Hence, we observed the importance of the association of the Ccr4-Caf1 proteins with Not1 for mRNA deadenylation . In contrast the Not-module (composed of Not2 and Not3/5 subunits bound to the C-terminal region of Not1) is dispensable for mRNA deadenylation or, if it has a role in this process, it is restricted to specific transcripts.

The work performed along these lines and our conclusions are described in the two attached manuscripts:

- Basquin J*, Vladimir V. Roudko*, Michaela Rode, Claire Basquin, Bertrand Seraphin, and Elena Conti. 2012. “Architecture of the Nuclease Module of the Yeast CCR4-NOT Complex: The Not1-Caf1-Ccr4 Interaction.” *Molecular Cell* 48 (2): 207–18. ** these authors contribute equally to the work.*
- Bhaskar, Varun, Vladimir Roudko, Jérôme Basquin, Kundan Sharma, Henning Urlaub, Bertrand Séraphin, and Elena Conti. 2013. “Structure and RNA-Binding Properties of the Not1-Not2-Not5 Module of the Yeast CCR4-NOT Complex.” *Nature Structural & Molecular Biology* 20 (11): 1281–88.

Molecular Cell
Article

Architecture of the Nuclease Module of the Yeast Ccr4-Not Complex: the Not1-Caf1-Ccr4 Interaction

Jérôme Basquin,[1,3] Vladimir V. Roudko,[2,3] Michaela Rode,[1] Claire Basquin,[1] Bertrand Séraphin,[2] and Elena Conti[1,*]
[1]Department of Structural Cell Biology, Max Planck Institute of Biochemistry, Am Klopferspitz 18, 82152 Martinsried, Germany
[2]Equipe Labellisée La Ligue, Institut de Génétique et de Biologie Moléculaire et Cellulaire (IGBMC), Institut National de Santé et de Recherche Médicale (INSERM) U964/Centre National de Recherche Scientifique (CNRS) UMR 7104/Université de Strasbourg, 67404 Illkirch, France
[3]These authors contributed equally to this work
*Correspondence: conti@biochem.mpg.de
http://dx.doi.org/10.1016/j.molcel.2012.08.014

SUMMARY

Shortening eukaryotic poly(A) tails represses mRNA translation and induces mRNA turnover. The major cytoplasmic deadenylase, the Ccr4-Not complex, is a conserved multisubunit assembly. Ccr4-Not is organized around Not1, a large scaffold protein that recruits two 3′-5′ exoribonucleases, Caf1 and Ccr4. We report structural studies showing that the N-terminal arm of yeast Not1 has a HEAT-repeat structure with domains related to the MIF4G fold. A MIF4G domain positioned centrally within the Not1 protein recognizes Caf1, which in turn binds the LRR domain of Ccr4 and tethers the Ccr4 nuclease domain. The interactions that form the nuclease core of the Ccr4-Not complex are evolutionarily conserved. Their specific disruption affects cell growth and mRNA deadenylation and decay in vivo in yeast. Thus, the N-terminal arm of Not1 forms an extended platform reminiscent of scaffolding proteins like eIF4G and CBP80, and places the two nucleases in a pivotal position within the Ccr4-Not complex.

INTRODUCTION

Since the discovery of the poly(A) tail over 40 years ago, a wealth of functional information has accumulated on the major influence it exerts on the posttranscriptional regulation of eukaryotic gene expression (Edmonds et al., 1971; reviewed in Zhang et al., 2010; Eckmann et al., 2011). The poly(A) tail consists of a long stretch of adenosine nucleotides and is coated by multiple poly(A)-binding proteins in the nucleus and in the cytoplasm (Mangus et al., 2003). The resulting structure of the mature messenger ribonucleoprotein particle (mRNP) protects the 3′ extremity of the messenger RNA (mRNA) from exoribonucleolytic degradation, thus increasing mRNA stability (reviewed in Zhang et al., 2010). It also increases translational efficiency by promoting the recruitment of translation initiation factors (Tarun et al., 1997; reviewed in Sonenberg and Dever, 2003). Conversely, poly(A) tail shortening, a process known as deadenylation, is linked to cytoplasmic mRNA decay and to translational repression (Decker and Parker, 1993; reviewed in Goldstrohm and Wickens, 2008; Zhang et al., 2010).

In yeast and mammalian cells, deadenylation begins with the Pan2-Pan3 complex (Boeck et al., 1996; Brown and Sachs, 1998; Yamashita et al., 2005) and continues with the Ccr4-Not complex (Daugeron et al., 2001; Tucker et al., 2001, 2002; Chen et al., 2002). Ccr4-Not is thought to reduce the poly(A) tail to a short oligo(A) tract before the body of the mRNA is degraded by subsequent enzymatic activities (the exosome-Ski complex, the decapping complex, and Xm1) (reviewed in Garneau et al., 2007). The core enzymes and regulators of this pathway are universally conserved throughout eukaryotes. Studies in yeast have shown that neither the Pan2-Pan3 nor the Ccr4-Not deadenylase activities are essential in vivo (Malvar et al., 1992; Boeck et al., 1996; Brown et al., 1996). Synthetic phenotypes observed in double mutants of the deadenylase complexes suggest that they act in a partially redundant manner (Tucker et al., 2001).

While the interplay between Pan2-Pan3 and Ccr4-Not is not fully understood, it is clear that their concerted action is often the rate-limiting step for mRNA decay (Cao and Parker, 2001) and a focal point for regulation. The direct recruitment of Ccr4-Not to specific regulators impacts for example ARE-mediated decay (Sandler et al., 2011), microRNA-mediated gene silencing (Braun et al., 2011; Chekulaeva et al., 2011; Fabian et al., 2011), and translational repression during developmental processes (de Moor et al., 2005). Finally, Ccr4-Not has been proposed to modulate mRNA levels by acting at the transcription level, via interactions with transcription factors (reviewed in Collart and Timmers, 2004) and with the elongating RNA polymerase II (Denis et al., 2001; Kruk et al., 2011). Recently, altered transcription in Ccr4-Not mutants was also shown to arise in compensation of reduced mRNA decay (Sun et al., 2012).

The core subunits of Ccr4-Not were first identified in the early nineties (reviewed in Collart and Timmers, 2004). Biochemical approaches later indicated that these gene products exist in the context of a multiprotein complex with an approximate mass of 1 MDa (Liu et al., 1998; Maillet et al., 2000; Chen et al., 2001). Yeast two-hybrid and coimmunoprecipitation studies suggest that Ccr4-Not is organized around Not1 (also

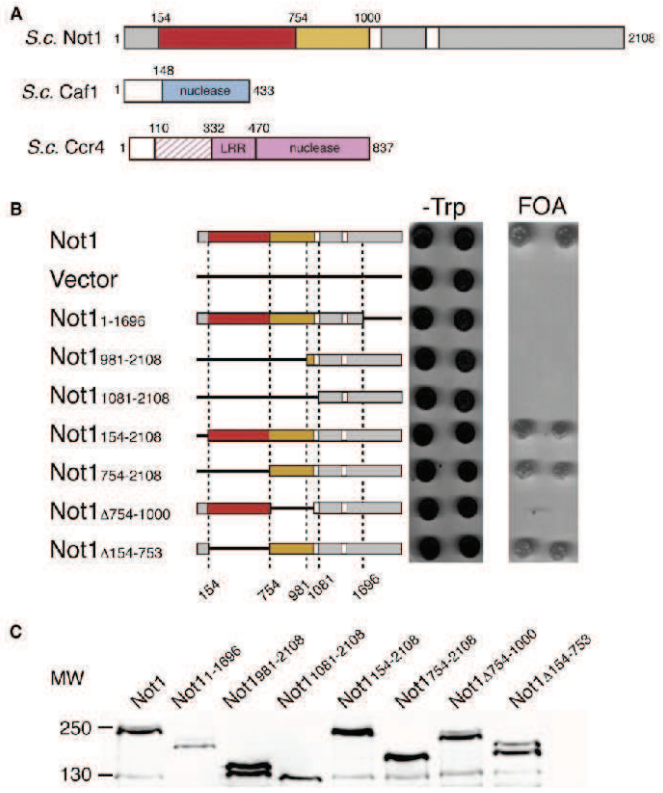

Figure 1. The Caf1-Ccr4-Binding Domain of Not1 Is Essential In Vivo

(A) Schematic representation of the domain arrangement of yeast Not1, Caf1, and Ccr4. The $Not1_{154–753}$ and $Not1_{754–1000}$ domains were identified biochemically (Figure S1) and are shown in red and orange, respectively. Other predicted structured regions in Not1 are colored in gray. The nuclease domain of Caf1 is in blue, and the LRR and nuclease domains of Ccr4 in pink. The N-terminal region of yeast Ccr4 present in the crystal structure reported in this manuscript is shaded in pink. Unstructured regions are in white.

(B) Analysis of the ability of Not1 truncation mutants to complement a Not1 deletion. *TRP1*-marked plasmids encoding different truncations of Not1 (fused to the TAP tag) are schematized on the left. The plasmids were introduced in strain T26N28 carrying a chromosomal deletion of *NOT1* complemented by a wild-type copy of the gene on a *URA3*-marked plasmid. Complementation was assayed by monitoring growth on FOA, growth on –Trp media serving as a control.

(C) Analysis of the levels of Not1 protein accumulating in the wild-type strain and mutants expressing truncated forms of the protein. Total proteins extracted from the various strains were fractionated by SDS-PAGE, transferred to a membrane, and detected through the TAP tag present at the C terminus of the proteins.

See also Figure S1.

known as Cdc39), a 240 kDa protein believed to function as a structural scaffold (Collart and Timmers, 2004). The N-terminal half of Not1 recruits the two interacting exoribonuclease subunits Caf1 (also known as Pop2 in yeast) and Ccr4, forming the "nuclease module" of the complex (Dupressoir et al., 2001; Draper et al., 1995; Bai et al., 1999). The C-terminal half of Not1 interacts with Not2, Not3, Not5, and Not4, forming the so-called "Not module" (Bai et al., 1999; Deluen et al., 2002). The overall architecture of the Ccr4-Not complex is likely conserved in humans, *Drosophila*, and trypanosomes, although the complexity of the interactions and the interplay of the nuclease activities differ (Albert et al., 2000; Temme et al., 2004; Schwede et al., 2008; Lau et al., 2009). Perhaps the most striking difference lies in the balance of the nuclease activities: while Ccr4 is the primary deadenylase in yeast (Chen et al., 2002; Tucker et al., 2002), in mammalian cells Caf1 contributes significantly, if not predominantly, to poly(A) tail shortening (Mauxion et al., 2008, Sandler et al., 2011).

Despite the importance of the Ccr4-Not complex, limited structural information is currently available. A negative-stain electron microscopy study of Ccr4-Not revealed an overall L-shape architecture (Nasertorabi et al., 2011) and the crystal structures of the individual nuclease domains of Caf1 and Ccr4 elucidated their different active sites (Thore et al., 2003; Jonstrup et al., 2007; Horiuchi et al., 2009; Wang et al., 2010). However, how the Not1-Caf1-Ccr4 network of interactions is established and how it positions the two exoribonucleases within the complex is unknown. To address these questions, we undertook a structural and functional analysis of the nuclease module of the Ccr4-Not complex.

RESULTS AND DISCUSSION

Domain Organization of the 114 kDa N-Terminal Region of Yeast Not1

S. cerevisiae Not1 is a 2,108 amino acid residue protein (Figure 1A). Yeast two-hybrid experiments previously mapped the interaction of Caf1 and Ccr4 to residues 667–1,152 of Not1 (Bai et al., 1999). To precisely identify the domains present in this portion of Not1, we used a combination of computational and experimental approaches. Sequence analysis and secondary structure predictions indicated the presence of a largely structured region in the first 1,000 residues of Not1, followed by a less-conserved, low-complexity segment. We expressed and purified a construct of yeast Not1 encompassing residues

1–1,000 ($Not1_{1–1000}$), subjected it to limited proteolysis, and identified the domain boundaries of the two largest fragments as corresponding to $Not1_{154–753}$ and $Not1_{754–1000}$ (Figure S1A available online). These proteolytically resistant fragments could be separately expressed and purified to homogeneity (Figure S1A) and did not coelute in size-exclusion chromatography (data not shown). These results indicated that $Not1_{154–753}$ and $Not1_{754–1000}$ are stable and folded as individual domains.

The $Not1_{754–1000}$ Domain Recruits Caf1-Ccr4 and Is Essential for Function in Yeast

Next, we identified the minimal domains required for the formation of a core Not1-Caf1-Ccr4 complex by mixing individually purified components in size-exclusion chromatography experiments (Figure S1B). These experiments were guided by previous coimmunoprecipitation studies showing that Caf1 bridges the interaction between Not1 and Ccr4 (Bai et al., 1999). We found that $Not1_{754–1000}$ was sufficient to form a ternary complex with the nuclease domain of Caf1 (hereafter referred to as Caf1) and with a construct of Ccr4 encompassing part of the N-terminal region, the leucine-rich repeat (LRR) domain and the nuclease domain (residues 110–837, hereafter referred to as Ccr4) (Figures 1A and S1B) (Simón and Séraphin, 2007). The interacting regions of Caf1 and Ccr4 include the functionally important residues that had been previously identified (Bai et al., 1999; Clark et al., 2004).

To delineate precisely the regions of the N-terminal half of Not1 important for function in vivo, we generated plasmids expressing Not1 full-length, Not1 truncation mutants ($Not1_{154–2108}$, $Not1_{754–2108}$, $Not1_{981–2108}$, $Not1_{1081–2108}$), and Not1 deletion mutants ($Not1\Delta_{754–1000}$, $Not1\Delta_{154–753}$) with a C-terminal tandem affinity purification (TAP) tag (Figure 1B). As a control, we generated a plasmid with a C-terminal truncation ($Not1_{1–1696}$) that eliminates an essential portion of Not1 involved in the interaction with Not2/3/5 (of unknown function) and Not4 (a ubiquitinating enzyme) (Maillet et al., 2000; Collart and Timmers, 2004). These plasmids were introduced into a *not1*⊿ haploid strain rescued by a *URA3*-marked *NOT1* plasmid. Growth phenotypes were assayed after counterselection of the *URA3* plasmid on 5-FOA. Wild-type Not1 as well as the $Not1_{154–2108}$ and $Not1_{754–2108}$ truncations complemented the chromosomal *not1* deletion (Figure 1B). In contrast, $Not1_{1081–2108}$ and $Not1_{1–1696}$ did not rescue cell growth on synthetic media (Figure 1B), consistent with the very slow growth reported only in rich media for $Not1_{1319–2108}$ and $Not1_{1151–2108}$ in a different genetic background (Maillet et al., 2000). Strikingly, the larger $Not1\Delta_{154–753}$ deletion was viable while the smaller $Not1\Delta_{754–1000}$ deletion was not (Figure 1B). Western blot detection of the TAP-tag confirmed that these phenotypes did not result from protein instability as all mutants accumulated at wild-type levels or higher (Figure 1C). We concluded that, in addition to the C-terminal region of Not1, the Caf1-Ccr4-binding domain ($Not1_{754–1000}$) is essential for Not1 function.

Overall Structure of the $Not1_{754-1000}$-Caf1-Ccr4 Complex

To determine the structure of the S. *cerevisiae* $Not1_{754-1000}$-Caf1-Ccr4 core complex, we proceeded in a stepwise manner. We first solved the structure of the $Not1_{754–1000}$ domain by iodine-based single anomalous diffraction (SAD) and refined it against a native data set at 1.4 Å resolution to an *R*free of 21.0% (Table 1). We then determined the crystal structure of the $Not1_{754–1000}$-Caf1 binary complex by molecular replacement (using the coordinates of $Not1_{754–1000}$ and of the previously published yeast Caf1 structure [Thore et al., 2003] and refined it at 2.3 Å resolution to an *R*free of 23.8% (Table 1). Finally, we determined the structure of the ternary $Not1_{754–1000}$-Caf1-Ccr4 complex by molecular replacement using the coordinates of $Not1_{754–1000}$-Caf1, followed by iterative rounds of model building and refinement.

The final model of $Not1_{754–1000}$-Caf1-Ccr4 was refined to 3.4 Å resolution with an *R*free of 27.4% and good stereochemistry (Table 1). The crystals contain four independent copies of the complex in the asymmetric unit. For each copy, the model includes Not1 residues 759–991, Caf1 residues 149–428 (with the exception of a disordered loop between 357–369), and Ccr4 residues 135–187 and 242–261 in the N-terminal region and 332–470 in the LRR domain (Figure S2). In two copies of the asymmetric unit, ordered electron density is also present for about half of the Ccr4 nuclease domain (Supplemental Experimental Procedures).

The $Not1_{754–1000}$-Caf1-Ccr4 complex is built by the sequential interaction of a MIF4G (*m*iddle domain of *i*nitiation *f*actor *4G*), nuclease, LRR, and nuclease domains (Figure 2). The relative orientation of the domains within the ternary complex is the same in the different copies of the asymmetric unit (Figure S3A). Below we describe the $Not1_{754–1000}$-Caf1-Ccr4 structure of one of the two copies in the asymmetric unit where the nuclease domain is partially ordered (Figure 2).

The $Not1_{754–1000}$ Domain Has a MIF4G Fold

The $Not1_{754–1000}$ domain contains ten antiparallel α helices (Figure 3A, left panel). The arrangement is characteristic of that observed in HEAT-repeat proteins. HEAT motifs consist of two antiparallel α helices (known as A and B helices) and pack against each other in an almost parallel fashion (Andrade et al., 2001). Database searches for structural similarities to $Not1_{754–1000}$ using the program Dali (Holm and Rosenström, 2010) indeed identified the HEAT-repeat fold of MIF4G (Figure 3A, left panel). The five HEAT repeats of $Not1_{754–1000}$ (residues 782–976) superpose with MIF4G domains of eIF4G (Schütz et al., 2008) and UPF2 (Kadlec et al., 2004) with a root-mean-square deviation (rmsd) of 2.8 Å for more than 70% of all α carbon atoms. In addition, $Not1_{754–1000}$ features two extended segments at the N and C termini (Figure 3A, left panel) that are anchored to the HEAT-repeat core by extensive hydrophobic interactions (Figure S3B), and thus form an integral part of the domain. The entire $Not1_{754–1000}$ domain is essentially unaltered when comparing the structures determined in the absence and presence of Caf1 (rmsd of 0.53 Å over more than 98% of α carbon atoms) (Figure S3C). Analysis of the $Not1_{754–1000}$ structure shows that the concave surface of the MIF4G domain is characterized by a large patch of conserved residues contributed by the B helices of HEAT 1 to 5 (Figure 3A, right panel). A small patch of conserved residues is also present on the opposite surface (Figure 3A, right panel), at the interrepeat loops connecting HEAT 3–4 and HEAT 4–5.

Table 1. Crystallographic Data Collection/Refinement Statistics

Data Set	$Not1_{754-1000}$	$Not1_{754-1000}$ (I SAD)	$Not1_{754-1000}$-Caf1	$Not1_{754-1000}$-Caf1-Ccr4	$Not1_{154-753}$ (Au SAD)
Data Collection					
Beamline	SLS PXII	Xcalibur Nova (CuKα)	SLS PXII	SLS PXII	SLS PXIII
Space group	$P4_12_12$	$P4_12_12$	$P2_12_12_1$	P1	$P2_1$
Unit cell parameters (Å)	a = b = 53.6, c = 187.2	a = b = 53.6, c = 183.5	a = 71.8, b = 76.56, c = 109.9	a = 122.6, b = 122.9, c = 126.4, α = 89.4, β = 89.7, γ = 64.2	a = 55.0, b = 164.5, c = 86.1, β = 100.1°
Wavelength (Å)	1.000	1.540	1.000	1.000	1.0396
Resolution range (Å)[a]	93.6–1.4 (1.48–1.41)	20.3–2.6 (2.74–2.60)	47.7–2.3 (2.42–2.30)	48.2–3.4 (3.6–3.4)	47.7–2.8 (2.95–2.8)
Unique reflections[a]	54,005 (7,437)	8,699 (1,265)	27,615 (3,835)	90,023 (13,150)	36,994 (5,266)
Multiplicity[a]	7.0 (6.9)	42.5 (23.9)	6.0 (5.9)	3.6 (3.7)	4.8 (4.8)
Completeness (%)[a]	99.8 (99.6)	97.3 (98.9)	99.5 (96.5)	98.5 (98.4)	99.5 (97.1)
Anomalous completeness (%)[a]		98.6 (99.1)			97.5 (93.2)
$I/\sigma(I)$[a]	22.2 (2.7)	40.4 (12.6)	15.3 (4.4)	10.0 (2.9)	20.0 (2.6)
R_{sym} (%)[a]	3.7 (59.4)	10.2 (30.0)	8.6 (45.0)	11.2 (51.1)	5.2 (53.0)
Refinement					
R_{work} (%)	19.5		19.0	23.5	23.7
R_{free} (%)	21.0		23.8	27.4	27.3
Rmsd bond (Å)	0.007		0.007	0.014	0.009
Rmsd angle (°)	1.16		1.05	1.64	1.28
Ramachandran values: Favored (%)	98.3		97.3	93.5	96.7
Ramachandran values: Disallowed (%)	0.0		0.0	0.0	0.0

[a]Values in parentheses correspond to the highest-resolution shell.

The Interaction of $Not1_{754-1000}$ with Caf1 Involves Evolutionary Conserved Residues

Caf1 is recognized by the small conserved patch of the $Not1_{754-1000}$ MIF4G domain formed by the interrepeat loops of HEAT 3–4 and HEAT 4–5 (Figures 3A and 3B). The structure of Caf1 has been previously described (Thore et al., 2003; Jonstrup et al., 2007; Horiuchi et al., 2009). In brief, Caf1 has an RNase D fold characteristic of the DEDD superfamily of exoribonucleases. The fold contains a β sheet to a large extent surrounded by α helices, with the exception of a small surface area that forms the active-site cavity (Figure 2A). The active site of *S. cerevisiae* Caf1 has a suboptimal Ser188-Glu190-Asp310-Gln394 (SEDQ) sequence as compared to the canonical DEDD sequence of the *S. pombe* or human orthologs (Thore et al., 2003; Jonstrup et al., 2007; Horiuchi et al., 2009). In the Ccr4-Not complex, Caf1 binds $Not1_{754-1000}$ at the opposite side of the molecule with respect to the active-site pocket (Figure 2A).

The interaction between Caf1 and $Not1_{754-1000}$ is mediated by conserved hydrophobic residues, in particular by Met290, Met296, and Trp333 in Caf1 and Pro897, Phe938, Pro943, and Trp944 in Not1 (Figure 3B). Overall, the $Not1_{754-1000}$-Caf1 interface buries only 8.4% of the total accessible solvent area (230 $Å^2$ for Caf1 and 420 $Å^2$ for Not1), leaving the large conserved patch on the concave surface of $Not1_{754-1000}$ exposed to solvent and accessible (Figure 2B, right panel). The active-site pocket of Caf1 is also solvent exposed in the ternary complex, since the binding of the Ccr4 LRR domain occurs at an adjacent and nonoverlapping surface (Figure 2B, right panel, and Figure S3C).

The Interaction of Caf1 with the LRR Domain of Ccr4 Forms a Contiguous Hydrophobic Core

The LRR domain of Ccr4 contains five leucine-rich repeats (Figure 2A, right panel). The repeats assemble side by side to form a crescent-shape structure, with the outer convex surface formed by α helices and the concave surface formed by parallel β strands. The concave surface of LRR domains is often the site of intermolecular interactions (Bella et al., 2008). In yeast Ccr4, the concave surface of the LRR domain interacts intramolecularly with the helices of the N-terminal region (Figure 2A). The 70 amino acid linker (residues 262–331) that connects the N-terminal region to the LRR domain is disordered. The ordered part of the N-terminal region buries the hydrophobic β sheet surface of the LRR domain (lined by Tyr363, Val384, Tyr407, Tyr409, Phe411, and Phe430). The structural analysis thus suggests that the N-terminal region and the LRR domain in yeast Ccr4 form a single structural unit. In vertebrates, Ccr4 lacks the N-terminal region (Figure S2), and the concave surface of the LRR domain is instead polar in nature.

The LRR domain of Ccr4 includes two helices that shield the leucine residues of the fifth repeat and lead directly into the

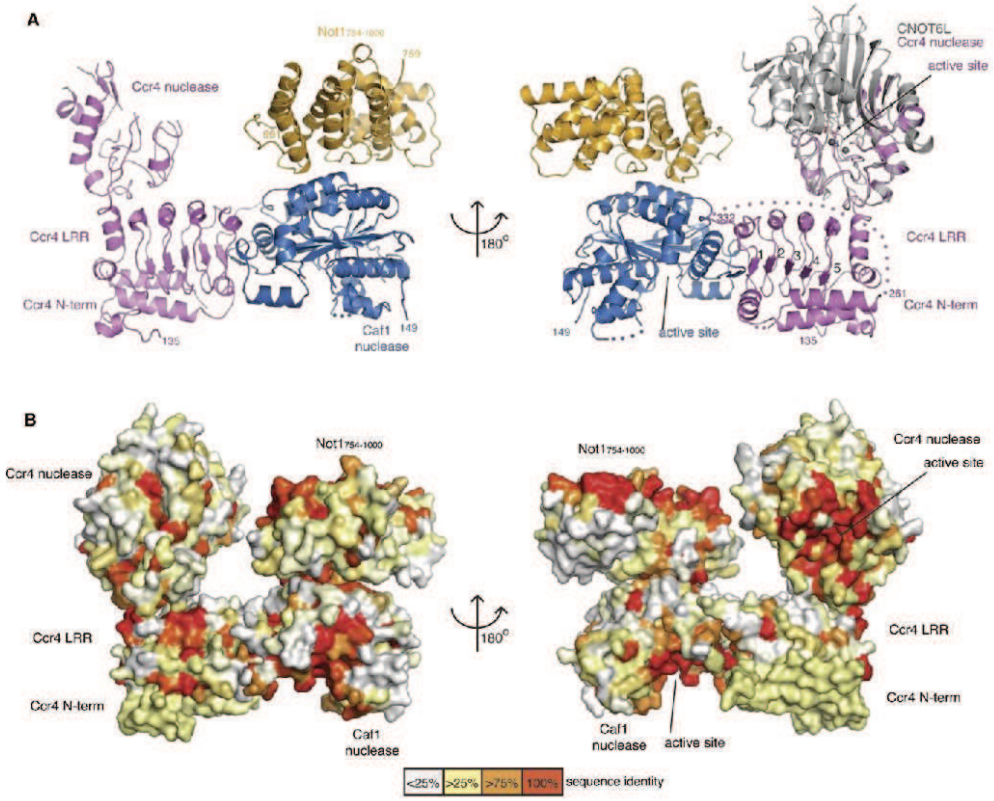

Figure 2. Structure of the Not1$_{754-1000}$-Caf1-Ccr4 Complex

(A) The complex is shown in two different orientations related by a 180° rotation around a vertical axis. Not1 is in orange, Caf1 in blue, and Ccr4 in pink. On the right, the complex is shown superposed to the structure of the nuclease domain of the human Ccr4 ortholog CNOT6L (in gray, PDB 3NGQ). The five LRR motifs and the N and C termini are labeled. Disordered loops are indicated with a dotted line. Residues at the active sites of Caf1 and Ccr4 are shown in stick representation. All structure figures in this manuscript were generated with Pymol (http://www.pymol.org/).

(B) Surface representation of the complex in similar orientations as in (A) and including the superposed CNOT6L nuclease domain. The surface is colored according to sequence conservation, ranging from white (variable residues) to dark orange (invariant residues). The conservation was mapped with the program Consurf (Ashkenazy et al., 2010) based on the alignment in Figure S2.

See also Figure S2.

Ccr4 nuclease domain (Figure 2A). It however lacks an analogous flanking region at the first repeat. The hydrophobic core of the first repeat is shielded intermolecularly by Caf1. Caf1 interacts with Ccr4 via a surface formed by a long loop (residues 193–206) and an α helix (residues 207–219) (Figure 3C). This region of Caf1 undergoes a localized conformational change as compared to the unbound Caf1 structure (Figure S3C). Caf1 residues 197–199 form a β strand that effectively extends the Ccr4 β sheet. The hydrophobic residues of the first LRR repeat (Leu339 and Leu341) contact nonpolar side chains of Caf1 (Ala215 and Phe219) (Figure 3C). The residues involved in the Caf1-Ccr4 interaction are conserved from fungi to animals (Figure S2), and the interaction surface is consistent with previous mutagenesis studies (Clark et al., 2004; Ohn et al., 2007).

The Nuclease Domain of Ccr4 Is Adjacent to the LRR Domain

Structural studies had shown that the catalytic domain of human CNOT6L, the ortholog of yeast Ccr4, belongs to the endonuclease-exonuclease-phosphatase (EEP) protein family (Wang et al., 2010). The fold is organized into two β sheets that face each other and are sandwiched between two outer layers of

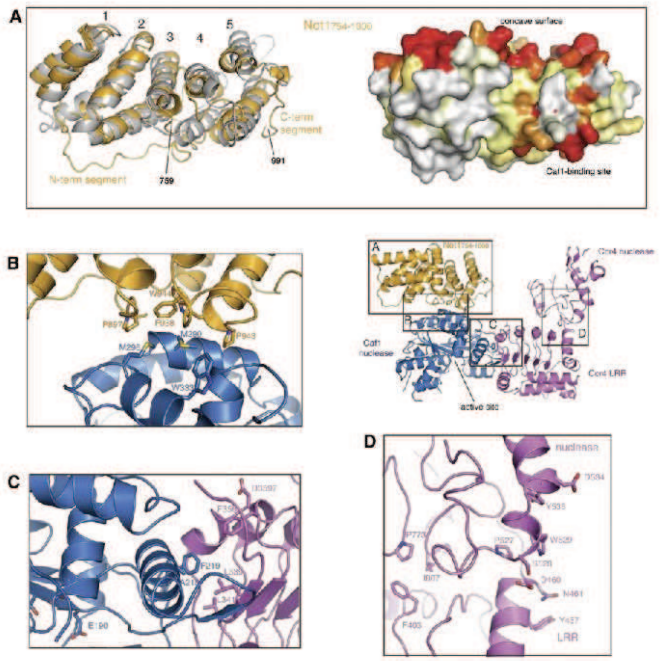

Figure 3. The Interactions in Not1$_{754–1000}$-Caf1-Ccr4 Are Conserved

The figure shows four enlarged regions of the complex discussed in the text.

(A) On the left, the crystal structure of the Not1$_{754–1000}$ domain is shown in orange superposed to a MIF4G domain of UPF2 (Kadlec et al., 2004, in gray). The five HEAT repeats are labeled and the N- and C-terminal segments are indicated. On the right, Not1$_{754–1000}$ is shown in the same orientation as a surface representation colored according to sequence conservation, ranging from white (variable) to dark orange (conserved), as described for Figure 2B.

(B) Zoom-in showing a subset of residues in stick representation at the Not1-Caf1 interface. Residues mutated in the functional assays in Figure 4 are indicated.

(C) Zoom-in showing a subset of residues in stick representation at the Caf1-Ccr4 interface. Residues mutated in the functional assays in Figure 4 are labeled. Also shown are residues reported in previous mutagenesis studies (Asp357, Phe358) (Clark et al., 2004) and residues at the Caf1 active site (Glu190, etc.).

(D) Zoom-in of the LRR-nuclease interaction of Ccr4. Hydrophobic residues at the interface are indicated, as well as conserved residues exposed on the surface.

See also Figure S3.

helices, forming a prominent active-site pocket (Figure 2, right panels). In two molecules of the asymmetric unit of the Not1$_{754–1000}$-Caf1-Ccr4 crystals, the helices in one half of the Ccr4 nuclease interact with the LRR domain, while the other half is disordered. The ordered part of the nuclease domain in the yeast structure has the same conformation as the corresponding part of human CNOT6L (rmsd of 1.1 Å upon superposition of 105 α carbon atoms) (Figure 2A, right panel).

The interaction between the LRR and nuclease domains of Ccr4 buries a surface of about 400 Å^2. The interface features hydrophobic contacts (between Phe403 from the β sheet surface of the LRR domain and Pro773 from the nuclease domain) and polar contacts (between Asp460 from the C-terminal helix of the LRR and Ser528 from the nuclease) (Figure 3D). Although the intramolecular interactions in Ccr4 appear to be weak and stabilized by lattice contacts, they are generally conserved (Figure S2) and create a continuous patch of evolutionary conserved solvent-exposed residues (Tyr457 and Asn461 from the LRR domain and Trp529, Asp534, and Tyr535 from the nuclease domain) (Figures 3D and S2). Moreover, an intramolecular contact between the nuclease domain and the LRR region had also been suggested by yeast two-hybrid studies (Clark et al., 2004). The relative arrangement of the two domains in Ccr4 results in an L-shape conformation, reminiscent of the central region in the L-shaped negative-stain EM structure of the Ccr4-Not complex (Nasertorabi et al., 2011).

Structure-Based Mutations Specifically Disrupt the Not1-Caf1 and the Caf1-Ccr4 Interfaces

Mutations based on the structural analysis were designed to specifically disrupt the interactions between Not1, Caf1, and Ccr4. To impair the Not1$_{754–1000}$-Caf1 interface, we engineered a M290K, M296K double substitution in Caf1 (Caf1-290/296 mutant) and a F938E, P943Y substitution in Not1 (Not1-938/943 mutant). In coimmunoprecipitation experiments using tagged Caf1, Ccr4, and Not1 proteins, the Caf1-290/296 mutant disrupted the interaction with Not1 and did not affect the Caf1-Ccr4 interaction (Figure 4A). Conversely, the Not1-938/943 mutant impaired the interaction with Caf1 without interfering with Not1 stability or the assembly of the Caf1-Ccr4 heterodimer (Figure 4A). Similar results were obtained using yeast two-hybrid assays (Figure S4A).

To disrupt the Caf1-Ccr4 interface, we engineered an A215E, F219E double substitution in Caf1 (Caf1-215/219 mutant) and a L339E, L341E in Ccr4 (Ccr4-339/341 mutant). The Caf1-215/219 mutant abolished the interaction with Ccr4, as shown by coimmunoprecipitation experiments (Figure 4B) and in yeast two-hybrid assays (Figure S4A), and slightly reduced interaction with Not1 (Figure 4B). Conversely, the Ccr4-339-341 mutant abolished the interaction with Caf1 but did not impact on the Caf1-Not1 interaction (Figure 4C and S4A). Importantly, the mutant proteins accumulated at normal level in all cases.

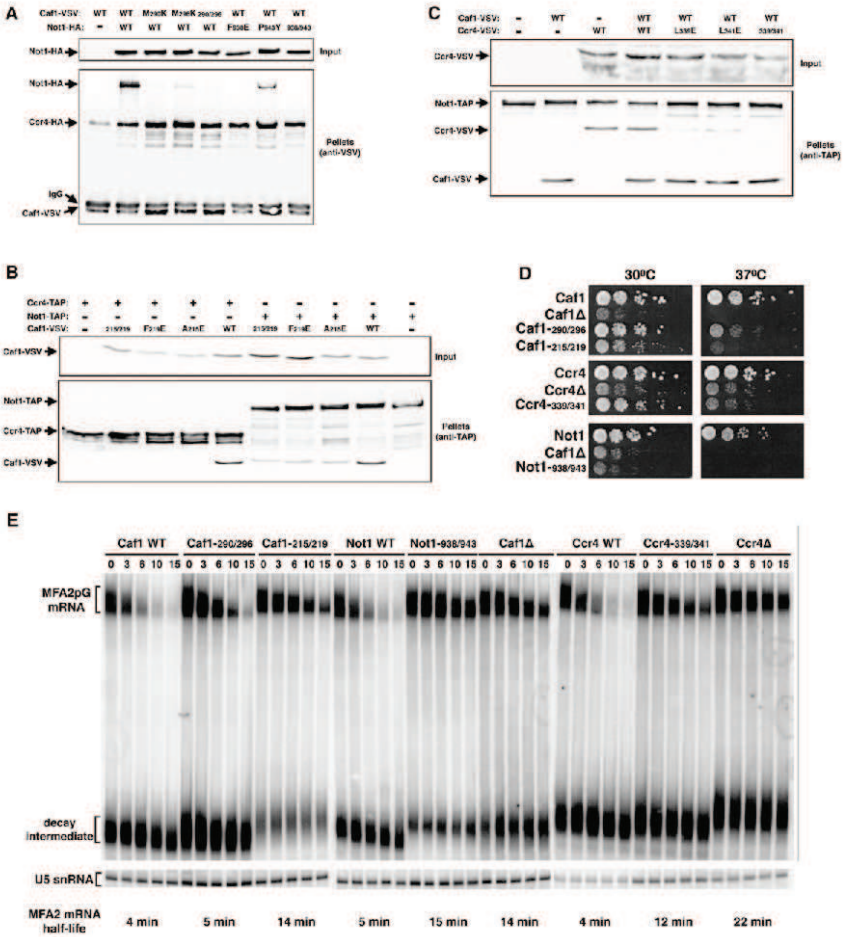

Figure 4. The Interactions in Not1$_{754-1000}$-Caf1-Ccr4 Are Essential for Normal Growth and mRNA Decay

(A–C) Coimmunoprecipitation was used to assay Not1-Caf1-Ccr4 interactions.

(A) VSV-tagged wild-type or mutant Caf1 present in strains expressing wild-type HA-tagged Not1 and HA-tagged Ccr4 were immunoprecipitated with anti-VSV antibodies. Parallel anti-VSV immunoprecipitations were performed from strains expressing VSV-tagged wild-type Caf1, HA-tagged mutant Not1, and wild-type HA-tagged Ccr4. Proteins present in the pellet fraction were detected by western blotting with anti-HA (Ccr4 and Not1) and anti-VSV (Caf1) antibodies.

(B) TAP-tagged wild-type Ccr4 (left lanes) or TAP-tagged Not1 (right lanes) present in strains expressing either wild-type or mutant VSV-tagged Caf1 were immunoprecipitated on IgG beads. Proteins present in the pellet fraction were detected by western blotting with anti-VSV antibodies (Caf1) and peroxidase-anti-peroxidase complex (Ccr4 or Not1).

(C) TAP-tagged wild-type Not1 present in strains expressing either VSV-tagged Ccr4 and/or VSV-tagged Caf1 was immunoprecipitated. Either wild-type or the indicated mutant forms of Ccr4 were used for this experiment. Proteins present in the pellet fraction were detected by western blotting with anti-VSV antibodies (Ccr4 and Caf1) and peroxidase-anti-peroxidase complex (Not1).

(D) Growth phenotypes resulting from mutations of interface residues. Plasmids encoding the Caf1, Ccr4, and Not1 mutants were introduced in strains deleted of the cognate wild-type gene, either directly (Caf1 and Ccr4) or by plasmid shuffling (Not1). Growth of the resulting strain was assayed on YPDA media at 30°C and 37°C.

(E) The plasmid encoding the MFA2pG reporter was introduced in the wild-type yeast strain, isogenic deletion strains lacking Ccr4 or Caf1 and point mutant of interface residues. The decay of the MFA2 mRNA was monitored in chase experiments. The MFA2 mRNA, decay intermediates and U5 small nuclear RNA were detected by northern blotting after fractionation in denaturing polyacrylamide gels.

See also Figure S4.

The Recruitment of Caf1 and Ccr4 to Not1 Is Essential for Their Biological Function

We used the structure-based mutants to test the physiological consequences of disrupting the Not1-Caf1 and the Caf1-Ccr4 interactions in vivo. To dissociate Caf1 from Not1, we introduced the Caf1-290/296 mutant in a strain carrying a chromosomal deletion of Caf1. Assaying the growth of the resulting strain demonstrated that preventing the association of Caf1 with Not1 results in a poor growth phenotype at high temperature (Figure 4D). In the latter conditions, the Caf1-290/296 mutant barely differed from the strain lacking Caf1.

In a complementary analysis, we introduced the Not1-938/943 mutant in the *not1*⊿ haploid strain rescued by a *URA3*-marked *NOT1* plasmid. The Not1-938/943 mutant was able to rescue the lethal phenotype conferred by Not1 inactivation, but the resulting strain grew at reduced rate at normal temperatures and very poorly at high temperatures (Figure 4D). The growth properties of the Not1-938/941 mutant strain were similar to those of an otherwise isogenic Caf1Δ strain (Figure 4D). The more severe phenotype observed with the Not1 mutant may reflect differences in residual interaction and/or the possibility that the mutated region of Not1 could be involved in additional functions. Nevertheless, because these mutations did not alter the level of Caf1, Ccr4, and Not1 or the formation of an active Ccr4-Caf1 dimer, these observations demonstrate that the association of Caf1-Ccr4 with Not1 is required for their biological activity. Interestingly, fusing Caf1 at the N terminus of the Not1-938/943 mutant partly rescued the slow growth phenotype of the Not1-938/943 protein, demonstrating that its inability to recruit Caf1 (and indirectly Ccr4) explains the poor activity of this factor (Figure S4B).

To dissociate Ccr4 from Caf1, we introduced the Caf1-215/219 and the Ccr4-339/341 mutants in strains devoid of Caf1 and Ccr4, respectively (Figure 4D). In both cases, the mutant strains grew at slightly reduced rate, a phenotype that was exacerbated at high temperature. We conclude that the recruitment of Ccr4 to the Ccr4-Not complex is essential for its biological activity.

Detachment of Caf1 and Ccr4 from Not1 Impairs Deadenylation and mRNA Decay

Next, we monitored the effect of the mutations on mRNA half-life. We introduced in the cognate mutants a reporter plasmid encoding the MFA2 mRNA under the control of a galactose-inducible promoter (Decker and Parker, 1993). Yeast cells were grown in galactose containing medium and transferred to glucose media to repress the reporter (time 0). Samples were withdrawn from the culture at various time points, to extract RNA and monitor the decay of the MFA2 reporter by northern blotting. The reporter mRNA was specifically detected with a probe hybridizing to a oligo(G) tract introduced in the reporter mRNA 3′ untranslated region (UTR) that also allowed the visualization of mRNA decay fragments by blocking the main 5′-3′ exonuclease, Xrn1.

Decay of the MFA2 reporter occurred with normal kinetic in control strains expressing wild-type Caf1, Ccr4 and Not1 (half-life [t½] of 4–5 min) but was strongly impaired in strains lacking Caf1 or Ccr4 (t½ of 14 and 22 min, respectively) (Figure 4E). In the absence of Caf1 and Ccr4, longer length intermediates that carried extended poly(A) tracts compared to their wild-type counterparts were detected (Figure 4E), as reported (Daugeron et al., 2001; Tucker et al., 2002). These intermediates extend from a stem loop in the reporter 3′ UTR to the mRNA 3′ end and originate from 5′-3′ exonucleolytic degradation of the mRNA body after decapping. Their increased length indicates that decapping proceedes despite the fact that poly(A) tails have not been shortened to the same length as in wild-type strains.

Upon assaying the disruption of the Not1-Caf1 interface (Figure 4E), we found that the reporter was only mildly affected in the Caf1-290/296 mutant (normal half life, moderately extended intermediates), while its decay was more severely impaired in the Not1-938/943 strain (t½ 15min, highly extended intermediates). When assaying the disruption of the Caf1-Ccr4 interface, both the Caf1-215/219 and the Ccr4-339/341 mutant strains resulted in the stabilization of the reporter (t½ of 14 and 12 min, respectively) and in extended decay intermediates (Figure 4E). These phenotypes were highly reproducible when the independent biological replicates were performed. Altogether, these observations demonstrate that the incorporation of Caf1 and Ccr4 in the Ccr4-Not complex (via the interaction with Not1) is essential for efficient deadenylation in vivo, as qualitatively evidenced by altered reporter mRNA half-life and the increased size of the decay intermediate. Quantitative differences observed between the mutants (i.e., the more severe phenotype of the Not1 mutation) may originate from different residual levels of interaction. It is also possible that the incorporation of Caf1-Ccr4 within the complex might differentially affect the deadenylation of different mRNAs. Finally, the Not1 mutant might also affect other properties or activities of the Ccr4-Not complex in addition to the recruitment of the deadenylases.

The Not1$_{154–754}$ Domain Is an Extended Platform of HEAT Repeats

To obtain a more complete view of the N-terminal arm of Not1, we also determined the structure of its largest domain. We solved the crystal structure of Not1$_{154–753}$ using Au-based SAD phasing and refined it at 2.8 Å resolution to an *R*free of 27.3% (see Table 1 for data collection and refinement statistics). The asymmetric unit of the crystals contains two independent copies of Not1$_{154–753}$, which have a rmsd of 0.62 Å over all α carbon atoms. The final model includes residues 193–745, with the exception of disordered loops at residues 211–232 and 268–270.

The Not1$_{154–753}$ structure is entirely built by antiparallel helices assembled side by side to form an elongated molecule with approximate dimensions of 120 Å × 25 Å × 25 Å (Figure 5A). Analysis of the structure identifies 13 helical hairpins related to HEAT repeats. HEAT repeats 1–9 have an overall parallel arrangement, with the exception of an unusually large rotation between HEAT 4 and 5. HEAT repeats 10–13 are also organized in a parallel fashion, but this region as a whole is rotated by about 90° with respect to HEAT 1–9 (Figure 5A). A search of the structural database using the Dali server (Holm and Rosenström, 2010) identified structural similarity between HEAT 10–13 (residues 571–746) and four HEAT repeats of MIF4G1 (rmsd of 3.9 Å over 115 Ca atoms after optimal superposition) (Figure S5).

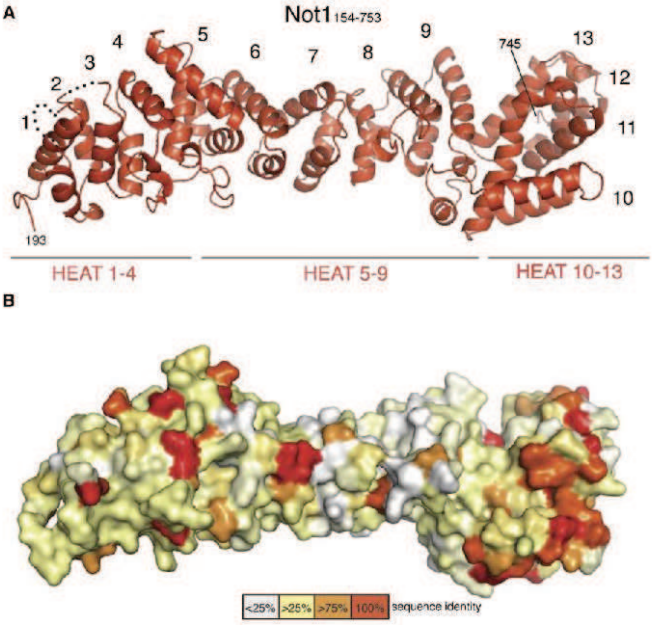

Figure 5. Not1$_{154-753}$ Is a HEAT-Rrepeat Platform
(A) Crystal structure of Not1$_{154-753}$ shown in a ribbon representation in red. The HEAT repeats and the ordered N and C termini are labeled. Disordered loops are indicated with a dotted line. (B) Not1$_{154-753}$ is shown in the same view as a surface representation colored according to sequence conservation as in Figure 2B.
See also Figure S5.

HEAT 10–13 is the most conserved portion of the Not1$_{154-753}$ domain (Figures 5B and S2). In particular, residues from the A helices of HEAT 10–11 form an evolutionary conserved patch on the outer surface of this domain. This conserved surface of Not1$_{154-753}$ (Figure 5B) and the conserved surface of Not1$_{754-1000}$ (Figure 2B, right panel) are prime targets for protein-protein interactions either within the core of the Ccr4-Not complex or for the recruitment of other factors.

Conclusions

The emerging picture from the current structural and functional information is that Not1 scaffolds the Ccr4-Not complex into two structural arms organized around the two halves of its 240 kDa polypeptide chain (Figure 6). In the N-terminal arm, the Not1$_{154-753}$ and Not1$_{754-1000}$ domains have a HEAT-repeat organization with regions related to MIF4G. This architecture is reminiscent of other scaffolding proteins involved in mRNA metabolism such as eIF4G (Schütz et al., 2008), CBC (Mazza et al., 2001), and UPF2 (Kadlec et al., 2004). The N-terminal arm of Not1 ends with a MIF4G domain that forms a rather rigid platform for the interaction with the Caf1 nuclease. Caf1 is sandwiched between Not1 and the LRR domain of Ccr4, which in turn tethers the nuclease domain with a covalent linkage and intramolecular interactions. The interactions between Not1, Caf1, and Ccr4 are evolutionarily conserved and functionally essential in vivo in yeast.

In vitro, Caf1-Ccr4 are active deadenylases in the absence of Not1 (Thore et al., 2003; Clark et al., 2004; Jonstrup et al., 2007). In the crystal structure, their active sites do not contact Not1$_{754-1000}$ and are accessible. In vivo, however, longer mRNA decay intermediates accumulate when disrupting the Not1-Caf1-Ccr4 interactions. These observations argue that the recruitment of Caf1-Ccr4 in the Ccr4-Not complex (via Not1) is required for full activity in yeast. It is possible that the complex might target the deadenylases to specific substrates and/or that the additional proteins in the Ccr4-Not complex might contribute. Indeed, studies in human cells have shown that depletion of Not2, a protein bound at the C-terminal arm of Not1 (Bai et al., 1999), affects the stability and enzymatic activity of the complex (Ito et al., 2011). Finally, the incorporation of Caf1-Ccr4 into the Not complex might also impact other processes in the cell, such as ubiquitination by Not4 or transcription.

The interpretation of the available data suggests that Not1$_{754-1000}$-Caf1-Ccr4 connects the two structural arms (Figures 6 and S6). The resulting model has interesting implications. First, it shows that the two nucleases are positioned centrally within the Ccr4-Not complex. Second, it rationalizes how regulators like BTG/Tob factors can be recruited to the surface of the complex to thread RNA substrates to the nuclease active sites (Figure S6). While BTG/Tob proteins bind directly to Caf1 (Horiuchi et al., 2009), it is possible to envisage that other regulators might be recruited to the extended HEAT-repeat platform in the N-terminal arm or to the C-terminal Not module. Finally, the model suggests that the nuclease domain of Ccr4 is adjacent to the Not module (Figures 6 and S6), rationalizing how a crosstalk between the nucleases and the Not proteins might be achieved. Understanding the structure and function of the Not module and the recruitment of regulators are open questions for future studies.

EXPERIMENTAL PROCEDURES

Protein Purification and Structure Determination

Not1 and Caf1 proteins were produced recombinantly in *E. coli*, while Ccr4 was obtained from insect-cell expression (Supplemental Experimental Procedures). The Not1$_{754-1000}$-Caf1 and Not1$_{754-1000}$-Caf1-Ccr4 complexes were reconstituted by mixing the purified components and by subsequent purification by size exclusion chromatography (Sephadex 200, GE

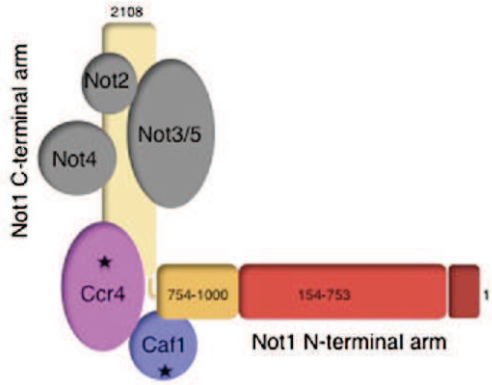

Figure 6. Structural Organization of the Yeast Ccr4-Not Complex
The scheme recapitulates the information from the crystal structures of $Not1_{754-1000}$-Caf1-Ccr4 and $Not1_{153-753}$ reported in this manuscript, combined with structural information from an EM study of the Ccr4-Not complex (Nasertorabi et al., 2011) (Figure S6) and previous interaction studies (reviewed in Collart and Timmers, 2004). Not1 is shown with the two structural arms colored from red (N terminus, residue 1) to yellow (C terminus, residue 2,108). Caf1 and Ccr4 are shown in blue and pink, with stars indicating their active sites. The Not2, Not3, Not4, and Not5 proteins that are part of the C-terminal "Not module" are shown in gray. Not shown here are Caf40 and Caf130, for which the interacting regions within the complex have yet to be precisely identified. See also Figure S6.

Healthcare). The samples were crystallized with the sitting-drop vapor diffusion technique at 18°C. Crystals were cryoprotected in mother liquor supplemented with 20% glycerol, mounted in nylon loops, and flash-frozen in liquid nitrogen for data collection at 100 K. Detailed procedures for crystallization and structure determination are in the Supplemental Experimental Procedures. The data statistics and quality of the models are summarized in Table 1.

Yeast Strains, Plasmids, and Growth Conditions

Yeasts were grown in standard media at 30°C, except when otherwise indicated. Yeast strains are listed in Table S1. Standard cloning, mutagenesis, and transformation procedures were used. Plasmids are listed in Table S2.

Reporter RNA Analysis, Western Blots and Coimmunoprecipitation Assays

RNA chase experiments were essentially performed as described previously (Daugeron et al., 2001). Details are in the Supplemental Experimental Procedures.

For coimmunoprecipitation assays, yeast total proteins were extracted from pellets prepared from 150 ml of yeast culture grown to OD_{600} 1.5. Coimmunoprecipitations were performed with 20 μl IgG-sepharose (GE Healthcare) for TAP-tagged proteins, or using protein G-sepharose preincubated with antiVSV IgG (Roche) for VSV-tagged proteins. Details are in the Supplemental Experimental Procedures. The input and precipitated fractions were analyzed by western blotting with antibodies described in the Supplemental Experimental Procedures.

ACCESSION NUMBERS

The coordinates and the structure factors have been deposited in the Protein Data Bank with accession numbers 4b8c ($Not1_{754-1000}$-Caf1-Ccr4), 4b8a ($Not1_{754-1000}$-Caf1), 4b89 ($Not1_{754-1000}$), and 4b8b ($Not1_{154-753}$).

SUPPLEMENTAL INFORMATION

Supplemental Information includes Supplemental Experimental Procedures, six figures, and two tables and can be found with this article online at http://dx.doi.org/10.1016/j.molcel.2012.08.014.

ACKNOWLEDGMENTS

We are grateful to E. Simon for defining stably expressing functional Ccr4-Caf1 truncations, to C. Carolis and D. Suck for the original expression vector of Ccr4-Caf1, to C. Gaudon, F. Wyers, F. Lacroute, V. Henriot, and C. Faux for plasmids and/or antibodies and the IGBMC for assistance. We gratefully acknowledge the Crystallization Facility and the Core Facilities at the Max Planck Institute of Biochemistry and A. Pauluhn, V. Olieric, and the staff of the PX beamlines at the SLS (Villigen, Zurich, Switzerland) for assistance during data collection. We also thank E. Lorentzen and F. Mauxion for useful discussions as well as members of our labs for critical reading of the manuscript. This study was supported by the Max Planck Gesellschaft, the European Research Council (ERC Advanced Investigator Grant 294371) and the Deutsche Forschungsgemeinschaft (DFG Sonderforschungsbereich SFB646, GRK1721, and the Gottfried Wilhelm Leibniz Program) to E.C. B.S. acknowledges support from the CERBM-IGBMC, the CNRS, the Ligue Contre le Cancer (Equipe Labellisée 2011) and the EU "3D-Repertoire" program (LSHG-CT-2005-512028).

Received: June 25, 2012
Revised: August 6, 2012
Accepted: August 16, 2012
Published online: September 6, 2012

REFERENCES

Albert, T.K., Lemaire, M., van Berkum, N.L., Gentz, R., Collart, M.A., and Timmers, H.T. (2000). Isolation and characterization of human orthologs of yeast CCR4-NOT complex subunits. Nucleic Acids Res. *28*, 809–817.

Andrade, M.A., Petosa, C., O'Donoghue, S.I., Müller, C.W., and Bork, P. (2001). Comparison of ARM and HEAT protein repeats. J. Mol. Biol. *309*, 1–18.

Ashkenazy, H., Erez, E., Martz, E., Pupko, T., and Ben-Tal, N. (2010). ConSurf 2010: calculating evolutionary conservation in sequence and structure of proteins and nucleic acids. Nucleic Acids Res. *38* (Web Server issue), W529–W533.

Bai, Y., Salvadore, C., Chiang, Y.C., Collart, M.A., Liu, H.Y., and Denis, C.L. (1999). The CCR4 and CAF1 proteins of the CCR4-NOT complex are physically and functionally separated from NOT2, NOT4, and NOT5. Mol. Cell. Biol. *19*, 6642–6651.

Bella, J., Hindle, K.L., McEwan, P.A., and Lovell, S.C. (2008). The leucine-rich repeat structure. Cell. Mol. Life Sci. *65*, 2307–2333.

Boeck, R., Tarun, S., Jr., Rieger, M., Deardorff, J.A., Müller-Auer, S., and Sachs, A.B. (1996). The yeast Pan2 protein is required for poly(A)-binding protein-stimulated poly(A)-nuclease activity. J. Biol. Chem. *271*, 432–438.

Braun, J.E., Huntzinger, E., Fauser, M., and Izaurralde, E. (2011). GW182 proteins directly recruit cytoplasmic deadenylase complexes to miRNA targets. Mol. Cell *44*, 120–133.

Brown, C.E., and Sachs, A.B. (1998). Poly(A) tail length control in Saccharomyces cerevisiae occurs by message-specific deadenylation. Mol. Cell. Biol. *18*, 6548–6559.

Brown, C.E., Tarun, S.Z., Jr., Boeck, R., and Sachs, A.B. (1996). PAN3 encodes a subunit of the Pab1p-dependent poly(A) nuclease in Saccharomyces cerevisiae. Mol. Cell. Biol. *16*, 5744–5753.

Cao, D., and Parker, R. (2001). Computational modeling of eukaryotic mRNA turnover. RNA *7*, 1192–1212.

Chekulaeva, M., Mathys, H., Zipprich, J.T., Attig, J., Colic, M., Parker, R., and Filipowicz, W. (2011). miRNA repression involves GW182-mediated recruitment of CCR4-NOT through conserved W-containing motifs. Nat. Struct. Mol. Biol. *18*, 1218–1226.

Chen, J., Rappsilber, J., Chiang, Y.C., Russell, P., Mann, M., and Denis, C.L. (2001). Purification and characterization of the 1.0 MDa CCR4-NOT complex identifies two novel components of the complex. J. Mol. Biol. *314*, 683–694.

Chen, J., Chiang, Y.-C., and Denis, C.L. (2002). CCR4, a 3′-5′ poly(A) RNA and ssDNA exonuclease, is the catalytic component of the cytoplasmic deadenylase. EMBO J. *21*, 1414–1426.

Clark, L.B., Viswanathan, P., Quigley, G., Chiang, Y.-C., McMahon, J.S., Yao, G., Chen, J., Nelsbach, A., and Denis, C.L. (2004). Systematic mutagenesis of the leucine-rich repeat (LRR) domain of CCR4 reveals specific sites for binding to CAF1 and a separate critical role for the LRR in CCR4 deadenylase activity. J. Biol. Chem. *279*, 13616–13623.

Collart, M.A., and Timmers, H.T. (2004). The eukaryotic Ccr4-not complex: a regulatory platform integrating mRNA metabolism with cellular signaling pathways? Prog. Nucleic Acid Res. Mol. Biol. *77*, 289–322.

Daugeron, M.C., Mauxion, F., and Séraphin, B. (2001). The yeast POP2 gene encodes a nuclease involved in mRNA deadenylation. Nucleic Acids Res. *29*, 2448–2455.

de Moor, C.H., Meijer, H., and Lissenden, S. (2005). Mechanisms of translational control by the 3′ UTR in development and differentiation. Semin. Cell Dev. Biol. *16*, 49–58.

Decker, C.J., and Parker, R. (1993). A turnover pathway for both stable and unstable mRNAs in yeast: evidence for a requirement for deadenylation. Genes Dev. *7*, 1632–1643.

Deluen, C., James, N., Maillet, L., Molinete, M., Theiler, G., Lemaire, M., Paquet, N., and Collart, M.A. (2002). The Ccr4-not complex and yTAF1 (yTaf(II)130p/yTaf(II)145p) show physical and functional interactions. Mol. Cell. Biol. *22*, 6735–6749.

Denis, C.L., Chiang, Y.C., Cui, Y., and Chen, J. (2001). Genetic evidence supports a role for the yeast CCR4-NOT complex in transcriptional elongation. Genetics *158*, 627–634.

Draper, M.P., Salvadore, C., and Denis, C.L. (1995). Identification of a mouse protein whose homolog in Saccharomyces cerevisiae is a component of the CCR4 transcriptional regulatory complex. Mol. Cell. Biol. *15*, 3487–3495.

Dupressoir, A., Morel, A.P., Barbot, W., Loireau, M.P., Corbo, L., and Heidmann, T. (2001). Identification of four families of yCCR4- and Mg2+-dependent endonuclease-related proteins in higher eukaryotes, and characterization of orthologs of yCCR4 with a conserved leucine-rich repeat essential for hCAF1/hPOP2 binding. BMC Genomics *2*, 9.

Eckmann, C.R., Rammelt, C., and Wahle, E. (2011). Control of poly(A) tail length. Wiley Interdiscip Rev RNA *2*, 348–361.

Edmonds, M., Vaughan, M.H., Jr., and Nakazato, H. (1971). Polyadenylic acid sequences in the heterogeneous nuclear RNA and rapidly-labeled polyribosomal RNA of HeLa cells: possible evidence for a precursor relationship. Proc. Natl. Acad. Sci. USA *68*, 1336–1340.

Fabian, M.R., Cieplak, M.K., Frank, F., Morita, M., Green, J., Srikumar, T., Nagar, B., Yamamoto, T., Raught, B., Duchaine, T.F., and Sonenberg, N. (2011). miRNA-mediated deadenylation is orchestrated by GW182 through two conserved motifs that interact with CCR4-NOT. Nat. Struct. Mol. Biol. *18*, 1211–1217.

Garneau, N.L., Wilusz, J., and Wilusz, C.J. (2007). The highways and byways of mRNA decay. Nat. Rev. Mol. Cell Biol. *8*, 113–126.

Goldstrohm, A.C., and Wickens, M. (2008). Multifunctional deadenylase complexes diversify mRNA control. Nat. Rev. Mol. Cell Biol. *9*, 337–344.

Holm, L., and Rosenström, P. (2010). Dali server: conservation mapping in 3D. Nucleic Acids Res. *38* (Web Server issue), W545–W549.

Horiuchi, M., Takeuchi, K., Noda, N., Muroya, N., Suzuki, T., Nakamura, T., Kawamura-Tsuzuku, J., Takahasi, K., Yamamoto, T., and Inagaki, F. (2009). Structural basis for the antiproliferative activity of the Tob-hCaf1 complex. J. Biol. Chem. *284*, 13244–13255.

Ito, K., Inoue, T., Yokoyama, K., Morita, M., Suzuki, T., and Yamamoto, T. (2011). CNOT2 depletion disrupts and inhibits the CCR4-NOT deadenylase complex and induces apoptotic cell death. Genes Cells *16*, 368–379.

Jonstrup, A.T., Andersen, K.R., Van, L.B., and Brodersen, D.E. (2007). The 1.4-A crystal structure of the S. pombe Pop2p deadenylase subunit unveils the configuration of an active enzyme. Nucleic Acids Res. *35*, 3153–3164.

Kadlec, J., Izaurralde, E., and Cusack, S. (2004). The structural basis for the interaction between nonsense-mediated mRNA decay factors UPF2 and UPF3. Nat. Struct. Mol. Biol. *11*, 330–337.

Kruk, J.A., Dutta, A., Fu, J., Gilmour, D.S., and Reese, J.C. (2011). The multifunctional Ccr4-Not complex directly promotes transcription elongation. Genes Dev. *25*, 581–593.

Lau, N.C., Kolkman, A., van Schaik, F.M., Mulder, K.W., Pijnappel, W.W., Heck, A.J., and Timmers, H.T. (2009). Human Ccr4-Not complexes contain variable deadenylase subunits. Biochem. J. *422*, 443–453.

Liu, H.Y., Badarinarayana, V., Audino, D.C., Rappsilber, J., Mann, M., and Denis, C.L. (1998). The NOT proteins are part of the CCR4 transcriptional complex and affect gene expression both positively and negatively. EMBO J. *17*, 1096–1106.

Maillet, L., Tu, C., Hong, Y.K., Shuster, E.O., and Collart, M.A. (2000). The essential function of Not1 lies within the Ccr4-Not complex. J. Mol. Biol. *303*, 131–143.

Malvar, T., Biron, R.W., Kaback, D.B., and Denis, C.L. (1992). The CCR4 protein from Saccharomyces cerevisiae contains a leucine-rich repeat region which is required for its control of ADH2 gene expression. Genetics *132*, 951–962.

Mangus, D.A., Evans, M.C., and Jacobson, A. (2003). Poly(A)-binding proteins: multifunctional scaffolds for the post-transcriptional control of gene expression. Genome Biol. *4*, 223.

Mauxion, F., Faux, C., and Séraphin, B. (2008). The BTG2 protein is a general activator of mRNA deadenylation. EMBO J. *27*, 1039–1048.

Mazza, C., Ohno, M., Segref, A., Mattaj, I.W., and Cusack, S. (2001). Crystal structure of the human nuclear cap binding complex. Mol. Cell *8*, 383–396.

Nasertorabi, F., Batisse, C., Diepholz, M., Suck, D., and Böttcher, B. (2011). Insights into the structure of the CCR4-NOT complex by electron microscopy. FEBS Lett. *585*, 2182–2186.

Ohn, T., Chiang, Y.-C., Lee, D.J., Yao, G., Zhang, C., and Denis, C.L. (2007). CAF1 plays an important role in mRNA deadenylation separate from its contact to CCR4. Nucleic Acids Res. *35*, 3002–3015.

Sandler, H., Kreth, J., Timmers, H.T., and Stoecklin, G. (2011). Not1 mediates recruitment of the deadenylase Caf1 to mRNAs targeted for degradation by tristetraprolin. Nucleic Acids Res. *39*, 4373–4386.

Schütz, P., Bumann, M., Oberholzer, A.E., Bieniossek, C., Trachsel, H., Altmann, M., and Baumann, U. (2008). Crystal structure of the yeast eIF4A-eIF4G complex: an RNA-helicase controlled by protein-protein interactions. Proc. Natl. Acad. Sci. USA *105*, 9564–9569.

Schwede, A., Ellis, L., Luther, J., Carrington, M., Stoecklin, G., and Clayton, C. (2008). A role for Caf1 in mRNA deadenylation and decay in trypanosomes and human cells. Nucleic Acids Res. *36*, 3374–3388.

Simón, E., and Séraphin, B. (2007). A specific role for the C-terminal region of the Poly(A)-binding protein in mRNA decay. Nucleic Acids Res. *35*, 6017–6028.

Sonenberg, N., and Dever, T.E. (2003). Eukaryotic translation initiation factors and regulators. Curr. Opin. Struct. Biol. *13*, 56–63.

Sun, M., Schwalb, B., Schulz, D., Pirkl, N., Etzold, S., Larivière, L., Maier, K.C., Seizl, M., Tresch, A., and Cramer, P. (2012). Comparative dynamic transcriptome analysis (cDTA) reveals mutual feedback between mRNA synthesis and degradation. Genome Res. *22*, 1350–1359.

Tarun, S.Z., Jr., Wells, S.E., Deardorff, J.A., and Sachs, A.B. (1997). Translation initiation factor eIF4G mediates in vitro poly(A) tail-dependent translation. Proc. Natl. Acad. Sci. USA *94*, 9046–9051.

Temme, C., Zaessinger, S., Meyer, S., Simonelig, M., and Wahle, E. (2004). A complex containing the CCR4 and CAF1 proteins is involved in mRNA deadenylation in Drosophila. EMBO J. *23*, 2862–2871.

Thore, S., Mauxion, F., Séraphin, B., and Suck, D. (2003). X-ray structure and activity of the yeast Pop2 protein: a nuclease subunit of the mRNA deadenylase complex. EMBO Rep. *4*, 1150–1155.

Tucker, M., Valencia-Sanchez, M.A., Staples, R.R., Chen, J., Denis, C.L., and Parker, R. (2001). The transcription factor associated Ccr4 and Caf1 proteins are components of the major cytoplasmic mRNA deadenylase in Saccharomyces cerevisiae. Cell *104*, 377–386.

Tucker, M., Staples, R.R., Valencia-Sanchez, M.A., Muhlrad, D., and Parker, R. (2002). Ccr4p is the catalytic subunit of a Ccr4p/Pop2p/Notp mRNA deadenylase complex in Saccharomyces cerevisiae. EMBO J. *21*, 1427–1436.

Wang, H., Morita, M., Yang, X., Suzuki, T., Yang, W., Wang, J., Ito, K., Wang, Q., Zhao, C., Bartlam, M., et al. (2010). Crystal structure of the human CNOT6L nuclease domain reveals strict poly(A) substrate specificity. EMBO J. *29*, 2566–2576.

Yamashita, A., Chang, T.-C., Yamashita, Y., Zhu, W., Zhong, Z., Chen, C.-Y.A., and Shyu, A.-B. (2005). Concerted action of poly(A) nucleases and decapping enzyme in mammalian mRNA turnover. Nat. Struct. Mol. Biol. *12*, 1054–1063.

Zhang, X., Virtanen, A., and Kleiman, F.E. (2010). To polyadenylate or to deadenylate: that is the question. Cell Cycle *9*, 4437–4449.

nature structural & molecular biology

Structure and RNA-binding properties of the Not1–Not2–Not5 module of the yeast Ccr4–Not complex

Varun Bhaskar[1], Vladimir Roudko[2,3], Jérôme Basquin[1], Kundan Sharma[4], Henning Urlaub[4], Bertrand Séraphin[2,3] & Elena Conti[1]

The Ccr4–Not complex is involved in several aspects of gene expression, including mRNA decay, translational repression and transcription. We determined the 2.8-Å-resolution crystal structure of a 120-kDa core complex of the *Saccharomyces cerevisiae* Not module comprising the C-terminal arm of Not1, Not2 and Not5. Not1 is a HEAT-repeat scaffold. Not2 and Not5 have extended regions that wrap around Not1 and around their globular domains, the Not boxes. The Not boxes resemble Sm folds and interact with each other with a noncanonical dimerization surface. Disruption of the interactions within the ternary complex has severe effects on growth *in vivo*. The ternary complex forms a composite surface that binds poly(U) RNA *in vitro*, with a site at the Not5 Not box. The results suggest that the Not module forms a versatile platform for macromolecular interactions.

The Ccr4–Not complex is a large assembly that regulates eukaryotic gene expression at multiple levels. The best-studied function of Ccr4–Not relates to its action as the major deadenylase involved in shortening the poly(A) tail of cellular mRNAs in the cytoplasm (reviewed in ref. 1). Deadenylation by Ccr4–Not is a key step in the constitutive and regulated turnover of mRNAs[2,3]. Ccr4–Not can also be targeted to *cis*-acting elements in the 3′ untranslated region (UTR) of specific transcripts to accelerate their decay (for example, in the case of ARE-containing mRNAs)[4,5] or to mediate microRNA-dependent repression[6–8] or translational repression (examples in refs. 9,10). In addition, Ccr4–Not has been implicated in transcription initiation and elongation in the nucleus as well as in ubiquitylation (reviewed in refs. 11,12). The nuclear and cytoplasmic functions of Ccr4–Not have long been thought of as disconnected. However, recent evidence is converging on the functional coupling between mRNA synthesis and degradation[13].

Ccr4–Not contains several evolutionarily conserved proteins (Not1, Caf1 (also called Pop2), Not2, Not3 or Not5 and Caf40) that are constitutive components of the complex in all species examined to date (yeast[14,15], humans[16,17], flies[18,19] and trypanosoma[20]). Other bona fide subunits of Ccr4–Not are peripheral (for example, Ccr4 and Not4)[16,18,21] and/or species specific[15,19,22,23]. Variants of the core complex are likely to exist, as homologs are present both in yeast (Not3 and Not5)[24] and humans (for Caf1 and for Ccr4)[16,17]. The core complex is built around Not1, a large scaffold protein of ~240 kDa (refs. 21,25). The N-terminal half of Not1 associates with the Caf1 and Ccr4 RNases and is involved in the formation of the deadenylase module of the complex[21,26]. The C-terminal half of Not1 binds Not2, Not3, Not4 and Not5 to form the so-called Not module[16,21,27]. Synthetic lethality between the yeast deadenylase subunits and Not subunits suggests that they have separate or only partially overlapping functions[21]. The deadenylase module is connected to the cytoplasmic activities of Ccr4–Not (reviewed in refs. 1,11) and has been studied at the structural and functional level[28,29]. How the Not module is structured and how it functions are far less clear (reviewed in ref. 30).

Genetic and biochemical studies have shown that Not2, Not3 and Not5 are closely associated[19,21]. *S. cerevisiae* Not3 and Not5 are currently thought of as paralogous proteins[30]. Yeast Not5 is reported to be crucial for vegetative growth, whereas Not3 deletion has milder phenotypes[24]. The only Not3 and Not5 homolog in metazoans (known as Not3) is essential in mice for embryonic development and for control of heart function[31] and metabolism[32] in adults. In metazoans, Not2 is believed to recruit Not3 into the complex[17,19], to be important for the integrity of Ccr4–Not[33,34] and to act as a repressor of promoter activity in the nucleus[35]. In yeast, Not2 and Not5 have been reported to interact with components of the transcription machinery, specifically with subunits of TFIID[36–38] and SAGA[33]. In addition to data pointing to connections with transcription (reviewed in refs. 11,12), the Not module has also been implicated in mRNA-decay pathways in the cytoplasm[18,39]. To shed light on how the Not module can mediate these different functions, we have determined the structure and biochemical properties of a core complex from *S. cerevisiae*.

RESULTS

Structure determination of a yeast Not1–Not2–Not5 complex

Yeast two-hybrid and coimmunoprecipitation assays have shown that Not1 (2,108 residues in *S. cerevisiae*) binds Not2, Not3 and Not5 in a region that spans approximately the last 700 residues[19,21,25] (**Fig. 1a**).

[1]Department of Structural Cell Biology, Max Planck Institute of Biochemistry (MPI Biochemistry), Martinsried, Germany. [2]Institut de Génétique et de Biologie Moléculaire et Cellulaire (IGBMC), Centre National de Recherche Scientifique (CNRS) UMR 7104, Institut National de Santé et de Recherche Médicale (INSERM), U964, Illkirch, France. [3]Université de Strasbourg, Illkirch, France. [4]Max Planck Institute of Biophysical Chemistry, Göttingen, Germany. Correspondence should be addressed to E.C. (conti@biochem.mpg.de).

Received 21 May; accepted 5 September; published online 13 October 2013; doi:10.1038/nsmb.2686

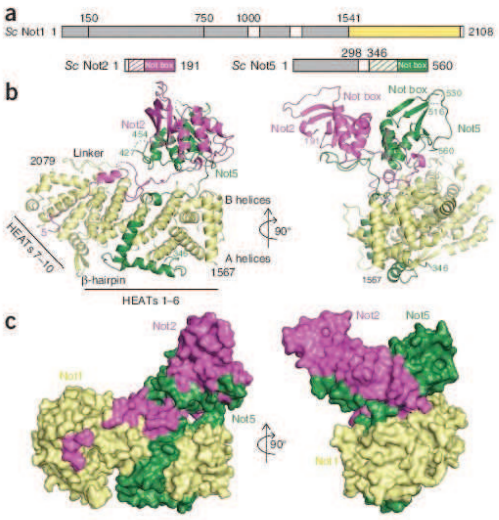

Figure 1 Structure of a yeast Not1–Not2–Not5 core complex. (**a**) Schematic representation of the domain organization of *S. cerevisiae* (*Sc*) Not1, Not2 and Not5. Color-filled rectangles indicate globular domains present in the crystal structure (yellow, Not1; magenta, Not2; green, Not5). Dashed rectangles indicate low-complexity regions of the molecules with ordered electron density. Gray rectangles indicate globular domains either from previous structures[28] or predicted from sequence analysis. (**b**) Structure of the complex shown in cartoon representation in two orientations (right, front view of the Not boxes; left, side view). Not1 features are labeled in black. Disordered regions are shown as dotted lines. The N- and C-terminal residues are indicated. The labeled linker and β-hairpin refer to the HEAT 6–7 and the HEAT 7–8 inter-repeat loops. This and all other cartoon drawings were generated with PyMOL (http://www.pymol.org/). (**c**) Surface representations of the complex in the same orientations and colors as in **b**.

Not2 (191 residues in *S. cerevisiae*) is predicted to contain a poorly structured N-terminal region followed by a conserved domain known as the Not-box domain[35] (**Fig. 1a**). Not5 (560 residues) contains an N-terminal coiled-coil region followed by a low-complexity linker and a C-terminal Not-box domain[35] (**Fig. 1a**). *S. cerevisiae* Not3 has a similar domain architecture as does Not5, but it could not be expressed as full length in a soluble form (V.B. and E.C., unpublished observations). We purified and reconstituted a complex containing the last ~750 residues of Not1, full-length (FL) Not2 and FL Not5, subjected it to limited proteolysis and identified the core complex composed of Not1 residues 1541–2093, Not2 FL and Not5 residues 298–560 (hereafter defined as Not1c, Not2 and Not5c, respectively) (**Supplementary Fig. 1**).

The Not1c–Not2–Not5c complex yielded crystals diffracting to 2.8-Å resolution. We determined the structure by SAD, using crystals derivatized with mercury, and refined it to an R_{free} of 22.6% and R_{work} of 18.1% with good stereochemistry (**Table 1**). The two independent copies of the Not1c–Not2–Not5c complex present in the crystal asymmetric unit are virtually identical (superposing with an r.m.s. deviation of 0.85 Å over all Cα atoms). The final model includes Not1 residues 1567–2079, Not2 residues 5–191 (with the exception of two disordered segments at residues 14–29 and 44–48) and Not5 residues 346–560 (with the exception of two loops at residues 428–453 and 517–529) (**Fig. 1b** and **Supplementary Fig. 2**).

The C-terminal region of Not1 is a scaffold of HEAT repeats

The Not1c–Not2–Not5c structure is organized around Not1 (**Fig. 1b**). Not1c is built almost entirely of antiparallel α-helices, forming an elongated molecule of the approximate dimensions 85 Å × 35 Å × 40 Å. The topology of the secondary-structure elements in Not1c is typical of that observed in HEAT-repeat proteins. Canonical HEAT repeats are characterized by a helix A–turn–helix B motif and are arranged in tandem in an almost-parallel fashion, with a 15° rotation between consecutive repeats[40]. Multiple repeats typically give rise to superhelical structures with a convex layer formed by the A helices and a concave layer formed by the B helices. Not1c contains ten HEAT repeats, which can be grouped into two units.

The first unit, comprising HEATs 1–6 (residues 1567–1849), has a regular architecture, albeit one less curved than for canonical HEAT-repeat proteins (**Fig. 1b**). The second unit, comprising HEATs 7–10 (residues 1888–2058), also adopts a regular architecture, with the exception of a long β-hairpin connecting HEATs 7 and 8 and of an additional C-terminal helix (residues 2059–2079). This unit contains four of the five HEAT repeats characteristic of the middle domain of eukaryotic initiation factor 4G (MIF4G)[41] and can therefore be described as an MIF4G-like domain. The 40-residue linker connecting HEATs 6 and 7 wraps around both units and contributes to formation of the extensive hydrophobic core of Not1c. The two HEAT-repeat units pack against each other in a perpendicular fashion resulting in a T-shaped architecture (**Fig. 1b** and **Supplementary Fig. 3a**). Interestingly, the domain formed by residues 193–745 in the N-terminal

Table 1 Data collection and refinement statistics

	Native	Hg derivative
Data collection[a]		
Space group	$P2_1$	$P2_1$
Cell dimensions		
a, *b*, *c* (Å)	110.45, 109.17, 133.62	109.67, 106.19, 136.02
α, β, γ (°)	90, 94.7, 90	90, 94.0, 90
		Peak
Wavelength	1.00004	1.00606
Resolution (Å)	49.15–2.80 (2.95–2.80)	47.77–3.20 (3.37–3.20)
R_{merge}	6.50 (42.90)	16.70 (80.60)
$I / \sigma I$	17.30 (2.90)	10.60 (2.40)
Completeness (%)	99.50 (97)	100 (100)
Redundancy	4.80 (4.50)	6.90 (7.20)
Refinement		
Resolution (Å)	49.15–2.80 (2.83–2.80)	
No. reflections	77,882	51,653
R_{work} / R_{free}	0.1812 / 0.2258	
No. atoms	14,019	
Protein	13,978	
Ligand/ion	36	
Water	5	
B factors	67.00	
Protein	67.10	
Ligand/ion	62.20	
Water	39.90	
r.m.s. deviations		
Bond lengths (Å)	0.009	
Bond angles (°)	1.12	

[a]One native and one Hg-derivative crystal were used for data collection. Values in parentheses are for highest-resolution shell.

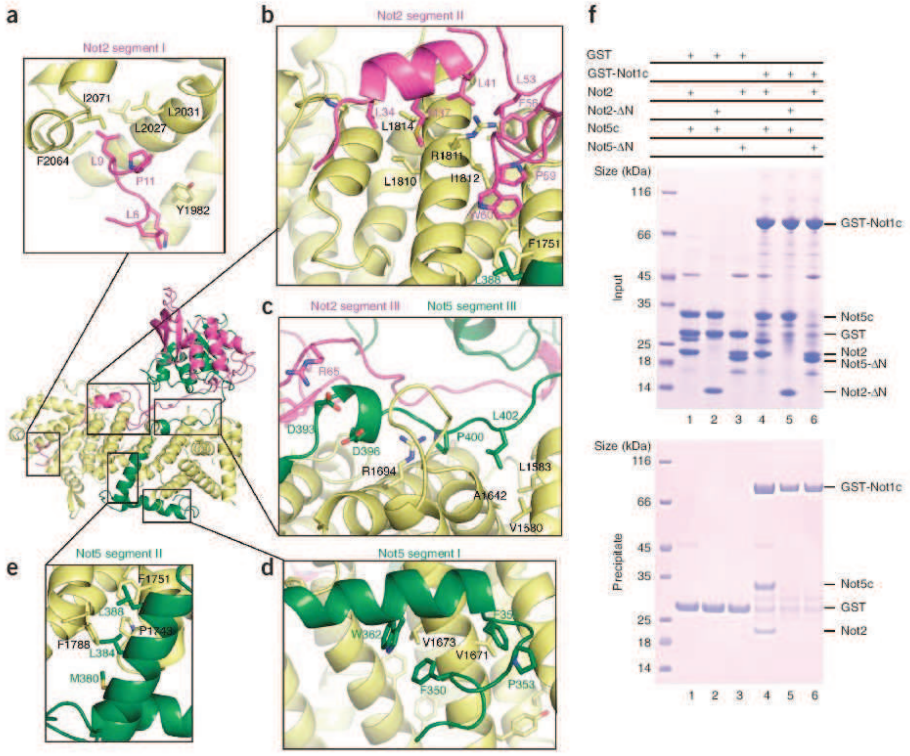

Figure 2 Not1 interacts with extended regions of Not2 and Not5. (**a**–**e**) Close-up views of the interactions of Not1 with Not2 and Not5 showing the three segments (I, II and III) of the N-terminal extensions of Not2 and Not5 that form the Not1-binding domains. The positions of the individual close-up views within the complex are indicated at center left. Interacting residues involved in evolutionarily conserved interactions are indicated and labeled (conservation shown in **Supplementary Fig. 2**). (**f**) Pulldown experiments of GST-tagged Not1c with untagged Not2, Not5c, Not2-ΔN and Not5-ΔN (ΔN refers to the removal of the N-terminal extension involved in Not1 binding). GST is shown as a control. Input samples (top) and samples precipitated on glutathione-agarose beads (bottom), analyzed on 4–12% Bis-Tris NuPAGE gel with MES running buffer, are shown. The proteins corresponding to the bands are indicated on the right.

arm of yeast Not1 is also formed by a MIF4G-like unit and a longer HEAT-repeat unit arranged perpendicularly to each other[28]. Although the relative orientations of the individual units differ in detail, the N-terminal and C-terminal arms of Not1 are built with remarkably similar principles (**Supplementary Fig. 3a**).

Extended regions of Not2 and Not5 wrap around Not1

Not2 and Not5 both contain a globular domain preceded by N-terminal extensions (**Fig. 1b**,**c**). In the N-terminal extensions, Not2 residues 5–75 and Not5 residues 346–404 mediate binding to Not1c, covering a distance of >100 Å each and burying a total surface of ~3,700 Å^2. The Not1-binding domain of Not2 can be described as composed of three segments (**Fig. 2**). The first segment (Not2 residues 5–13) binds the MIF4G-like unit of Not1c, mainly at the A helices of HEATs 9 and 10. Here, a conserved hydrophobic pocket of Not1 recognizes Not2 Leu9 (**Fig. 2a**), a conserved residue that has been shown to be functionally important in *in vivo* studies[33]. The second segment (Not2 residues 31–64) binds Not1c at the adjacent HEAT-repeat unit, zigzagging over the B helices of HEATs 4–6 (**Fig. 2b**). This segment of Not2 forms a short helix and a hairpin. The helix docks with hydrophobic residues on the conserved surface of HEAT 5 centered at Arg1811 and Leu1814. The hairpin wedges into another set of hydrophobic residues in a conserved groove at HEATs 4–5 (from Phe1751 to Ile1812). The third segment (Not2 residues 65–75) extends over the B helices of Not1c toward HEAT 3 (**Fig. 2c**).

The Not1-binding domain of Not5 wraps around HEATs 1–5 of Not1 (**Fig. 1b**) and can also be subdivided into three segments. The first segment (Not5 residues 346–373) contains an α-helix and binds the A helices of Not1c with apolar interactions (**Fig. 2d**). The second segment (Not5 residues 374–391) contains another α-helix and binds the edge of Not1c formed at the intrarepeat connections of HEATs 3–5 through hydrophobic interactions (**Fig. 2e**). The third segment (Not5 residues 392–404) stretches over the B helices of Not1c between HEATs 1–3, making both polar and apolar contacts (**Fig. 2c**). The third segment of Not5 flanks the third segment of Not2 and directly interacts with it through a salt bridge (between Asp393 and Arg65) (**Fig. 2c**). The structure suggests that the Not1-binding domains of Not2 and Not5 bind Not1c synergistically. We tested the effect of

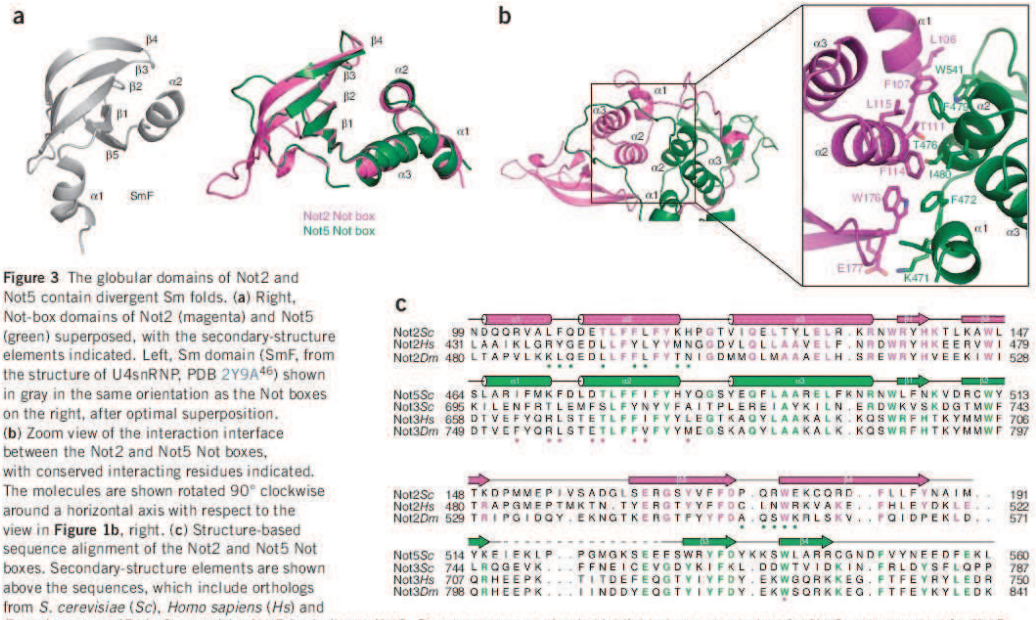

Figure 3 The globular domains of Not2 and Not5 contain divergent Sm folds. (**a**) Right, Not-box domains of Not2 (magenta) and Not5 (green) superposed, with the secondary-structure elements indicated. Left, Sm domain (SmF, from the structure of U4snRNP, PDB 2Y9A[46]) shown in gray in the same orientation as the Not boxes on the right, after optimal superposition. (**b**) Zoom view of the interaction interface between the Not2 and Not5 Not boxes, with conserved interacting residues indicated. The molecules are shown rotated 90° clockwise around a horizontal axis with respect to the view in **Figure 1b**, right. (**c**) Structure-based sequence alignment of the Not2 and Not5 Not boxes. Secondary-structure elements are shown above the sequences, which include orthologs from *S. cerevisiae* (*Sc*), *Homo sapiens* (*Hs*) and *D. melanogaster* (*Dm*). *S. cerevisiae* Not5 is similar to Not3. Sequence conservation is highlighted as magenta text for Not2 and green text for Not5. Below the sequences, the residues of Not2 that interact with Not5 are indicated with green circles, and residues of Not5 that interact with Not2 are indicated with magenta circles.

deleting either domain on Not1 binding in pulldown assays with purified proteins. As a control, Not2 and Not5c coprecipitated with glutathione S-transferase (GST)-tagged Not1c (**Fig. 2f**, lane 4). In this assay, Not5c was not coprecipitated with Not1c when Not2 was truncated (to Not2-ΔN, residues 76–191) (**Fig. 2f**, lane 5). Analogously, Not2 did not coprecipitate with Not1c when Not5c was truncated (to Not5-ΔN, residues 405–560) (**Fig. 2f**, lane 6). We concluded that formation of the core of the Not module requires the cooperative binding of Not2 and Not5.

The Not boxes of Not2 and Not5 have divergent Sm-like folds

The globular domains of Not2 and Not5 are positioned on top of the B helices of Not1 HEATs 1–4, sandwiching in between parts of the Not2 and Not5 N-terminal extensions (**Fig. 1b,c**). The globular domains contain the so-called Not boxes. The Not box of Not2 (residues 99–191) consists of three N-terminal helices (α1, α2 and α3) and a β-sheet formed by four antiparallel β-strands adjacent to each other (**Fig. 3a**, **Supplementary Fig. 3b** and **Supplementary Fig. 3c**). The β-sheet is highly bent: strands β3 and β4 are long and curved, with a conserved glycine residue (Gly166) at the bending point of β3. A short C-terminal extension packs against β1, creating a small β-barrel. The Not box of Not5 (residues 464–560) is similar in structure to that of Not2, superposing with an r.m.s. deviation of <1.3 Å over all Cα atoms (**Fig. 3a** and **Supplementary Fig. 3b**). The main difference is that in Not5 all the β-strands are short, thus resulting in a rather flat β-sheet.

Database searches on the DALI server[42] for structural similarities to the Not-box domains identified Sm domains as the most similar in fold (r.m.s. deviation of 2.2 Å and 2.7 Å with SmD3 and SmF, respectively[43]) (**Fig. 3a**). The Not boxes, however, differ from canonical Sm folds in several aspects. First, they lack the characteristic Sm1 and Sm2 signature motifs in the amino acid sequence. At the structural level, the Not boxes lack the fifth β-strand that in Sm proteins mediates the interaction forming dimeric Sm–Sm subcomplexes[43] and ring-like structures[44–46] (**Supplementary Fig. 3b**). The Not boxes of Not2 and Not5 also interact with each other, but in the absence of a fifth β-strand they do so with a different dimerization mechanism that involves the N-terminal α-helices (**Fig. 3b** and **Supplementary Fig. 3b**). Helix α1 of the Not2 Not box packs against the base of the β-sheet of the Not5 Not box and vice versa. Between them, the α2 helices of Not2 and Not5 pack against each other. The dimerization interface is mediated by extensive interactions centered at the conserved Phe114 and Leu115 of Not2 and the corresponding Phe479 and Ile480 of Not5 (**Fig. 3b,c**). Finally, the globular domains are also formed by parts of the N-terminal extensions. Residues 67–93 of Not2 wrap around the Not box of Not5, and residues 408–427 of Not5 wrap around the Not box of Not2 (**Fig. 3b**). The interactions of the N-terminal extensions effectively clamp the Not boxes on the Not1 scaffold (**Fig. 1b,c**).

Not1–Not2–Not5 mutations lead to growth defects *in vivo*

It has previously been shown that deletion of ~400 residues from the C terminus of Not1 is lethal in yeast[25,28]. In hindsight, these deletions generated Not1 proteins that lacked the last eight HEAT repeats (HEATs 3–10 in the Not1c structure). To test the functional importance of the Not module, we used the structural information to design point mutations that would disrupt specific interactions in the context of tagged full-length proteins.

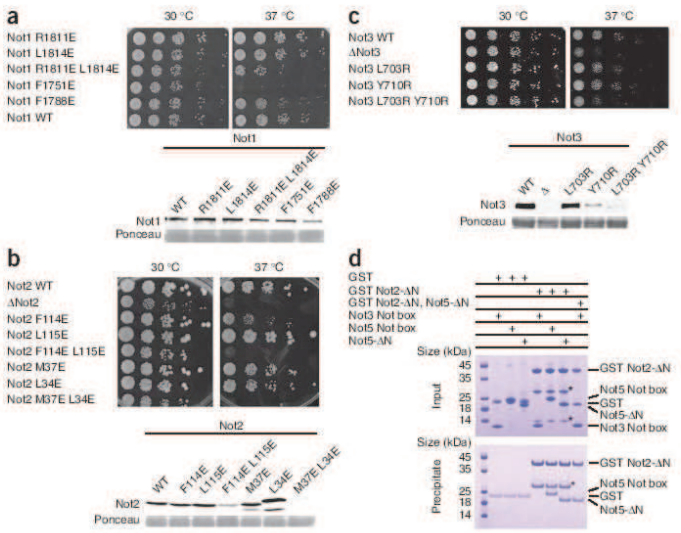

Figure 4 Analysis of mutants targeting interaction surfaces of the Not module. (**a**) Top, growth assays of Not1 mutants. Serial dilutions of cultures of strains expressing the indicated mutants incubated on YPDA medium at the indicated temperature are shown. Bottom, western blot analysis of Not1-TAP protein from cells expressing the wild-type (WT) or mutant proteins at 30 °C detected by peroxidase–antiperoxidase complex (PAP) prepared in rabbit. Ponceau staining of the membrane, used to assess equal loading in the different lanes, is shown. (**b**) Top, growth assays of Not2 mutants. Mutant strains were analyzed as for Not1 in **a**. Bottom, western blot analysis of Not2 mutant protein levels. Mutant strains were analyzed as for Not1 in **a**, with anti-VSV antibodies. (**c**) Top, growth assays of Not3 mutants. Serial dilutions of cultures of strains expressing the indicated mutant on YPDA medium containing 1 M NaCl at the indicated temperature is shown. Bottom, western blot analysis of Not3 mutant protein levels. Mutant strains were analyzed as for Not2 in **b**. (**d**) Pulldown experiment of GST Not2-ΔN with Not3 Not box, Not5 Not box and Not5-ΔN. The experiment was carried out as in **Figure 2f**. The Not3 Not box, Not5-ΔN and Not5 Not box include residues 685–800, 405–560 and 460–560 (with an N-terminal His-Z tag). The asterisks indicate a degradation product of GST Not2-ΔN.

We constructed four substitutions of Not1 residues contributing to the interaction with Not2 and Not5 (R1811E, L1814E, F1751E or F1788E) and a double mutant (R1811E L1814E) in a tandem affinity purification (TAP)-tagged plasmidic copy of the gene. R1811E and L1814E target the conserved binding site for the second segment of Not2 (**Fig. 2b**). Phe1751 is sandwiched between Not2 Trp60 and Not5 Leu388 and thus is expected to affect the binding of both proteins (**Fig. 2b**,**e**). F1788E targets the binding to the second segment of Not5 (**Fig. 2e**). Mutants were introduced in a *not1*Δ strain rescued by a *NOT1* gene (official symbol CDC39) on a *URA3*-marked plasmid. We recovered strains expressing only the mutant protein after counter selection for the *URA3* plasmid and scored the growth phenotypes at different temperatures. This revealed that Not1 R1811E or L1814E had little effect on cell growth at 30 °C and 37 °C, whereas strains expressing Not1 R1811E L1814E, F1751E or F1788E had a slow-growth phenotype at 30 °C that was exacerbated at 37 °C, particularly for the F1751E mutant (**Fig. 4a**). Western blot analyses demonstrated that the Not1 mutant proteins were expressed at comparable levels to those of the wild type (**Fig. 4a**). Coimmunoprecipitation experiments showed that the Not1 R1811E L1814E and F1751E mutants indeed blocked the interaction of Not1 with Not2 but maintained a normal interaction with Pop2 (**Supplementary Fig. 4a**).

Next, we engineered substitutions in Not2. The Not2 mutants L34E, M37E and the double mutant combining these substitutions target the Not1-binding site (**Fig. 2b**). The Not2 mutants F114E, L115E and combination of these substitutions target the binding to the Not5 Not box (**Fig. 3b**). We did not test the corresponding mutations in Not5 because of the lack of easily scorable phenotypes of Not5 mutants in our strain background (V.R. and B.S., unpublished observations). We introduced the Not2 mutants in yeast cells with the corresponding wild-type gene deleted and assayed the growth phenotypes of the resulting strains at various temperatures on appropriate medium. At 30 °C, the different mutations had no detectable effect, whereas growth of the double-mutant strains was severely impaired at 37 °C (**Fig. 4b**). Western blot analyses revealed that the double-mutant proteins were barely detectable (**Fig. 4b**). This observation that interfering with the dimerization of the Not2 Not box destabilizes Not2 is consistent with previous analyses of Not2 mutants showing protein instability with a concomitant reduction of Not5 protein level[33].

Differences between yeast and human Not3

In coimmunoprecipitation experiments, mutation on the surface of Not1 that interacts with Not2–Not5 also prevented the association with Not3 (**Supplementary Fig. 4a**), a result reinforcing the parallel between Not3 and Not5. The Not box of Not3 is predicted to have a similar fold and dimerization interface as those of Not5 or Not2. The central residues at the putative dimerization interface of the Not3 Not box are conserved, including Leu703 and Tyr710 (which are equivalent to *S. cerevisiae* Not5 Phe472 and PheF479; **Fig. 3b**,**c**). Using strategies described above, we constructed and evaluated yeast strains with the Not3 L703R and Y710R substitutions and a combination of both. As in the case of Not2, the single mutants had no growth phenotypes, whereas the growth of the double-mutant strain was severely impaired at 37 °C (**Fig. 4c**). Similarly as for the Not2 double mutants, low levels of the Not3 protein were present for the Not3 L703R Y710R double mutant (**Fig. 4c**). These results are consistent with the notion that Not3 is also destabilized if the Not-box domain is mutated at the putative dimerization interface.

Yeast Not3 and Not2 have been shown to associate *in vivo*[21,47,48] (**Supplementary Fig. 4b**), although with the caveat that the interaction might be indirect. The interaction between human Not2 and Not3 Not boxes has been shown to be direct by *in vitro* assays[19]. To test for direct interactions of the yeast proteins *in vitro*, we engineered a fragment of yeast Not3 encompassing a minimal Not-box region (residues 685–800). In contrast to that of Not5, the Not3 Not box failed to interact with GST Not2-ΔN in pulldown assays with purified proteins (**Fig. 4d**, comparison of lane 4 with lanes 5 and 6). The Not3 Not box also did not bind on top of the GST Not2-ΔN–Not5-ΔN complex (**Fig. 4d**, lane 7). A close inspection of the amino acid sequences revealed that a subset of residues at the putative dimerization interface

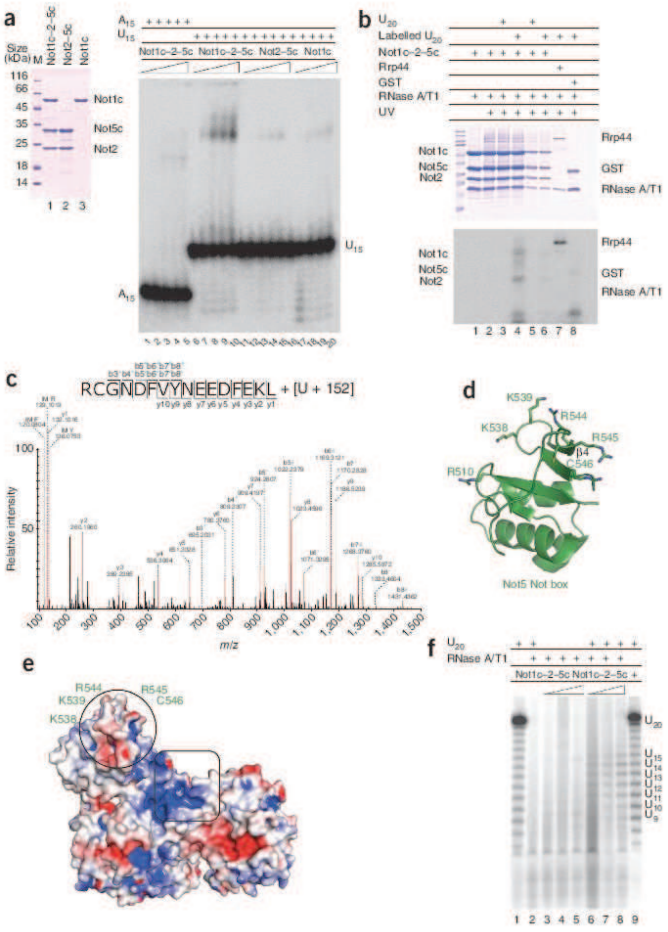

Figure 5 Not1c–Not2–Not5c binds poly(U) RNA. (**a**) Left, Coomassie-stained 13.5% SDS-PAGE gel with the protein samples used for the biochemical assays. Right, EMSA with A_{15} or U_{15} RNA (50 nM) labeled at the 5′ end with [γ-^{32}P]phosphate and incubated with increasing amounts of proteins. M, molecular weight marker. (**b**) Protein-RNA cross-linking. Proteins and γ-^{32}P body-labeled poly(U) 20-mer RNAs cross-linked under UV light and separated on 13.5% SDS PAGE are shown. The gel was stained with Coomassie blue (top) and analyzed by phosphorimaging (bottom). A/T1, mixture of RNases A and T1. (**c**) Tandem mass spectrum of Not5 residues 545–560, identifying an additional mass of 476.0338 Da corresponding to a U nucleoside with an adduct of 152 Da (associated with a cysteine). Peptide sequence and fragment ions are indicated at top. b ions with a mass shift corresponding to U-H_3PO_4 + 152 and to U + 152 are shown with an asterisk and hash mark, respectively. IM, immonium ions. (**d**) Structure of the Not5 Not box showing the position of the U–cross-linked Cys546 surrounded by a patch of positively charged residues. (**e**) Surface representation of the ternary complex colored by electrostatic potential (positive in blue and negative in red), calculated with PyMOL APBS tools. The structure is shown after a 180° rotation around a vertical axis with respect to **Figure 1b**, left. Circle, RNA-binding site; square, positively charged surface patch at the intersection of Not1, Not2 and Not5. (**f**) RNase protection assay. The protected RNA fragments obtained after treatment with a mixture of RNase A and T1 (A/T1), labeled at the 5′ end with γ-^{32}P, resolved by denaturing PAGE and analyzed by phosphorimaging are shown.

is conserved between Not5 and metazoan Not3 but diverges in *S. cerevisiae* Not3 (for example, *S. cerevisiae* Not3 Thr702, Phe706, Asn711 and Ala715 in **Fig. 3c**), thus rationalizing the different behavior of the yeast Not3 protein.

The Not1–Not2–Not5 complex is a binding platform for proteins

The interaction of the Not2 and Not5 Not boxes creates a V-shaped surface (**Fig. 1b**,**c**). In one molecule of the asymmetric unit, the β-sheet of Not2 is extended by a loop that mediates a crystal contact with the β4 strand of Not5 from a symmetry-related molecule (**Supplementary Fig. 3c**). Another interaction is present between the β4 strand of Not2 and the β-hairpin of Not1 from a symmetry copy (**Supplementary Fig. 3c**). These crystal-packing contacts are somewhat reminiscent of canonical Sm-Sm interactions and point to the Not boxes as possible interaction surfaces. Genetic evidence suggests that the Not box of Not5 interacts with Not4 (ref. 24), a conserved subunit of the complex with ubiquitin-ligase activity[49]. The Not box of Not2 interacts with ADA2, a component of the transcription-regulatory histone-acetylation complex SAGA[33]. Mutation of Not2 Arg165 has been shown to abrogate the interaction with ADA2 without affecting the integrity of the Ccr4–Not complex in yeast[33]. In the structure, Arg165 protrudes on the surface of the β-barrel and is indeed accessible to solvent (**Supplementary Fig. 5a**).

Not1–Not2–Not5 is a binding platform for poly(U) RNA

Mapping of the electrostatic potential on the molecular surface of the Not1c–Not2–Not5c complex showed patches of positively charged residues. We therefore tested whether the Not module can mediate RNA binding. In electrophoretic mobility shift assays (EMSAs), a single-stranded poly(U) 15-mer RNA (U_{15}) bound the Not1c–Not2–Not5c complex, whereas we detected no binding with a poly(A) 15-mer RNA (A_{15}) (**Fig. 5a**). The Not module recognized poly(U) RNA specifically, albeit with low affinity (in the low-micromolar range; **Supplementary Fig. 5b**). The EMSAs showed no binding of U_{15} RNA to either Not1c or the Not2–Not5c subcomplex in isolation (**Fig. 5a**), suggesting that the different portions of the Not module contribute together to RNA recognition. Indeed, after incubation of the Not1c–Not2–Not5c complex with a body-labeled U_{20} RNA and exposure to UV irradiation at 254 nm, all bands showed RNA cross-linking, which was strong in the case of Not1c and Not2 and less pronounced in the case of Not5c (**Fig. 5b**). In this experiment, Rrp44 and GST were positive and negative controls, respectively (**Fig. 5b**).

Next, we used MS to identify residues of the complex cross-linked to the U_{20} RNA. This approach is based on the detection and sequencing by LC-MS/MS of peptides conjugated to the mass of an RNA nucleotide (reviewed in ref. 50). The advantage of this approach is that RNA-contact sites are determined in an unbiased manner. The caveat is that the identification is limited to sites where the ribonucleotide is in proximity to amino acids with reactive groups (for example, thiol groups in cysteine residues) and is limited by the amounts of the cross-linked species and the complexity of the spectra. The MS analysis identified a Not5 peptide corresponding to residues 545–560, with a single U nucleoside cross-linked to Cys546 (**Fig. 5c**). In the structure, Cys546 is positioned at the top of the Not-box β-sheet and is part of a surface patch with positively charged residues (Lys515, Arg533, Arg544 and Arg545; **Fig. 5d**). This RNA-binding site (circle in **Fig. 5e**) differs from the U nucleoside–binding site of canonical Sm folds (**Supplementary Fig. 5a**) and is contiguous to a positively charged surface patch at the intersection of Not1, Not2 and Not5 (square in **Fig. 5e**). To estimate the length of the RNA-binding path on the complex, we carried out RNase protection assays. We found that fragments of 11–15 nucleotides accumulated in the presence of Not1c–Not2–Not5c (**Fig. 5f**, lanes 6–8). Fragments of this size could easily span a distance of 40–60 Å.

DISCUSSION

The core of the Not module that we investigated in this work is built around the C-terminal arm of Not1 by the cooperative binding of Not2 and Not5. The C-terminal arm of Not1 has a HEAT-repeat architecture similar to that found in the N-terminal arm[28]. It is thus possible to imagine that the two arms of Not1 might have originated from a duplication event. Not2 and Not5 interact through their C-terminal Not-box domains. At the structural level, the Not boxes resemble Sm folds. The similarity extends to their biochemical properties in terms of the ability of the Not boxes to dimerize and to bind poly(U) RNA stretches, although the interaction mechanisms have diverged from those of canonical Sm folds. The heterodimerization of the two Not boxes in the Not1–Not2–Not5 complex serves multiple purposes.

First, heterodimerization of the Not boxes tethers the N-terminal regions of Not2 and Not5, promoting their synergistic binding to Not1. Previous studies have shown that the N-terminal region of Not2 is essential for the structural integrity of the Not module because it recruits Not5 into the complex[33]. We found that the N-terminal region of Not5 is equally important in recruiting Not2. The two Not boxes thus contribute indirectly to Not1 binding by bringing the two separate N-terminal regions into spatial proximity, thus probably increasing their effective local concentration. Not-box heterodimerization is also important for the stability of the individual proteins *in vivo*, as shown by mutational analysis of Not2 as well as Not3. Yeast Not3 and Not5 are currently considered homologs with partially redundant functions[24,30]. Unexpectedly, we found that the yeast Not3 Not box has diverged from that of Not5 and does not interact with the Not2 Not box *in vitro*. The Not2-Not5 dimerization interface is instead conserved in Not2-Not3 from higher eukaryotes, thus suggesting that the protein that we currently refer to as metazoan Not3 is an ortholog of *S. cerevisiae* Not5. The identity of the direct interactions that mediate the recruitment of *S. cerevisiae* Not3 Not box in the complex is currently unclear and is an important question for future studies.

Second, the Not boxes together with Not1 form a composite platform for macromolecular interactions. Extensive data indicate that the Not module is closely connected to the transcriptional machinery and physically recruits transcription factors, such as ADA2 (ref. 33; reviewed in refs. 11,12). Evidence is also accumulating on the ability of the Not modules to mediate protein-protein interactions important for cytoplasmic mRNA metabolism. For example, in *Drosophila melanogaster* Not3 binds the translational repressor BicC[51], and in mice the C-terminal arm of Not1 binds the mRNA developmental regulator NANOS2 (ref. 52). We found that the Not module creates a composite RNA-binding surface for U nucleosides, with a specific site in the Not box of Not5. Although this RNA-binding activity of the Not module was unexpected, it rationalizes previous observations. In yeast, the decay of the Edc1 mRNA has been shown to proceed through a deadenylation-independent decapping pathway that depends on the Not proteins and on a poly-U tract in its 3′ UTR[39]. A model is conceivable in which binding of the Not module to this 3′ UTR might bring the mRNA into proximity of Dhh1, a decapping activator (known as DDX6 or RCK in metazoans) that is recruited to Ccr4–Not[27,53,54]. Interestingly, mouse Not3 has been shown to regulate the deadenylation of specific mRNAs by recruiting their 3′ UTRs[32], which also contain U-rich stretches. The emerging picture is that the Not module of the Ccr4–Not complex creates a platform for protein and nucleic acid interactions that is able to contribute to the many functions of the Ccr4–Not complex, including the degradation of specific mRNAs.

METHODS

Methods and any associated references are available in the online version of the paper.

Accession codes. Coordinates and structural factors have been deposited in the Protein Data Bank under accession code 4BY6.

Note: Any Supplementary Information and Source Data files are available in the online version of the paper.

ACKNOWLEDGMENTS

We thank the MPI Biochemistry Crystallization Facility and Core Facility. We thank F. Bonneau and C. Basquin (MPI Biochemistry) for help with biochemical assays and for **Supplementary Figure 5b**; F. Lacroute, F. Gabriel and M.C. Daugeron (Centre de Génétique Moléculaire) for yeast strains; the staff of the Swiss Light Source synchrotron for assistance during data collection; and members of our laboratories for discussions and for critical reading of the manuscript. E.C. acknowledges support from the Max Planck Gesellschaft, the European Research Council (ERC Advanced Investigator Grant 294371, Marie Curie Initial Training Network RNPnet 289007) and the Deutsche Forschungsgemeinschaft (DFG SFB646, SFB1035, GRK1721, FOR1680, CIPSM). B.S. acknowledges support from the Centre Européen de Recherche en Biologie et en Médecine (CERBM)-IGBMC, the CNRS and the Ligue Contre le Cancer (Equipe Labellisée 2011).

AUTHOR CONTRIBUTIONS

V.B. and J.B. carried out the structure determination and the *in vitro* experiments; V.R. carried out the *in vivo* experiments; K.S. and H.U. carried out the MS analysis; E.C. and B.S. supervised the project; and E.C., V.B. and B.S. wrote the manuscript.

COMPETING FINANCIAL INTERESTS

The authors declare no competing financial interests.

1. Wahle, E. & Winkler, G.S. RNA decay machines: deadenylation by the Ccr4-Not and Pan2-Pan3 complexes. *Biochim. Biophys. Acta* **1829**, 561–570 (2013).
2. Tucker, M. *et al.* The transcription factor associated Ccr4 and Caf1 proteins are components of the major cytoplasmic mRNA deadenylase in *Saccharomyces cerevisiae*. *Cell* **104**, 377–386 (2001).
3. Daugeron, M.C., Mauxion, F. & Séraphin, B. The yeast POP2 gene encodes a nuclease involved in mRNA deadenylation. *Nucleic Acids Res.* **29**, 2448–2455 (2001).

4. Sandler, H., Kreth, J., Timmers, H.T.M. & Stoecklin, G. Not1 mediates recruitment of the deadenylase Caf1 to mRNAs targeted for degradation by tristetraprolin. *Nucleic Acids Res.* **39**, 4373–4386 (2011).
5. Fabian, M.R. *et al.* Structural basis for the recruitment of the human CCR4–NOT deadenylase complex by tristetraprolin. *Nat. Struct. Mol. Biol.* **20**, 735–739 (2013).
6. Braun, J.E., Huntzinger, E., Fauser, M. & Izaurralde, E. GW182 proteins directly recruit cytoplasmic deadenylase complexes to miRNA targets. *Mol. Cell* **44**, 120–133 (2011).
7. Chekulaeva, M. *et al.* miRNA repression involves GW182-mediated recruitment of CCR4–NOT through conserved W-containing motifs. *Nat. Struct. Mol. Biol.* **18**, 1218–1226 (2011).
8. Fabian, M.R. *et al.* miRNA-mediated deadenylation is orchestrated by GW182 through two conserved motifs that interact with CCR4–NOT. *Nat. Struct. Mol. Biol.* **18**, 1211–1217 (2011).
9. Goldstrohm, A.C., Hook, B.A., Seay, D.J. & Wickens, M. PUF proteins bind Pop2p to regulate messenger RNAs. *Nat. Struct. Mol. Biol.* **13**, 533–539 (2006).
10. Suzuki, A., Igarashi, K., Aisaki, K.-I., Kanno, J. & Saga, Y. NANOS2 interacts with the CCR4-NOT deadenylation complex and leads to suppression of specific RNAs. *Proc. Natl. Acad. Sci. USA* **107**, 3594–3599 (2010).
11. Collart, M.A. & Panasenko, O.O. The Ccr4-Not complex. *Gene* **492**, 42–53 (2012).
12. Miller, J.E. & Reese, J.C. Ccr4-Not complex: the control freak of eukaryotic cells. *Crit. Rev. Biochem. Mol. Biol.* **47**, 315–333 (2012).
13. Sun, M. *et al.* Comparative dynamic transcriptome analysis (cDTA) reveals mutual feedback between mRNA synthesis and degradation. *Genome Res.* **22**, 1350–1359 (2012).
14. Liu, H.Y. *et al.* The NOT proteins are part of the CCR4 transcriptional complex and affect gene expression both positively and negatively. *EMBO J.* **17**, 1096–1106 (1998).
15. Chen, J. *et al.* Purification and characterization of the 1.0 MDa CCR4-NOT complex identifies two novel components of the complex. *J. Mol. Biol.* **314**, 683–694 (2001).
16. Albert, T.K. *et al.* Isolation and characterization of human orthologs of yeast CCR4-NOT complex subunits. *Nucleic Acids Res.* **28**, 809–817 (2000).
17. Lau, N.C. *et al.* Human Ccr4-Not complexes contain variable deadenylase subunits. *Biochem. J.* **422**, 443–453 (2009).
18. Temme, C. *et al.* Subunits of the *Drosophila* CCR4-NOT complex and their roles in mRNA deadenylation. *RNA* **16**, 1356–1370 (2010).
19. Bawankar, P., Loh, B., Wohlbold, L., Schmidt, S. & Izaurralde, E. NOT10 and C2orf29/NOT11 form a conserved module of the CCR4-NOT complex that docks onto the NOT1 N-terminal domain. *RNA Biol.* **10**, 228–244 (2013).
20. Schwede, A. *et al.* A role for Caf1 in mRNA deadenylation and decay in trypanosomes and human cells. *Nucleic Acids Res.* **36**, 3374–3388 (2008).
21. Bai, Y. *et al.* The CCR4 and CAF1 proteins of the CCR4-NOT complex are physically and functionally separated from NOT2, NOT4, and NOT5. *Mol. Cell Biol.* **19**, 6642–6651 (1999).
22. Mauxion, F., Prève, B. & Seraphin, B. C2ORF29/CNOT11 and CNOT10 form a new module of the CCR4-NOT complex. *RNA Biol.* **10**, 267–276 (2013).
23. Färber, V., Erben, E., Sharma, S., Stoecklin, G. & Clayton, C. Trypanosome CNOT10 is essential for the integrity of the NOT deadenylase complex and for degradation of many mRNAs. *Nucleic Acids Res.* **41**, 1211–1222 (2013).
24. Oberholzer, U. & Collart, M.A. Characterization of NOT5 that encodes a new component of the Not protein complex. *Gene* **207**, 61–69 (1998).
25. Maillet, L., Tu, C., Hong, Y.K., Shuster, E.O. & Collart, M.A. The essential function of Not1 lies within the Ccr4-Not complex. *J. Mol. Biol.* **303**, 131–143 (2000).
26. Draper, M.P., Liu, H.Y., Nelsbach, A.H., Mosley, S.P. & Denis, C.L. CCR4 is a glucose-regulated transcription factor whose leucine-rich repeat binds several proteins important for placing CCR4 in its proper promoter context. *Mol. Cell Biol.* **14**, 4522–4531 (1994).
27. Maillet, L. & Collart, M.A. Interaction between Not1p, a component of the Ccr4-Not complex, a global regulator of transcription, and Dhh1p, a putative RNA helicase. *J. Biol. Chem.* **277**, 2835–2842 (2002).
28. Basquin, J. *et al.* Architecture of the nuclease module of the yeast Ccr4-Not complex: the Not1-Caf1-Ccr4 interaction. *Mol. Cell* **48**, 207–218 (2012).
29. Petit, A.-P. *et al.* The structural basis for the interaction between the CAF1 nuclease and the NOT1 scaffold of the human CCR4-NOT deadenylase complex. *Nucleic Acids Res.* **40**, 11058–11072 (2012).
30. Collart, M.A., Panasenko, O.O. & Nikolaev, S.I. The Not3/5 subunit of the Ccr4-Not complex: a central regulator of gene expression that integrates signals between the cytoplasm and the nucleus in eukaryotic cells. *Cell Signal.* **25**, 743–751 (2013).
31. Neely, G.G. *et al.* A global *in vivo Drosophila* RNAi screen identifies NOT3 as a conserved regulator of heart function. *Cell* **141**, 142–153 (2010).
32. Morita, M. *et al.* Obesity resistance and increased hepatic expression of catabolism-related mRNAs in *Cnot3*$^{+/-}$ mice. *EMBO J.* **30**, 4678–4691 (2011).
33. Russell, P., Benson, J.D. & Denis, C.L. Characterization of mutations in NOT2 indicates that it plays an important role in maintaining the integrity of the CCR4-NOT complex. *J. Mol. Biol.* **322**, 27–39 (2002).
34. Ito, K. *et al.* CNOT2 depletion disrupts and inhibits the CCR4-NOT deadenylase complex and induces apoptotic cell death. *Genes Cells* **16**, 368–379 (2011).
35. Zwartjes, C.G.M., Jayne, S., van den Berg, D.L.C. & Timmers, H.T.M. Repression of promoter activity by CNOT2, a subunit of the transcription regulatory Ccr4-Not complex. *J. Biol. Chem.* **279**, 10848–10854 (2004).
36. Badarinarayana, V., Chiang, Y.C. & Denis, C.L. Functional interaction of CCR4-NOT proteins with TATAA-binding protein (TBP) and its associated factors in yeast. *Genetics* **155**, 1045–1054 (2000).
37. Lemaire, M. & Collart, M.A. The TATA-binding protein-associated factor yTafII19p functionally interacts with components of the global transcriptional regulator Ccr4-Not complex and physically interacts with the Not5 subunit. *J. Biol. Chem.* **275**, 26925–26934 (2000).
38. Deluen, C. *et al.* The Ccr4-not complex and yTAF1 (yTaf(II)130p/yTaf(II)145p) show physical and functional interactions. *Mol. Cell Biol.* **22**, 6735–6749 (2002).
39. Muhlrad, D. & Parker, R. The yeast EDC1 mRNA undergoes deadenylation-independent decapping stimulated by Not2p, Not4p, and Not5p. *EMBO J.* **24**, 1033–1045 (2005).
40. Andrade, M.A., Petosa, C., O'Donoghue, S.I., Müller, C.W. & Bork, P. Comparison of ARM and HEAT protein repeats. *J. Mol. Biol.* **309**, 1–18 (2001).
41. Marcotrigiano, J. *et al.* A conserved HEAT domain within eIF4G directs assembly of the translation initiation machinery. *Mol. Cell* **7**, 193–203 (2001).
42. Holm, L. & Rosenström, P. Dali server: conservation mapping in 3D. *Nucleic Acids Res.* **38**, W545–W549 (2010).
43. Kambach, C. *et al.* Crystal structures of two Sm protein complexes and their implications for the assembly of the spliceosomal snRNPs. *Cell* **96**, 375–387 (1999).
44. Törő, I. *et al.* RNA binding in an Sm core domain: X-ray structure and functional analysis of an archaeal Sm protein complex. *EMBO J.* **20**, 2293–2303 (2001).
45. Khusial, P., Plaag, R. & Zieve, G.W. LSm proteins form heptameric rings that bind to RNA via repeating motifs. *Trends Biochem. Sci.* **30**, 522–528 (2005).
46. Leung, A.K.W., Nagai, K. & Li, J. Structure of the spliceosomal U4 snRNP core domain and its implication for snRNP biogenesis. *Nature* **473**, 536–539 (2011).
47. Azzouz, N. *et al.* Specific roles for the Ccr4-Not complex subunits in expression of the genome. *RNA* **15**, 377–383 (2009).
48. Tarassov, K. *et al.* An *in vivo* map of the yeast protein interactome. *Science* **320**, 1465–1470 (2008).
49. Albert, T.K. *et al.* Identification of a ubiquitin–protein ligase subunit within the CCR4–NOT transcription repressor complex. *EMBO J.* **21**, 355–364 (2002).
50. Schmidt, C., Kramer, K. & Urlaub, H. Investigation of protein-RNA interactions by mass spectrometry: techniques and applications. *J. Proteomics* **75**, 3478–3494 (2012).
51. Chicoine, J. *et al.* Bicaudal-C recruits CCR4-NOT deadenylase to target mRNAs and regulates oogenesis, cytoskeletal organization, and its own expression. *Dev. Cell* **13**, 691–704 (2007).
52. Suzuki, A., Saba, R., Miyoshi, K., Morita, Y. & Saga, Y. Interaction between NANOS2 and the CCR4-NOT deadenylation complex is essential for male germ cell development in mouse. *PLoS ONE* **7**, e33558 (2012).
53. Hata, H. *et al.* Dhh1p, a putative RNA helicase, associates with the general transcription factors Pop2p and Ccr4p from *Saccharomyces cerevisiae*. *Genetics* **148**, 571–579 (1998).
54. Coller, J.M., Tucker, M., Sheth, U., Valencia-Sanchez, M.A. & Parker, R. The DEAD box helicase, Dhh1p, functions in mRNA decapping and interacts with both the decapping and deadenylase complexes. *RNA* **7**, 1717–1727 (2001).

ONLINE METHODS

Protein purification. All the proteins were cloned and expressed individually in *E. coli* BL21(DE3) pLysS cells (Stratagene) in TB medium with IPTG induction overnight at 18 °C. Not1$_{1541–2093}$ (Not1c), Not5 FL and Not5$_{298–560}$ (Not5c) were expressed with an N-terminal His-SUMO tag (cleavable with the Senp2 protease). The Not1 C-terminal arm (starting at 1348), Not2 FL and Not5$_{460–560}$ (Not5 Not box) were expressed with an N-terminal His-Z tag (cleavable with TEV protease). Not3$_{685–800}$ (Not3 Not box) was expressed with an N-terminal His tag (cleavable with TEV protease). The cells were lysed in buffer A (50 mM sodium phosphate buffer, pH 7.5, 250 mM NaCl and 20 mM imidazole) by sonication. The lysates were cleared by centrifugation and were loaded on a 5-ml His-trap column (GE Healthcare). The column was washed with buffer B (50 mM phosphate buffer, pH 6.5, 1 M NaCl, 20 mM imidazole, 50 mM KCl, 10 mM $MgSO_4$ and 2 mM ATP) and with buffer A. The proteins were eluted by a gradient of buffer A and buffer C (buffer A supplemented with 500 mM imidazole). Except for the Not5 Not box and Not2, all other proteins were dialyzed overnight in gel-filtration buffer (without DTT) in the presence of TEV or Senp2 proteases and were then applied to the His-trap column to remove the cleaved tag (second affinity step). The proteins were further purified by size-exclusion chromatography in the gel-filtration buffer (20 mM Tris-Cl buffer, pH 7.5, 250 mM NaCl and 2 mM DTT). The complex of Not1c–Not2–Not5c was formed by mixing the purified protein in a 1:1.25:1 molar ratio and was incubated with TEV protease overnight at 4 °C to cleave the N-terminal His-Z tag of Not2. The complex was applied onto the 5-ml His-trap column (GE Healthcare) to remove the cleaved tag and was purified by gel filtration (Superdex 200 16/60, GE Healthcare) in the gel-filtration buffer.

For the pulldown assays, Not5c, Not5-ΔN and Not2-ΔN were expressed as N-terminal His-GST fusion proteins, whose tags were cleavable with 3C protease. Not2, Not5c and Not5-ΔN were affinity purified with a 5-ml His-trap column (GE Healthcare) as described above. Not2-ΔN was affinity purified at a pH of 8.5 (with buffer A and C at pH 8.5) instead of pH 7.5. Not2–Not5c, Not2-ΔN–Not5c and Not2–Not5-ΔN complexes were formed by mixing a 1:1.5 molar ratio of the larger to smaller protein and dialyzed in gel-filtration buffer (without 2 mM DTT) in the presence of 3C protease and TEV protease. The dialyzed proteins were subjected to a second His-affinity purification with a 5-ml His-trap column (GE Healthcare) and subsequent incubation with glutathione-agarose beads (Protino) for 2 h at 4 °C to remove the GST-tag contamination. The proteins were then purified by gel filtration (Superdex 75 10/30, GE Healthcare) in gel-filtration buffer. Not1c-GST was affinity purified as described above. The protein was dialyzed against heparin buffer A (20 mM Tris, pH 7.5, and 100 mM NaCl), applied onto the 5-ml heparin column (GE Healthcare) and purified with a gradient elution with heparin buffer A and heparin buffer A supplemented with 1 M NaCl. Not1c-GST was further purified by gel filtration (Superdex 200 10/30, GE Healthcare). The Not3 Not box was expressed as TEV protease–cleavable His_6 fusion protein and purified in a similar way as mentioned above.

For the RNA-binding experiments, Not2 and Not5c were expressed and purified as individual proteins as described above. The Not2–Not5c complex was formed by mixing the proteins in a 1.25:1 molar ratio and subsequent overnight incubation with TEV protease. The cleaved protein was subjected to His-affinity purification to remove the cleaved tag and a subsequent heparin-column purification. The complex was further purified by gel filtration (Superdex 200 16/60, GE Healthcare). Not1c was expressed and purified as above, with an additional step of heparin purification included after the second His-affinity step. Not1c–Not2–Not5c was purified by mixing Not1c and Not2–Not5c in a 1:1.25 molar ratio and subsequent gel filtration (Superdex 200 16/60, GE Healthcare).

Limited proteolysis experiment. 0.6 mg/ml of the Not1Δ1347–Not2–Not5 complex was incubated with elastase (Roche) at a 1:10 (w/w) enzyme/protein ratio for 30 min on ice. The products of the proteolysis were identified by N-terminal sequencing and MS analysis. The interacting core complex was identified by size-exclusion chromatography of the proteolyzed sample.

Crystallization and structure solution. The Not1c–Not2–Not5c complex was concentrated to 16 mg/ml and crystallized at room temperature in 8.5% (w/v) PEG 8000, 100 mM MES, pH 6.5, and 200 mM calcium acetate. The mercury derivative was prepared by cocrystallization of a solution of Not1c–Not2–Not5c with ethyl mercury phosphate (EMP) at 0.55 mM final concentration. The crystals were frozen in the presence of 20% glycerol as cryoprotectant. X-ray data were collected at 100 K at the SLS synchrotron (PXII and PXIII beamlines), with tuning of the wavelength at the Hg edge in the case of the EMP-containing crystals for SAD data collection. The data were processed with XDS[55]. The crystals belong to a monoclinic space group ($P2_1$) with two molecules per asymmetric unit. We used PHENIX.autosol[56] for phasing and Buccaneer[57] for the initial automatic model building. We completed the model with iterative rounds of manual model building with Coot[58] and restrained refinement with PHENIX[56]. The final model has 97.3% residues in the most-favored regions of the Ramachandran plot, as calculated with MolProbity[59].

Pulldown assays. For the experiments in **Figure 2f**, 50 pmol of bait (GST or GST-Not1c) were incubated with 100 pmol of prey (Not2–Not5c, Not2-ΔN–Not5c and Not2–Not5-ΔN) for 1 h at 4 °C in 40 mM Tris, pH 7.5, 150 mM NaCl, 2 mM DTT, 12.5% (v/v) glycerol and 0.1% (w/v) NP-40 (binding buffer). The protein mix was incubated with 20 µl of GSH-agarose beads (Protino) for 1 h with gentle rocking at 4 °C. The resin was washed three times with the binding buffer, and the proteins were eluted in 15 µl of binding buffer containing 100 mM glutathione. Input and precipitates were mixed with SDS loading dye, resolved on 4–12% Bis-Tris NuPAGE gel (Invitrogen) with MES as running buffer, and visualized by Coomassie-blue staining. A similar protocol was used for the GST pulldown assays in **Figure 4d** with 40 mM Tris, pH 8.5, 100 mM NaCl, 2 mM DTT and 12.5% (v/v) glycerol as binding buffer.

Sequence alignments and superpositions. All the sequence alignments were done with ClustalW[60] and ALINE[61], and the structural superpositions were done with SSM in Coot[58]. The r.m.s. deviations reported are from the output of Coot. Structure-based sequence alignment was done in STRAP[62] with the Aligner3D method and manually edited in ALINE.

Yeast strains. Yeast strains used in this study are all derivatives of W303 (*ade2-1, can1-100, leu2-3,112, his3-11,15, ura3-1, trp1-1*). Genes differing from W303 are as follows: T26N28 (*MATa, Δtrp1, ΔNOT1::HIS3 pFL38 (NOT1)*), BSY1110 (*MATa, Δtrp1, not2::HISMX6*), BSY1111 (*MATa, Δtrp1, not3::HISMX6*), BSY1230 (*MATa, Δtrp1, NOT3-VSV, NOT2-3HA::hisMX6*), BSY1231 (*MATa, Δtrp1, POP2-VSV, NOT2-3HA::hisMX6*), BSY1240 (*MATa, Δtrp1, NOT3-TAP::TRP1$_{Kl}$, POP2-VSV, NOT4-HA::hisMX6*) and BSY1242 (*MATa, Δtrp1, NOT3-TAP::TRP1$_{Kl}$, POP2-VSV, NOT2-HA::hisMX6*).

Coprecipitation assays. Protein extract preparation and coimmunoprecipitation were performed as described previously[28].

Mutant analyses. Mutations in Not1, Not2 and Not3 were constructed in plasmids pBS4806 (ref. 28) (Not1-TAP), pBS4968 (Not2-VSV) and pBS4975 (Not3-VSV) by one or multiple rounds of site-directed mutagenesis. The presence of the desired mutation was ascertained by sequencing. The resulting plasmids were introduced into yeast strains with the lithium acetate transformation procedure. Plasmid shuffling, growth assays, protein extraction and western blot analyses were performed with standard procedures as previously described[28].

Electrophoretic mobility shift assays. Proteins at 3, 10, 13 and 20 µM concentration (30, 100, 130 and 200 pmol, respectively) were incubated with 50 nM (0.5 pmol) of 5′-labeled RNA (A_{15} or U_{15}) at 4 °C overnight in 20 mM HEPES, pH 7.5, 5 mM EDTA, 0.1% NP-40 and 2 mM DTT (EMSA buffer). The reaction mixtures were complemented with gel-filtration buffer to a final NaCl concentration of 54 mM, resolved on a 6% (w/v) native PAGE and visualized by phosphorimaging.

RNA cross-linking. 200 pmol (20 µM) of Not1–Not2–Not5c complex were incubated with 2.5 pmol (250 nM) of body-labeled U_{20} RNA overnight in EMSA buffer at 4 °C. The cross-linking was performed by irradiation of the mix at a wavelength of 254 nm for 5 min on ice. The mixture was then treated with 1% SDS and 0.5 µl of RNase A/T1 mixture at 37 °C for 5 min. The samples were heated with SDS loading dye at 70 °C for 2 min, separated on 13.5% (w/v) SDS-PAGE gel and visualized by phosphorimaging and Coomassie-blue staining.

Mass spectrometry. *UV-induced protein-RNA cross-linking and enrichment of cross-linked peptides.* UV cross-linking and enrichment of cross-linked peptides was performed according to the established protocols described in ref. 63. Briefly, 1 nmol of the single-stranded U_{15} RNA oligonucleotide and 1 nmol of

Not1c–Not2–Not5c complex were mixed in a 1:1 molar ratio, and the total reaction volume was brought to 100 µl in 20 mM HEPES, pH 7.5, 50 mM NaCl, 2 mM DTT and 5 mM EDTA. The mixture was incubated on ice overnight for complex formation. The samples were then transferred to black polypropylene microplates (Greiner Bio-One) and irradiated at 254 nm for 10 min. After ethanol precipitation, the samples were denatured in 4 M urea and 50 mM Tris-HCl, pH 7.9, and digested for 2 h at 52 °C with 1 µg RNase A (Ambion, Applied Biosystems). After RNA digestion, proteolysis with trypsin (Promega) was performed overnight at 37 °C. The sample was desalted on an in-house–prepared C18 (Dr. Maisch GmbH) column, and the cross-linked peptides were enriched on an in-house–prepared TiO_2 (GL Sciences) column with the protocol described in ref. 63. The samples were dried and then resuspended in 10 µl sample solvent (5% v/v ACN and 1% v/v FA) for MS analysis.

Nano–liquid chromatography and MS analysis. 5 µL of the above sample was injected onto a nano–liquid chromatography system (Agilent 1100 series, Agilent Technologies) including a C18 trapping column of length ~2 cm and inner diameter 150 µm, in line with a C18 analytical column of length ~15 cm and inner diameter 75 µm (both packed in house; C18 AQ 120 Å 5 µm, Dr. Maisch GmbH). Analytes were loaded on the trapping column at a flow rate of 10 µL/min in buffer A (0.1% v/v FA) and subsequently eluted and separated on the analytical column with a gradient of 7–38% buffer B (95% v/v acetonitrile and 0.1% v/v FA) with an elution time of 33 min (0.87%/min) and a flow rate of 300 nL/min. Online ESI-MS was performed with an LTQ-Orbitrap Velos instrument (Thermo Scientific), operated in data-dependent mode with a TOP10 method. MS scans were recorded in the m/z range of 350–1,600 and for subsequent MS/MS the top ten most-intense ions were selected. Both precursor ions as well as fragment ions were scanned in the Orbitrap. Fragment ions were generated by higher-energy collision dissociation (HCD) activation (normalized collision energy = 40) and recorded from m/z = 100. As precursor ions as well as fragment ions were scanned in the Orbitrap, the resulting spectra were measured with high accuracy (<5 p.p.m.), both in the MS and MS/MS level.

Data analysis. The MS .raw files were converted into the .mzML format with msconvert[64]. Protein-RNA cross-links were analyzed with OpenMS[65,66] and OMSSA[67] as a search engine. Data-analysis workflows were assembled as described[11]. The high-scoring cross-linked peptides were manually annotated for confirmation. Protein-RNA interactions between the complex and poly(U) RNA were analyzed with UV-induced protein-RNA cross-linking followed by MS. Peptide RCGNDFVYNEEDFEKL in Not5 (position 545–560) was observed carrying an additional mass of 476.0338 Da corresponding to U nucleoside with an adduct of 152. The y-ion series could be observed from 1 to 10, unshifted. In contrast, b ions from b3 until b8 were observed with a mass shift corresponding to U-H_3PO_4 and 152 adduct (**Fig. 5c**). Also, the b ions from b5 until b8 were observed with a mass shift corresponding to U and 152. We have always observed that the 152 adduct is observed as a shift associated with cysteine, which could be the amino acid that is cross-linked. In the corresponding figure (**Fig. 5c**), the b ions that were observed with a mass shift corresponding to U-H_3PO_4 + 152 and to U + 152 are shown with an asterisk (*) and hash (#), respectively, and the immonium ions with IM.

RNase protection assays. 100, 150 and 200 pmol (10, 15 and 20 µM) of Not1c–Not2–Not5c complex were incubated with 0.5 pmol (50 nM) of U_{20} RNA in the EMSA buffer overnight at 4 °C. The reaction mixtures were treated with 0.5 µl of RNase A/T1 mix for 30 min at 4 °C. RNA was purified with phenol/chloroform/isoamyl alcohol extraction and ethanol precipitation. The purified RNA was 5′ labeled with [γ-^{32}P]ATP with T4 polynucleotide kinase, repurified by phenol/chloroform/isoamyl alcohol extraction and ethanol precipitation, separated on 22% (w/v) denaturing PAGE with 5 M urea and visualized by phosphorimaging.

Fluorescence anisotropy. 5′-6-carboxy-fluorescein (6-FAM)-labeled U_{15} RNA was used in fluorescence anisotropy measurements at 20 °C with Genios Pro (Tecan). RNA was 9.1 nM at final concentration and was incubated with varying concentrations of Not1c–Not2–Not5c complex in the gel-filtration buffer supplemented with 10 mM EDTA. We used 250 mM NaCl in the buffer for the measurement because the protein was not stable at 100 or 150 mM salt in such high concentration at 20 °C. The excitation and emission wavelengths were 485 nm and 535 nm, respectively. Each titration point was measured three times with ten reads with an integration time of 40 µsec. The data were analyzed by nonlinear regression fitting with Origin (OriginLab; http://www.originlab.com/).

55. Kabsch, W. Integration, scaling, space-group assignment and post-refinement. *Acta Crystallogr. D Biol. Crystallogr.* **66**, 133–144 (2010).
56. Adams, P.D. *et al.* PHENIX: a comprehensive Python-based system for macromolecular structure solution. *Acta Crystallogr. D Biol. Crystallogr.* **66**, 213–221 (2010).
57. Cowtan, K. The Buccaneer software for automated model building. 1. Tracing protein chains. *Acta Crystallogr. D Biol. Crystallogr.* **62**, 1002–1011 (2006).
58. Emsley, P., Lohkamp, B., Scott, W.G. & Cowtan, K. Features and development of Coot. *Acta Crystallogr. D Biol. Crystallogr.* **66**, 486–501 (2010).
59. Davis, I.W., Murray, L.W., Richardson, J.S. & Richardson, D.C. MOLPROBITY: structure validation and all-atom contact analysis for nucleic acids and their complexes. *Nucleic Acids Res.* **32**, W615–W619 (2004).
60. Larkin, M.A. *et al.* Clustal W and Clustal X version 2.0. *Bioinformatics* **23**, 2947–2948 (2007).
61. Bond, C.S. & Schüttelkopf, A.W. ALINE: a WYSIWYG protein-sequence alignment editor for publication-quality alignments. *Acta Crystallogr. D Biol. Crystallogr.* **65**, 510–512 (2009).
62. Gille, C. & Frömmel, C. STRAP: editor for structural alignments of proteins. *Bioinformatics* **17**, 377–378 (2001).
63. Kramer, K. *et al.* Mass-spectrometric analysis of proteins cross-linked to 4-thio-uracil- and 5-bromo-uracil-substituted RNA. *Int. J. Mass Spectrom.* **304**, 184–194 (2011).
64. Kessner, D., Chambers, M., Burke, R., Agus, D. & Mallick, P. ProteoWizard: open source software for rapid proteomics tools development. *Bioinformatics* **24**, 2534–2536 (2008).
65. Sturm, M. *et al.* OpenMS: an open-source software framework for mass spectrometry. *BMC Bioinformatics* **9**, 163 (2008).
66. Bertsch, A., Gröpl, C., Reinert, K. & Kohlbacher, O. OpenMS and TOPP: open source software for LC-MS data analysis. *Methods Mol. Biol.* **696**, 353–367 (2011).
67. Geer, L.Y. *et al.* Open mass spectrometry search algorithm. *J. Proteome Res.* **3**, 958–964 (2004).

doi:10.1038/nsmb.2686

2.1.2 The Not1 essential function(s) and potential structural heterogeneity of the CCR4-NOT complex *in vivo*

The yeast CCR4-NOT complex has two peculiar features:

- First, the yeast CCR4-NOT complex contains one, and only one, subunit essential for yeast viability, namely the scaffold subunit Not1. This is surprising because in many complexes essential for vegetative life (such as polymerase II, translation initiation factors, cell-cycle dependent kinases…) deletion of all or most of the complex subunits results in similar or related phenotypes. Some exceptions are obviously known, particularly when some subunits are encoded by duplicated genes. This feature makes the yeast CCR4-NOT complex markedly different from many other protein assemblies;
- The yeast CCR4-NOT complex has two paralogous subunits, Not3 and Not5, whereas a single homologue is found in other species such as mammals. This situation suggests that the two proteins probably bind to the same Not1 surface and raise questions whether the two subunits are present simultaneously in the complex.

The requirement of yeast Not1 for viability could suggest that Not1 by itself has some particular functionality that makes it essential. Alternatively, Not1 could coordinate various activities that are each independently non-essential but that are simultaneously required for cell growth. To gain insight into these questions and define the region of Not1 essential for cell viability, I built several deletion mutants, trimming the Not1 sequence from either the N-terminus or the C-terminus, and also by deleting some internal regions. The ability of the resulting construct to complement a yeast *not1* deletion mutant was tested using a plasmid shuffling assay. This test allowed me to map the minimal Not1 sequence sufficient to carry out its essential function.

Yeast Not1 is 2108 amino acid long protein, which can be divided in at least 4 domains, based on published structural studies and sequence comparisons:

- amino acids (aa) 1-750: N-terminal HEAT repeat domain;
- aa750-1000: Caf1-Ccr4 interaction MIF4G-like domain;
- aa 1500 – 2108: Not2-Not3/5 interaction HEAT-repeat domain, termed Not1-domain;

- and 1000 – 1500 aa residues linker domain, which is believed mediates interaction with the rest CCR4-NOT subunits, such as Caf40 and Caf130.

Thus, taking into account these regions involved in protein interaction , I constructed the deletion mutants (Figure 36). To allow me to monitor expression on the mutant proteins, these constructs were built in a context where Not1 was carrying a TAP tag.

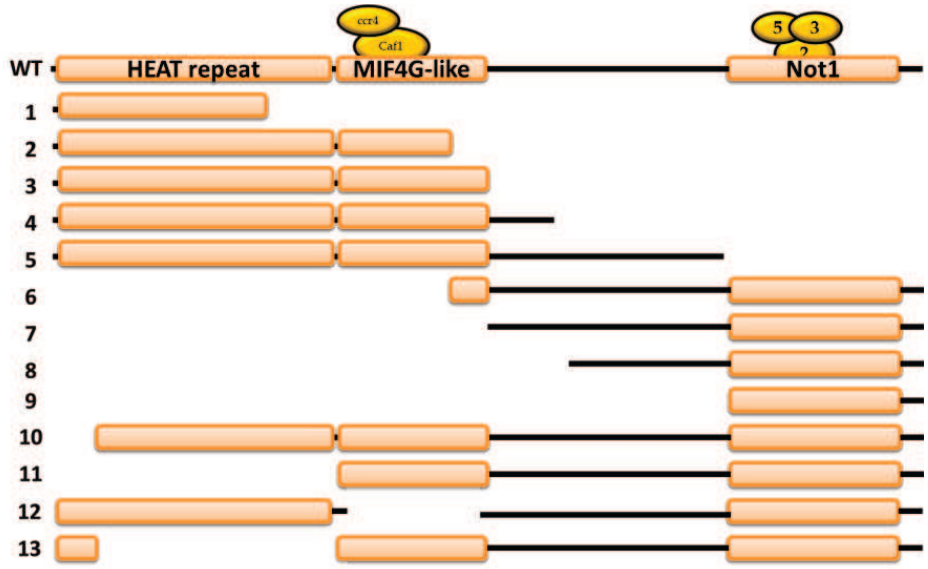

Figure 36. 13 different yeast Not1 deletion mutants (numbers 1 - 13) constructed in this study and analysed for their ability to rescue the lethality of a not1 deletion. Full length wild type Not1 protein is represented as a diagram with the three main domains indicated: the N-terminal HEAT repeat domain (aa 1 – 750); the central MIF4G-like domain (aa 750-1000), and the C-terminal Not1-domain (aa 1500 – 2108).

The yeast plasmid shuffling strategy that was used to test the complementation activity of these plasmids is described below. Briefly, a yeast strain carrying a chromosomal *not1* deletion (BMA64Δnot1) and expressing full-length Not1 from a centromeric plasmid with a URA3 selection marker, was transformed with plasmids carrying the various *not1* deletion mutants present on a TRP1 marked backbone. After transformation, several colonies were picked, subcloned on selective media, and replicated on plates containing 5-Fluoroorotic acid (FOA). 5-FOA is toxic to yeast cells that synthesize the enzyme orotidine-5'-phosphate decarboxylase encoded by the URA3 gene. Such cells are therefore unable to grow on 5-FOA-containing media. Thus, this chemical allows us to recover yeast cells that have lost the URA3-marked plasmid (Figure 37). As *NOT1* is essential, the appearance of positive clones

after FOA selection indicates that the *not1* mutant carried by the *TRP1* marked plasmid is functional. In contrast, if no clone is recovered, one can conclude that the *not1* mutant was not sufficient for yeast growth.

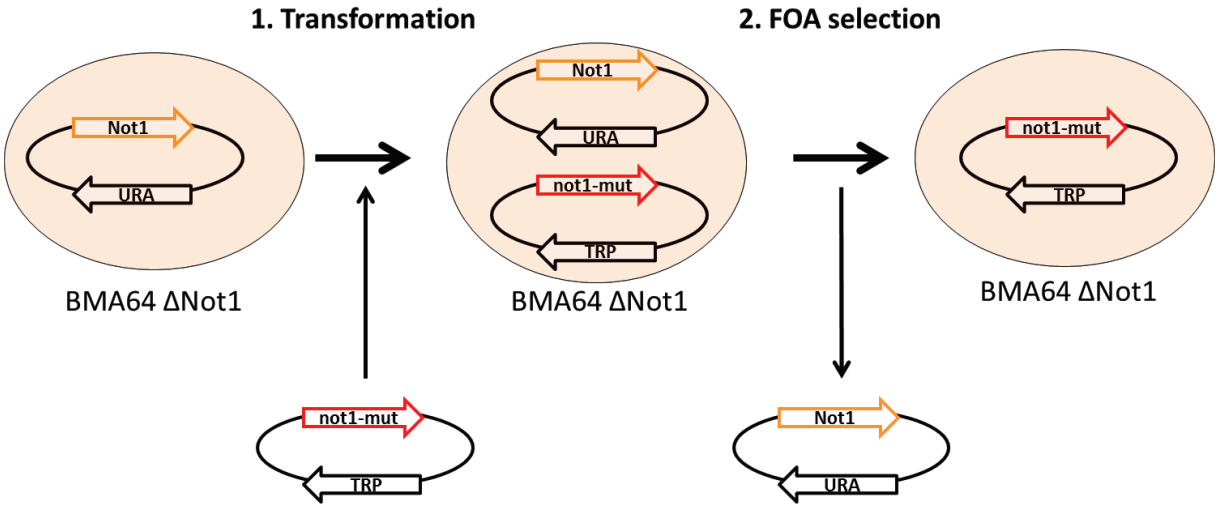

Figure 37. Yeast FOA-based plasmid shuffling assay.

Interestingly, Not1 mutants that lack either the ability to form the Caf1-Ccr4 module (mutants 1, 6-9, 11 and 12, Figure 34) or the Not module (mutants 1-5, Figure 36), are non viable. In contrast, deletion of the N-terminal HEAT-repeat domain (mutants 10, 11, 13, Figure 36) has little or no effect on yeast viability. The smallest functional Not1 corresponds to Not1 mutant 11 and carries interaction surfaces to form both the Caf1-Ccr4 and Not2-3-5 modules. Although additional constructs could be tested, this observation suggests that the Not1 essential function may be to keep these two interaction modules linked together by one interacting scaffold protein (Figure 38).

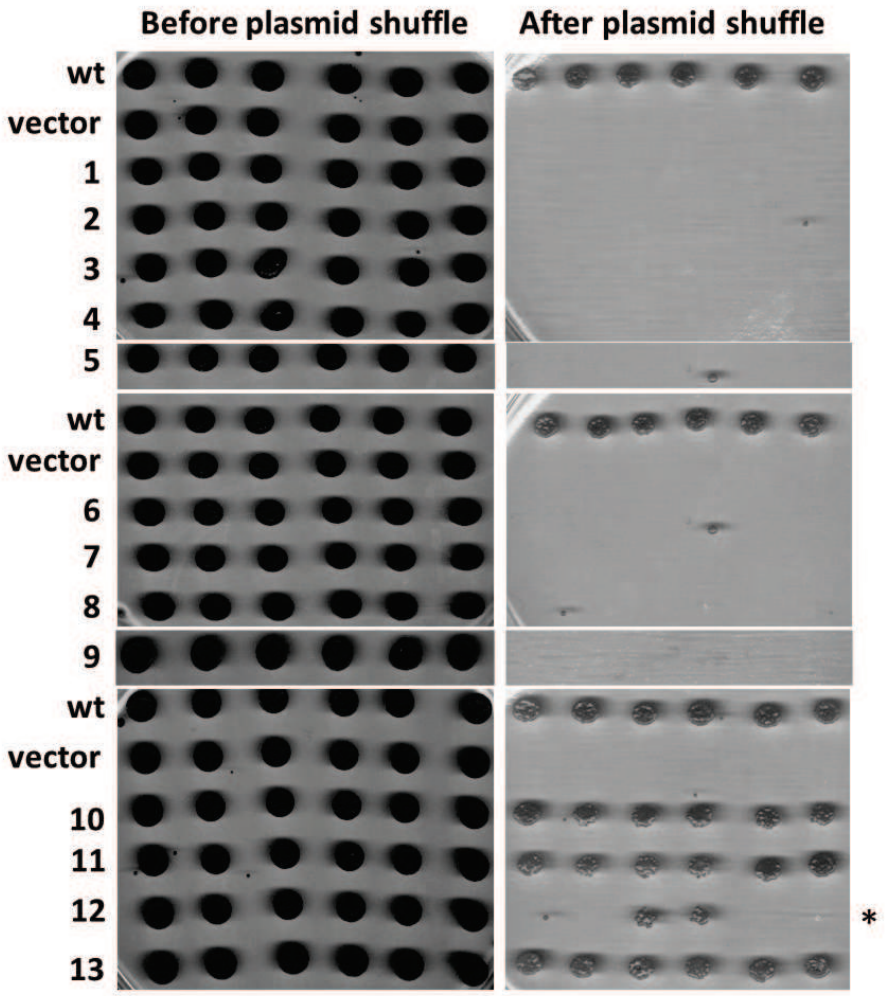

Figure 38. Result of the plasmid shuffling assay. The Not1 deletion mutants (numbers correspond to Figure 32) were tested for their ability to complement an yeast Δnot1 strain as described in the text. * corresponds to yeast revertant clones, as confirmed by PCR.

In order show that the observed effects were not due to instability of the deletion mutant protein, I checked the expression levels of each deletion in a wild type yeast strain background (where wild type Not1 is also present), after transformation with the various plasmids. Western blot analysis using the TAP-tag indicated that all deletion mutants are well expressed (Figure 39). This indicated that the effects observed above result from the function of Not1 and not from Not1 instability

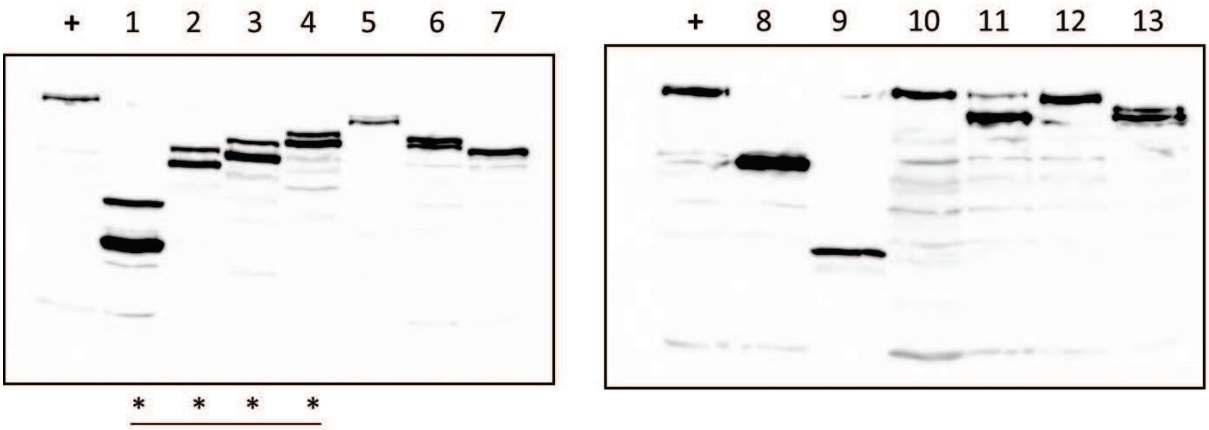

Figure 39. Protein expression analysis of Not1 deletion mutants (numbers correspond to Figure 32). *: corresponds to mutants 1-4 for which the tagged protein migrate as two bands.

During the mutant protein expression analysis I observed that several Not1 C-terminal truncations, particularly mutants 1-4, appeared as two bands. It is possible that this difference is present in other construct containing the N-terminal extremity of the protein but masked by the larger size of the polypeptide (constructions 5, 12 and 13). This observation suggests that protein might be post-translationally modified or that it has alternative translation initiation sites (possibly due to alternative transcription). To determine the basis for the observed differences in migration, I performed a TAP-purification of Not1 mutant 1 (Figure 40A). The two bands were cut out and analysed by mass-spectrometry. The results revealed a clear difference in peptide coverage for the two bands (Figure 40B), suggesting that at least two different Not1 isoforms with different N-termini exist. While I cannot rule out proteolytic processing, the Not1 protein primary indicate the presence of a possible alternative translation start site at position 163.

In summary, the Not1 mutant analysis allows us to suggest that the essential Not1 function could be to bring two interaction modules: the Caf1-Ccr4 and the Not modules, into close proximity. However, at this stage, it is not possible to rule out other hypotheses involving other subunits of the CCR4-NOT complex (Caf40, Not4,…), or as yet unknown partners of Not1. These experiments also revealed the presence of Not1 protein isoforms *in vivo* suggesting that different CCR4-NOT complexes might exist in yeast cells. Both isoforms of the complex would most likely be functional, as the shorter Not1 isoform lacks a in non-

essential region of Not1 sequence. The presence of different Not1 isoforms prompted me to investigate whether complexes of different protein composition could coexist (see below).

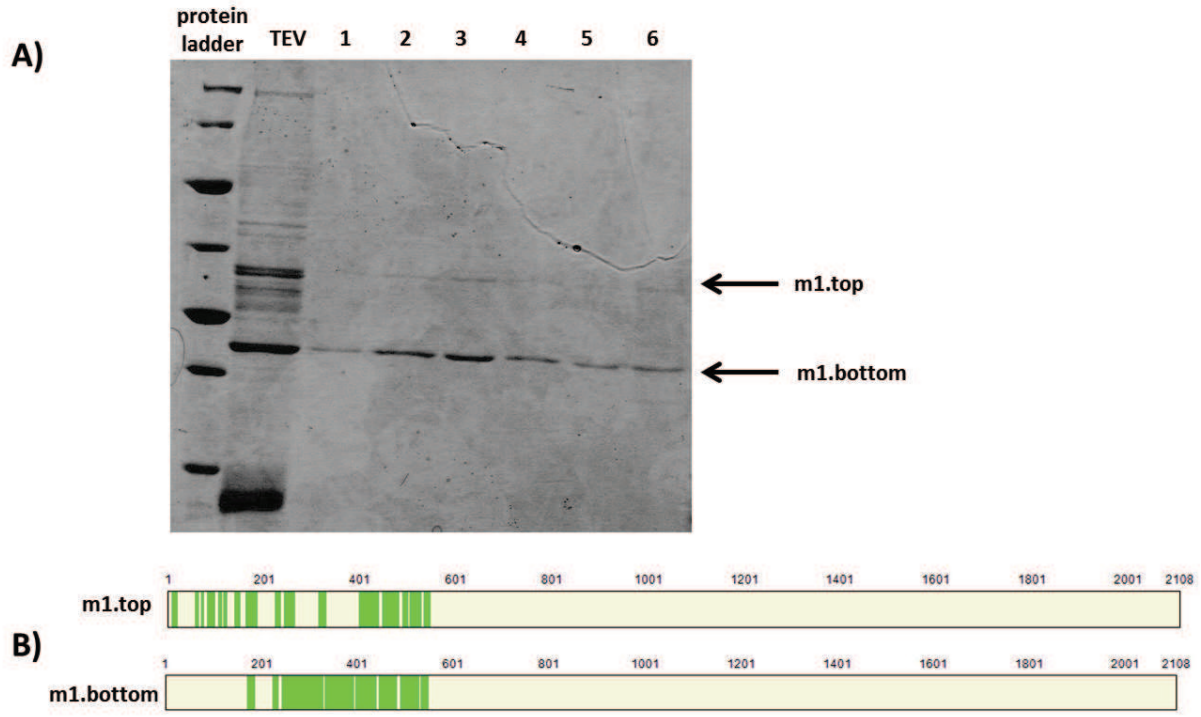

Figure 40. A) TAP purification of Not1 deletion mutant 1, A Coomassie blue stained gradient polyacrylamide gel is shown. Lane TEV: TEV-protease cleavage elution fraction after the first binding with IgG beads; lanes 1 – 5: elution fractions after second affinity chromatography on calmoduline beads; lane 6: 1%SDS elution fraction after the two purification steps. Two protein bands (m1.top and m1.bottom) were further analyzed by mass spectrometry. B) Location of the peptides detected by mass-spectrometry (green) on a 1 – 2108 ruler representing Not1 sequence length. The two protein bands appears to be different in the first 200 aa residues suggesting that the different protein isoforms could result from alternative translation start-site usage. (A methionine is present at residue 163 of the longest protein.)

To gain further insight into the organization of the CCR4-NOT complex and of the subunit interaction network, I performed binary two-hybrid interaction assays between the different protein pairs (with the exception of the non-conserved Caf130 subunit for which the plasmids were not obtained). The two-hybrid assay that I used is based on GAL4 transcription activation system (Figure 39). GAL4 is a transcription enhancer, and is composed of two-domains: an N-terminal DNA-binding domain, which specifically binds to its cognate DNA sequence, called the upstream activation sequence (UAS); and a C-terminal activation domain, which enhances the target gene expression by stimulating RNA

polymerase II. The link between the two Gal4 domains is functionally, but not structurally, important and can be replaced by other sequences or can even be substituted by two interacting domains. Expressing the two proteins, the first protein of interest linked to the GAL4-activation domain (AD, Prey) and the second fused to the GAL4 DNA-binding domain (DB, Bait), in yeast it reconstitutes a functional Gal4 transcription factor if the two proteins interact in the yeast nucleus. If a LacZ gene encoding β-galactosidase driven by a promoter containing GAL4-UAS is present in the same strain, interaction of the two test proteins will drive LacZ transcription and β-galactosidase production (Figure 41). The latter can be easily monitored in cell lysates using sensitive activity assays. Normalization of the resulting signal to yeast cell quantities (assessed by optical density reading) allows one to gain some evidence for protein interaction. It is important to stress, however, that this assay is not foolproof and that artefacts can limit interpretation (for example non-functional fusion protein or fusion of a protein containing a transcription activation domain to the Gal4 DAN binding domain).

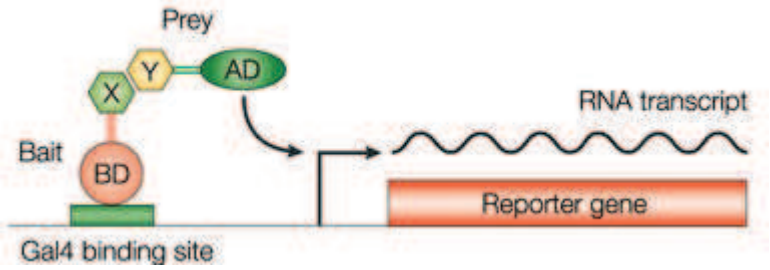

Figure 41. Principle of the two-hybrid interaction assay in yeast using β-galactosidase as a readout. The reporter gene (LacZ encoding β-galactosidase in my case) is expressed under the control of a Gal4 UAS (Gal4 binding site). If two proteins (X and Y) interact, this brings the Gal4-activation domain close to the RNA polymerase II transcription start site, thus enhancing transcription of reporter gene (Stynen et al. 2012).

Pairwise testing of different combinations of subunits of the CCR4-NOT complex in the two-hybrid interaction assay gave insight into the organization of the complex (Table 1). Significant interactions between the Caf1 and Ccr4 deadenylase subunits and the Not1 scaffold were observed. This confirmed their association in the complex. Strong β-galactosidase activity (1147842 and 317956 units in Not5-Not2 and Not5-Not2 respectively) was detected for interaction between Not2 and Not5, supporting a direct interaction between these proteins. However, association of Not2 with the paralogous protein Not3 was

not easily detected, and if so, only in one orientation, perhaps due to low levels of protein expression. Unexpectedly, a significant Not2-Not2 interaction was observed, as testified by a relatively high normalized β-galactosidase activity (9886 units comparing to 1163 and 157 in control measurements). This could suggest that Not2 might form dimers in the CCR4-NOT complex. Alternatively, this result could be artificial and result from the propensity of Not-Box to form dimers. Finally a significant β-galactosidase activity was observed for the Not1 and Caf40 pair (only in one direction, Caf40-Not1), supporting the association of these two subunits within the complex. The detection of this signal allowed me to delineate the region of Not1 interacting with Caf40.

AD / DB	empty-AD	Not1	Not2	Not3	Not4	Not5	Caf1	Ccr4	Caf40
EMPTY-DB	30	1378	157	840	169	200	47	68	60
Not1	10270 12081	11026	7954 12621	5031 9745	2818 9515	5499 7920	77634	37255	24740
Not2	1163	1946	9886	2147	1306	317956	5130	977	27951
Not3	1752	1289	800	742	552	362	7254	670	1811
Not5	2077	1506	1147842	2348	2384	2262	2185	1885	1227
Caf1	22948	89794	53467	15442	12849	14999	21282	198460	15419
Ccr4	383	19938	627	364	719	453	118811	344	539
Caf40	4006 5898	49366	26520	3666	4535	4796	11273	8125	4420

Table 1. Measurement of normalized β-galactosidase activity in two-hybrid assay for CCR4-NOT complex subunits. Horizontal rows represent proteins linked to the DNA-binding domain, while vertical columns indicate proteins fused to the activation domain. The background for each protein pair is determined by two control measurements: protein1 with empty vector containing the AD (first column numbers) and empty vector with DB together with protein2 (first row numbers). Different colours correspond to the intensity of normalized β-galactosidase activities compared to the signals of background level. Thus, light yellow means around a two-fold difference in the signal compared to highest of the two background signals. Dark yellow is for signals at least three-fold above background. All measurements were done with three biological replicates and the signal means are presented. Variability was less then 5%.

Using the same assay to map the Caf40 binding region in Not1, I tested several deletion mutants of Not1 (deletion of N-terminal 980, 1080, 1695 amino acids, Table 2) in combination with full length Caf40. The β-galactosidase signals observed between Caf40 and

the Not1 N-terminal truncation mutants Not1 Δ(1-980), Not1 Δ(1-1080) together with the absence of signal for the Caf40 - Not1 Δ(1-1680) pair, suggests that the central part of Not1, locaed between amino acid 1080 – 1680 is required for Caf40 binding. Indeed, this Not1 Caf40-binding region was confirmed by more recent studies for the mammalian CCR4-NOT orthologous complex (Bawankar et al. 2013; Y. Chen et al. 2014; Mathys et al. 2014).

		DNA-binding fusion	
		vector	**Caf40**
activation domain fusion	**vector**	200	3385
	Not1	981	29931
	Δ(1-980)	804	43795
	Δ(1-1080)	873	22570
	Δ(1-1695)	942	3207
		activation domain fusion	
		vector	Caf40
DNA binding domain fusion	**vector**	200	197
	Not1	15068	25898
	Δ(1-980)	38497	47669
	Δ(1-1080)	6139	33964
	Δ(1-1695)	299	264

Table 2. Assaying interaction between Caf40 subunit and Not1 mutants in two different orientations using the two-hybrid system. Normalized β-galactosidase activities are presented. Yellow coloring correspond to significantly strong β-galactosidase units comparing to control measurements (vector rows and columns).

My two-hybrid data results together with the Not1 truncation analysis allowed me to suggest an interaction scheme for the CCR4-NOT complex with defined regions of interaction within Not1. In particular, my results indicated that association of the Caf40 subunit with Not1 requires a region of Not1 located between amino acids 1000 – 1600 (Figure 42A). As this region is found in the essential fraction of Not1, it is possible that linkage of Caf40 to the Caf1-Ccr4 and/or the Not module(s) contributes to making Not1 essential for yeast life. My two-hybrid data further suggested that a layer of complex heterogeneity could come from the composition of the Not-interaction module as these experiments could suggest the presence of two copies of Not2 in (some) CCR4-NOT complexes (Figure 42B).

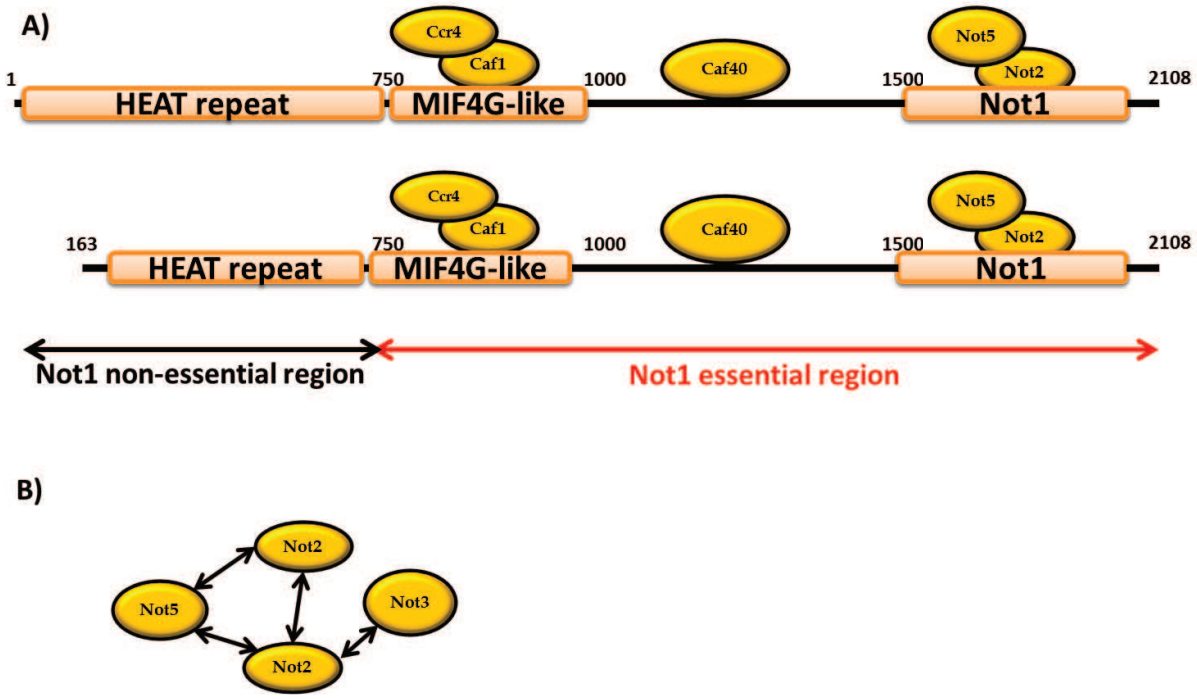

Figure 42. A) Interaction map of yeast CCR4-NOT complex. The Not1 scaffold subunit is represented as a line overlaid with boxes with its three domains indicated: the N-terminal HEAT repeat; the central MIF4G-like domain; and the C-terminal Not1 domains. Not1 essential region (750 – 2108aa. residues) is marked by a red arrow. Sites of binding of Caf1-Ccr4, Caf40, and Not2-Not5 are indicated. B) Two-hybrid interactions detected between Not2-Not3-Not5 subunits. The putative Not2 dimerization is also represented.

As mentioned above, the yeast CCR4-NOT complex contains two paralogous protein subunits, Not3 and Not5, that appear to be present simultaneously in complex immunoprecipitation experiments. Interestingly, overexpression of Not5 was shown to be sufficient to complement a *not3* deletion, suggesting that these proteins could be partly exchangeable. Also, the three subunits Not2 Not3 and Not5 share an N-terminal domain, called the NOT-box. Taken together, these observations suggest that several CCR4-NOT complexes containing different subunits (e.g., Not2-Not5 versus Not2-Not3) might coexist in the yeast cell. To test this hypothesis, I performed co-immunoprecipitation assays with different tagged subunits in order to gain insight into complex composition *in vivo*.

Different subunits of the CCR4-NOT complex were tagged with 3 different protein tags: the tandem affinity purification tag (TAP-tag); the VSV-G peptide tag; and the HA peptide tag. These tags allowed protein detection, precipitation, and eventually elution. Tagging was done for up to three proteins in a given yeast strain. This allowed me to perform two

successive precipitations: pulling first the complex by the TAP-tagged subunit, eluting with TEV protease, and then precipitating eluted proteins through the VSV tag. The presence of proteins carrying the VSV- and HA-tags in the final precipitate was then detected by western blotting. This strategy was aimed at deciphering whether some subunit combinations were present in one CCR4-NOT complex or in two different ones as explained below (see also Figure 39). If one wants to test whether protein A can be present in a complex with protein B and C or whether protein B and C are mutually exclusive for their interaction with protein A, three fusions have to be constructed: A-TAP, B-VSV and C-HA (Figure 43). After a first step of binding to IgG-beads and elution with TEV protease, the two partner proteins, B-VSV and C-HA, are expected to be detected by western blotting in the eluate in the two configuration. However, if one uses the eluate from this first step for a second precipitation with IgG-anti-VSV and elution with saturating amounts of VSV-peptide, different results are expected: if B-VSV and C-HA bind to same A subunit, the elution fraction is expected to contain of both a VSV and HA signals after western blot analysis; if B-VSV and C-HA bind to different A subunits, the elution fraction will only be positive for VSV (Figure 43).

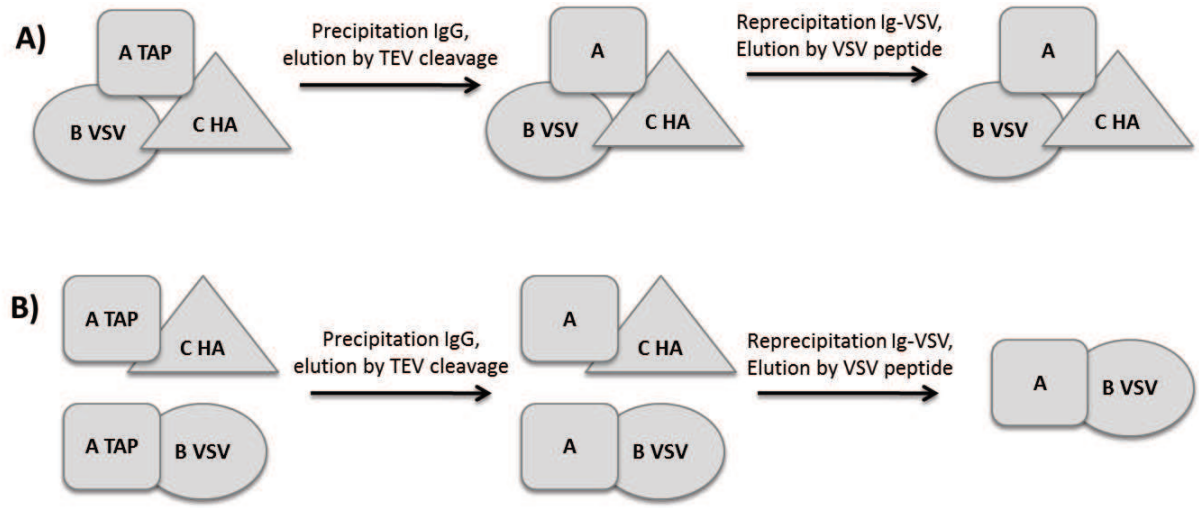

Figure 43. Two step co-immunoprecipitation protocol. A) The process and expected compositions of the two successive eluates if the A-TAP, B-VSV and C-HA proteins are present in a single complex. B) The process and expected compositions of the two successive eluates if A-TAP, B-VSV and C-HA are present in two distinct complexes.

Several yeast strains with different combinations of tagged subunits of the CCR4-NOT complex were tested using this strategy. A strain carrying Not1-TAP + Caf1-VSV + Not4-HA

was used to demonstrate that both the deadenylase Caf1 and the E3-ubiquitin ligase Not4 subunits are present in one CCR4-NOT complex (Figure 44B). Precipitation experiments with lysate from a Not1-TAP + Not3-VSV + Not2-HA yeast strain showed that Not3 and Not2 are not efficiently co-precipitating suggesting that they bind to different Not1 subunits (Figure 44A). Because it was observed in my two-hybrid experiments that Not2 might be associated with the CCR4-NOT complex in two copies, I tested the possibility of this putative dimerization of Not2 by performing co-precipitation experiments from yeast diploid strains where each alleles of Not2 was tagged; one with the TAP tag and the other with the HA tag. In parallel, a diploid strain carrying two differentially tagged version of Not5 was prepared. In both cases, the TAP-tagged protein efficiently bound to the beads. However, HA-tagged Not2 or HA-tagged Not5 did not co-precipitate with Not2-TAP or Not5-TAP respectively (Figure 45A and 45B). This suggested that the dimerization of Not2 or Not5 does not happen efficiently.

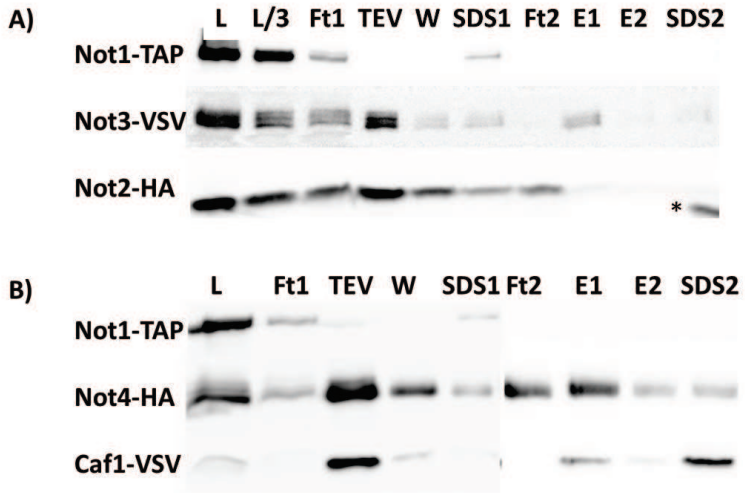

Figure 44. Two-step co-immunoprecipitation purifications. L and L/3: lysate fractions and its dilution 3 times; Ft1: flowthrough after first step of binding to IgG beads; TEV: elution fraction with the TEV protease; W: wash from IgG beads; SDS1: 1% sds elution from IgG beads; Ft2: flowthough after second binding to IgG-VSV beads; E1 and E2: two successive elutions of IgG-VSV beads with saturated quantities of VSV-peptide; SDS2: 1% SDS elution from IgG-VSV beads. A) Lysate from a yeast strain containing Not1-TAP + Not3-VSV + Not2-HA. The first binding step confirmed the association of Not3 and Not2 subunits with Not1, however second binding step suggests that Not3 and Not2 associate with different Not1 subunits. B) A Not1-TAP + Not4-HA + Caf1-VSV yeast strains was tested and the results indicate that Not4 and Caf1 are simultaneously present in one CCR4-NOT complex.

Figure 45. Co-immunoprecipitation from diploid yeast strains. L and L/3: lysate fractions and its dilution 3 times; Ft: flow-through after binding to IgG beads; TEV: elution with TEV protease; SDS1: 1% SDS elution from IgG beads. A) The diploid yeast strain Not2-TAP + Not2-HA + Not3-VSV was tested and the result shows no evidence for Not2-Not2 dimerization. B) The diploid yeast strain Not5-TAP + Not5-VSV wad tested and the result show no evidence for Not5-Not5 dimerization.

In conclusion, taken together with the structural data obtained by our collaborators and those reported in the literature, my analysis of the CCR4-NOT complex using the two-hybrid system and co-immunoprecipitation assays, as well as the Not1 protein analysis allows me to propose plausible models of the yeast CCR4-NOT complex organization *in vivo*:

- A first layer of heterogeneity originates from variation in the length of Not1 (Not1 long and Not1 short isoforms);
- A second layer of heterogeneity probably arises from the composition of the Not module: Not1-Not2-Not3 and Not1-Not3-Not5 are present at the same moment. Surely, this conclusion should be taken with caution, as during the co-immunoprecipitation assays, that were used to reach this conclusion, subunits might dissociate.
- Caf40 binds to the region located between the deadenylase- and Not- modules.
- Altogether, this would suggest that at least 4 structurally different CCR4-NOT complexes co-exist in yeast (Figure 46). The biological significance of this heterogeneity is unknown.

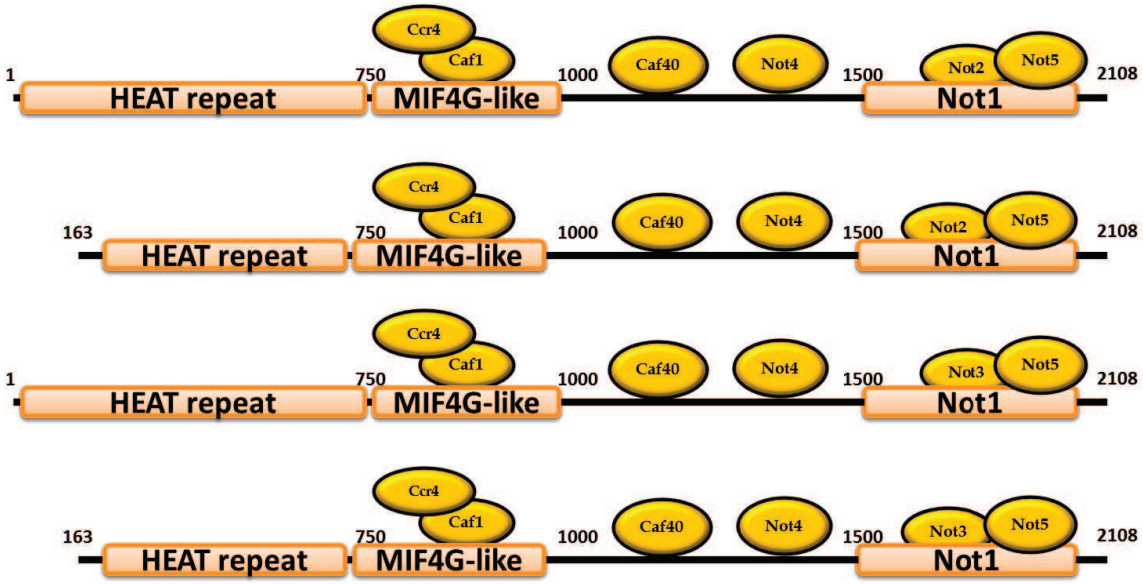

Figure 46. Proposed structural organization of yeast CCR4-NOT complexes *in vivo*. Two sources of heterogeneity are proposed: length of the Not1 scaffold subunit and identity of Not1 C-terminal binding partners.

2.1.3 Translation repression by the CCR4-NOT complex

Two groups uncovered the basic principle of miRNA-mediated gene expression repression: translation shutdown precedes the deadenylation step (Djuranovic et al. 2012; Bazzini et al. 2012). This conclusion indicates that before being degraded, mRNAs targeted by miRNA quit the pool of actively translated polysomal templates because of a block in translation initiation. This situation may apply to many mRNAs that are targeted by the degradation machinery. It is thus very important to determine the molecular bases for such a translation initiation block. Molecular clues came from the determination of the structure of Ccr4-Caf1-Not1 module. This revealed that the corresponding Not1 domain adopts an MIF4G-like fold. The same fold is adopted by a segment of the translation initiation factor eIF4G that interacts with the eIF4A helicase (Schütz et al. 2008). Superimposition of Not1 MIF4G-like domain with eIF4G MIF4G domain revealed high structural similarity of these two protein fragments. This similarity, together with the surface conservation, further suggests that a specific helicase could bind to Not1 in a manner similar to eIF4A binding eIF4G (Figure 47). Such a helicase could somehow affect translation regulation directly implicating the CCR4-NOT complex in this regulation of protein production beside its role in mRNA decay.

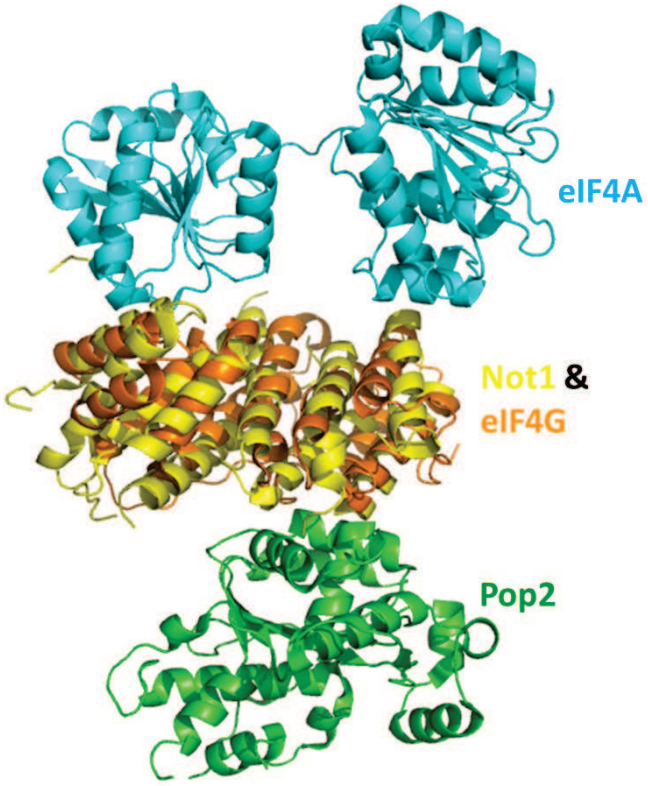

Figure 47. Structural alignment of the Not1(MIF4G-like)-Caf1 and eIF4G(MIF4G)-eIF4A complexes (Petit et al. 2012; Schütz et al. 2008). The Not1 and eIF4G MIF4G(-like) domains show a high level of structural similarity that provided the basis for the structural alignment (in the middle of the figure). The surfaces of interaction of Not1 with Caf1 and of Not1 with a predicted helicase binding in a similar manner to eIF4A are opposite to each other. Importantly, the latter surface is highly conserved in Not1.

Some of my additional experimental data indeed indirectly supports the involvement of the CCR4-NOT complex in translation regulation. Disruption of the *ccr4* or *caf1* genes results in a yeast growth defect at non-permissive temperature (temperature sensitive (ts-) phenotype). I observed that the same was true for point mutations affecting the interaction of Ccr4 and Caf1, or of Caf1 and Not1. To find genes that are able to suppress these ts-phenotypes, I screened a yeast library in a vector and identified several multicopy suppressors. Interestingly, among the genes identified was Stm1 which is known to inhibit the ribosome by blocking mRNA interaction with the 40S subunit in glucose deprivation conditions (Ben-Shem et al. 2011).

Taking into account the structural comparisons and the suppressor screening results, we hypothesized the involvement of the CCR4-NOT complex in translation repression. More specifically, in this project I addressed three questions:

- Is the putative helicase interaction surface of Not1 functionally important for cell growth?
- Do specific RNA helicases bind to the yeast CCR4-NOT complex? Is this interaction structurally similar to the eIF4G-eIF4A translation initiation complex?

Structural alignment together with sequence alignment identified three conserved amino acids exposed on the putative helicase interaction surface of Not1: two asparagines, N794 and N795, and a glutamic acid, E832 (Figure 48A). I constructed yeast strains carrying point mutations in the target amino acid residues: a double mutant Not1 (N794A, N795A) and the Not1(E832R) single mutant. Western blot analysis confirmed that Not1 protein expression was not affected by these mutations (Figure 48B). However, these mutations strongly impaired cell growth at non-permissive temperature (Figure 48C). This observation suggests that the putative surface of interaction is functionally important and that the designed mutations are likely to affect/disrupt an interaction, possibly with an RNA helicase. These data encouraged me to identify a putative interaction partner(s).

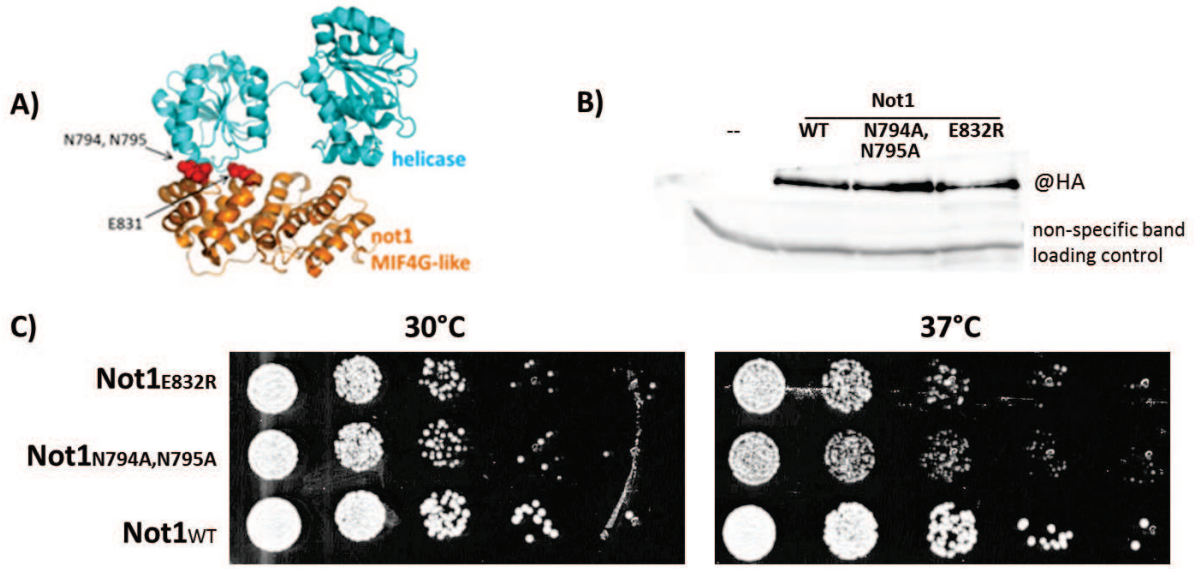

Figure 48. Designed mutations in putative surface of interaction (A) were introduced in Not1 and corresponding yeast strains were tested in growth assay (C). Introduced mutations

strongly affected yeast growth at non-permissive temperature (37^0C). The observed effect suggests the functional importance of the mutated region, as protein level of Not1 expression was approximately the same as for non-mutated protein (B).

To identify the putative partner of Not1, I first performed TAP-purifications of the CCR4-NOT complex using Not1-TAP. Purifications were done using wild type and mutants of Not1 in parallel. TAP-purified proteins were loaded on a denaturing gel and subjected to mass-spectrometry analysis. I then selected putative RNA helicases from this list for further analyses, namely:

- Translation initiation factors eIF4A1 and eIF4A2;
- Ded1: a DEAD-family protein helicase, involved in translation regulation of select RNA targets;
- Dhh1: a DEAD-family protein helicase, involved in mRNA decapping and mRNA translation repression regulation.

I performed co-immunoprecipitation interaction assays, expressing either Not1-TAP in eIF4A1-HA, eIF4A2-HA and Ded1-HA yeast strains (the chromosomal copies of the genes were tagged with HA-tag or Dhh1-TAP yeast strain was used, previously constructed by C. Gaudon). Protein complexes were pulled-down via IgG-beads and elutions were analysed by western blotting. Strong non-specific binding of eIf4A1, eIF4A2 and Ded1 to the IgG beads was observed suggesting either that the interaction with Not1-TAP protein was non specific, or that the HA-tagged proteins bound directly to the beads (Figure 49A and B). Also pull-downs with Dhh1-TAP did not reveal a specific interaction with Not1, suggesting that Dhh1 does not interact with the yeast CCR4-NOT complex, at least under the conditions tested (Figure 49C).

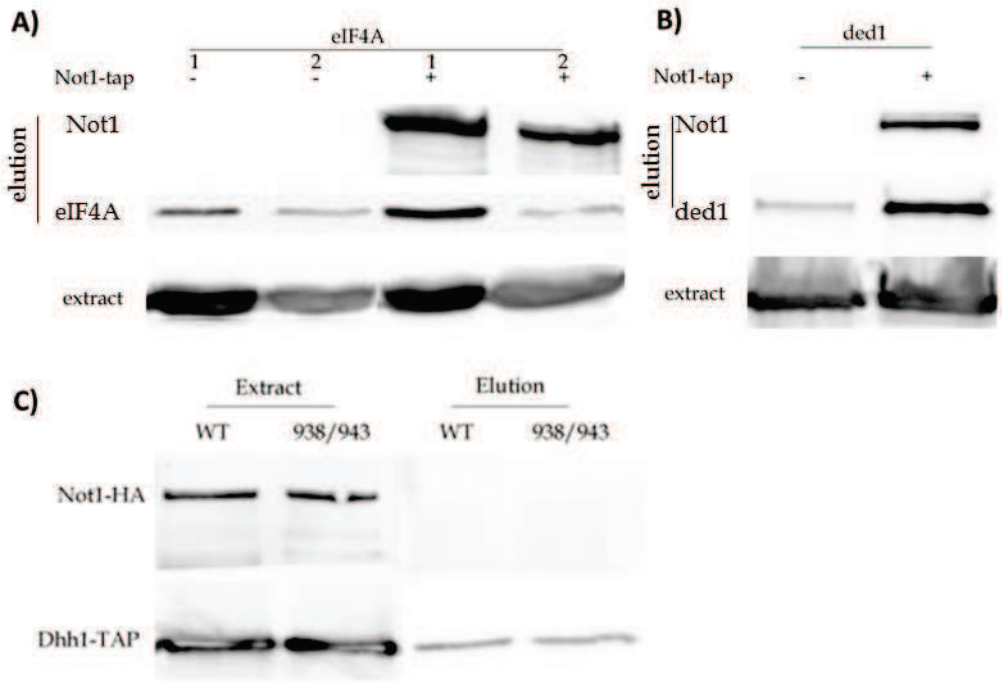

Figure 49. Co-immunoprecipitation analyses with selected helicase targets. Chromosomal copies of the indicated factors (eIF4A1, eIF4A2, Ded1) were tagged with HA-tag, thus allowing protein detection by western blotting. Dhh1-TAP had previously been constructed by C. Gaudon in our lab. Co-immunoprecipitation analyses with A) eIF4A1-HA and eIF4A2-HA and B) Ded1-HA resulted in a non-specific signal possibly because of non-specific binding of the helicases to the IgG beads. C) Co-immunoprecipitation assay using wild type Not1 or a Not1 mutant unable to interact with Caf1 did not reveal an interaction with Dhh1.

While these experiments were in progress, two papers were published showing that the mammalian CCR4-NOT complex interacts with the Dhh1 orthologue Ddx6 (p54) (Y. Chen et al. 2014; Mathys et al. 2014). These manuscripts also showed that this interaction was involved in translational repression mediated by miRNA. While it is likely that Dhh1 also binds to this surface on Not1 in yeast, I could not observe this interaction. This could suggest that the Not1-Dhh1 interaction is regulated and only occurs in specific conditions.

2.1.4 Genome-wide mRNA expression profiles of mRNA processing factors: Puf3-mediated CCR4-NOT complex recruitment

Recently a genome-wide mRNA transcription and decay profiling microarray-based method, called comparative Dynamic Transcriptome Analysis (cDTA), was developed (Miller et al. 2011; Sun et al. 2012; Sun et al. 2013). This approach allows the simultaneous measurement

of mRNA transcription and decay rates for each mRNA, genome-wide. The principle of the method is based on the ability of yeast and other eukaryotic cells to use 4-thiouracil added to the growth media as a source of uracil. Thus, addition of 4-thiouracil (4-tU) to yeast growing in rich media during short time period (~6 min) allows the labelling of nascent transcripts containing a few modified 4tU nucleotides. Cells are then lysed and total the mRNA recovered. These are then chemically biotinylated. Briefly, activated biotin (biotin-HPDP) specifically reacts with the thiol groups of the labeled mRNAs forming covalent S-S bonds. Subsequently, biotinylated mRNAs are recovered on streptavidin-coated magnetic beads. Theose mRNAs are then eluted with a reducing agent, such as dithiothreitol (DTT). Two mRNA fractions are recovered from these protocol: the total cellular mRNA that contains newly made and older mRNAs; and the nascent mRNA transcripts that represent transcripts synthesized during the pulse period. These two mRNA pools are analysed using Affymetrix microarrays allowing the quantitation of new and older mRNAs. The authors of one of these studies (Sun et al. 2012) developed an R-based statistical algorithm that allows the estimation of mRNA transcription and decay rates based on the data obtained on the microarray (Figure 50).

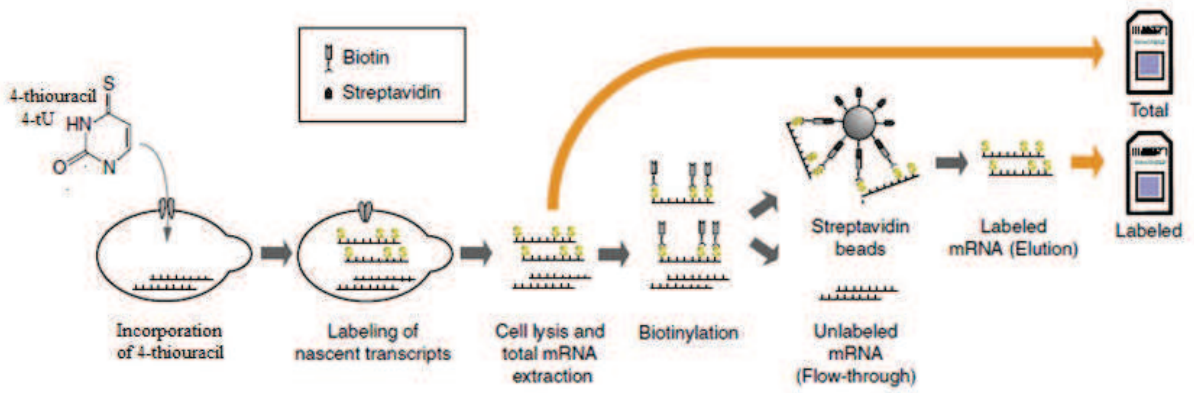

Figure 50. Dynamic transcriptome analysis (DTA) experimental procedure. Adopted from (Miller et al. 2011).

Subsequently, Sun et al. modified the original protocol making it possible to assay and compare the estimated mRNA transcription and decay rates of different yeast strains. The authors applied the resulting comparative DTA (cDTA) approach for a collection of 46 yeast deletion mutants of genes affecting different steps of mRNA processing, degradation, and

quality control. In the published manuscript, the authors built a correlation plot for estimated mRNA degradation rates. This plot indicated that the measured expression profiles, for genes involved in the same pathway or for genes encoding proteins physically interacting in the same mRNA processing complex, are clustered together. I took these available data and decided to reconstitute the analytical steps. More specifically, I took the measured total mRNA expression profiles and estimated mRNA decay rates and built the correlation plots (Figure 51). Confirming published data (Sun et al. 2012), only the correlation plot based on mRNA degradation rates allows the detection of a correlation between genes encoding proteins involved in the same functional processes. For example, ΔCaf1 and ΔCcr4 mRNA decay profiles are clustered together, while Caf1 and Ccr4 are physically associated with the CCR4-NOT complex. Intriguingly, in the same expression cluster two subunits of the PAT-LSM complex are detected: Dhh1 and Pat1 (Figure 51 left). Finally, several other highly correlated expression profiles of proteins physically interacting in same processing complexes are observed:

- Upf1-Upf2 cluster: Upf1-Upf2 are proteins involved in same quality control pathway NMD, and Xrn1 is exoribonuclease involved in NMD-decay mRNA intermediate scavenging;

- Lsm1-Lsm6-Lsm7 cluster: LSM-ring components of PAT-LSM complex, playing role in basic mRNA degradation pathway, probably by targeting partly deadenylated mRNA fragments for decapping enzymes;

- Ski2-Ski3-Ski8 expression cluster: components of Ski-complex, cytoplasmic binding partner for RNA exosome, believed to participate in RNA unfolding and presenting to the exosome for degradation;

- and Pan2-Pan3 cluster: proteins physically interacting and forming a deadenylation complex, believed to perform the first deadenylation reaction by trimming the poly(A) tail (Figure 50 left).

While Sun et al. did not analyse these results deeper, I decided to get a more detailed insight into mRNA decay from these correlations.

The high correlation observed between expression profiles of Ccr4-Caf1-Pat1-Dhh1 and Pan2-Pan3 mutants encouraged me to build pairwise comparison plots between them based on mRNA decay rate estimations. Each dot on the plot has its coordinates (X,Y), which correspond to the measured degradation rates in mutant X (first coordinate number) and in mutant Y (second coordinate number). Because each estimated mRNA degradation rate also has its confidence measurement (p-value), I also included this information in the plot as a colour function:

- If (X,Y) has both p-value(X) and p-value (Y) less than the confidence threshold (p(X)<0,05 and p(Y)<0,05), the dot is coloured red;
- If both p-value(X) and p-value(Y) are higher than 0,05, then the dot is coloured black.

For all other cases one of the colours in the gradient from red to black is assigned (basically the colour is set from the average of the p-values).

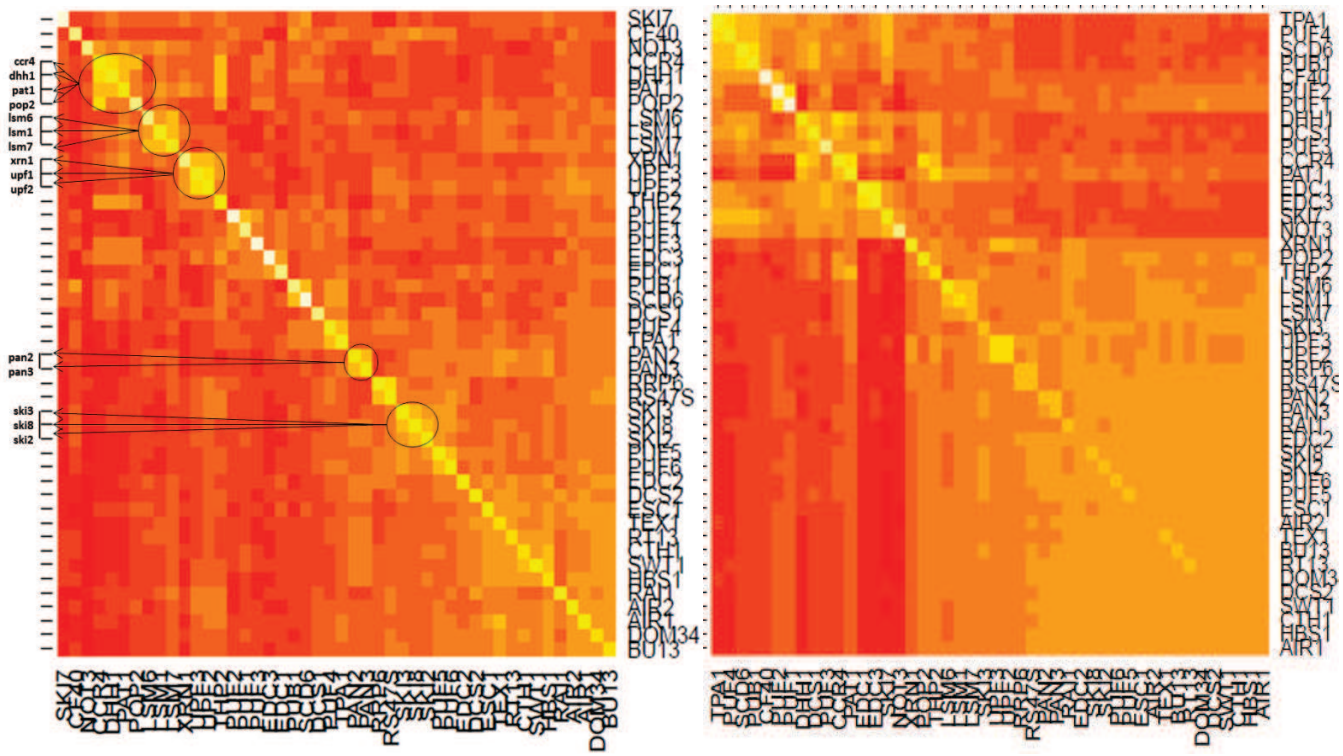

Figure 51. Correlation plots based on cDTA measurements obtained by Sun et al. 2012. Gradient colour from red to yellow reflects the correlation coefficient between pairs of compared mutants (red – correlation coefficient equals 0, yellow – correlation coefficient equals 1). *Left plot* – correlation plot based on genome-wide mRNA decay rate estimations. *Right plot* – correlation plot based on genome-wide total mRNA expression estimates. Only the correlation plot based on mRNA decay rate calculations allows to detect correlation

between closely-regulated genes, genes known to interact physically, or genes participating to the same biological process.

As expected, the profiles were highly correlated for pairs in the group Ccr4-Caf1-Pat1-Dhh1 and for Pan2-Pan3. This can be observed by linear trends of the distributions (Figure 52 A, B, C, D). It is worth noting, that disruption of genes encoding factors in the Ccr4-Caf1-Pat1-Dhh1 group leads to strong mRNA expression misregulation, both stabilizing specific mRNAs (as expect after disrupting protein factors involved in mRNA degradation) but also unexpectedly strongly destabilization of other mRNAs (Figure 52A, B, C, red coloured extreme fractions). The nature of this opposite effect is not known. It may perhaps reflect some conserved cellular mechanism that buffers the total mRNA quantity in the cell. Mechanistically it is also important to note, that another deadenylase, the Pan2-Pan3 complex, has a totally different impact on mRNA decay rates, as the fraction of statistically significant mRNAs mostly concentrate around the unaffected fraction (Figure 52D, red fraction) with just a few outliers found in the mRNA stabilized corner. Analysing the correlation between the impact of a deletion of deadenylase subunit Ccr4 and of another CCR4-NOT complex subunit, namely Not3, revealed little correlation between the resulting consequences in mRNA decay rates. A similar observation was made for Caf1-Not3. Moreover, this is in agreement with previously published genome-wide data (Cui et al. 2008). This indirectly suggests that, at least for the Not3 subunit, the C-terminal binding partners of Not1 are probably involved in cellular processes that differ from the general role of Ccr4 and Caf1 in basic mRNA deadenylation, as has already been suggested by results obtained during our structural and functional study of the Not module (Bhaskar et al. 2013).

It is also worth analysing the amplitude of mRNA decay rate changes. In *ccr4*, *caf1*, *pat1* and *dhh1* mutants the quantitative impact is quite strong, the amplitude of the effect being around four-fold in both the stabilizing and destabilizing directions. This indicates that these factors significantly affect gene expression. For *pan2*, *pan3* and *not3* mutants, the amplitude is narrower with a maximum two-fold effect. This indicates that the Pan2-Pan3 complex and Not3 have a more modest role in mRNA expression regulation and/or that the effect of their deletions are better buffered *in vivo*. The former conclusion is in agreement with the

proposed role of the Pan2-Pan3 complex in initial poly(A) tail trimming, resulting in just few adenine bases being removed from the transcript (Funakoshi et al. 2007).

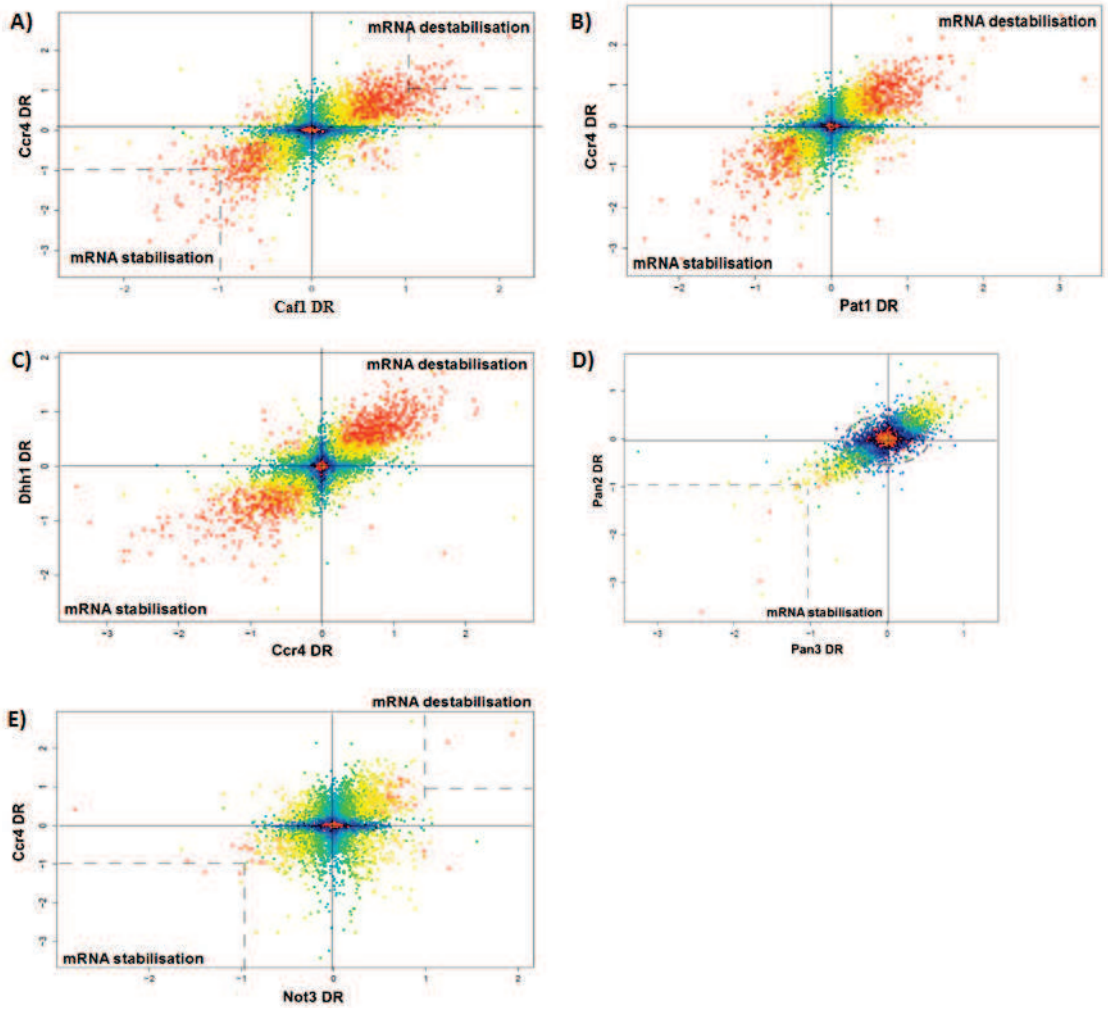

Figure 52. Pairwise log-scaled correlation plots of effects of pairs of mutants affecting proteins linked to mRNA decay. Colour function: if (X,Y) has both p-value(X) and p-value (Y) less than confident threshold (p(X)<0,05 and p(Y)<0,05), the colour red is assigned for the (X,Y) dot; if both p-value(X) and p-value(Y) are higher than the threshold, then black colour is assigned; for all other cases one of the colours in the gradient from red to black is assigned (colour = coef*(p(x)+p(y))/2). The X and Y axes represent log-values of mRNA decay rate estimates. The windows of mRNA stabilized (X<0 and Y<0) or mRNA destabilized (X>0 and Y>0) are labelled. A) Pairwise plot of Ccr4 deletion mutant mRNA decay rates and Δcaf1 mutant mRNA decay rates (Ccr4 DR vs Caf1 DR). B) Pairwise plot of Ccr4 deletion mutant mRNA decay rates and Pat1 deletion mutant mRNA decay rates (Ccr4 DR vs Pat1 DR). C) Pairwise plot of Dhh1 deletion mutant mRNA decay rates and Ccr4 deletion mutant mRNA decay rates (Dhh1 DR vs Ccr4 DR). D) Pairwise plot of Pan2 deletion mutant mRNA decay rates and Pan3 deletion mutant mRNA decay rates (Pan2 DR vs Pan3 DR). D) Pairwise plot of Ccr4 deletion mutant mRNA degradation rates and Not3 deletion mutant mRNA degradation rates (Ccr4 DR vs Not3 DR).

Following the increasing evidence that mRNA binding factors play a role in RNA decay regulation (Fabian et al. 2013; Leppek et al. 2013), I was interested in extracting information about mRNAs whose decay was affected by specific RNA-binding proteins from the previous profiles. Such information might, for example, reveal the molecular role of this RNA-binding protein in recruiting the CCR4-NOT complex to specific mRNAs. The genome-wide mRNA binding profiles of over 40 mRNA binding proteins have been reported (Hogan et al. 2008; Gerber, Herschlag, and Brown 2004). Thus combination of these data with the impact of mRNA factors on mRNA decay rates allowed me to build enrichment plots, which represent the relative enrichment of a given RNA-binding protein target in cDTA mRNA decay rate profiles. Following this idea, I build two main plots: one for enrichment of RNA-binding protein targets in mRNAs with statistically significant decreased decay rate (Figure 53A, C) and another for enrichment of RNA-binding protein targets in mRNAs with significantly increased decay rate (Figure 53B, D). This analysis was done for *ccr4*, *caf1*, *pat1* and *dhh1* mutants, as I have shown above that these mutants strongly affect mRNA decay rates in both directions (Figure 52). This analysis revealed a more than three-fold enrichment of Puf3-mRNA binding targets in all mutant profiles. This effect is highly specific and was not detected to a comparable extent with any of the other 27 RNA binding protein analysed. More specifically, one can observe that Puf3-bound mRNAs are highly represented in the mRNA fraction with decreased mRNA decay rates, while completely under-represented in the mRNA fraction with increased mRNA decay rates. This observation indicates that mRNAs targeted by Puf3 are affected in a concerted manner by these mRNA decay factors, with their half-lives being increased when these factors are deleted. This observation also supports the involvement of the Puf3 RNA-binding protein in mRNA decay regulation.

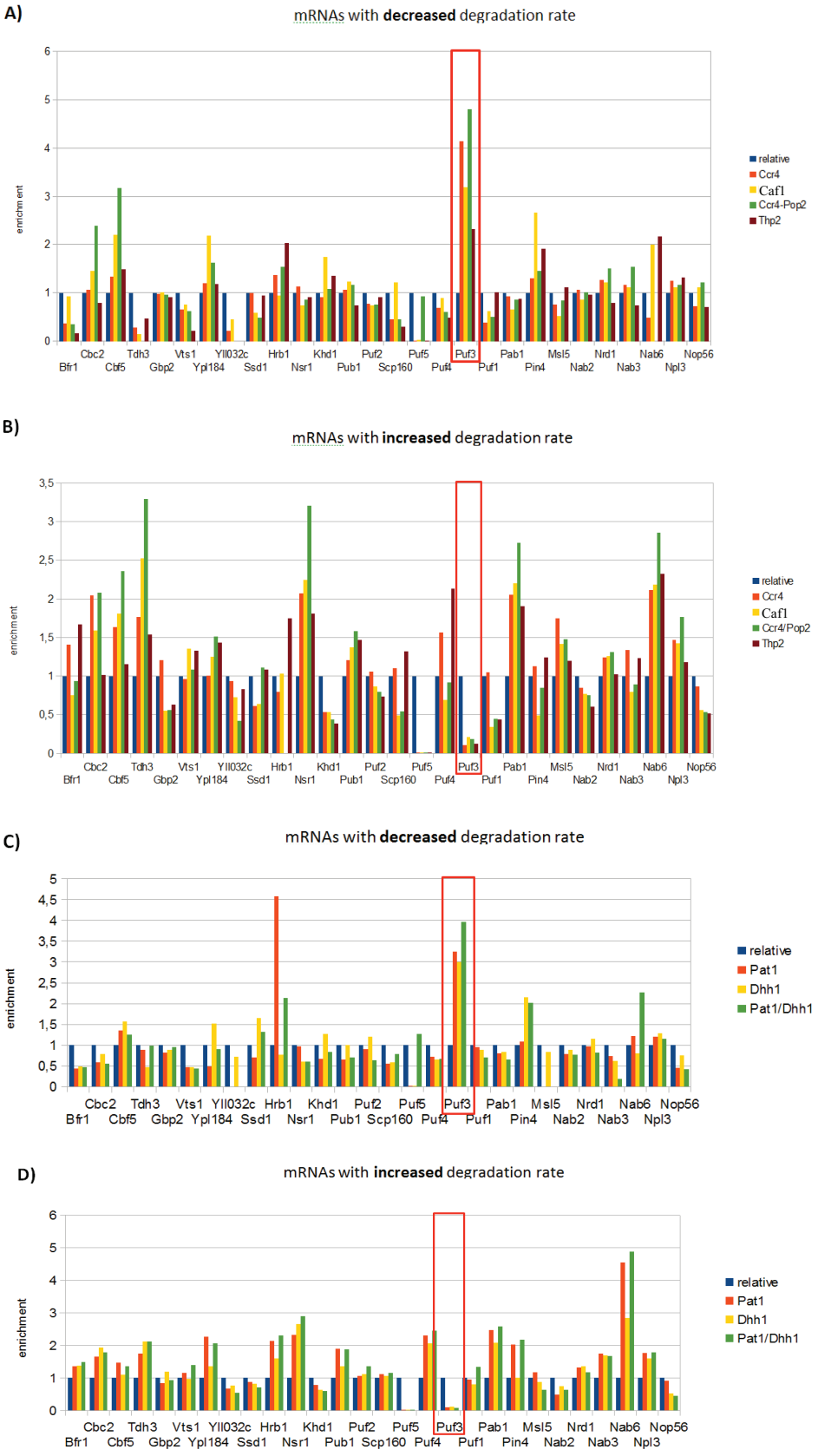

Figure 53. Enrichment analysis. Plots represent the fold-enrichment of mRNAs containing a binding site for a given RNA-binding protein. Analysis was performed for mRNAs classified as destabilized or stabilized by the cDTA analysis. mRNAs, significantly stabilized in *ccr4*, *caf1*,

pat1 and *dhh1* mutants, are highly enriched in mRNAs being targets of Puf3. Interestingly, the same class of mRNAs is strongly underrepresented in mRNAs being destabilized by the same mutants.

To gain a deeper insight into the biological function of mRNAs stabilized in cDTA profiles of the *ccr4*, *caf1*, *pat1* and *dhh1* mutants, a GO-term analysis was performed. This revealed at least four statistically significant clusters of genes involved in related biological functions. Amongst them, three were specific to some of the mutants, while the latter group was affected by inactivation of the 4 factors. Hence transcripts, whose products are involved in the yeast reproduction process, such as pheromone signalling, are stabilized in the *ccr4* and *caf1* mutants. The glucose catabolism pathway is up-regulated in the absence of the Ccr4, Pat1, and Dhh1 factors, while respiration regulation is affected only by *ccr4* deletion. These mutant-specific mRNA stability changes might reflect adaptation of the mutant cell to the environment. For one cluster of stabilized transcripts all four mutant profiles were coordinativly affected. This cluster represents mRNAs whose protein products are part of mitochondrial translation apparatus, namely nuclear-encoded mitochondrial ribosome proteins or translation factors (Figure 54A). Interestingly, most of them are also Puf3-binding targets.

Does disruption of Puf3 leads to stabilization of its target mRNAs? To address this question, I took the ΔPuf3 cDTA profiles, the list of mRNAs with decreased decay rate (stabilized mRNA fraction), and compared it with the list of mRNAs bound by Puf3 (Sun et al. 2012; Hogan et al. 2008; Gerber, Herschlag, and Brown 2004). This analysis reveals that indeed deletion of Puf3 affects the stability of a relatively small fraction of mRNAs (decreasing the stability of 20 mRNAs and increasing the stability of 72 transcripts). The fraction of mRNAs bound by Puf3 is relatively larger, with around 250 mRNAs targeted. Interestingly, of the latter mRNAs, the decay rate of only 50 was significantly decreased (Figure 54B). It is unclear why such a small fraction of the Puf3 targets had altered decay rates. This could suggest that not all Puf3-binding events are productive, or alternatively, that the resulting changes in the decay rate were too small to be observed.

Altogether, the statistical and correlational analyses suggest a functional link between Puf3-RNA binding events and mRNA decay regulation by the Ccr4, Caf1, Pat1 and Dhh1 factors.

For a set of 50 mRNAs that are bound by Puf3 and whose decay rates are altered in the absence of Puf3, their stability is affected by inactivation of the Ccr4, Caf1, Pat1, and Dhh1 factors. Interestingly, these mRNAs encode proteins involved in mitochondrial translation.

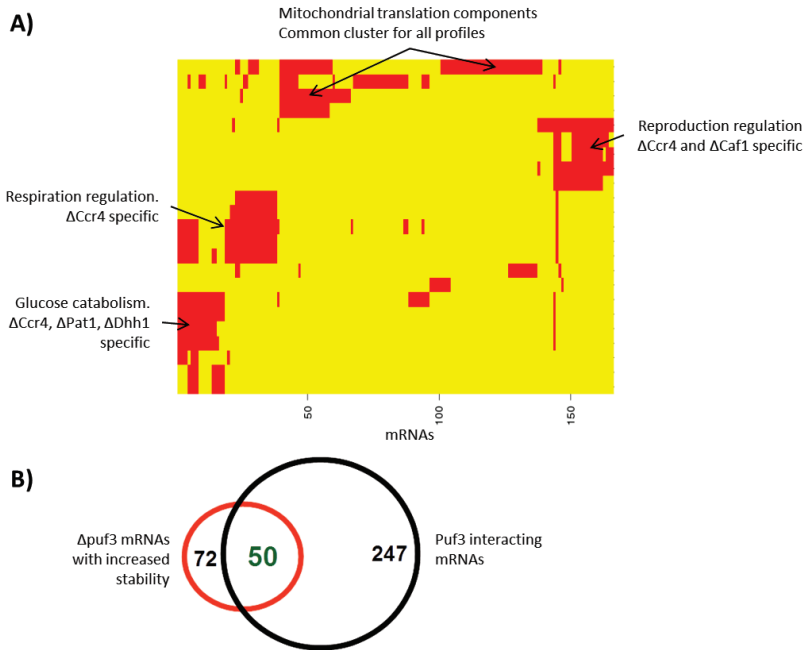

Figure 54. A) GO-term analysis of significantly stabilized mRNAs in selected mutant cDTA profiles (Δccr4, Δcaf1, Δpat1 and Δdhh1). Selected mRNAs are aligned on the horizontal axis, while GO-terms are plotted on the vertical axis. Red color corresponds to mRNAs enriched in same GO-term cluster. This analysis revealed four statistically significant GO clusters, reflecting the biological function of the genes affected in these mutants: mitochondrial translation, respiration, reproduction regulation, and glucose catabolism. B) Venn-diagram of Puf3-bound mRNAs (Puf3 interacting mRNA pool) and mRNAs significantly stabilized in a *puf3* deletion mutant as revealed by cDTA (Δpuf3 mRNAs with increased stability). 50 mRNAs are common to these two pools, representing mRNAs bound by Puf3-binding whose decay is regulated by Puf3.

This correlation analysis led me to hypothesize that Puf3 binding targets specific mRNAs to be degraded by recruiting the CCR4-NOT complex. To test this hypothesis, I performed two-hybrid and co-immunoprecipitation interaction assays between Puf3 and CCR4-NOT components. As yeast Puf3 has two distinguishable regions: an N-terminal non-conserved extension and a C-terminal conserved armadillo-repeat domain, I tested three protein versions in the two hybrid assay: the full-length protein; the N-terminal region; and the C-terminal region (Nterm and Cterm respectively, Figure 55A). Indeed significant β-galactosidase levels (two-fold above negative control) were detected: between full-length

Puf3 and Ccr4; and Puf3 C-terminal armadillo-repeat domain with Caf1. The detected interactions suggest that the RNA-binding domain of Puf3 contacts the CCR4-NOT complex (Figure 55B, C).

To confirm these results by an independent method and to gain insight into the subunit of CCR4-NOT complex involved in the interaction with Puf3, I tested co-immunoprecipitation assays of Not1, the scaffold subunit of the CCR4-NOT complex, with Puf3 (Figure 55D). Strong non-specific binding of Puf3 to the beads obscured conclusion in one tested orientation (Not1-TAP + Puf3-HA, pull-down through Not1-TAP precipitation). But the Puf3-TAP subunit did indeed co-precipitate Not1, well above background levels. Moreover, testing a Not1 mutant version, which does not interact with the Caf1 subunits (Not1 939/943) indicates that this interaction is not mediated by Caf1 or Ccr4. Moreover, pretreatment of the the yeast lysates with RNAse A reveals that the Puf3 association with the CCR4-NOT complex is RNA-independent, arguing for the involvement of direct protein-protein interactions. However, the precise identification of the Puf3 binding partner in the CCR4-NOT complex remains to be determined.

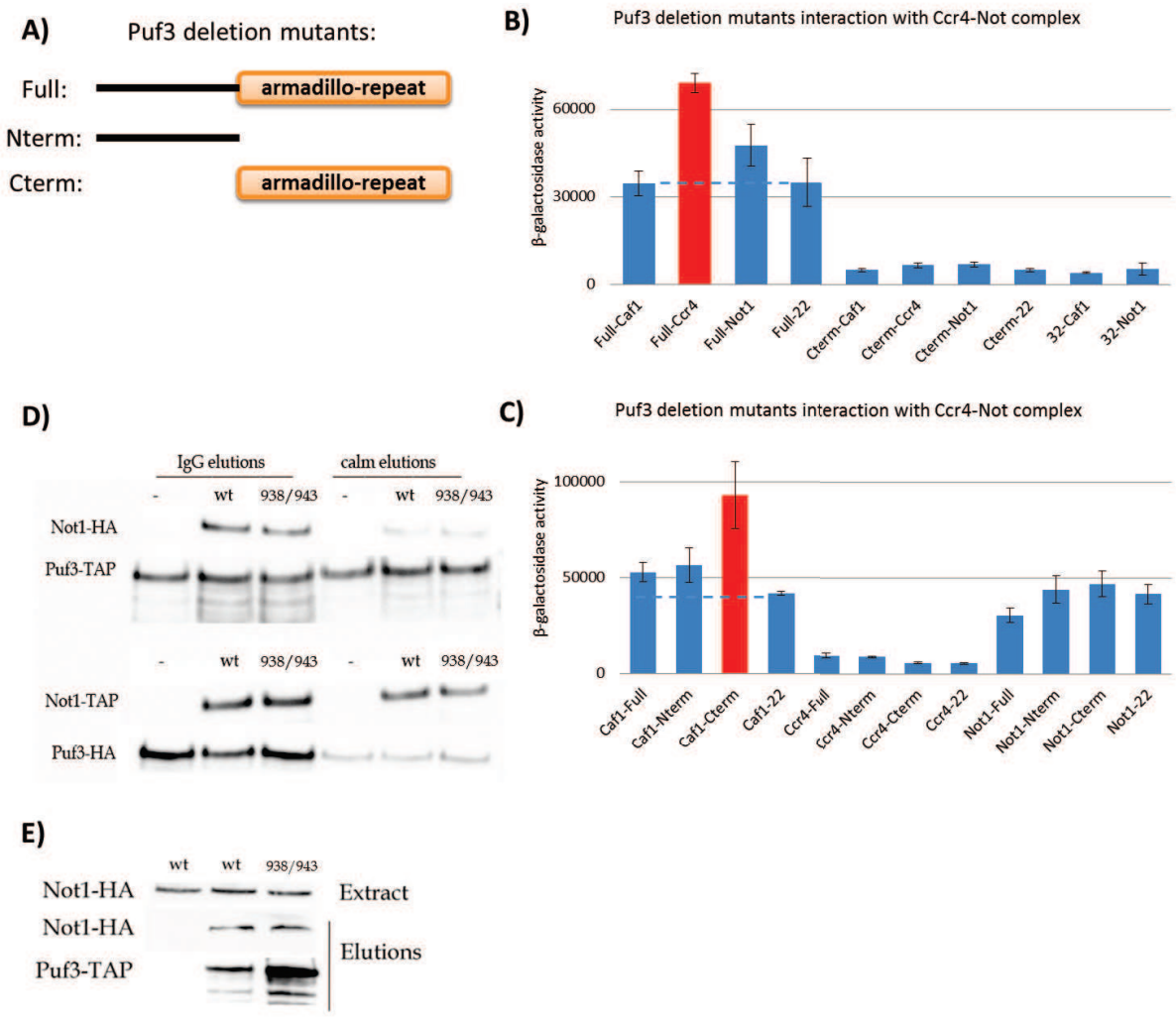

Figure 55. Interaction of Puf3 with the CCR4-NOT complex. A) Structural organization of the of yeast Puf3 protein and truncation mutants tested in two hybrid assay. B) Two-hybrid interaction assay between Puf3 variants fused to the Gal4 DNA-binding domain and some CCR4-NOT complex subunits fused to the Gal4 activation domain. A significant interaction between the full-length Puf3 protein and Ccr4 is detected. The corresponding bar is coloured in red. C) Two-hybrid interaction assay between Puf3 variants fused to the Gal4 activation domain and CCR4-NOT complex subunits linked to the Gal4 DNA-binding domain. A significant interaction between the Puf3 C-terminal domain and Caf1 is detected. The corresponding bar is coloured in red. D) Co-immunoprecipitation assay between the Not1 subunit of the CCR4-NOT complex and Puf3. Protein extracts were incubated with either IgG-beads or calmodulin resin that recognizes different modules of the TAP tag. Co-precipitation of extracts containing Not1-TAP (WT or the 938/943 mutant) and Puf3-HA resulted in non-specific retention of Puf3-HA to the beads. However, co-precipitation of extracts containing Puf3-TAP and Not1-HA (WT or the 938/943 mutant) revealed a co-precipitation of both WT and mutant Not1 with Puf3. Co-precipitation of the Not1-HA 939/943 mutant, which has previously been shown not to interact with the Caf1-Ccr4 module, indicates that the interaction does not occur through Caf1 or Ccr4. E) RNAse pre-treatment of lysates containing Puf3-TAP and Not1-HA before co-immunoprecipitation analysis reveals that the interaction between Puf3 and the CCR4-NOT complex is RNA independent.

The interaction detected between Puf3 and the CCR4-NOT complex suggests that a molecular basis for the Puf3-directed targeting of mRNA to deadenylation is mediated by the CCR4-NOT complex. What is the mode of RNA recognition by Puf family members? Published data suggests two crucial specificity determinants are required for efficient binding by Puf proteins: RNA primary sequence and its single-stranded nature (Figure 56A and B). Curiously, mapping the Puf recognition motif on available yeast mRNA secondary structure models built by the parallel analysis of RNA structure (PARS) method (Kertesz et al. 2010), revealed potential strong base-pairing between some Puf3-binding motifs located in 3'-UTR of the target and the complementary RNA sequence located in the mRNA open reading frame (Figure 56C).

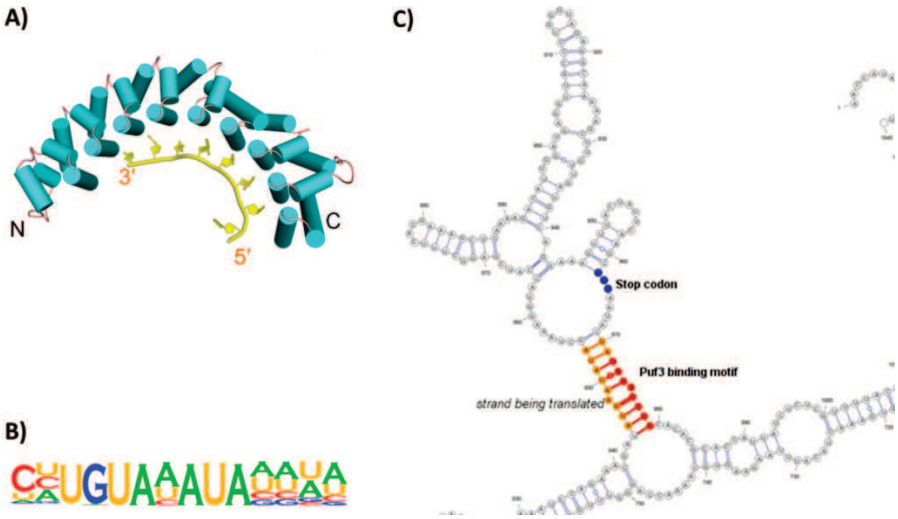

Figure 56. Features of Puf-family proteins and of its mRNA targets. A) Structure of the Puf3 homologue Pum1 in complex with its single-stranded RNA substrate. Adapted from Wang et al. 2002. B) Puf3 recognition motif in MotifScan representation. The height of the base reflects its conservation score. The motif UGUA[A/U/C]AUA can be defined as the recognition sequence. Adapted from Hogan et al. 2008. C) Mapping the location of the Puf3-binding motif (red) and translation stop site on the secondary structure model of the YBR251W mRNA. The latter mRNA encodes the mrps5 mitochondrial ribosomal protein of the small subunit. This structural model reveals that the Puf3-recognition sequence located in the 3'-UTR of mRNA (red) could base pair with a complementary sequence located in the open reading frame (orange). The mRNA secondary structure model was taken from Kertesz et al. 2010.

Surprisingly, most mRNAs that display a similar organization with Puf3-recognition motifs predicted to be present in a stem, encode proteins of the mitochondrial ribosome.

Additionally, the decay of such mRNAs is strongly inhibited in *ccr4*, *caf1*, *pat1*, *dhh1*, and *puf3* deletion mutants, according to the cDTA analysis.

How is the decay of these mRNAs induced if the Puf3-recognition sequence is hidden in a stem? An obvious possibility was that the base-pairing between the open-reading frame region and Puf3-binding motif would be unfolded during translation, thus making the Puf3-recognition sequence accessible to Puf3 (Figure 57A). Puf3 binding would then recruit the CCR4-NOT complex and induce deadenylation followed by mRNA degradation.

To test this model, I decided to introduce mutations into the two strands forming the stem encompassing the Puf3 binding site and to analyse the half-life of the resulting mRNAs. Indeed, one would predict that introducing a mutation into the RNA sequence complementary to the Puf3-binding motif would make the latter permanently accessible. Thus such mutant mRNA would be a good substrate for Puf3 binding leading to faster decay compared to the wild type mRNA (Figure 57B). Conversely, mutating the Puf3-recognition sequence is expected to lead to greater mRNA stability as the mutant mRNA would be unable to recruit the CCR4-NOT deadenylation complex (Figure 57C). Also, according to the model, blocking the translation of this mRNA is also expected to have an impact on mRNA decay. Thus, blocking translation of the wild type mRNA should stabilize the mRNA, as the putative stem would no longer be unfolded (Figure 57D). In contrast specifically inhibiting translation of an mRNA mutated in the RNA sequence complementary to the Puf3-binding motif would not affect its stability, as it would constitutively be targeted by Puf3 and the CCR4-NOT complex (Figure 57E).

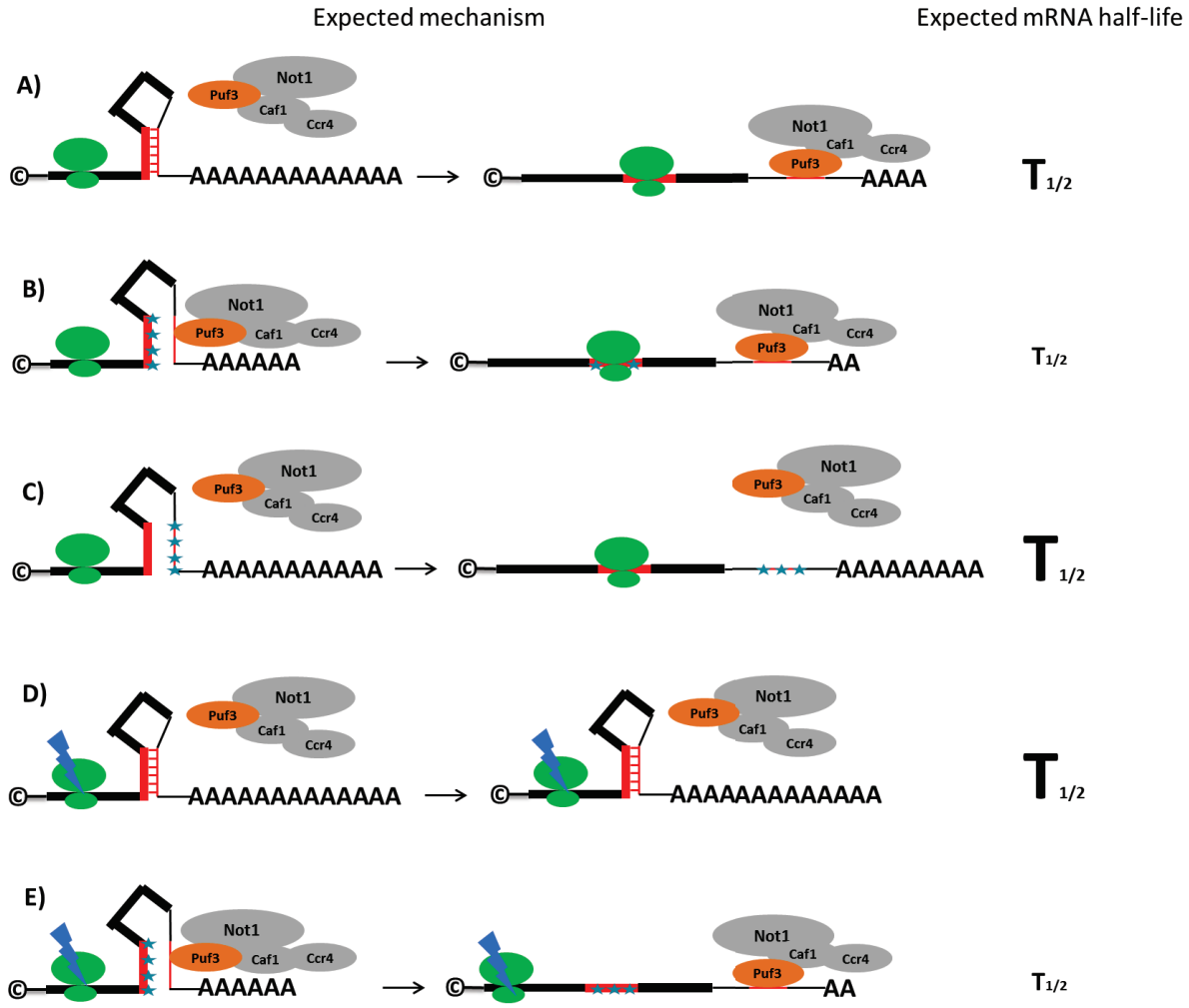

Figure 57. Proposed model of translationally-regulated Puf3-mediated mRNA decay and experiments designed for its verification. The relative sizes of the half-life symbol (T1/2) indicate the relative stability of the corresponding mRNAs. A) Wild type context: the Puf3 binding sequence is hidden in a stem that will be opened by translation thus promoting Puf3 binding, mRNA deadenylation and mRNA decay. B) Disruption of the stem by mutating the strand complementary to the Puf3 binding sequence would favour Puf3 binding and mRNA decay. C) Disruption of the stem by mutating the Puf3-recognition sequence would prevent Puf3 binding and increase mRNA half-life. D) Inhibition of translation of the wild-type mRNA would prevent unfolding of the mRNA and stabilize it. E) Inhibition of translation of the mRNA containing a stem carrying a mutation in the strand complementary to the Puf3 binding sequence would not impact its stability.

To test this model, I selected two mRNAs having the required characteristics:

- Targeted to degradation by Ccr4, Caf1, Pat1, and Dhh1;
- Regulated by Puf3;

- -Containing a Puf3 binding site in a predicted stem structure, as revealed by high throughput secondary structure determination experiments (Kertesz et al. 2010).

These two mRNAs are encoded by the YDR115W and YBR251W loci. They both encode mitochondrial ribosome proteins (mrpl34 of the large subunit for YDR115W, and mrps5 of the small subunit for YBR251W. To be able to monitor mRNA decay rates, the production of these mRNA was driven by a doxycycline-repressible promoter. Doxycycline addition thus allows performing of a classical chase experiments with these reporters. Then, mutations, predicted to disrupt the putative stem were introduced in both reporter plasmids. Mutations affecting the sequence complementary to the Puf3-binding motif formed reporters called the “complement mutant”. Mutations of the Puf3-binding motif itself generated reporters called the “motif mutant”. (Details of the mutations are listed in the Materials and Methods section.) Chase experiments were performed with the resulting reporters. Total RNA was then extracted and analysed by Northern blot using probes specific for one or the other of the reporters. (Briefly, oligonucleotide probes were designed to hybridize to the first nucleotides of the transcript encoded by the doxycycline promoter initiation site and to the reporter mRNA, thus avoiding cross-detection of mRNAs encoded by the corresponding genomic-loci).

In contrast with my expectations, no significant changes in the mRNA half-lives after mutating either the “complement” or “motif” sequences were detected (Figure 58A and B). This could suggest that these mRNAs are not regulated by Puf3-induced mRNA decay or that Puf3 is inactive under the conditions tested. The latter is, however, unlikely because previous analyses of the Cox17 mRNA that demonstrated that its stability was controlled by Puf3 were performed under similar conditions (Olivas and Parker 2000). Alternatively, the access of Puf3 to its binding sequence may not be rate limiting for the decay process, thus altering this kinetic would have no impact on mRNA stability. Interestingly, the YDR115W transcript is detected on the northern blot as two-bands with a major band of shorter size. Mutating the Puf3-binding site resulted in an almost total disappearance of the shortertranscript and accumulation of large quantities of the longer one. These two-migrating species most likely represent two isoforms resulting from alternative polyadenylation (as the doxycyclin-regulated promoter generates rather homogenous 5’ ends, see the YBR251W construct as control). The mutations of the Puf3-binding sequence

could interfere with usage of the first polyadenylation signal. RACE-experiments will need to be performed to identify the exact polyadenylation site used by mRNAs encoded by this reporter plasmid.

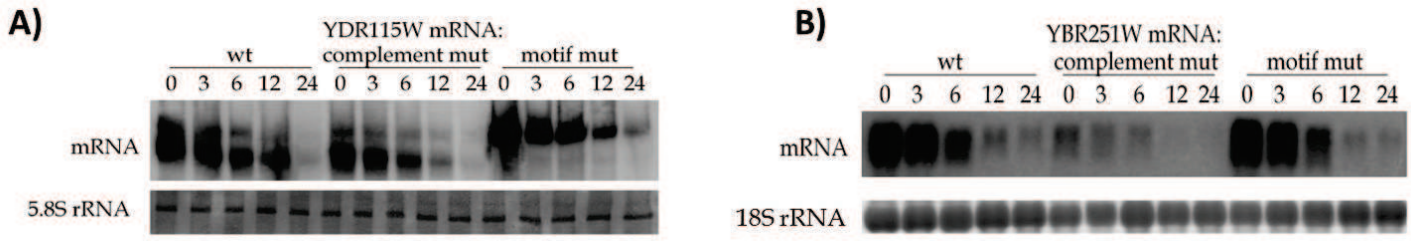

Figure 58. Experimental testing of the model presented in Figure 56. (A) Analysis of the half-lives of the wild type, complement mutant and motif mutant of the YDR115W mRNA. (B) Analysis of the half-lives of the wild type, complement mutant and motif mutant of the YBR215W mRNA. For YDR115W Northern blots, 5,8S rRNA was used as loading control, while for YBR215W – 18S rRNA was used.

In conclusion, in this part of my work I analysed genome-wide mRNA degradation profiles of mRNA binding proteins. This gave some insight into particular cases of Puf3-induced mRNA decay. I obtained evidence for an interaction between the Puf3 RNA-binding protein and the CCR4-NOT deadenylation complex. Then based on the integration of different published genome-wide data, I identified an intriguing RNA secondary structure element involving the base pairing of the Puf3-binding sequence element with the complementary sequence found in the coding sequence of the same transcript. This allowed me to propose a model linking translation and Puf3-induced decay. I tested several features of this model using two reporters. My results did not confirm the starting hypothesis but other unexpected observations were made. Those will be the focus of subsequent research.

3. Discussion and Perspectives

During my PhD work, I extensively analysed the role of the CCR4-NOT complex in post-transcriptional gene expression and regulation. In collaboration with the group of Elena Conti (Max Plank Institute, Munich, Germany), the high-resolution crystal structures of two CCR4-NOT subcomplexes, Ccr4-Caf1-Not1 and Not1-Not2-Not5, were determined and I investigated the functional importance of these interactions in mRNA deadenylation. I also addressed the question of a putative link between mRNA translation repression and mRNA decay. While no definitive conclusion was obtained for the yeast system, our hypothesis is supported by recent results obtained in higher eukaryotes. Finally, using biocomputing and biochemical analyses, I identified a link between the Puf3 RNA-binding protein and the CCR4-NOT complex and investigated possible underlying regulatory mechanisms, providing a basis for further research in this area.

3.1 Structural and functional characterization of the CCR4-NOT complex.

For a long time, the role of the CCR4-NOT complex was unclear. Originally described as a transcription regulator (NOT means *Negative on TATA-less promoters*), the CCR4-NOT complex was initially believed to regulate transcription initiation by affecting the activity of the SAGA factor (Cui et al. 2008; Landrieux and Collart 2007). Even though the complex was described to localize in the nucleus under certain conditions (Chicoine et al. 2007; Collart and Struhl 1994), its localization, which is principally cytoplasmic, was difficult to reconcile with its proposed role in transcription regulation. These observations argued for some additional or alternative biological role(s). Evidence for additional functions originated from the observation of the presence of a nuclease fold in the Caf1 and Ccr4 factors, and the demonstration that these proteins have exonuclease activity and are involved in deadenylation both *in vitro* and *in vivo* (Daugeron et al. 2001; Chen et al. 2002; Tucker et al. 2001; Bianchin et al. 2005). If this finding focused attention towards the role of these factors in mRNA degradation control, the role of the other subunits of the CCR4-NOT complex in this process remained elusive, or even contradictory. Moreover, whether the deadenylation reaction is catalysed by the Ccr4 and Caf1 subunits as part of the CCR4-NOT complex, or whether these factors can act independently, was unclear. These important biological

questions motivated me to undertake the analyses of the complex function by integrated strategies.

Our collaborative experiments uncovered some fundamental principles of the organization and function of this major eukaryotic deadenylase. The solved structure of the ternary complex containing fragments of Ccr4-Caf1-Not1 highlighted two binding surfaces, between Ccr4 and Caf1, and between Caf1 and Not1. This confirmed earlier data suggesting that Caf1 bridges the Not1 scaffold subunit with the Ccr4 deadenylase, which in yeast appears to mediate most of the exonucleolytic degradation of poly(A) tails (Tucker et al. 2001). Interestingly, Ccr4 interacts with Caf1 through its leucine-rich repeat domain, while its exonuclease domain is linked to the complex through a flexible arm composed of alpha-helices, suggesting that the Ccr4 catalytic site may explore different locations while still remaining attached to the complex. From a functional viewpoint, the two interactions (between Ccr4 and Caf1, and between Caf1 and Not1) are required for efficient deadenylation *in vivo*. Given that mutations of Not1 preventing the recruitment of the Caf1-Ccr4 dimer affect deadenylation, one can conclude for the first time that the Not1 scaffold subunit is implicated in deadenylation. Indeed, in this mutant a fully functional (wild type) Caf1-Ccr4 dimer is present at normal level in the cell, yet deadenylation is blocked. Interestingly, even though the interface between Not1 and Caf1 is formed by conserved amino acids located in both Not1 and Caf1, the geometry of interaction is not essential for activity as a covalent linkage of a Not1 mutant, defective in Caf1 recruitment, to the Caf1 subunit partially restores mRNA decay and cell growth. The absence of the requirement for a precise geometry of the complex is in agreement with both the flexible positioning of the Ccr4 catalytic site relative to the remainder of the complex, and the fact that two spatially distant catalytic sites appear to be used for deadenylation in evolutionarily divergent complexes: Caf1 only in plants and trypanosomes; Caf1 and Ccr4 in metazoans, and principally Ccr4 in yeast.

Why is a bulky complex including the large, approximately 250kDa, Not1 protein required for deadenylation *in vivo*, if the active subunit(s) Ccr4 and/or Caf1 can efficiently degrade poly(A) sequences *in vitro*? One obvious possibility was that the Not1 protein, which forms the scaffold of the CCR4-NOT complex, could also serves as a platform for transient interactions with different protein “adaptors” which would serve as mediators between

mRNA targets and the RNA degradation machinery. While this possibility remained hypothetical for several years, recent results have provided definitive proof for this concept. Thus, in mammalian miRNA-mediated decay, GW-repeat proteins were shown to interact with the CNOT9 subunit in the CCR4-NOT complex, thus bridging the interaction between the "executor" deadenylases and the mRNA recognition "reader" miRNA-AGO complex (Y. Chen et al. 2014; Mathys et al. 2014). Similarly for ARE-mediated RNA decay, the structural basis for TTP interaction with Not1 has been described at the atomic level (Fabian et al. 2013). In this case, the "executor" complex is directly recruited by the mRNA-binding protein that associates with target mRNAs. Related mechanisms probably apply to nanos-induced mRNA decay (Bhandari et al. 2014), Puf-mediated mRNA deadenylation (Goldstrohm et al. 2007) (see also results above for Puf3), and perhaps also to the Roquin-mediated TNF-α mRNA degradation (Leppek et al. 2013). However in these last cases, the structural organization of the link connecting the "executor" and the "reader" still remains to be deciphered. It is possible that every mRNA in a given cell has its own "adaptor", which targets this transcript for deadenylation by the CCR4-NOT complex (or other deadenylase). This would argue that mRNA decay is a highly specific and regulated process (Figure 59). However, one cannot exclude that in addition to its targeted actions, the CCR4-NOT complex has also a generic deadenylase activity that may randomly shorten the poly(A) tails of any mRNA. Such activity could result from the direct mRNA-binding activity of some core subunits of the CCR4-NOT complex. Consistent with the latter, the Caf40 (CNOT9 in mammals) subunit of the complex has been described as non-specific RNA/DNA-binding armadillo-repeat protein *in vitro* (Garces et al. 2007).

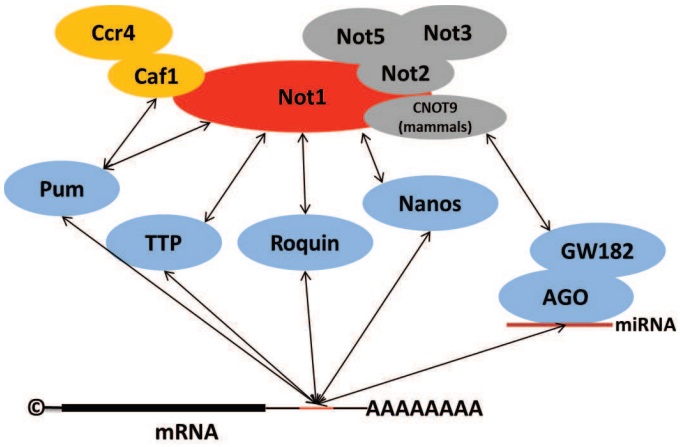

Figure 59. The CCR4-NOT complex targeting to its mRNA substrates is mediated by plethora of adaptor proteins and complexes that bind to the Not1 scaffold factor or other CCR4-NOT complex subunits. Hence mRNA decay mediated by the CCR4-NOT complex can be induced by miRNA-associated complexes (AGO-GW182), Nanos, Roquin1/2, TTP, and Pum1/2 RNA-binding proteins. Each mediator targets specific group of mRNAs, binding to its response element, generally located in the mRNA 3' UTR. CCR4-NOT complex subunit names are given in respect to the yeast homologous complex, while Caf40 (CNOT9 subunit in mammals) is named as CNOT9, as this subunit was shown to mediate interaction between GW182 and CCR4-NOT complex (Mathys et al. 2014; Y. Chen et al. 2014).

Another related question is how general is the involvement of the CCR4-NOT complex for mRNA deadenylation and decay? In other words, are all mRNAs subjected to CCR4-NOT mediated deadenylation or are some mRNAs not affected by its activity? It is obvious that mRNas targeted by quality control processes such as NMD do not require the activity of the CCR4-NOT complex for their degradation. However, available transcriptome-wide data (Sun et al. 2012) suggests that the decay of some "normal" mRNAs is not affected in *ccr4* and *caf1* mutants. Some of those RNAs may use alternative mRNA decay routes like the deadenylation-independent mechanism described for particular transcripts (Badis et al. 2004). Defining the mRNA decay factors and pathway(s) used by each mRNA at the transcriptome level would provide clues on the determinants directing one mRNA to a given degradation pathway.

Focusing on one mRNA, another interesting question relates to the stoichiometry of mRNA deadenylation machinery relative to the target mRNA. In other words, how many CCR4-NOT complexes can be recruited for a given transcript? Indeed, many mRNAs in cells have long, sometimes highly-structured 3'-UTRs, which generally carry multiple binding motifs for RNA-

binding factors. If several of these factors interact with the CCR4-NOT complex, how is this organized? For example, in the TNF-α 3'-UTR there are at least two sequence motifs, one binding TTP and the other interacting with Roquin1/2. If these proteins bind simultaneously to one mRNA molecule, do they interact simultaneously with one CCR4-NOT complex, enhancing its local concentration by preventing its release? Or in contrast, could the two proteins bind two different CCR4-NOT complexes? The latter situation might have a reduced impact on deadenylation as only one complex would be able to access the poly(A) tail 3' end at any given time. Obviously, mixed models are also possible between these two extremes. Additional analyses, possibly involving single-molecule approachs *in vitro*, will be required to answer this question (Figure 60).

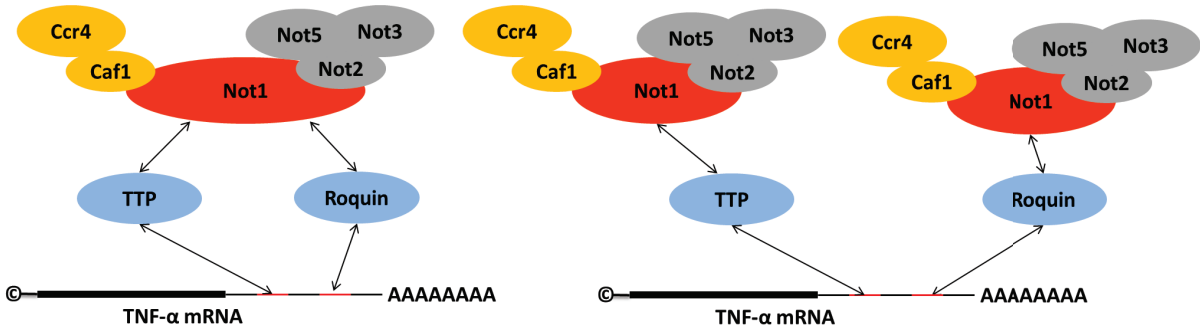

Figure 60. How many CCR4-NOT complex(es) are recruited on a given mRNA? Co-occurrence in a given mRNA of binding motifs for different RNA-binding proteins interacting with the CCR4-NOT complex might result in two extreme situations: recruitment of one CCR4-NOT complex tethered by several links to the target transcript or engagement of several CCR4-NOT complexes.

Beside our structural and functional analysis of the Ccr4-Caf1-Not1 ternary module, we also investigated, in collaboration with the group of Elena Conti, the Not1-Not2-Not5 module. This work revealed an intricate network of interactions connecting each pairs of proteins present in the structure. A particular feature of the yeast NOT-module is that it contains two paralogous subunits, Not3 and Not5, for which a single orthologue is present in many other species. A simple model compatible with the structural data would be that Not3 and Not5 are mutually exclusive alternate subunits.

Interestingly, when the Not2 or Not3 subunits are unable to enter the CCR4-NOT complex, they appear to be subjected to rapid protein degradation *in vivo*, probably reflecting the stabilizing role of the their interaction with the Not1 subunit. Mutations specifically disrupting interactions within the NOT-module are functionally important as they affect cell growth. However, they do not seem to perturb mRNA decay *in vivo* suggesting that they affect another biological function, or a restricted number of mRNAs. It is important to note that Not1 deletion mutants lacking the C-terminal region, which is involved in interaction with Not2 and Not5 modules, are non viable. This suggests that the yeast Not1 essential function requires interaction with the NOT-module.

What might be the biological role of the NOT-module? One hypothesis was that the module is required for specific mRNA decay regulation, as this module was reported to bind poly(U) *in vitro* (Bhaskar et al. 2013). However, *in vivo* studies of the mRNA decay kinetics of an mRNA containing a poly(U) stretch in its 3'-UTR important for its stability, namely the EDC1 mRNA, did not not reveal alteration of its decay kinetic when the NOT-module was genetically disrupted. If the function of the NOT module in mRNA decay remains elusive in yeast, it is worth remembering that inactivation of this module in fly resulted in altered decay of the Hsp70 mRNA (Boland et al. 2013). Further work will be necessary to unravel the molecular mechanism(s) to which the NOT module contributes. Understanding this function is of high importance, as recently several SNPs associated with an acute form of T-cell lymphoblastic leukemia (ALL) were identified in the human CNOT3 gene. These alterations resulted in complete protein loss (De Keersmaecker et al. 2013). Thus, careful characterization of the NOT-module might contribute to better ALL treatment in the future.

3.2 Translation repression by CCR4-NOT complex.

The Caf1-Ccr4-Not1 complex structure revealed a specific MIF4G-like fold in the Not1 domain involved in interaction with Caf1. The same fold is adopted by a segment of the translation initiation factor eIF4G interacting with the eIF4A helicase. This interaction is required for efficient translation initiation. Intriguingly, superposition of the Not1- and eIF4G- MIF4G domains reveals their high structural similarity. Interestingly, Caf1 and eIF4A interact with different MIF4G surfaces. Moreover, the surface of Not1 corresponding in eIF4G to the region of interaction with eIF4A is highly conserved. This suggested that Not1

might interact with an RNA helicase in a manner similar to eIF4G. As I observed that some multi-copy suppressors of the temperature sensitive phenotype of Ccr4-Caf1-Not1 interaction mutants were identified as translational repressors, I hypothesized that the CCR4-NOT complex could be involved in translation regulation. Indeed, two papers provided evidence for a two-step process of mRNA repression by miRNAs, first involving a translation initiation repression step and then induction of deadenylation (Bazzini et al. 2012; Djuranovic et al. 2012). It was thus tempting to speculate that the Not1-putative helicase interaction, suggested by structure and sequence similarities, could be involved in translation repression. Preliminary experiments failed to support this model in yeast. However, the human Ddx6 helicase (homologous to the of yeast Dhh1 protein) was recently identified as a Not1-MIF4G interacting partner which is functionally required for the translation repression step (Tarn and Chang 2014; Hilliker et al. 2011). The failure to identify this interaction in yeast may indicate that it is fragile, or too transient, to be detected by standard methods.

These observations raise numerous questions. Amongst them, one can wonder whether Not1 is always part of a CCR4-NOT complex or if some DHH1-NOT complexes lacking Ccr4 do also exist? In such cases, CRR4-NOT1-DHH1 complexes could also be present. In other words, is the interaction between Dhh1-Not1 and Not1-Caf1 mediated by one Not1 subunit or restricted to different Not1 subunits? along the same line, does one CCR4-NOT complex mediate both activities, translation repression and mRNA decay induction, through the successive binding of Dhh1 and then with Caf1-Ccr4 to one molecule of Not1, or are two Not1 proteins successively targeted to one transcript, the first associated with Dhh1 and the second associated with Caf1-Ccr4? Interestingly, if the first activity, namely translational repression, could be restricted to one complex lacking the Caf1 and Ccr4 subunit, this could suggest a role of Not1-containing complexes in mRNA storage. Indeed, one could speculate, that the DHH1-NOT complex targeted to mRNA could induce its silencing without subsequent mRNA degradation (Figure 61). Such molecular mechanisms could have a great biological significance for neuron function, where many mRNAs are known to be stored in a translationally repressed state before a local activation during the synaptic activation processes (Udagawa et al. 2012; Bramham et al. 2008). Whether Not1-containing complexes are involved in this neuron plasticity regulation might be an intriguing line of research.

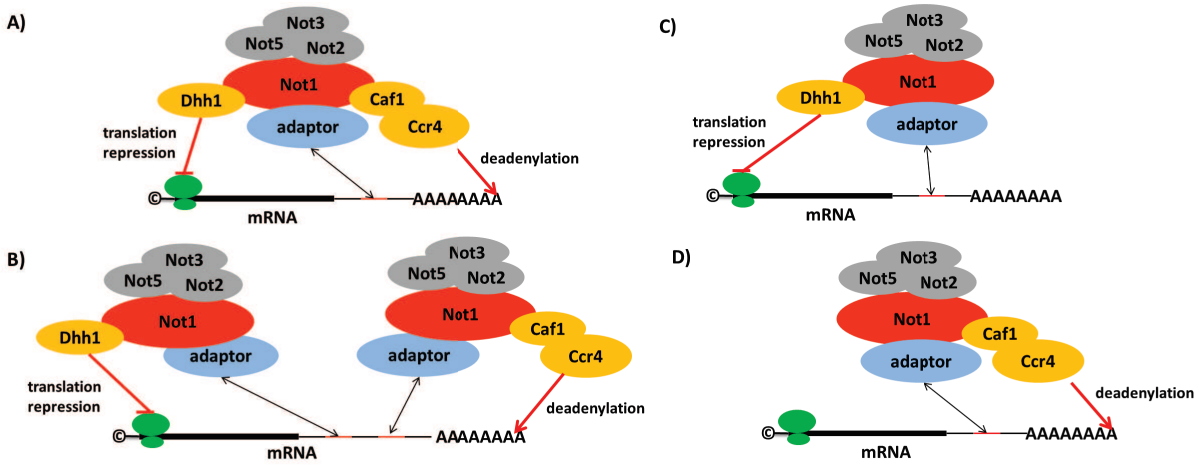

Figure 61. Concomitant or mutually exclusive association of partners to Not1 could provide specific biological functions. A) Dhh1 and Caf1-Ccr4 modules might associate with one Not1 scaffold, thus allowing one complex to simultaneously repress translation and induce deadenylation. B) Both functional activities might be separated to different Not1-containing complexes, DHH1-NOT and CCR4-NOT. C) Some mRNAs might escape the degradation step, forming mRNPs translationally silenced by a DHH1-NOT complex. D) Some mRNAs might be subjected directly to degradation by a CCR4-NOT complex skipping an initial translation inhibition step.

Taking the observation of helicase association with Not1 and translational repression together with the role of RNA-binding proteins in targeting the CCR4-NOT complex discussed in the previous paragraph, it would be interesting to determine whether RNA-binding proteins trigger preferentially (or exclusively) translational repression or mRNA decay or whether this outcome is purely dependent upon the composition of the complex recruited. If many recent results have provided us with insights into the organization and function of the CCR4-NOT complex, it may seem worrisome that these findings provide less answers than the number of new questions that they raise.

3.3 Genome-wide mRNA expression profiles of mRNA processing factors: Puf3-mediated CCR4-NOT complex recruitment.

The last part of my thesis work was using large sets of data published by the Cramer lab as part of their genome-wide cDTA analysis of different RNA processing factor mutants in an attempt to extract information of the regulation of the CCR4-NOT complex. Correlating expression profiles with RNA-protein genome-wide interaction data sets revealed a correlation between Puf3 bound mRNAs and those whose regulation is mediated by the CCR4-NOT complex. This suggests a putative interaction between the Puf3 RNA binding protein and the CCR4-NOT complex. Experimental evidence for this interaction and thus indirectly in the role of Puf3 in mRNA degradation (or translational repression) was provided by two-hybrid analyses and co-immunoprecipation assays. I have discussed the interplay between RNA-binding proteins and the CCR4-NOT complex in the above text. Thus, I would like to focus here on a part of the work where I tried to establish the role of putative mRNA secondary structures in linking the decay of specific mRNAs to their translation. Experimental determination of yeast mRNA secondary structures in a transcriptome-wide manner by the PARS approach (Kertesz et al. 2010) revealed the complex structural organization of mRNAs that are far from being just single-stranded nucleic acid polymers. Moreover, mapping Puf3-response elements (UGUA[AU]AUA) within the sequences of identified Puf3 target mRNAs detected their presence in stems in these secondary structures. Such locations probably prevent the Puf3 protein from accessing these binding sites, as Puf3 is known to bind only single-stranded RNA sequences. However, as the Puf3

binding-motifs were base-pairing with a complementary sequence located in the open reading frame of the target mRNAs, this suggests that Puf3 binds to its response element as soon as the ribosome travels along the complementary RNA strand. Indeed, this would unfold the stem and expose the Puf3 binding motif (Figure 56). Consistently, in the literature one can find examples of base-pairing of Pum1/2 response elements with miRNA binding sites in the p27 mRNA in mammals (Kedde et al. 2010). Moreover, genome-wide data suggests a statistically significant co-occurrence of Pum motifs with miRNA binding sites in many other mRNAs (Galgano et al. 2008). In yeast, a link between translation and binding of the Puf3 binding motif was already established. Indeed, it was shown that Puf3 binds to its target mRNAs, relocates them towards the mitochondrial outer membrane, and also represses their expression (Quenault et al. 2011). While the translational repression role might be mediated by the CCR4-NOT complex, the localization of mRNAs towards mitochondrial membrane was shown to be a co-translational process. However, the molecular nature of this process was not elucidated (Saint-Georges et al. 2008; Eliyahu et al. 2010; Gadir et al. 2011). In one of the models proposed it was hypothesized that during active translation the ribosome unfolds the stem thus allowing Puf3 to bind to its response element. This would simultaneously promote the relocation of the mRNA to the mitochondrial outer membrane, while initiating deadenylation of the transcript. Thus, a simple dynamics of secondary structure element resulting from the pairing of a segment of a 3'-UTR with a complementary sequence located in the ORF of a given mRNA could regulate the effects previously associated with Puf3-binding: co-translational localization and induction of co-translational mRNA decay (Figure 62). The experiments that I performed did not provide a definitive evidence for this model. Nevertheless, I believe that the role of mRNA secondary structural elements and of their dynamics in mRNA regulation is underestimated (Mortimer, Kidwell, and Doudna 2014). Several examples of dynamic RNA secondary structure elements and of their involvement in regulation do exist: the Vts1 protein has been shown to bind shape-specifically to its response element and regulates its mRNA stability by recruiting the CCR4-NOT complex in yeast (Rendl et al. 2008; Oberstrass et al. 2006). Another biological example is Staufen-mediated decay, as has been shown, Staufen specifically binds to double-stranded RNA regions and induces mRNA degradation partly involving NMD-machinery (Laver et al. 2013). However, these examples are restricted to a limited number of mRNA targets. Perhaps, future improvements in mRNA secondary

structure probing, both *in vivo* and *in vitro* (Kertesz et al. 2010; Rouskin et al. 2014; Ding et al. 2014), coupled with functional annotation of detected secondary structure elements in mRNA regulation, would provide unprecedented understanding of mRNA functioning in living cells.

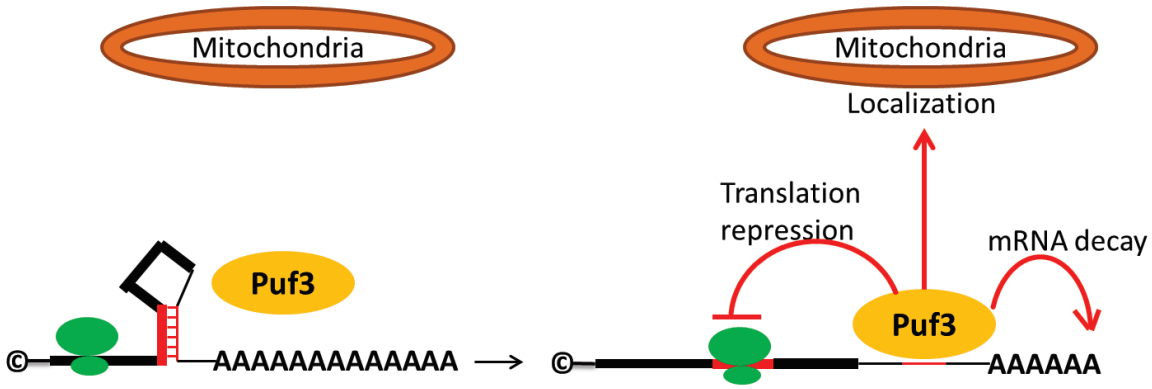

Figure 62. Hypothesis of Puf3-mediated mRNA localization and repression mediated by co-translational changes in targeted mRNA secondary structure.

4. Materials and Methods

4.1 Strains and media

4.1.1 Bacterial media

E .coli MH1 bacteria were used for molecular cloning and plasmid production. After transformation, bacteria were grown on LB plates (10g/l tryptone, 5g/l yeast extract, 5 g/l NaCl, 10% agar per liter) with the required antibiotic (see below). For plasmid recovery, bacteria cells were grown in liquid LB media (10g/l tryptone, 5g/l yeast extract, 5 g/l NaCl per liter). Depending on selection marker, used during transformation or plasmid production, the following antibiotics were added to the plates or liquid medium at the indicated concentration: 50 µg/ml ampicillin, 50 µg/ml kanamycin, 50 µg/ml gentamicin. Bacteria were grown at 37^0C unless otherwise indicated, and shaken at 170 rpm for liquid cultures.

4.1.2 Yeast media

Both haploid and diploid yeast cells were grown either in rich media or in synthetic defined drop out media, lacking one or several amino acids or bases. Synthetic media either contained 2% glucose or 2% galactose as source of carbon and energy.

Rich media was usually prepared from YPDA dry stocks (10g/l yeast extract, 30 g/l bacto peptone, 20g/l glucose, 40 mg/l adenine sulfate for 1 liter).

Synthetic defined drop out media contained per liter the recommended quantity of Complete Supplement Mixture lacking the appropriate amino acid(s) and/or base(s) combination (X) (CSM-X, (Bio101)), 6,7 g/l Difco yeast nitrogen base without amino acids, 20g/l glucose or galactose, 50 ml Sorensen's phosphate buffer (20x).

If media prepared in solid form, 2% bacto agar was added. Yeast were grown at 30^0C unless otherwise indicated it was indicated, and shaken at 170 rpm for liquid cultures.

4.1.3 Yeast strains and plasmids

Table 3. Yeast strains.

Name	Yeast strain	Genotype
BMA64	BMA64	*ade 2-1 his3-11,115 leu2-3,112 trp1Δ ura3-1 can1-100 Mat a*
T26 N28	Δnot1+(Not1)	*ura3-1, Δtrp1, ade2-1, leu2-3,112, his3-11,15, NOT1::HIS3 pFL 38 (NOT1) Mat a*
T23 N4	Δpop2	*ura3-1, Δtrp1, ade2-1, leu2-3,112, his3-11,15 ,*

		POP2::TRP1 Mat a
T23 N10	Δccr4	*ura3-1, Δtrp1, ade2-1, leu2-3,112, his3-11,15 , CCR4::TRP1 Mat a*
T23 N214	Puf3-TAP	*ura3-1, Δtrp1, ade2-1, leu2-3,112, his3-11,15 , PUF3 TAP tag 3', TRP1 Mat a*
T24 N13	PUF3-3HA	*ura3-1, Δtrp1, ade2-1, leu2-3,112, his3-11,15 , PUF3 tag 3' HA ::HIS3 Mat a*
MAV203		*Mat a; leu2-3,112; trp1-901; his3-200; ade2-101; cyh2R; can1R; gal4-542; gal-80; GAL1::lacZ; HIS3UASGAL1::HIS3@LYS2; SPAL10 UASGAL1::URA3*
HF7c		*Mat α; Ura3-52 his3-200 ade2-101 lys2-801 trp1-901 leu 2-3, 112 gal4-542 gal80-538 LYS2::GAL$_{UAS}$-GAL1$_{TATA}$-HIS3 URA3::GAL4$_{17mers(x3)}$-CYC1$_{TATA}$-lacZ*

Table 4. Yeast plasmids.

Name	Vector	Insert	Selection marker
pBS4039	pFL39	empty	TRP1
pBS4802	pFL39	5'UTR-Not1-TAP-3'UTR	TRP1
pBS4824	pFL39	5'UTR-Not1(981-2108)-TAP-3'UTR	TRP1
pBS4825	pFL39	5'UTR-Not1(1081-2108)-TAP-3'UTR	TRP1
pBS4826	pFL39	5'UTR-Not1(1296-2108)-TAP-3'UTR	TRP1
pBS4827	pFL39	5'UTR-Not1(1696-2108)-TAP-3'UTR	TRP1
pBS4829	pFL39	5'UTR-Not1(754-2108)-TAP-3'UTR	TRP1
pBS4828	pFL39	5'UTR-Not1(154-2108)-TAP-3'UTR	TRP1
pBS4819	pFL39	5'UTR-Not1(1-550)-TAP-3'UTR	TRP1
pBS4820	pFL39	5'UTR-Not1(1-981)-TAP-3'UTR	TRP1
pBS4821	pFL39	5'UTR-Not1(1-1081)-TAP-3'UTR	TRP1
pBS4822	pFL39	5'UTR-Not1(1-1291)-TAP-3'UTR	TRP1
pBS4823	pFL39	5'UTR-Not1(1-1696)-TAP-3'UTR	TRP1
pBS4830	pFL39	5'UTR-Not1Δ(754-1000)-TAP-3'UTR	TRP1
pBS4831	pFL39	5'UTR-Not1 Δ(154-754)-TAP-3'UTR	TRP1
pBS4868	pFL39	5'UTR-Not2-VSV-3'UTR	TRP1
pBS4975	pFL39	5'UTR-Not3-VSV-3'UTR	TRP1
pBS5154	pRS415	5'UTR-Not2-VSV-3'UTR	LEU2
pBS5155	pRS415	5'UTR-Not3-VSV-3'UTR	LEU2
pBS5156	pRS426	tetO2$_{repressible}$-CYC1$_{promoter}$-luciferase$_{fyrefly}$-PGK1(3'UTR)-U1A$_{BindingSite}$	URA3

pBS5157	pRS426	$tetO2_{repressible}$-$CYC1_{promoter}$-$luciferase_{fyrefly}$-PGK1(3'UTR)-$U1A_{reverse}$	URA3
pBS5158	pRS426	$tetO2_{inducible}$-$CYC1_{promoter}$-$luciferase_{fyrefly}$-PGK1(3'UTR)-$U1_{BindingSite}$	URA3
pBS5159	pRS426	$tetO2_{inducible}$-$CYC1_{promoter}$-$luciferase_{fyrefly}$-PGK1(3'UTR)-$U1_{BindingSite}$	URA3
pBS5161	pRS415	5'UTR-Ccr4-$U1A_{RNAbinding\ domain}$-3HA-3'UTR	LEU2
pBS5162	pRS415	5'UTR-Ccr4-L339E/L341E-$U1A_{RNAbinding\ domain}$-3HA-3'UTR	LEU2
pBS5163	pRS413	5'UTR-Caf1-M290K/M296K-$U1A_{RNAbinding\ domain}$-3VSV-3'UTR	HIS3
pBS2872	pDEST22	Not1	TRP1
pBS2816	pDEST22	Not2	TRP1
pBS4185	pDEST22	Not3	TRP1
pBS4188	pDEST22	Not5	TRP1
pBS4190	pDEST22	Caf40	TRP1
pBS2672	pDEST22	Caf1	TRP1
pBS2702	pDEST22	Ccr4	TRP1
pBS2876	pDEST32	Not1	LEU2
pBS2819	pDEST32	Not2	LEU2
pBS4282	pDEST32	Not3	LEU2
pBS4189	pDEST32	Not5	LEU2
pBS4218	pDEST32	Caf40	LEU2
pBS2661	pDEST32	Caf1	LEU2
pBS5170	pDEST32	Ccr4	LEU2
pBS4838	pDEST22	Δ(1-980)	TRP1
pBS4840	pDEST22	Δ(1-1080)	TRP1
pBS4842	pDEST22	Δ(1-1695)	TRP1
pBS4839	pDEST32	Δ(1-980)	LEU2
pBS4841	pDEST32	Δ(1-1080)	LEU2
pBS4843	pDEST32	Δ(1-1695)	LEU2
pBS5164	pDEST22	Puf3	TRP1
pBS5165	pDEST22	Puf3-$N_{terminus}$	TRP1
pBS5166	pDEST22	Puf3-$C_{terminus}$	TRP1
pBS5167	pDEST32	Puf3	LEU2
pBS5168	pDEST32	Puf3-$N_{terminus}$	LEU2
pBS5169	pDEST32	Puf3-$C_{terminus}$	LEU2

4.2 Bacterial manipulations

4.2.1 Molecular cloning

4.2.1.1 Plasmid DNA isolation from E.coli

Plasmids were purified from *E. coli* using the NucleoSpin Plasmid kit (Macherey Nagel) for miniprep size preparations, or NucleoBond Xtra Midi kit (Macherey Nagel) for midiprep size preparations. Manipulations were performed following manufacturer's instructions.

4.2.1.2 PCR and restriction

PCRs for cloning in yeast expression plasmids were performed using Phusion high-fidelity DNA polymerase (Finnzymes), PfuUltra II fusion HS DNA polymerase (Agilent) or Q5 high-fidelity DNA polymerase (NEB) with their corresponding buffers following the manufacturer's recommendations and instructions. The resulting PCR products, purified from the gel, were digested by the appropriate restriction enzymes (New England Biolans, Fermentas), following the manufacturers' instructions in a 50 µl total volume.

4.2.1.3 Ligation

Digested plasmids and PCR products were fractionated by electrophoresis in low melting agarose at 4^0C. Appropriate bands were excised from the gel and placed in an Eppendorf tube. The band was melted at 65^0C for 10 minutes. The tube was then transferred to 42^0C. Approximately equimolar quantities of purified plasmids and PCR products were mixed with 2x ligation mix (T4 DNA ligase 20U/µl, 2x T4 DNA ligase buffer (New England Biolabs)) and incubated at 16^0C overnight. Before bacterial transformation, ligation mixes were melted at 65^0C and mixed with 50 µl 50mM $CaCl_2$. After cooling on ice, competent cells were added to ligation reactions and transformation proceeded as described below.

4.2.1.4 Bacterial transformation

100 µl competent *E. coli* MH1 cells were added to 1 µl plasmid or 50µl of cooled ligation products (see above). After 20 min incubation on ice, cells were heat-shocked at 42^0C for 90 seconds, then returned back on ice and kept for additional 5 min. After addition of 1ml LB, cells were incubated for 1 hour at 37^0C. A fraction or entire transformation was plated on solid LB mediua containing the appropriate antibiotic for plasmid selection.

4.2.1.5 Restriction analysis of E. coli transformants

A selected number of colonies recovered after transformation, were grown in LB media containing appropriate antibiotic. Plasmids were purified using the miniprep kit. Correct insertion of the PCR products was verified by restriction analysis with select restriction endonucleases, which allowed the discrimination of empty plasmid from the ones with the desired insertion. Digestions were analyzed by electrophoresis in agarose gels. Inserts of positive plasmids then were sequenced (GATC Biotech).

4.2.1.6 QuickChange site-directed mutagenesis

Point mutations were generated following principles of the QuickChange site-directed mutagenesis strategy. Briefly, a pair of complementary primers containing the desired mutation flanked on both sides by 15-20 nucleotides were designed and ordered. These primers were used to PCR-amplify the plasmid DNA containing the wild type target sequence using the PfuII DNA polymerase. The resulting PCR products were treated with DpnI (New England Biolabs) at 37^{0}C for 2-3 hours, to digest the non-mutated plasmid DNA used as template for PCR reaction. DNA was extracted with phenol:chloroform:isoamyl alcohol, ethanol precipitated and resuspended in water and then transformed in MH1.

4.3 Yeast manipulation

4.3.1 Yeast methods used for cloning and strain construction

4.3.1.1 Isolation of yeast genomic DNA

1.5 ml of saturated yeast culture was collected at in an Eppendorf tube 14 000 rpm (20 000 g) for 5 min and resuspended in 300 µl of yeast lysis buffer (see list of buffer below). 300 µl of glass beads and 700 µl phenol was added. The mixture was vortexed 4 times for 2-3 minutes, cooling it on ice between each vortexing cycle. The mixture was centrifuged at 14000 rpm (20 000 g) for 5 minutes at 4°C. The upper phase containing the DNA was taken and transfered to a second tube containing XX µl of phenol:chloroform:isoamyl alcohol and second round of PCI extraction was performed. The second upper phase was recovered and DNA was precipitated by ethanol as follows: 1/10 volume of 3M NaAc pH 5.2, 2.5 volume of 100% ethanol and 1µg of glycogen were added and the final mix was incubated at -20^{0}C for a minimum of 1 hour. Following centrifugation at 14000 rpm (20 000 g) for 30 min. at 4^{0}C, the pellet was washed with 70% ethanol and spun again at 14000 rpm (20 000 g) for 10 min at

4^0C. After drying, the pellet was dissolved in water. For gene disruption verification, the DNA was dissolved in 200 µl H_2O of which 1 µl was used for a 20 µl PCR.

4.3.1.2 Yeast plasmid DNA isolation

1.5 ml of saturated yeast culture, grown in selective media, was pelleted and resuspended in 100 µl of SCE buffer. A pinch of zymolyase enzyme was added and total mixture was incubated at 30^0C for 1 hour. After incubation, the extract was processed with miniprep protocol for bacterial plasmid purification. Then recovered DNA was transformed in MH1 *E. coli* cells. Plasmid DNA was extracted from select transformants as described above.

4.3.1.3 Yeast gene disruption and verification

The selection marker used for gene disruption, was amplified in a polymerase chain reaction (PCR), using Taq DNA polymerase in Thermopol buffer following the manufacturer recommendations. Primers were designed to contain 40-60 nucleotides sequence overhang, corresponding to flanking regions of the gene targeted for disruption. The 20 nucleotides at 3'-end of the primers corresponded to cassette region being amplified. The size and quantity of PCR product were verified by gel electrophoresi. The DNA product was then purified by adding 1 volume of phenol:chloroform:isoamyl alcohol extraction and precipitated with ethanol as described above. The precipitated PCR product was dissolved in 10 µl H_2O and used for yeast transformation as it described in next paragraph.

Selected yeast colonies were inoculated in liquid YPDA and genomic DNA was recovered as described above. Gene deletions were verified by two PCR reactions using Taq DNA polymerase that overlapped the 5' and 3' recombination sites respectively. PCR products were analyzed by electrophoresis in TBE agarose 1% gels.

4.3.1.4 Yeast DNA transformation

50 ml of yeast culture grown in YPDA to an OD_{600} 0.8-1 was pelleted at 5000 rpm (4500 g), washed in 50l ml 10 mM Tris-Cl pH 7.5 and pelleted again. The resulting pellet was resuspended in 1mM LiT containing 10 mM DTT, followed by incubation at room temperature for 40 minutes with gentle shaking. Yeasts were pelleted again and resuspended in 750 µl LiT containing 10 mM DTT. 100 µl of these competent yeast cells was added to 5 µl of plasmid DNA, 5 µl of denatured carrier DNA (10mg/ml) and 50 µl LiT. This mixture was then incubated at room temperature for 10 min. Then 300 µl of PEG4000

dissolved in LiT (1g/ml) was added to the transformation tube. The tube was then incubated 10 minutes at room temperature and 15 minutes at 42^{0}C. Cells were pelleted at 14000 rpm (20000 g) for 10 seconds, resuspended in 1 ml YPDA and incubated at 30^{0}C for 1 hour. Then cells were pelleted at 14000rpm (20000 g) for 60 seconds, resuspended in 100 µl 10mM Tris pH 7.5 and plated on the appropriate synthetic defined drop out medium plate or on antibiotic containing rich-media.

4.3.1.5 Yeast diploid strain sporulation and dissection

Two haploid yeast strains of opposite mating types (a and α) carrying the genes to be combined and compatible selection markers were mixed on YPDA plates. After overnight incubation, the YPDA mating plate was replica-plated on doubly selective media, allowing selection of mated diploid yeast cells. This plate was incubated over night at 30^{0}C. Some diploid cells were transferred on a plate containing sporulation media and incubated 3-4 days, until 50-90% of cells were sporulated. Yeast sporulation is detected by appearance of characteristic 4-spore containing assemblies (tetrads), visible under the microscope. Once sporulation was detected, a pinch of yeast was dissolved in 450 µl SSC buffer (Invitrogen UltraPure™ 20X, 15557-036) containing zymolyase and incubated for 5-7 minutes at room temperature. Zymolyase treatment greatly facilitates tetrad dissection by disrupting cell wall of the mother cell that keeps the 4 spores together. 20 µl of zymolyase-treated yeast culture was deposited on a fresh YPDA plate and dissected using a Zinger MSN 400 dissection microscope. The resulting dissection plate was incubated at 30^{0}C for 2-3 days.

Once yeast colonies originating from each of the spores were grown enough on dissection plate, they were transferred to a YPDA master plate and incubated over night at 30^{0}C. This master plate was then replicated on selective media to ascertain the segregation of the markers present in the starting parent cells. The desired combination of mutants were selected and used for further analyses.

4.3.2 Yeast phenotypic assays

4.3.2.1 Yeast drop growth assay

A yeast overnight pre-culture was diluted in the early morning and grown till mid-log phase in YPDA or synthetic defined drop out media. OD_{600} was measured and an aliquot of the culture diluted in sterile water to OD_{600} 0.1. 10-fold serial dilutions were made. 2 µl of each

dilution was spotted on the solid medium, either YPDA rich medium plate or synthetic defined drop out medium plate. Plates were let to dry and incubated at different temperatures, 16^{0}C, 25^{0}C, 30^{0}C and 37^{0}C, for 2-6 days.

4.4 Biochemical methods

4.4.1 RNA analysis methods

4.4.1.1 RNA extraction

For analysis of RNA levels and half-life estimations, 10 ml of yeast culture at OD_{600} 1.0 grown in selective media were pelleted at 5000 rpm (4500 g). The pellet was frozen in liquid nitrogen. If RNA extraction was postponed to following days, pellets were stored at -80^{0}C.

RNA was isolated using the hot phenol extraction method. 450 µl phenol saturated with water (pH 4.5-5) were added to the frozen pellet. The mixture was shaken at 1400 rpm at 65^{0}C during 1 min. Then, 450 µl of TES buffer was added and the extraction reaction was kept foran additional 30 min at 65^{0}C. During these 30 min of incubation, each 6 min the tubes were vigorously shaken at 1400 rpm for 1 min. Then tubes were incubated at 4^{0}C for 10 min to facilitate phase separation. Finally, the tubes were spun at 14000 rpm (20000 g) for 5 min at room temperature. The upper phase was recovered and re-extracted with 450 µl of phenol. For this second extraction, the upper phase was manually shaken with phenol and the extraction reaction was incubated 5 min at 4^{0}C. After phase separation by centrifugation (as above), the upper phase re-extracted with 400 µl chloroform as described for the second extraction above. 250 µl of upper phase was mixed with25 µl 3M NaAc pH 5.2 and 625 µl ethanol (stored at -20^{0}C) . After mixing, tubes were incubated at -20^{0}C for at least 1 hour. After 30 min of centrifugation at 4^{0}C, the nuclei acids pellet was washed with 500 µl 70% ethanol (-20°C) and spun at 14000 rpm (20000 g) for 5 minutes at room temperature. Collected RNA was resuspended in 50 µl H_2O.

4.4.1.2 Northern blot analysis

4.4.1.2.1 RNA analysis after RNA fractionation on agarose-formaldehyde gel

10 µg of RNA sample were mixed with 2 µl RNA loading due, 2 µl 10x MOPS buffer, 3.5 µl formaldehyde and 10 µl formamide. Samples were then incubated at 65^{0}C for 15 minutes, cooled on ice for 10 minutes, and loaded on a 2% agarose-formaldehyde gel in MOPS buffer. After 4-5 hours of migration at 100V in 1x MOPS buffer, the gel was washed in 10x SSC

(Invitrogen) for 10 minutes. RNAs were transferred to a Hybond-XL membrane (GE Healthcare) in 10x SSC by capillary blotting overnight. RNAs were cross-linked to the membrane by exposure to 240 mJ UV light (Stratalinker). The membrane was stained in 0,1% methylene blue 0.5 NaAc pH 5.2. Excess of dye was washed with H_2O. The quality of RNA transfer was assessed from the RNA migration profile revealed by methylene blue staining.

After fixation and methylene blue coloration, the membrane was pre-hybridized in Church buffer for 1 hour, followed by overnight hybridization in fresh Church buffer containing the desired probe. Hybridization temperature was selected below the calculated melting temperatures of DNA oligonucleotide probes (see below). The next day, membranes were washed at hybridization temperature in 2x SSC 0.5% SDS (3x 15 minutes washes) and 0.1x SSC 0.5% SDS (1x 15 minutes wash). Signals were visualized with a Typhoon 8600 Variable Mode Imager and quantified using ImageQuant 5.2 software (Molecular Dynamics).

4.4.1.2.2 RNA analysis after polyacrylamide-urea gel separation

10 µg of RNA sample (e.g., containing MFA2pG mRNA) were mixed with 5 µl loading dyee, heated at 65^0C for 15 minutes. and then cooled on ice. 20 cm X 20 cm 6% polyacrylamide 8.0 M urea gels were pre-run at 15 W for 15 minutes. RNA was loaded and electrophoresis was performed in TBE at 20 W at room temperature. RNA present in the gel was transferred to a Hybond-XL membrane in a wet electroblotting system at 200 mA, 1.5 hours at 4^0C. Membrane staining and hybridization were performed as indicated above.

4.4.1.2.3 Probe labeling

All probes were labeled by incubating 15 pmol of the desired oligonucleotide with 10 pmol γ-^{32}P ATP (1 mCi, HARTMANN ANALYTIC, SRP-501) and 10 U T4 polynucleotide kinase in enzyme buffer A (Fermentas) in a 30 µl reaction for 45 minutes at 30^0C. The reaction was stopped by adding 2 µl 0.5 M EDTA. After addition of 30 µl H_2O, unincorporated nucleotides were removed by passage through a Micro Bio-Spin 6 column (BioRad) at 3000 rpm for 1 minute. Oligonucleotides used for RNA detection were:

MFA2pG: OBS1298: ATTCCCCCCCCCCCCCCCCCA (55^0C),

YBR251W: OBS6461: CTTGTATGGTTGGATCCCCCG (55^0C)

YDR115W: OBS6464: CAGTGAGTTTCGGATCCCCCG (55^0C).

Hybridization temperatures are indicated in brackets.

4.4.1.3 mRNA half-life estimation

100 ml yeast cultures expressing the reporter mRNA construct were grown at 30^0C in synthetic defined drop out medium containing either 2% galactose (for the MFA2pG mRNA construct under the control of a galactose-inducible promoter) or 2% glucose (for the YDR115W and YBR251W reporters under the control of a doxycyclin-repressible promoter). At OD_{600} ~ 1.0, the cultures were pelleted at 5000 rpm (4500 g) for 5 minutes at 30^0C. Pellets were resuspended in 10 ml of the same drop out medium, but containing 2% glucose instead of galactose for the MFA2pG reporter, or containing 50 µg/ml doxycycline additionally ifor the YDR115W and YBR251W reporters. In both case, this treatment induced the switch off of the reporter promoter). Cultures were divided into 1 ml aliquots in Eppendorf tubes, which were shaken at 1400 rpm at 30^0C. At defined time-points, aliquots were pelleted for 15 seconds in a microcentrifuge and cell pellets immediately frozen in liquid nitrogen. RNA was isolated by the hot phenol extraction method (see above) and dissolved in 50 µl H_2O. 10 µg of each sample was loaded for northern blot analysis.

4.4.2 Protein analysis

4.4.2.1 Rapid protein extraction

2 ml yeast cultures were grown overnight. 1 ml aliquot of these cultures were pelleted at 14000 rpm (20000 g) for 1 minute and resuspended in 100 µl H_2O. 100 µl 0.2 M NaOH were added. After 5 minutes of incubation at room temperature, cells were pelleted by centrifugation at 14000 rpm (20000 g) for 5 minutes. Pellets were resuspended in 50 µl protein loading dye. This protocol is based on a published method (Kushnirov, 2000).

4.4.2.2 Native protein yeast extract

A 100 ml yeast culture was grown at 30^0C in rich YPDA or selective drop out medium till OD_{600} ~ 2.0. Cells were recovered by centrifugation at 5000 rpm (4500 g), washed with sterile water, and frozen in liquid nitrogen if samples were not processed immediately. For cell lysis, pellets were transferred to COREX tubes and resuspended in 500 µl buffer A with protease inhibitors cocktail. 300 µl of glass beads were added. Cell lysis was performed at 4^0C by repeating 5 cycles of vigorous vortexing for 1 minute interrupted with pauses on ice of 1 minute. The lysate was then spun at 5000 rpm (4500 g) and the liquid phase was

transferred to an Eppendorf tube. 100 µl of NaCl 5M were added and lysate was centrifuged at 14000 rpm (20000 g) for 10 minutes. After centrifugation, the upper phase was transferred to Beckman tubes and lysate was ultracentrifuged at 55000 rpm for 40 minutes (rotor TLA120.2). The liquid phase was transferred to new Eppendorf tubes and protein concentration was estimated using the Bradford method.

4.4.2.3 Protein gel analysis by SDS-PAGE

Except for "Kushnirov" extractions (sse above), protein extracts were mixed with 3x protein loading dye. Before loading on gel, tubes were heated at 90^0C for 5 minutes and spun at 14000 rpm for 5 minutes. For small scale analysis, 8.5 cm x 6 cm SDS polyacrylamide gels (SDS-PAGE) were used for protein fractionation. Proteins purified by TAP-method were analyzed on large 16 cm x 20 cm SDS-PAGE. All gels were run in Laemmli buffer. Small gels were run at 120 V, large ones at 200 V. Proteins were stained using Coomassie staining followed by destaining in 20% ethanol 10% acetic acid, or by silver staining using a SilverQuest kit (Invitrogen) following the manufacturer's instructions.

4.4.2.4 Mass spectrometry

Bands cut from the silver or Coomassie stained gels were analyzed by mass spectrometry. For silver stained gels, bands were destained by incubating them for 15 minutes in a 1:1 mixture of solutions A and B from the SilverQuest kit shaking at 14000 rpm. The mixture was removed, then 200 µl H_2O was added followed by shaking for 10 minutes. Water was removed and the bands were incubated with 200 µl acetonitrile with shaking for 20 minutes. The bands were analyzed by nanoLC-MS/MS by the Proteomics platform at the IGBMC.

4.4.2.5 Western analysis

Proteins were transferred from SDS-PAGE to a Protran nitrocellulose membrane (Whatman) in a wet tank electroblotting system in transfer buffer at 100 V for 1 hour at 4^0C. The membrane was washed in water and blocked in 5% milk in PBS-Tween. It was then incubated with a primary antibody in 5% milk-PBS-Tween for 1 hour at room temperature or overnight at 4^0C. When necessary, following 4 washes in PBS-Tween each of 10 minutes, the membrane was incubated with the secondary antibody for 1 hour at room temperature. After 4 additional washes as above, the membrane was incubated with ECL (GE Healthcare), Luminata Crescendo (Millipore) or SuperSignal West Fempto (Thermo Scientific)

chemiluminescent reagents. Signals were visualized using an ImageQuant LAS 4000 system (GE Healthcare).

Table 5. Antibodies used for western blot analyses.

Name	Against	Source	concentration
AbBS8	Stm1	Rabbit, polyclonal	1 : 2000
HA.11 Clone 16B12	HA-tag	Mouse, monoclonal Covance MMS-101P	1 : 1000
VSV-G Clone P5D4	VSV-tag	Mouse, monoclonal Roche #11667351001	1 : 1000
Goat anti-Rabbit IgG + IgM Secondary antibody, HRP conjugate	Rabbit IgG + IgM secondary antibody	Pierce 31460	1 : 5000
Goat anti-Mouse IgG + IgM Secondary antibody, HRP conjugate	Mouse IgG + IgM secondary antibody	Jackson 115-035-068	1 : 5000
Peroxidase anti-peroxidase	Binds to protein A	Sigma P1291	1 : 3000

4.4.2.6 Co-immunoprecipitation protein interaction analysis

100 ml of a yeast culture of the strain expressing the two tagged proteins being analyzed for interaction was grown till OD_{600} ~ 2.0. If both proteins were tagged by genomic integration of the tag sequence, yeast cultures were grown in YPDA. If at least one of the tagged proteins was expressed from a plasmid, yeasts were grown in synthetic drop out medium. Native protein yeast extracts were prepared as described above. The protein concentration of the extract was measured using the Bradford reagent. 3 mg of total protein was mixed with 50 µl of IgG-agarose beads (if proteins were precipitated via the TAP-tag), or IgVSV-agarose beads (if proteins were precipitated via the VSV-tag). IPP150 buffer was added to a final volume of 400 µl. Binding to beads was performed at 4^0C with rotation for 1,5 hours. Tubes were spun at 4000 rpm (2880 g) 4^0C for 5 minutes. The liquid phase, named flow)though, was transferred to a fresh tube and frozen. Beads were washed 3 times with IPP150 buffer, each time with rotation for 15 minutes at 4^0C. Proteins, precipitated on beads, were eluted by adding 50 µl of IPP150 1% SDS solution and agitated at 60^0C during 3 minutes. After elution, beads were spun at 10000 rpm (20000 g) and 50 µl of the elution fraction was collected in new tubes. 50 µl of protein loading dye was added to denature the eluted proteins and to facilitate the loading on the protein gel for the subsequent western blot analysis. Proteins, tested for interaction, were detected using specific antibodies recognizing the tag sequences.

4.4.2.7 Yeast two-hybrid analysis

Two-hybrid vectors containing the CCR4-NOT subunit coding sequences were prepared using GATEWAY cloning strategy following the manufacturer instructions (Invitrogen). The MAV203 yeast strain transformed with two plasmids (one with a DNA-binding fusion the other with an activation domain fusion) was grown to mid-log phase. 1 ml of culture was pelleted, resuspended in 500 µl buffer Z and 200 µl water saturated ether. After a quick centrifugation for 1 minute, ether was left to evaporate under the hood for 10 min. Reaction tubes were pre-warmed at 30^0C for 5 minutes before addition of 100 µl ONPG (4mg/ml in buffer Z). Reactions were incubated at 30^0C until their color changed into bright yellow. Reactions were then stopped by addition of 250 µl 1M Na_2CO_3.Reactions were spun for 5 minutes and OD_{420} of the liquid phase devoid of cell debris was measured. The following formula was used to calculate β-galactosidase activity:

Activity = 1000 x OD_{420}/(OD_{600} x culture volume x reaction time)

In some cases, a luminescence-based kit was used (Invitrogen). In such cases, 100 µl of yeast culture was mixed with 100 µl reaction buffer, containing both the luminescence substrate and the yeast lysis reagent. The reaction was incubated at 30°C for 1 hour. Both the yeast culture density (OD_{600}) and luminescence activity were measured. β-galactosidase activity was estimated as following:

Activity = Luminescence/OD_{600}

4.5 List of Buffers

Table 6. List of Buffers.

Buffer	**Composition**
Buffer A (native protein purification)	10 mM Hepes-KOH pH7.9; 10 mM NaCl; 10 mM $MgCl_2$; 0.5 mM DTT; 0.5 mM PMSF; 2 mM benzamidine; 1 mM leupeptin; 2 mM pepstatin A; 4 mM chymostatin; 2.6 mM Aprotinin, 1 tablet of protease inhibitor mix.
Coomassie staining	1 g/l Coomassie R-250; 45% ethanol; 10% acetic acid
IPP150	10 mM Tris-Cl pH8.0; 150 mM NaCl; 10 mM $MgCl_2$; 0.1% Igepal
IPP150 calmodulin binding buffer	10 mM β-mercaptoethanol; 10 mM Tris-Cl pH8.0; 100 mM NaCl; 10 mM $MgCl_2$; 1 mM Mg-acetate; 1mM imidazole; 2mM $CaCl_2$; 0.1% Igepal
IPP150 calmodulin	10 mM β-mercaptoethanol; 10 mM Tris-Cl pH8.0; 100 mM NaCl; 10

elution buffer	mM $MgCl_2$; 1 mM Mg-acetate; 1mM imidazole; 2mM EGTA; 0.1% Igepal
Laemmli buffer	0.1% SDS; 1.44% glycine; 0.3% Tris base
LiT	10 mM Tris-Cl pH 7.5; 100 mM LiOAc
Luciferine mix	470 µM luciferine; 530 µM ATP; 270 µM coenzyme A; 20 mM Tris-phosphate pH7.8; 1.07 mM $MgCl_2$; 2.7 mM $MgSO_4$; 100 µM EDTA; 33.3 mM DTT
Loading dye 3x (protein gel)	0.05% bromophenol blue; 50 mM Tris pH6.8; 10% glycerol; 2% SDS
MOPS buffer	0.1M MOPS; 40 mM Na-acetate; 5 mM EDTA; adjust to pH7
PBS-Tween	PBS; 0.2% Tween 20
Polyacrylamide gel (RNA)	6.0% polyacrylamide; 8.0M urea; 1x TBE; 0.06% ammonium persulfate; 0.1% N,N,N',N'-Tetramethyl-ethlenediamine
RNA loading dye (polyacrylamide gel)	0.25% bromphenol blue; 0.25% xylene cyanol; 95% formamide; 18 mM EDTA; 0.025% SDS
RNA loading dye (agarose gel)	0.25% bromphenol blue; 0.25% xylene cyanol; 50% glycerol; 1.0 mM EDTA
SDS-PAGE	acrylamide:bis-acrylamide 37.5:1 as required for gel concentration; 378 mM Tris pH 8.8; 0.1% SDS; 0.1% ammonium persulfate; 0.1% N,N,N',N'-Tetramethyl-ethlenediamine
Stacking gel	5% acrylamide:bis-acrylamide 37.5:1; 126 mM Tris pH 6.8; 0.1% SDS; 0.1% ammonium persulfate; 0.1% N,N,N',N'-Tetramethyl-ethlenediamine
TA buffer	40 mM Tris base; 1.14% acetic acid
TBE buffer	8.9 mM Tris base; 8.9 mM boric acid; 2.0 mM EDTA
TES buffer	10 mM Tris pH 7.5; 10 mM EDTA; 0.5% SDS
TEV cleavage buffer	10 mM β-mercaptoethanol; 10 mM Tris-Cl pH8.0; 100 mM NaCl; 10 mM $MgCl_2$; 0.5mM EDTA; 0.1% Igepal
Transfer buffer (western)	3 g/l Tris base; 3 g/l glycine; 0.05% SDS; 20% ethanol
Yeast lysis buffer for DNA purification	10 mM Tris pH7.5; 1 mM EDTA; 3.0% SDS
SCE buffer	1 M sorbitol, 10 mM EDTA, 10 mM DTT, 100 mM sodium citrate pH5.8

4.6 Bioinformatics

Computational studies were carried out using Perl scripting in Komodo IDE 8 environment and R i386 3.0.2 in Rstudio shell.

5. French introduciton. Introduction

5.1 L'expression des gènes eucaryotes: tous les chemins passent par l'ARN.

Le dogme central de la biologie moléculaire de la transmission de l'information génétique est basé sur trois événements principaux: l'ADN est transcrit en ARN messager (ARNm) qui, après une séquence d'événements, est utilisé comme matrice pour la synthèse des protéines. Cela est vrai dans tous les domaines de la vie: les procaryotes, les archées et les eucaryotes. Dans le cas des eucaryotes cette séquence d'événements est spatialement et temporellement divisée en raison de la présence d'une enveloppe nucléaire. Elle est également strictement régulée à plusieurs niveaux : la molécule précurseur de l'ARNm résultant de la transcription passe à travers de multiples étapes de maturation et de contrôle qualité avant d'être finalement traduite en une protéine fonctionnelle. Les produits finaux de l'expression des gènes - les protéines - subissent également des étapes de maturation à l'aide de chaperonnes et sont parfois la cible de modifications post-traductionnelles (Madhani 2013).

Grâce à la régulation de l'expression des gènes, chaque type cellulaire dans un organisme hautement organisé obtient sa propre identité et sa spécialisation. Pour cela, les molécules d'ARNm produites seront constamment reconnues par une grande variété de protéines qui auront une influence sur leur localisation au sein de la cellule, leur traduction et leur stabilité. Ces voies complexes d'expression des gènes soulignent fortement l'importance de la régulation des ARN dans la cellule.

Ce travail de thèse porte sur la caractérisation fonctionnelle du complexe CCR4-NOT, complexe requis pour le contrôle de la stabilité des ARNm. Une base importante pour ce travail est l'analyse structurelle de l'ensemble CCR4-NOT. En raison de sa grande conservation chez les différentes espèces eucaryotes, le système de levure modèle *Saccharomyces cerevisiae* a été utilisé pour cette étude. Après une brève introduction concernant la synthèse des ARNm, de leur maturation et de leur export dans le cytoplasme, ce manuscrit se concentrera sur les divers mécanismes utilisés par les voies de dégradation des ARNm.

5.2 La transcription, la maturation et l'export des ARNm

La transcription peut être définie comme la synthèse d'une molécule d'ARN en utilisant un brin d'ADN comme matrice. Chez les eucaryotes la transcription a lieu dans le noyau de la cellule et est régie par une multitude de facteurs. Cette réaction est effectuée par les ARN polymérases I, II et III, chacune étant nécessaire pour la synthèse d'une classe spécifique d'ARN. L'ARN polymerase II est responsable de la synthèse de tous les ARNm cytoplasmiques de la cellule. Le processus débute à l'extrémité 5' du gène, dans la région du promoteur et nécessite le recrutement et l'assemblage de nombreux facteurs d'initiation de la transcription. Ensuite, la machinerie transcriptionnelle se

déplace le long du gène et l'ARNm s'allonge de plus en plus et, finalement, la synthèse se termine à l'extrémité 3' du gène. La molécule d'ARN produite est reconnue par un complexe protéique qui va induire un clivage puis ajouter la queue polyadénylée. De manière remarquable, la transcription peut être régulée à n'importe quelle étape par des facteurs protéiques et même par des régions éloignées de l'ADN, appelés « enhancers ».

Les transcrits primaires eucaryotes sont fortement transformés (Figure 1). Cela inclut l'introduction de la coiffe à l'extrémité 5' de l'ARNm, leur épissage alternatif, l'introduction de modifications dans les nucléotides et la polyadénylation de l'extrémité 3'. La coiffe de l'ARNm, un nucléotide 7-méthyl-guanine attaché à la séquence de l'ARNm par une liaison 5'-5' triphosphate, ainsi que la queue poly(A) sont nécessaires pour une traduction efficace des ARNm dans le cytoplasme. Ces modifications affectent aussi la stabilité des ARNm, ayant un rôle protecteur contre la dégradation des ARNm par les exoribonucléases cellulaires. En raison de la nature continue de l'élongation de la transcription, les transcrits d'ARNm primaires contiennent à la fois des exons, qui servent ensuite de séquences codantes pour la traduction, et des introns, qui sont des séquences non codantes. Afin d'éliminer ces dernières, un complexe moléculaire hautement organisé appelé le spliceosome agira sur les molécules d'ARN. Pour cela, le produit de la transcription primaire est coupé au niveau des jonctions exon-intron puis les exons sont reliés pour former l'ARNm mature. Dans certains cas, des sites d'épissage alternatifs peuvent être utilisés, certains exons pouvant être omis et certains introns pouvant être retenus, ce qui permet de générer une grande variété d'ARNm à partir d'un seul gène. Finalement, les nucléotides modifiés de type méthyl-6-adénine ont longtemps été connus pour être présents dans les ARNm (Desrosiers et al 1975; Wei et al 1976). La fonction moléculaire précise de cette modification post-transcriptionnelle doit encore être déterminée mais des expériences récentes suggèrent qu'elles affectent la stabilité des ARNm. Durant et après le processus de maturation, différentes protéines se fixent sur les transcrits d'ARNm ce qui permet la formation d'un complexe ribonucléoprotéique (mRNP). Ce complexe est ensuite dirigé vers les pore nucléaires en vue de l'export dans le cytoplasme (Figure 1).

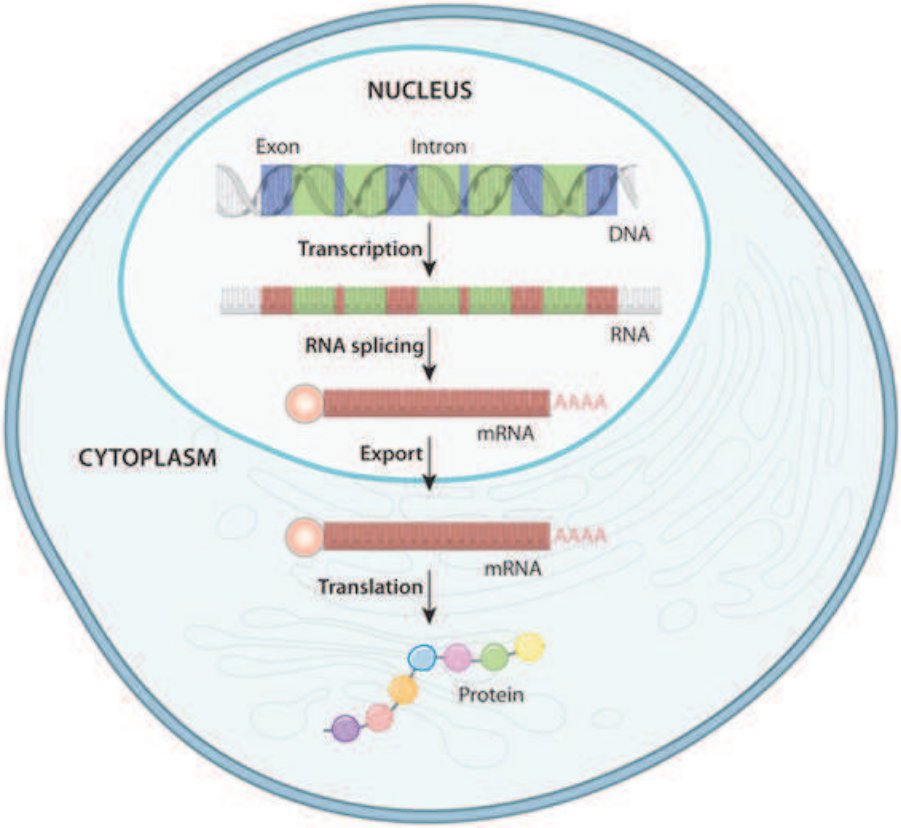

Figure 1. Expression génétique chez les eucaryotes (Nature, 2010)

Une fois qu'ils atteignent le cytoplasme, les ARNm passent par plusieurs étapes de contrôle qualité qui permettent de détecter et de dégrader toutes les molécules d'ARN présentant des défauts (Madhani 2013). L'un des facteurs déterminants est l' « Exon Junction Complex » (EJC), impliqué dans la voie de dégradation des ARNm nonsense (NMD). Ce complexe est déposé à proximité d'une liaison exon-exon, normalement de 20 à 24 nt en amont de la jonction d'épissage. L'EJC est composé de plusieurs sous-unités hautement conservées, eIF4III, Magoh, Y14 et MLN51, qui forment un noyau auquel s'associent des protéines périphériques. L'EJC sert d'empreinte sur les événements d'épissage qui se produisent sur l'ARNm dans le noyau. Fait intéressant, l'EJC est également lié de manière fonctionnelle à la traduction de l'ARNm. En effet, si un ribosome rencontre un codon stop prématuré en amont d'un EJC lors de la traduction, ce dernier va jouer un rôle important dans l'induction du mécanisme de sauvetage, appelé dégradation des ARNm nonsense (NMD).

5.3 Traduction

L'information portée par les ARNm doit être décodée pour produire une protéine - le but final de chaque ARNm. La traduction de l'ARNm en protéine est effectuée par les ribosomes qui sont de grands complexes ribonucléoprotéines conservés. La traduction est un processus cyclique, divisée en

4 étapes: l'initiation, l'élongation, la terminaison et le recyclage des ribosomes. Au cours de l'initiation, les ribosomes vont s'assembler sur l'ARNm et devenir actifs. Lors de l'élongation le ribosome ajoute les acides aminés dans la chaîne polypeptidique en croissance. A la fin, le ribosome rencontre le signal de terminaison et libére la protéine nouvellement synthétisée. Les ribosomes utilisés sont alors recyclés pour démarrer un autre cycle de traduction (Figure 2). Afin de décrire correctement la façon dont ces différentes étapes sont reliées entre elles , je vais entrer dans le détail du processus de traduction des ARNm eucaryotes.

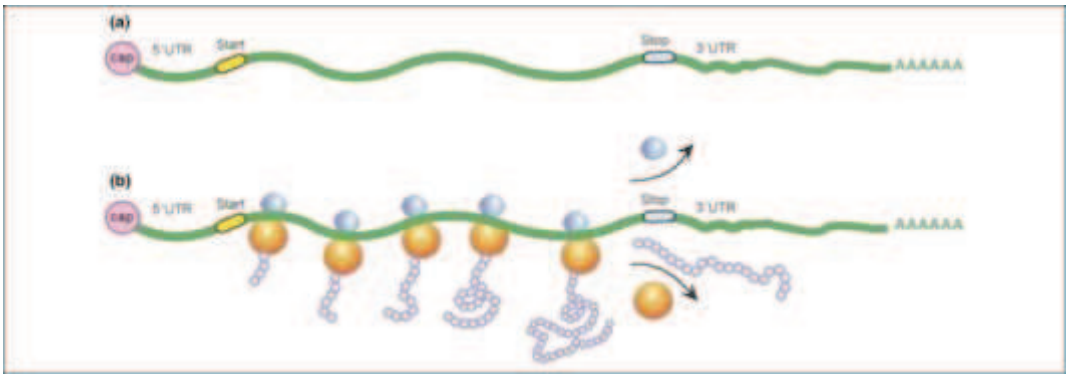

Figure 2. Synthèse des protéines (Lodish 2008)

5.3.1 Composantes du cycle de traduction

5.3.1.1 L'ARNm

La séquence de l'ARNm eucaryote peut être subdivisée en: une coiffe; une région 5' non traduite (5' UTR); un cadre de lecture (ORF); une région 3' non traduite (3' UTR); et une queue poly(A). L'ORF en elle-même est divisée en triplets de bases appelés codons, chacun correspondant à un résidu d'acide aminé spécifique ou à un signal d'arrêt (Figure 3).

1st letter	Second Letter: U	Second Letter: C	Second Letter: A	Second Letter: G	3rd letter
U	UUU Phe UUC UUA Leu UUG	UCU UCC Ser UCA UCG	UAU Tyr UAC UAA Stop UAG Stop	UGU Cys UGC UGA Stop UGG Trp	U C A G
C	CUU CUC Leu CUA CUG	CCU CCC Pro CCA CCG	CAU His CAC CAA Gln CAG	CGU CGC Arg CGA CGG	U C A G
A	AUU AUC Ile AUA AUG Met	ACU ACC Thr ACA ACG	AAU Asn AAC AAA Lys AAG	AGU Ser AGC AGA Arg AGG	U C A G
G	GUU GUC Val GUA GUG	GCU GCC Ala GCA GCG	GAU Asp GAC GAA Glu GAG	GGU GGC Gly GGA GGG	U C A G

Figure 3. Le code génétique "standard" (Lodish 2008)

Le ribosome, aidé par des facteurs d'initiation, se lie à la coiffe puis se déplace le long de la région 5' UTR jusqu' à reconnaître le codon d'initiation AUG. La synthèse peptidique commence au moyen d'un aminoacyl-ARNt chargé avec la méthionine puis continue le long de l'ORF en incorporant un nouvel acide aminé pour chaque codon, jusqu'à ce que il atteint l'un des trois codons stop. Les séquences des régions 5' UTR et 3' UTR servent principalement à des fins de régulation: ainsi plusieurs sites de protéines liants l'ARN sont situés en 3 'UTR (figure 4) (Castello et al 2013; Castello et al 2012).

Figure 4. L'organisation de l'ARNm eucaryote typique (Lodish 2008)

5.3.1.2 Les ARN de transfert aminoacylés (aa-ARNt)

Afin de synthétiser une protéine qui correspond à la séquence des codons de l'ARNm, des molécules intermédiaires sont nécessaires. Les ARN de transfert (ARNt) sont ces adaptateurs. Pour cela, ils adoptent une structure tridimentionelle caractéristique à partir d'élements de structure secondaire particuliers. L'un de ces éléments contient dans une boucle la séquence anticodon qui reconnaît le codon apparenté dans l'ARNm par appariement de paires de bases. Un autre élément, appelée la tige accepteur, porte un résidu d'acide aminé spécifique pour cet ARNt (Figure 5). Par conséquent, lors de la traduction les ribosomes incorporent dans la chaîne polypeptidique en croissance les résidus d'acides aminés apportés par les ARNt en suivant la séquence de l'ARNm à travers l'appariement de bases codons-anticodons.

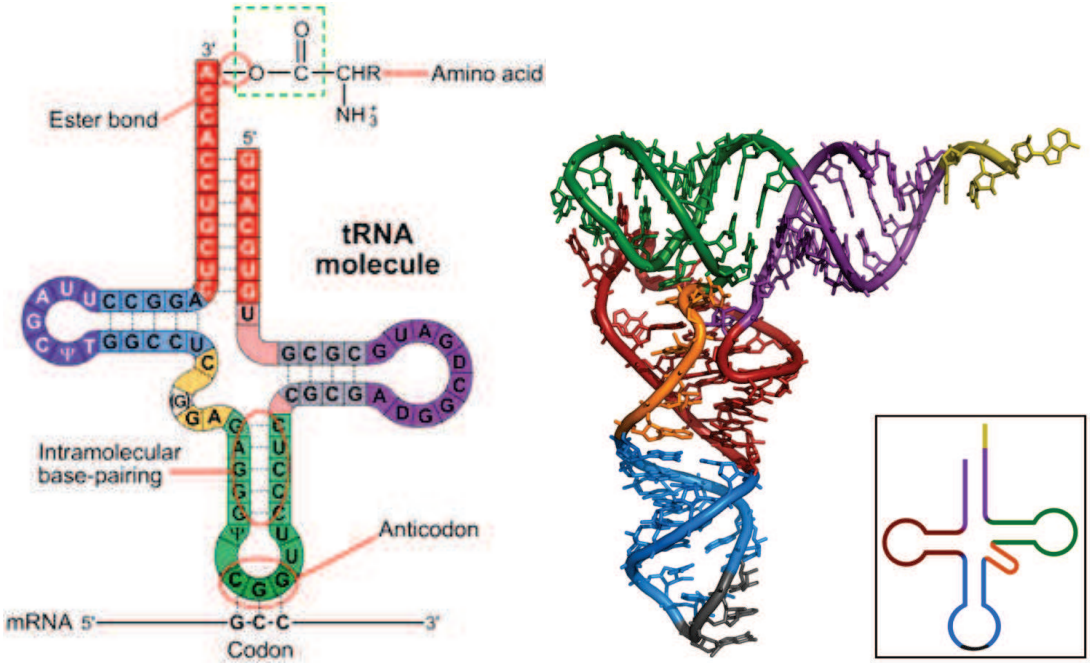

Figure 5. Deux représentations de l'ARNt: structure secondaire de la forme aminoacylée (à gauche) et de la structure tertiaire sans le résidu d'acide aminé (à droite) (Lodish 2008)

5.3.1.3 Le Ribosome

Le ribosome est le catalyseur de la synthèse des protéines. Le ribosome eucaryotes, appelé ribosome 80S, est constitué de deux sous-unités: la petite sous-unité 40S et la grande sous-unité 60S. Chaque sous-unité est composée de plusieurs protéines ribosomales spécifiques et d'un ou plusieurs ARN ribosomaux (ARNr). Chez les eucaryotes, la sous-unité 40S contient 33 protéines et l'ARNr 18S tandis que la sous-unité 60S est composé de 47 protéines ribosomales et des ARNr 5,8 S, 28S et 5S (Melnikov et al. 2012). Les dernieres structures cristallographiques du ribosome eucaryote complet de *S. cerevisiae* ont fourni des détails sur l'organisation tridimentionelle de cette machinerie

moléculaire et sur les interactions moléculaires qui se produisent dans ce grand complexe (Figure 6) (Jenner et al 2012; Ben-Shem et al 2011).

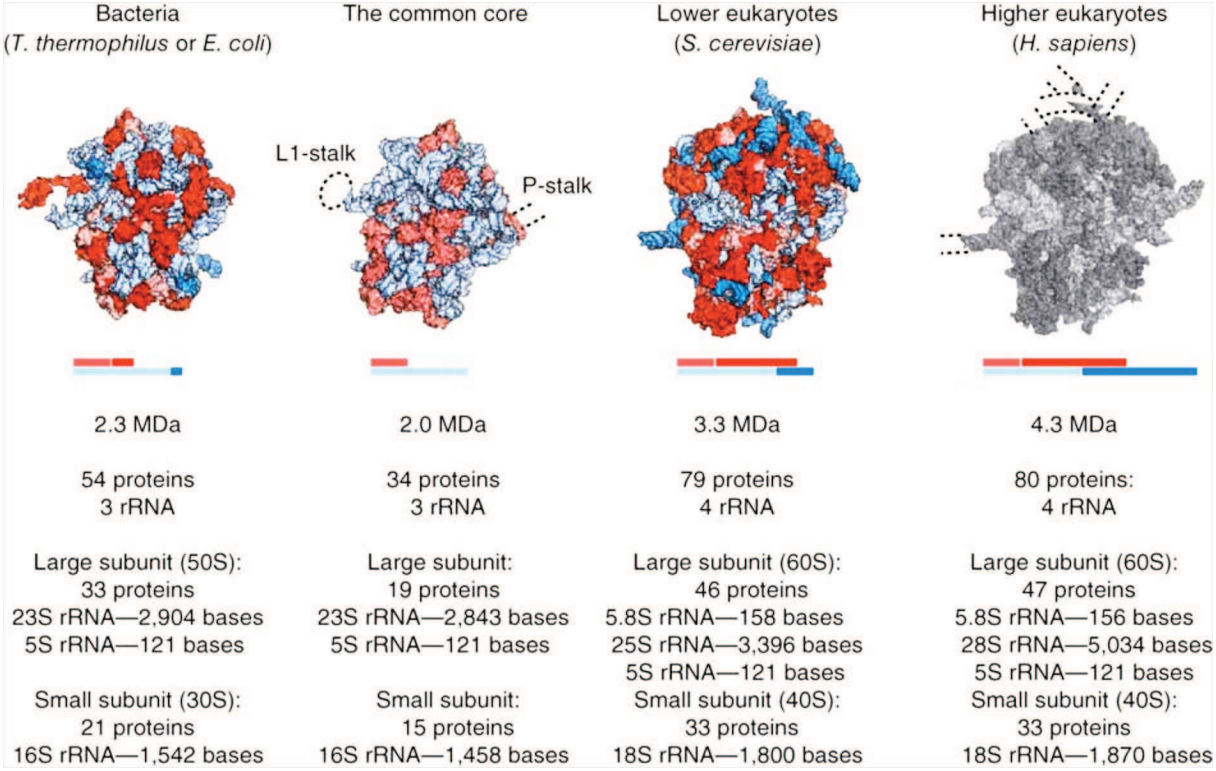

Figure 6. Composition des ribosomes de différents règnes du vivant. L'ARNr est représenté en bleu, les protéines ribosomales sont en rouge. La structure cristallographique du ribosome humain n'est pas encore connue, par conséquent, le modèle correspondant est en gris (Melnikov et al. 2012).

Un ribosome contient trois régions fonctionnelles conservées, conçues pour accueillir les ARNt et arbitrer les acides aminés de la chaîne polypeptidique en croissance (Figure 7). Ces sites sont appelés A - aminoacyl ARNt, P - peptidyl transférase et E - sites de sortie (Steitz 2008).

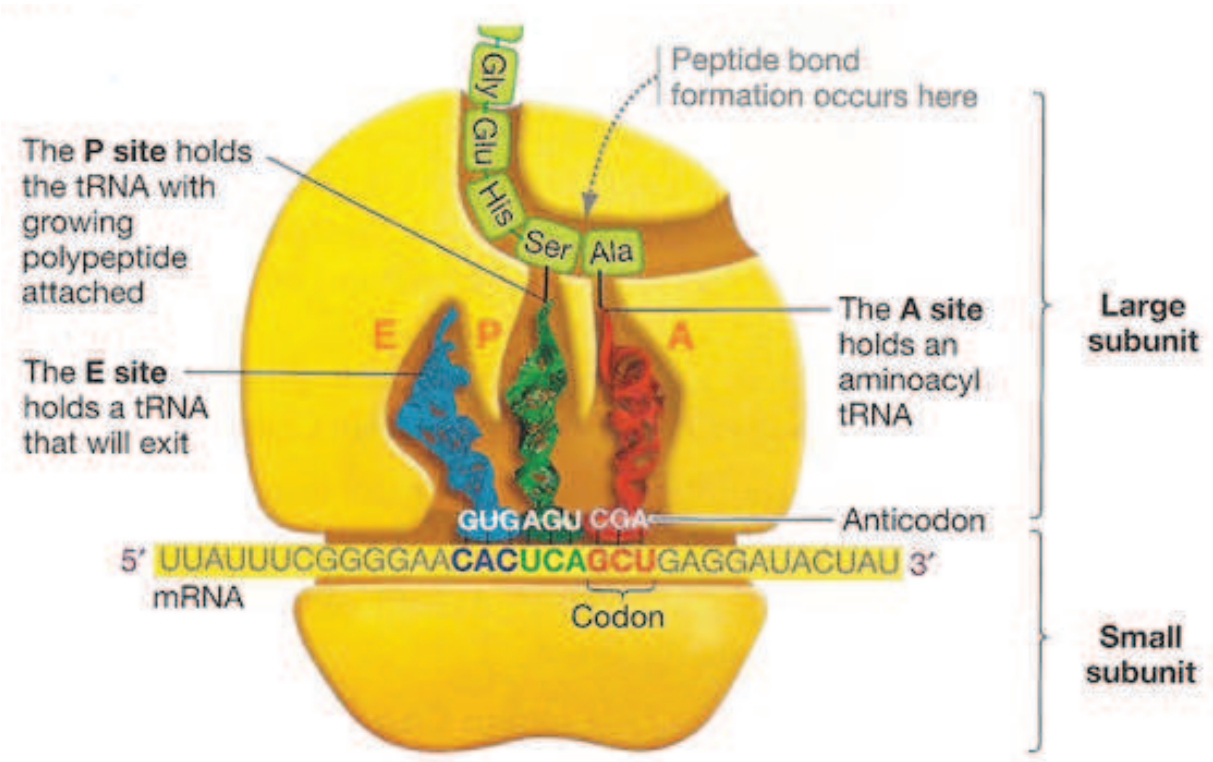

Figure 7. Sites de liaison des aa-ARNt dans le ribosome (discoveryandinnovation.com)

Au cours de chaque étape de la traduction, à l'exception de l'étape d'initiation, le peptide en croissance est maintenu par l'ARNt dans le site P. L'aa-ARNt entrant est possitionné dans le site A. Si la reconnaissance codon-anticodon a lieu avec succès, l'aa-ARNt est lié de manière stable au ribosome et une liaison peptidique est formée avec la séquence peptidique portée par le peptidyl-ARNt présent dans le site P. Ensuite, le nouvellement formé peptidyl-ARNt migre du site A vers le site P, tandis que l'ancien peptidyl-ARNt, désormais vide, sort par le site E (Rodnina et al 2007; Beringer et Rodnina 2007a; Beringer et Rodnina 2007b). Ce cycle est répété pour chaque nouveau codon de l'ARNm. Dans le paragraphe suivant, je vais décrire les étapes essentielles de la traduction, initiation, l'élongation et la terminaison chez les eucaryotes que les détails de ce processus fournissent des indices sur la façon dont la traduction est liée à la vie de l'ARNm, et la décroissance en particulier.

5.4 La dégradation des ARNm.

Toutes les ARNm qui ont été synthétisés doivent à un moment donné être dégradés. La dégradation des ARNm eucaryotes est médiée par des complexes de protéines qui sont hautement régulés et optimisés pour des besoins cellulaires spécifiques. La vitesse de dégradation des ARNm spécifie le temps de demi-vie de chaque transcript, qui, avec le taux de synthèse du à la transcription, détermine le niveau total d'un ARNm dans une cellule donnée (Garneau, Wilusz, et Wilusz 2007). Les

temps de demi-vie des ARN peuvent être modulés de manière spécifique après la transcription par les protéines liant l'ARN, les microARN ou les siARN. En outre, des voies spécialisées qui ciblent les ARNm ayant des défauts dans leur séquence ou présentant des difficultés lors de la traduction existent. La traduction d'un ARNm aberrant ou anormal peut entraîner la production de protéines non fonctionnelles. Plusieurs processus existent, appelés dégradation des ARNm nonsense (NMD), dégradation des ARNm sans codon stop (NSD), dégradation des ARNm bloqués lors de la traduction (NGD) et dégradation des ribosomes non fonctionnels (BDNI). Ces systèmes d'élimination des ARNm aberrants et des complexes de traduction sont des systèmes de contrôle de qualité (Behm-Ansmant et al 2007; Chang et al, 2007).

Les principales voies de dégradation des ARNm eucaryotes ont été analysées en détail dans des modèles différents comme la levure, *C. elegans* et l'homme. Comme mon travail de thèse a porté sur le système présent chez la levure, je vais me concentrer principalement sur les mécanismes qui se produisent dans *S. cerevisiae*, tout en décrivant brièvement les différences avec le système humain ou d'autres espèces. Une attention particulière sera accordée à la dégradation des ARNm modulée par des protéines se liant spécifiquement aux ARNm. L'importance physiologique de la dégradation des ARNm dans différents contextes sera également abordée. Enfin, je vais donner une description des mécanismes moléculaires de base impliqués dans la dégradation des ARNm, en me concentrant sur le complexe CCR4-NOT qui a été au cœur de mon projet.

5.4.1 Le mécanisme de la dégradation des ARNm dans le cytoplasme

Compte tenu du fait que les ARNm ont une séquence ribonucléique coiffé à son extrémité 5' et se terminant avec une queue poly(A) à son extrémité 3', trois grandes voies existent pour initier leur dégradation: de manière exonucléolytique en partant de l'extrémité 3' avec le raccourcissement de la queue poly(A); de manière exonucléolytique en partant de l'extrémité 5' en supprimant la coiffe protectrice; ou par un clivage endonucléolytique dans le corps de l'ARNm. En général, la dégradation des ARNm commence par le raccourcissement de la queue poly(A), ce qui conduit à la formation d'un ARNm oligoadenylé. Ceux-ci sont ensuite traitées à leur extrémité 5' par le complexe d'élimination de la coiffe DCP1/DCP2 et finalement dégradés par l'exonucléase XRN1 dans la direction 5' vers 3'. Les molécules d'ARNm résultant de la déadénylation peuvent également être dégradés par les exosomes à partir de leurs extrémités 3'. Les ribonucléotides résultant de cette dégradation peuvent ensuite être recyclés en entrant dans la voie de sauvetage des nucléotides. Néanmoins, la coiffe doit être traitées ultérieurement par le complexe DcpS/Dcs1 qui semble être la principale enzyme impliquée dans le métabolisme de la coiffe (Beelman et Parker, 1995; Decker et Parker, 1993). Je vais maintenant donner une image détaillée de la dégradation des ARNm, sa régulation et ses connexions à d'autres processus cellulaires (Figure 8).

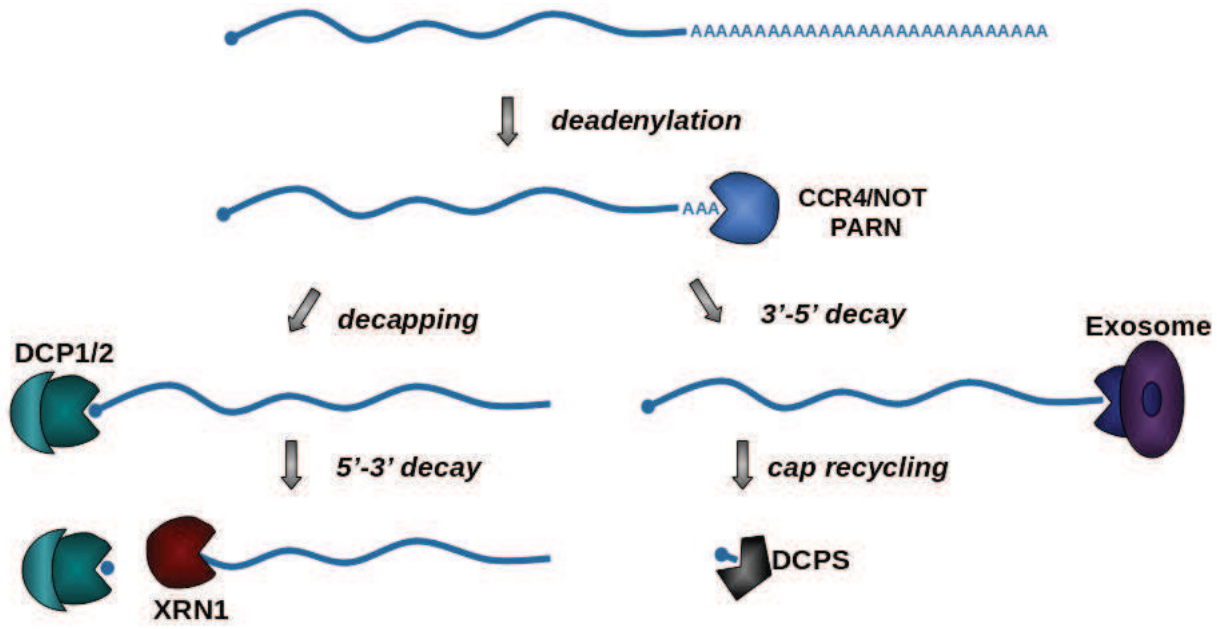

Figure 8. Les voies de dégradation des ARNm eucaryotes (Beelman et Parker, 1995)

5.4.1.1 Première étape de la dégradation des ARNm – la déadénylation.

Comme décrit ci-dessus, la déadénylation est la première étape clé dans la dégradation de la plupart des ARNm. Le complexe CCR4-NOT contribue à l'étape initiale de raccourcissement de la queue poly(A) et à l'inhibition de la traduction. L'inhibition de la formation du complexe d'initiation de la traduction entraine le recrutement des facteurs d'élimination de la coiffe puis la dégradation des ARN dans la direction 5' vers 3'. Dans ce chapitre, je me concentre sur les facteurs induisant la déadénylation des ARNm, en mettant l'accent sur le complexe CCR4-NOT qui a fait l'objet de mes études.

Architecture globale du complexe de déadénylation de levure CCR4-NOT

Le complexe CCR4-NOT est un assemblage de protéines hautement conservé chez les eucaryotes avec une masse approximative de 1 MDa (Figure 9). Le complexe de levure est composé de neuf sous-unités de base et de protéines supplémentaires nécessaires pour exercer ses fonctions. CCR4-NOT a d'abord été décrit comme un complexe transcriptionnel modulant négativement les niveaux d'ARNm par des expériences génétiques liées à la transcription (Collart et Panasenko 2012; Collart et Struhl 1994). Plus récemment, il est devenu largement accepté que le complexe CCR4-NOT a un rôle majeur dans la déadénylation des ARNm (Daugeron et al., 2001). Le complexe CCR4-NOT de levure contient deux sous-unités ayant une activité nucléase sur l'ARN, à savoir Caf1 et CCR4; une sous-unité protéique contenant un domaine de type ubiquitine ligase E3, à savoir Not4; la sous-unité

Not1, une protéine qui forme l'échafaudage du complexe et donc sur laquelle les autres protéines vont se lier; et les protéines Not2-3-5, Caf40 et Caf130 (J Chen et al, 2001; Bai et al 1999). La purification du complexe CCR4-NOT de mammifère a révélé plusieurs différences: Caf130 n'est pas conservé chez les mammifères et une seule protéine est présente à la place de Not3 et Not5. Il est également intéressant de noter qu'une sous-unité Not4 est codée dans les génomes de mammifères, mais qu'elle n'a pas été retrouvée associer au complexe CCR4-NOT humain, contrairement à la levure. A l'inverse, CNOT10 et CNOT11 sont présents dans le complexe humain mais absents chez la levure (Ito et al 2011; Collart et Timmers 2004; Mauxion et al 2013). Une variation supplémentaire est trouvée dans le complexe humain avec, dans certains cas, deux gènes codant pour des sous-unités du complexe CCR4-NOT (par exemple, deux sous-unités "CAF1" avec CNOT7 et CNOT8) et dans d'autres cas des variants provenants de processus d'épissage alternatif. En regardant des organismes phylogénétiquement plus éloignés on trouve plus de surprises. Par exemple, les homologues CCR4 sont absents des trypanosomes et des plantes. Comme ma recherche visait à disséquer, à la fois structurellement et fonctionnellement, le complexe CCR4-NOT de levure, chacune des sous-unités de cet ensemble est présenté ci-dessous. Cela comprend des données qui ont été publiées lorsque mon projet était en cours.

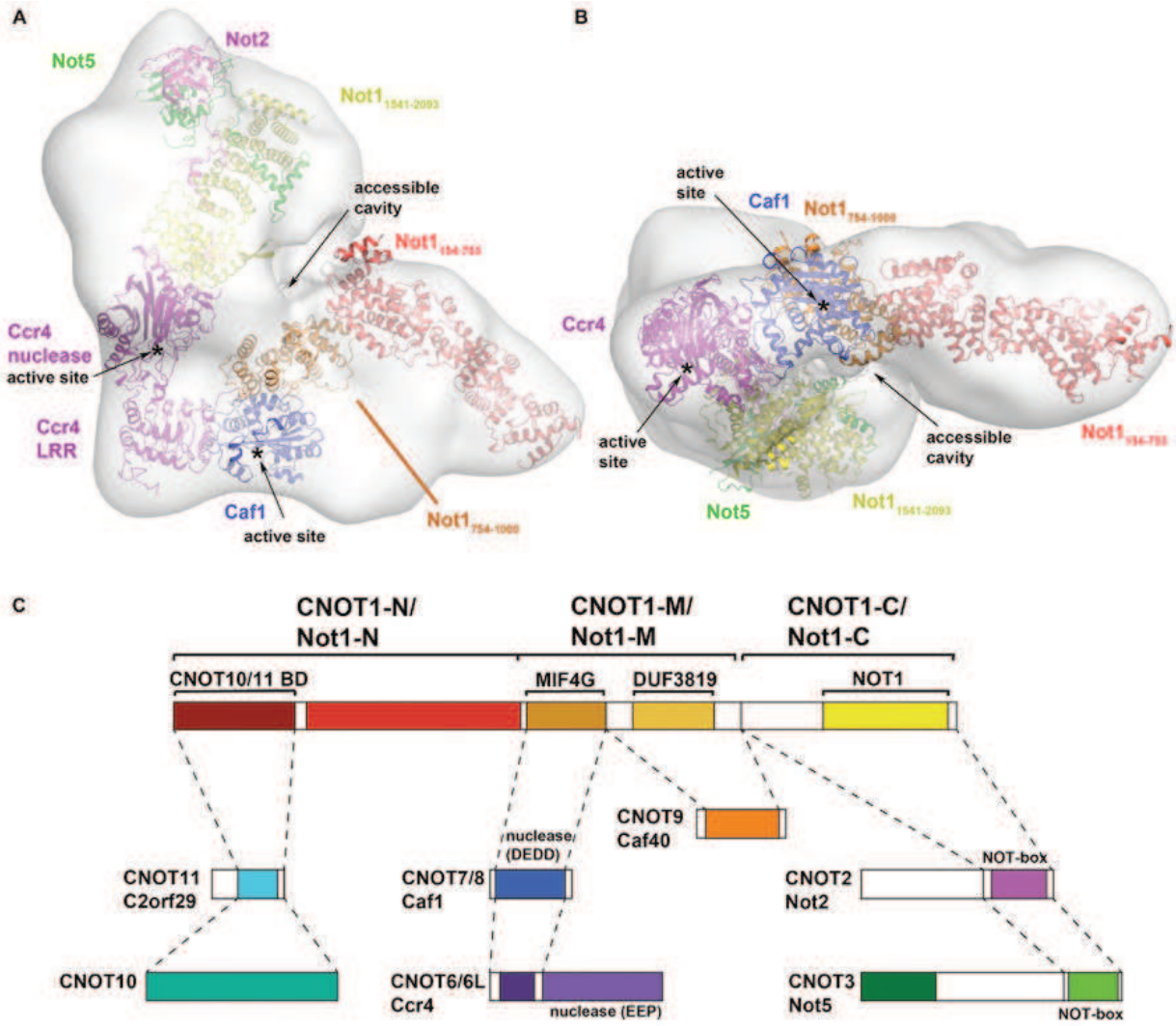

Figure 9. Architecture du complexe CCR4-NOT. A) et B) récente cryo-EM structure à basse résolution du complexe CCR4-NOT qui révèle un complexe en forme de L. Des structures résolus par diffraction aux rayons X de certains composants ont été installées dans cette enveloppe. C) Représentation schématique des sous-unités du complexe CCR4-NOT connus, indiquant les partenaires de liaison et les domaines d'interaction. Tant chez l'humain (en haut) que chez la levure (en bas) les noms des protéines sont indiqués. (Basquin et al. 2012a)

Les études d'interaction ont montré que la protéine de 240 kDa Not1 constitue l'échafaudage du complexe de levure CCR4-NOT (CNOT1 chez l'homme). Les analyses structurales ont démontré qu'elle est principalement formée de répétitions de type « HEAT », qui sont des structures en hélice alpha. Cette grande protéine est essentielle pour la viabilité de la levure et l'inhibition de son expression dans les cellules humaines entraîne la mort des cellules par apoptose (Ito et al. 2011).

Des analyses ont révélé au moins trois domaines d'interactions au sein de Not1 (Figure 10). Ceux-ci sont situés principalement dans sa partie centrale et C-terminale: la surface d'interaction avec la

sous-unité Caf1 est située dans le domaine central. Il adopte une structure apparentée au domaine MIF4G du facteur d'initiation eIF4G. Cette surface recrute indirectement la sous-unité CCR4 qui se lie, grâce à un domaine répété riche en leucine (LRR), à Caf1 (Chen et al. 2002). De manière remarquable, alors que dans les complexes humains et de drosophile les deux sous-unités CAF1 et CCR4 sont activement impliquées dans la déadénylation, chez la levure seule CCR4 semble être impliquée dans cette activité. En revanche, chez les plantes et les trypanosomes, l'absence d'un homologue CCR4 suggère que Caf1 est totalement responsable de l'activité nucléase du complexe.

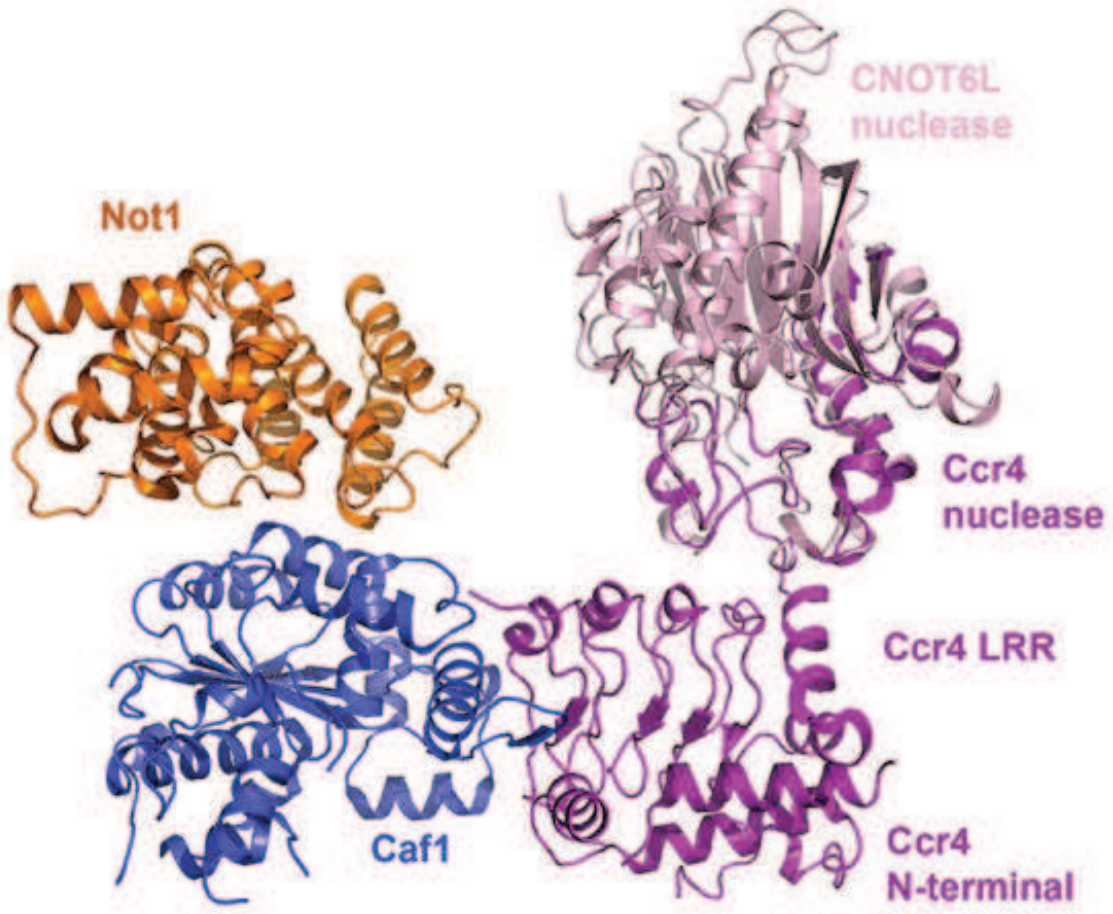

Figure 10. Structure d'un complexe hétérotrimérique contenant des fragments de Not1, Caf1, et CCR4 associés. Cette structure montre que la sous-unité Caf1 fait un pont entre Not1 et CCR4 (Basquin et al. 2012a).

La structure de la partie C-terminale de Not1 révéle deux surfaces d'interaction pour les sous-unités Not2 et Not5 du complexe CCR4-NOT (Figure 11). On pense que Not3 peut interagir d'une manière similaire à Not5. Not1 forme un domaine avec des répétitions de type « HEAT » étendues, autour desquels les sous-unités Not2 et Not5 sont assemblées. Fait intéressant, ces deux sous-unités

partagent le même repliement pour leur domaine N-terminal qui promeut leur interaction et l'interaction avec la partie C-terminale de Not1. Chez la levure, deux protéines paralogues existent, Not3 et Not5. L'idée que ces deux facteurs interagissent avec Not1 et Not2 d'une manière similaire suggére que le complexe CCR4-NOT est hétérogène, avec Not3 et Not5 étant mutuellement exclusives: certains complexes contiendraient Not3 tandis que d'autres contiendraient Not5. Cependant, étant donné les similitudes de séquences et de structures entre l'extrémité N-terminale de Not2, Not3 et Not5, on pourrait aussi envisager que certains complexes peuvent contenir des hétérodimères Not3-Not5 (Bhaskar et al 2013; Boland et al 2013).

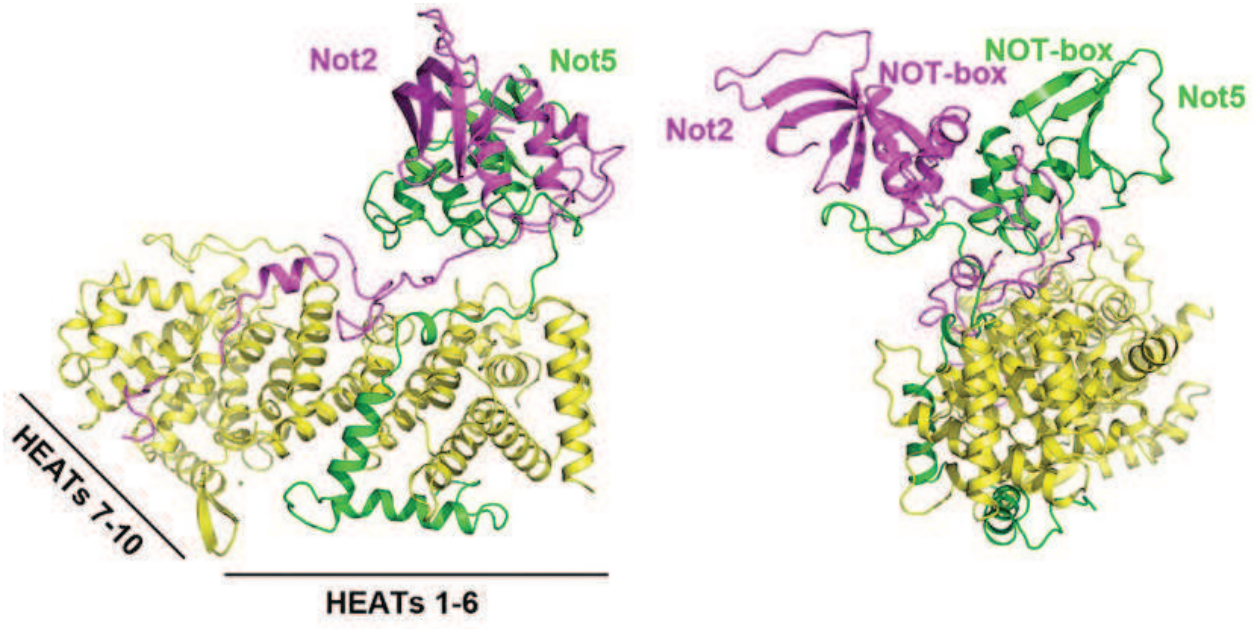

Figure 11. Structure d'un complexe contenant le domaine C-terminal de Not1 avec les parties N-terminales de Not2 et Not5. Cette structure révèle l'organisation régulière avec des répétition de type « HEAT » de Not1. Not2 et Not5 interagissent ensemble grâce à leurs domaines NOT-box conservés. Les deux sous-unités interagissent directement avec Not1 (Bhaskar et al. 2013).

Des études structurales de la partie N-terminale de Not1 révèlent les mêmes répétitions de type « HEAT » étendues (Basquin et al. 2012b). Cette région pourrait se lier à des protéines accessoires diverses, comme des protéines liant l'ARN ou d'autres facteurs de régulation. En effet, l'homologue de Not1 chez les mammifères interagit avec les sous-unités spécifiques CNOT10 et CNOT11 (Mauxion et al 2013; Bawankar et al 2013).

D'autres sous-unités du complexe de levure, comme Not4, Caf40 et Caf130, et d'autres partenaires de liaison semblent se lier soit au domaine central de Not1 ou dans sa proximité. La détermination

des modèles d'interactions de tous les partenaires de régulation du complexe CCR4-NOT est actuellement un domaine de recherche intensive (Panasenko et Collart 2011; Azzouz et al, 2009).

5.4.1.7 Rôle particulier du complexe CCR4-NOT de levure dans la dégradation de l'ARNm induite par les protéines de liaison aux ARN: le cas de la protéine Puf

Après avoir présenté la composition de base et la structure du complexe CCR4-NOT de levure, je vais décrire comment cet assemblage de protéines peut être ciblée au substrat ARNm par des facteurs tels que les protéines liant les ARN spécifiquement. Un cas bien décrit est celui de la dégradation des ARNm médiée par les protéines de la famille Puf.

La famille de protéines Puf liant les ARN est composée de six membres bien décrits dans la levure, appelés Puf1 à Puf6. Chez les eucaryotes supérieurs, les protéines orthologues correspondantes sont appelés FBF chez *C. elegans*, Pumulio chez la drosophile et chez l'homme (chez ce dernier, deux orthologues ont été identifiés: Pum1 et Pum2). D'un point de vue structurel, ces protéines adoptent une répétition de type « armadillo », qui, dans le cas des protéines Puf est nécessaire pour la liaison à l'ARN (Jenkins et al 2009; Caro et al., 2006). Fait intéressant, les différents acides aminés présents à la surface de liaison à l'ARN dictent les préférences de substrat. Ces préférences ont été décrites pour chaque protéine de levure Puf (Figure 12). Les motifs correspondants se retrouvent fréquemment dans les régions 3' UTR des ARNm. Ainsi, la protéine de levure Puf3 se lie principalement à des ARNm codants pour des protéines mitochondriales, alors que Puf4 interagit avec les ARNm codants pour des facteurs de la biogenèse des ribosomes (Galgano et al 2008; Gerber, Herschlag, et Brown, 2004; Kershner Kimble et 2010). Structurellement, le complexe formé par les protéines Puf entre son domaine de liaison à l'ARN et les ARN cibles consiste à empiler les interactions entre les nucléotides conservés et des résidus d'acides aminés aromatiques (Figure 12). Ce réseau d'interaction explique les spécificités strictes de chaque paire Puf-ARNm. Les protéines Puf utilisent une variété de mécanismes pour réguler l'expression des ARNm cibles: en fonction de l'ARNm et de l'organisme, les protéines peuvent Puf soit réprimer sa traduction de l'ARNm et/ou induire sa dégradation. Une tendance générale est que les protéines exercent leur fonction à un emplacement défini. Ces points seront discutés en mettant l'accent sur les fonctions des protéines Puf de levure.

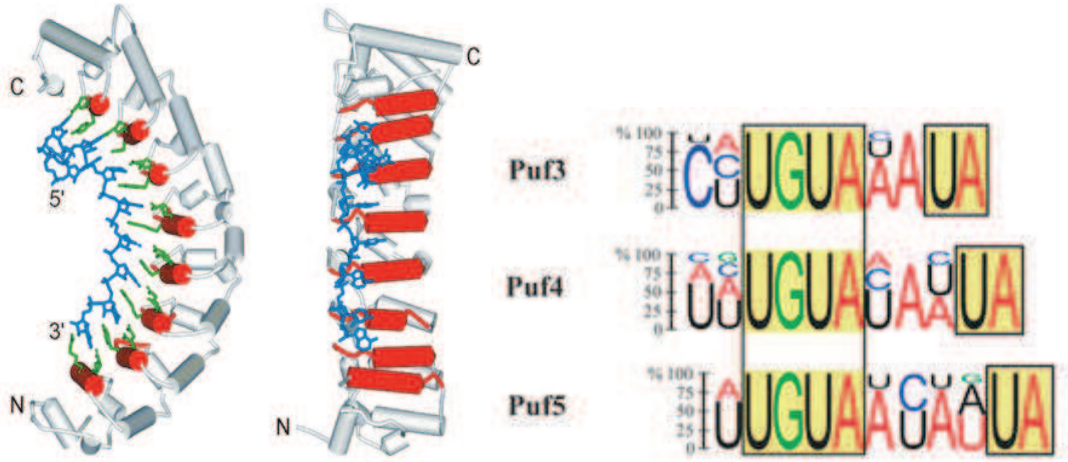

Figure 12. Schéma illustrant l'interaction de Pumillio1 humain à son motif de liaison dans l'ARN (gauche). Les α-hélices sont présentés sous forme de cylindres rouges, les chaînes latérales d'acides aminés sont en vert et l'ARN est en bleu. Divers motifs de liaison aux protéines Puf retrouvés dans les ARN. Les nucléotides conservés sont encadrés (droite) (Jenkins, Baker-Wilding, et Edwards, 2009).

Comme mentionné plus haut, la levure a six protéines orthologues Puf différentes. Les facteurs les mieux étudiés sont Puf3, Puf5 et Puf6. L'une des fonctions de ces protéines est la localisation de l'ARNm. Plusieurs sources de données suggèrent que la protéine Puf3 localise ses ARNm cibles à proximité des mitochondries, facilitant ainsi l'importation de protéines ciblés sur la mitochondrie. La suppression de puf3 entraîne ainsi la délocalisation des protéines Cox17 et Oxa1, deux protéines dont les ARNm sont des substrats de Puf3 (Gadir et al 2011; Eliyahu et al. 2010). Fait important, l'incubation de cellules avec de la cycloheximide, un inhibiteur de la traduction, pour un court laps de temps supprime aussi la localisation des ARNm, suggérant que le ciblage médié par Puf3 dépend d'une traduction active (Saint-Georges et al 2008; Gadir et al 2011). Cette observation remet également en cause le mécanisme associé à la localisation des ARNm associés à Puf3: Puf3 est-il le principal facteur de localisation ou bien est-ce la séquence d'importation mitochondriale, encodée par le signal en N-terminal des protéines ciblée? La combinaison de ces deux signaux est certainement importante et, en accord avec les données biochimiques, la disruption simultanée des gènes codants pour Puf3 et pour le récepteur d'importation mitochondriale Tom20 conduit à une interaction génétique léthale, avec des levure incapables de croître sur des milieux contenant une source de carbone non fermentable, tel que le glycérol (Eliyahu et al. 2010).

Une fonction de localisation similaire a été décrite pour Puf6 (Figure 13). En effet, Puf6 est impliquée dans la régulation de l'ARNm ASH1 par la promotion de sa localisation et de sa traduction dans les cellules de levure filles, après division. ASH1 code pour un facteur de transcription actif uniquement

dans les cellules de levure filles. Ce schéma spécifique d'expression est obtenu par la localisation asymétrique de l'ARNm ASH1 dans le bourgeonnement qui donnera la cellule fille. La traduction de cet ARNm est également contrôlée et ne se produit que peu de temps après la division cellulaire, assurant que seule la cellule fille hérite de la protéine ASH1. Puf6 est nécessaire pour inhiber la traduction de l'ARNm au cours de son transport par la liaison à l'extrémité 3' UTR de l'ARNm ASH1 et en interagissant avec le facteur d'initiation eIF5B, empêchant l'assemblage des sous-unités ribosomiques 60S au complexe d'initiation 48S. Fait intéressant, la localisation de l'ARNm ASH1 implique également l'interaction de la sous-unité protéique She2 du complexe de localisation avec des éléments ARN présents au sein du cadre de lecture. Ainsi, l'inhibition de la traduction par Puf6 facilite certainement cette liaison et la localisation de l'ARNm. Lorsque l'ARNm ASH1 atteint sa destination, l'activation de la traduction se produit: Puf6 est phosphorylé et se dissocie de son motif de reconnaissance (Gu et al, 2004; Quenault et al 2011..).

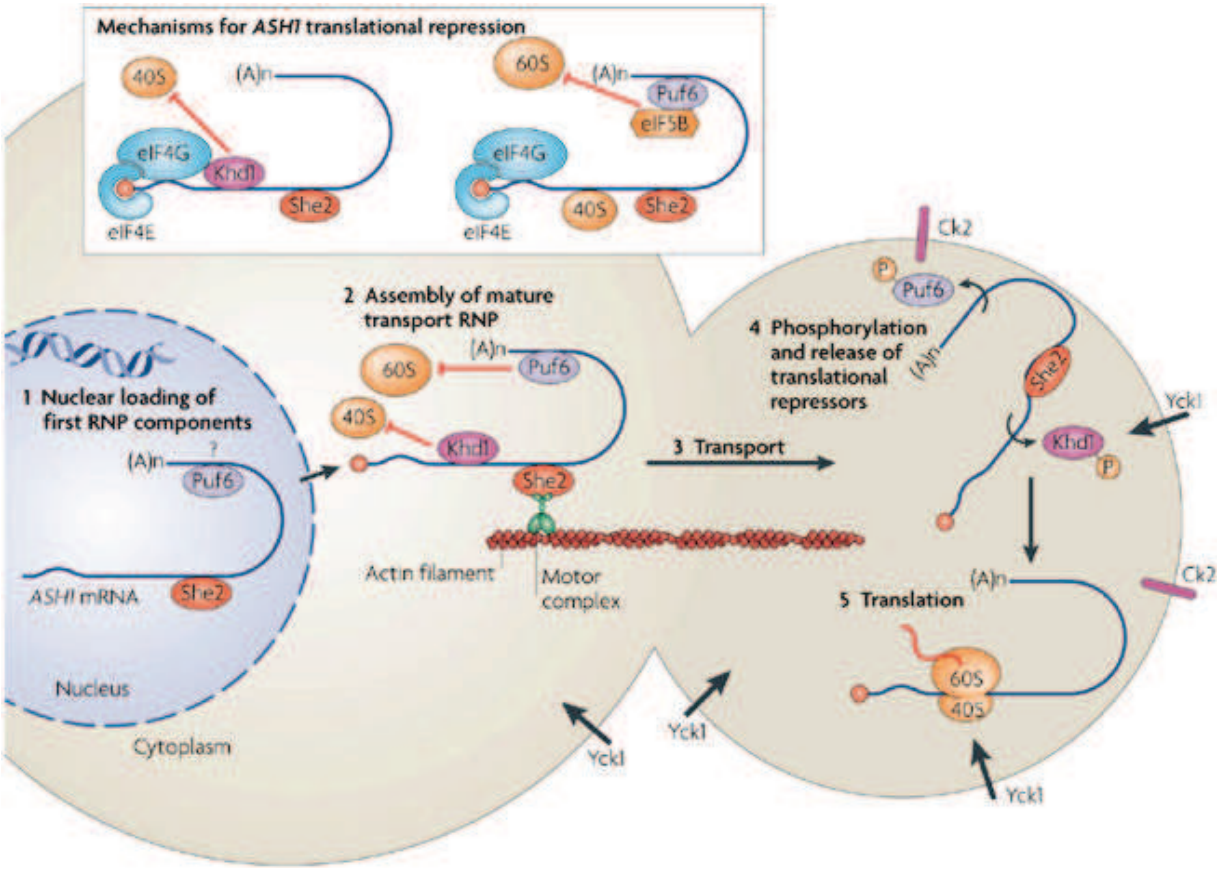

Figure 13. Rôle de la répression de la traduction de l'ARNm dans sa localisation. Pendant le transport de l'ARNm ASH1, Puf6 interagit avec eIF5B, inhibant ainsi l'assemblage des sous-unités 60S de ribosome avec le complexe 48S. La répression de la traduction est également obtenue par l'action de la protéine Khd1, qui inhibe le déplacement de la sous-unité 40S. Dans la cellule fille, la traduction de l'ARNm ASH1 est activée par la phosphorylation des protéines inhibitrices Puf6 et Khd1 et leur libération de l'ARNm (Besse et Ephrussi 2008).

Le mécanisme de répression de la traduction médiée par Puf5 diffère de ceux identifiés pour Puf3 et Puf6. Il a été démontré que Puf5 s'associe avec la sous-unité Caf1 du complexe CCR4-NOT, réprimant ainsi l'expression de l'ARNm cible par induction de sa déadénylation (Goldstrohm et al 2006; Chritton et Wickens, 2010).

En conclusion, les protéines Puf sont des répresseurs polyvalents. Le recrutement de la machinerie de déadénylation et de dégradation CCR4-NOT semble être une voie conservée entre la levure et les métazoaires et être le mécanisme principal pour la mise en place de la repression. A ce stade, cependant, on ne peut exclure l'existence d'autres mécanismes de répression.

Notre connaissance de plus en plus approfondie du complexe CCR4-NOT fournit des preuves sur son importance dans la physiologie cellulaire, le développement embryonnaire, la réponse immunitaire, le fonctionnement des neurones et la régulation de l'homéostasie chez la levure. De multiples rôles dans la régulation de la stabilité des ARNm et du contrôle de leur qualité ont été proposées, soit par une régulation de la dégradation des ARNm ou par la répression de leur traduction. Ces étapes nécessitent de nombreux facteurs fonctionnels supplémentaires qui se lient souvent transitoirement au noyau du complexe CCR4-NOT. Le complexe CCR4-NOT est donc au coeur d'un réseau d'interactions protéine-protéine très étendu dans lequel il est un effecteur important. Ces observations font qu'il est important de comprendre l'organisation structurelle de ce complexe, la fonction de ses sous-unités et de ses protéines associées, et les mécanismes par lesquels il affecte la traduction des ARNm et leur dégradation.

5.5 Aperçu du projet

Au cours de mon travail de thèse, j'ai étudié la fonction du complexe CCR4-NOT chez la levure *S. cerevisiae*. La première partie de mon travail a été de déchiffrer le rôle des interactions protéine-protéine qui se produisent à l'intérieur de ce complexe et leur rôle dans le mécanisme de déadénylation *in vivo*. Ces études fonctionnelles ont été basées sur la détermination de la structure de certaines parties du complexe CCR4-NOT par nos collaborateurs et ont permis de répondre à certaines questions liées à l'hétérogénéité structurale de ce complexe. Par la suite, je me suis intéressé à la nature essentielle de la protéine Not1 chez la levure *S. cerevisiae*. Enfin, j'ai analysé le mécanisme de répression de la traduction par le complexe CCR4-NOT et le mécanisme de ciblage de ce complexe sur un ARNm par la protéine Puf3.

5.5.1 Caractérisation structurale et fonctionnelle du complexe CCR4-NOT

Quand j'ai commencé à travailler sur ce projet, peu d'informations sur l'organisation structurelle du complexe CCR4-NOT étaient disponibles. Plusieurs modèles d'architecture du complexe ont été proposées sur la base d'études *in vivo* et *in vitro*. L'importance de chaque sous-unité du complexe dans l'activité de déadénylation était également mal définie. En collaboration avec le laboratoire d'Elena Conti, la structure de deux sous-complexes de levure ont été résolus, à savoir les fragments de Not1-Caf1-CCR4 et un fragment de Not1 avec Not2 et l'extrémité N-terminale de Not5. Sur la base de ces informations structurelles, j'ai effectué la caractérisation fonctionnelle des interactions entre ces sous-unités. En particulier, j'ai vérifié si:

• Les interactions entre Not1-Caf1, Caf1-CCR4, ou dans le module Not, sont importantes pour l'activité de déadénylation *in vivo*?

• Les interactions au sein de ces modules sont physiologiquement importants et nécessaires à la croissance cellulaire?

5.5.2 Fonction essentielle de Not1 et l'hétérogénéité structurelle du complexe CCR4-NOT *in vivo*

• Il est surprenant de constater que Not1 est la seule sous-unité essentielle du complexe CCR4-NOT. Par conséquent, j'ai essayé de découvrir pourquoi. Par l'utilisation de protéine Not1 tronquées, j'ai essayé de déterminer la séquence minimale de Not1 requise pour remplir sa fonction essentielle dans les cellules.

• En parallèle, en raison de la nature des sous-unités paralogues Not3 et Not5 que l'on trouve dans la levure mais pas chez les mammifères, j'ai essayé de comprendre si le complexe CCR4-NOT a une composition unique de protéines ou s'il s'agit d'un assemblage hétérogène.

5.5.3 Mécanisme d'action du complexe CCR4-NOT: répression de la traduction et recrutement par la protéine Puf3

La dégradation des ARNm est associée à la sortie des ARNm cibles de la traduction active. Par conséquent, les mécanismes de répression de la traduction peuvent être intimement liés à la dégradation des ARNm. La structure du module d'interaction Not1-Caf1-CCR4 suggére un mécanisme possible pour la répression de la traduction par le complexe CCR4-NOT. Des criblages de suppression génétiques que j'ai effectué m'ont permis d'identifier plusieurs protéines candidates comme partenaire fonctionnel du complexe CCR4-NOT dans la répression de la traduction. Sur la base de ces observations, j'ai fait l'hypothèse de l'existence d'une hélicase à ARN spécifique de Not1 responsable

de la répression de la traduction par le complexe. J'ai effectué des essais de liaison avec plusieurs partenaires potentiels et aussi développé un test basé sur un gène rapporteur luciférase pour mesurer quantitativement les activités de répression de la traduction des différents sous-unités du complexe CCR4-NOT.

Les analyses de l'expression des ARNm au niveau du transcriptome a révélé un enrichissement significatif des ARNm ciblés par les facteurs Puf3 dans les ARNm affectés dans les souches mutantes de CCR4-NOT. Pour comprendre les bases moléculaires de cet effet, j'ai effectué des études de liaison entre la protéine Puf3 et le complexe CCR4-NOT dans des conditions de croissance différentes. Ce projet a donné lieu à des résultats préliminaires intéressants qui devront être étudiés de manière plus approfondie à l'avenir.

Les résultats de mon travail sont présentés dans les sections suivantes et comprennent deux articles publiés dans Molecular Cell en 2012, et Nature Structural and Molecular Biology en 2013 et dont je suis co-auteur.

6. References

Aitken, Colin Echeverría, and Jon R Lorsch. 2012. “A Mechanistic Overview of Translation Initiation in Eukaryotes.” *Nature Structural & Molecular Biology* 19 (6): 568–76.

Alkalaeva, Elena Z, Andrey V Pisarev, Lyudmila Y Frolova, Lev L Kisselev, and Tatyana V Pestova. 2006. “In Vitro Reconstitution of Eukaryotic Translation Reveals Cooperativity between Release Factors eRF1 and eRF3.” *Cell* 125 (6): 1125–36.

Allmang, C, J Kufel, G Chanfreau, P Mitchell, E Petfalski, and D Tollervey. 1999. “Functions of the Exosome in rRNA, snoRNA and snRNA Synthesis.” *The EMBO Journal* 18 (19): 5399–5410.

Allmang, C, P Mitchell, E Petfalski, and D Tollervey. 2000. “Degradation of Ribosomal RNA Precursors by the Exosome.” *Nucleic Acids Research* 28 (8): 1684–91.

Andersen, Gregers R, Poul Nissen, and Jens Nyborg. 2003. “Elongation Factors in Protein Biosynthesis.” *Trends in Biochemical Sciences* 28 (8): 434–41.

Araki, Y, S Takahashi, T Kobayashi, H Kajiho, S Hoshino, and T Katada. 2001. “Ski7p G Protein Interacts with the Exosome and the Ski Complex for 3’-to-5' mRNA Decay in Yeast.” *The EMBO Journal* 20 (17): 4684–93.

Arraiano, Cecília Maria, Fabienne Mauxion, Sandra Cristina Viegas, Rute Gonçalves Matos, and Bertrand Séraphin. 2014. “Intracellular Ribonucleases Involved in Transcript Processing and Decay: Precision Tools for RNA.” *Biochimica et Biophysica Acta* 1829 (6-7): 491–513.

Aslam, Akhmed, Saloni Mittal, Frederic Koch, Jean-Christophe Andrau, and G Sebastiaan Winkler. 2009. “The Ccr4-NOT Deadenylase Subunits CNOT7 and CNOT8 Have Overlapping Roles and Modulate Cell Proliferation.” *Molecular Biology of the Cell* 20 (17): 3840–50.

Azzouz, Nowel, Olesya O Panasenko, Cécile Deluen, Julien Hsieh, Grégory Theiler, and Martine a Collart. 2009. “Specific Roles for the Ccr4-Not Complex Subunits in Expression of the Genome.” *RNA (New York, N.Y.)* 15 (3): 377–83

Badis, Gwenael, Cosmin Saveanu, Micheline Fromont-Racine, and Alain Jacquier. 2004. “Targeted mRNA Degradation by Deadenylation-Independent Decapping.” *Molecular Cell* 15 (1): 5–15.

Baggs, Julie E, and Carla B Green. 2003. “Nocturnin, a Deadenylase in Xenopus Laevis Retina: A Mechanism for Posttranscriptional Control of Circadian-Related mRNA.” *Current Biology : CB* 13 (3): 189–98.

Bai, Y, C Salvadore, Y C Chiang, M a Collart, H Y Liu, and C L Denis. 1999. “The CCR4 and CAF1 Proteins of the CCR4-NOT Complex Are Physically and Functionally Separated from NOT2, NOT4, and NOT5.” *Molecular and Cellular Biology* 19 (10): 6642–51.

Basquin, Jerome, Vladimir V. Roudko, Michaela Rode, Claire Basquin, Bertrand S??raphin, and Elena Conti. 2012a. “Architecture of the Nuclease Module of the Yeast ccr4-Not Complex: The not1-caf1-ccr4 Interaction.” *Molecular Cell* 48 (2): 207–18.

———. 2012b. “Architecture of the Nuclease Module of the Yeast ccr4-Not Complex: The not1-caf1-ccr4 Interaction.” *Molecular Cell* 48 (2): 207–18.

Bawankar, Praveen, Belinda Loh, Lara Wohlbold, Steffen Schmidt, and Elisa Izaurralde. 2013. “NOT10 and C2orf29/NOT11 Form a Conserved Module of the CCR4-NOT Complex That Docks onto the NOT1 N-Terminal Domain.” *RNA Biology* 10 (2): 228–44.

Bazzini, a. a., M. T. Lee, and a. J. Giraldez. 2012. “Ribosome Profiling Shows That miR-430 Reduces Translation Before Causing mRNA Decay in Zebrafish.” *Science* 336 (6078): 233–37.

Becker, Thomas, Jean-Paul Armache, Alexander Jarasch, Andreas M Anger, Elizabeth Villa, Heidemarie Sieber, Basma Abdel Motaal, Thorsten Mielke, Otto Berninghausen, and Roland Beckmann. 2011. “Structure of the No-Go mRNA Decay Complex Dom34-Hbs1 Bound to a Stalled 80S Ribosome.” *Nature Structural & Molecular Biology* 18 (6): 715–20.

Beelman, C a, and R Parker. 1995. “Degradation of mRNA in Eukaryotes.” *Cell* 81 (2): 179–83.

Beelman, C A, A Stevens, G Caponigro, T E LaGrandeur, L Hatfield, D M Fortner, and R Parker. 1996. “An Essential Component of the Decapping Enzyme Required for Normal Rates of mRNA Turnover.” *Nature* 382 (6592): 642–46.

Behm-Ansmant, Isabelle, David Gatfield, Jan Rehwinkel, Valérie Hilgers, and Elisa Izaurralde. 2007. “A Conserved Role for Cytoplasmic poly(A)-Binding Protein 1 (PABPC1) in Nonsense-Mediated mRNA Decay.” *The EMBO Journal* 26 (6): 1591–1601.

Behm-Ansmant, Isabelle, Isao Kashima, Jan Rehwinkel, J??r??me Sauli??re, Nadine Wittkopp, and Elisa Izaurralde. 2007. “mRNA Quality Control: An Ancient Machinery Recognizes and Degrades mRNAs with Nonsense Codons.” *FEBS Letters* 581 (15): 2845–53.

Ben-Shem, Adam, Nicolas Garreau de Loubresse, Sergey Melnikov, Lasse Jenner, Gulnara Yusupova, and Marat Yusupov. 2011. “The Structure of the Eukaryotic Ribosome at 3.0 Å Resolution.” *Science (New York, N.Y.)* 334 (6062): 1524–29.

Beringer, Malte, and Marina V Rodnina. 2007a. “The Ribosomal Peptidyl Transferase.” *Molecular Cell* 26 (3): 311–21.

———. 2007b. “Importance of tRNA Interactions with 23S rRNA for Peptide Bond Formation on the Ribosome: Studies with Substrate Analogs.” *Biological Chemistry* 388 (7): 687–91.

Berndt, H., C. Harnisch, C. Rammelt, N. Stohr, a. Zirkel, J. C. Dohm, H. Himmelbauer, J.-P. Tavanez, S. Huttelmaier, and E. Wahle. 2012. “Maturation of Mammalian H/ACA Box

snoRNAs: PAPD5-Dependent Adenylation and PARN-Dependent Trimming." *Rna* 18 (5): 958–72.

Berthelot, Karine, Mark Muldoon, Lukas Rajkowitsch, John Hughes, and John E G McCarthy. 2004. "Dynamics and Processivity of 40S Ribosome Scanning on mRNA in Yeast." *Molecular Microbiology* 51 (4): 987–1001.

Besse, Florence, and Anne Ephrussi. 2008. "Translational Control of Localized mRNAs: Restricting Protein Synthesis in Space and Time." *Nature Reviews. Molecular Cell Biology* 9 (12). Nature Publishing Group: 971–80.

Bhandari, Dipankar, Tobias Raisch, Oliver Weichenrieder, Stefanie Jonas, and Elisa Izaurralde. 2014. "Structural Basis for the Nanos-Mediated Recruitment of the CCR4-NOT Complex and Translational Repression." *Genes & Development* 28 (8): 888–901.

Bhaskar, Varun, Vladimir Roudko, Jérôme Basquin, Kundan Sharma, Henning Urlaub, Bertrand Séraphin, and Elena Conti. 2013. "Structure and RNA-Binding Properties of the Not1-Not2-Not5 Module of the Yeast Ccr4-Not Complex." *Nature Structural & Molecular Biology* 20 (11): 1281–88.

Bianchin, Claire, Fabienne Mauxion, Stéphanie Sentis, Bertrand Séraphin, and Laura Corbo. 2005. "Conservation of the Deadenylase Activity of Proteins of the Caf1 Family in Human." *RNA (New York, N.Y.)* 11 (4): 487–94.

Bloch, D B, R a Nobre, G a Bernstein, and W H Yang. 2011. "Identification and Characterization of Protein Interactions in the Mammalian mRNA Processing Body Using a Novel Two-Hybrid Assay." *Experimental Cell Research* 317 (15). Elsevier Inc. 2183–99.

Boland, Andreas, Ying Chen, Tobias Raisch, Stefanie Jonas, Duygu Kuzuoğlu-Öztürk, Lara Wohlbold, Oliver Weichenrieder, and Elisa Izaurralde. 2013. "Structure and Assembly of the NOT Module of the Human CCR4-NOT Complex." *Nature Structural & Molecular Biology* 20 (11): 1289–97.

Bonneau, Fabien, J??r??me Basquin, Judith Ebert, Esben Lorentzen, and Elena Conti. 2009. "The Yeast Exosome Functions as a Macromolecular Cage to Channel RNA Substrates for Degradation." *Cell* 139 (3): 547–59.

Bouveret, E, G Rigaut, A Shevchenko, M Wilm, and B Séraphin. 2000. "A Sm-like Protein Complex That Participates in mRNA Degradation." *The EMBO Journal* 19 (7): 1661–71.

Bramham, Clive R, Paul F Worley, Melissa J Moore, and John F Guzowski. 2008. "The Immediate Early Gene arc/arg3.1: Regulation, Mechanisms, and Function." *The Journal of Neuroscience : The Official Journal of the Society for Neuroscience* 28 (46): 11760–67.

Brandt, Florian, Stephanie A Etchells, Julio O Ortiz, Adrian H Elcock, F Ulrich Hartl, and Wolfgang Baumeister. 2009. "The Native 3D Organization of Bacterial Polysomes." *Cell* 136 (2): 261–71.

Braun, Joerg E., Eric Huntzinger, Maria Fauser, and Elisa Izaurralde. 2011. “GW182 Proteins Directly Recruit Cytoplasmic Deadenylase Complexes to miRNA Targets.” *Molecular Cell* 44 (1). Elsevier Inc. 120–33.

Buchan, J Ross, Denise Muhlrad, and Roy Parker. 2008. “P Bodies Promote Stress Granule Assembly in Saccharomyces Cerevisiae.” *The Journal of Cell Biology* 183 (3): 441–55.

Caro, F, N Bercovich, C Atorrasagasti, M J Levin, and M P Vazquez. 2006. “Trypanosoma Cruzi: Analysis of the Complete PUF RNA-Binding Protein Family.” *Exp.Parasitol.* 113 (0014-4894 (Print) LA - eng PT - Journal Article PT - Research Support, Non-U.S. Gov’t): 112–24

Castello, Alfredo, Bernd Fischer, Katrin Eichelbaum, Rastislav Horos, Benedikt M Beckmann, Claudia Strein, Norman E Davey, et al. 2012. “Insights into RNA Biology from an Atlas of Mammalian mRNA-Binding Proteins.” *Cell* 149 (6): 1393–1406.

Castelló, Alfredo, David Franco, Pablo Moral-López, Juan J Berlanga, Enrique Alvarez, Eckard Wimmer, and Luis Carrasco. 2009. “HIV- 1 Protease Inhibits Cap- and poly(A)-Dependent Translation upon eIF4GI and PABP Cleavage.” *PloS One* 4 (11): e7997.

Castello, Alfredo, Rastislav Horos, Claudia Strein, Bernd Fischer, Katrin Eichelbaum, Lars M Steinmetz, Jeroen Krijgsveld, and Matthias W Hentze. 2013. “System-Wide Identification of RNA-Binding Proteins by Interactome Capture.” *Nature Protocols* 8 (3): 491–500.

Chamieh, Hala, Lionel Ballut, Fabien Bonneau, and Hervé Le Hir. 2008. “NMD Factors UPF2 and UPF3 Bridge UPF1 to the Exon Junction Complex and Stimulate Its RNA Helicase Activity.” *Nature Structural & Molecular Biology* 15 (1): 85–93.

Chang, Yao-Fu, J Saadi Imam, and Miles F Wilkinson. 2007. “The Nonsense-Mediated Decay RNA Surveillance Pathway.” *Annual Review of Biochemistry* 76 (January): 51–74.

Chen, J, J Rappsilber, Y C Chiang, P Russell, M Mann, and C L Denis. 2001. “Purification and Characterization of the 1.0 MDa CCR4-NOT Complex Identifies Two Novel Components of the Complex.” *Journal of Molecular Biology* 314 (4): 683–94.

Chen, Junji, Yueh Chin Chiang, and Clyde L. Denis. 2002. “CCR4, a 3???-5??? poly(A) RNA and ssDNA Exonuclease, Is the Catalytic Component of the Cytoplasmic Deadenylase.” *EMBO Journal* 21 (6): 1414–26.

Chen, Ying, Andreas Boland, Duygu Kuzuoğlu-Öztürk, Praveen Bawankar, Belinda Loh, Chung-Te Chang, Oliver Weichenrieder, and Elisa Izaurralde. 2014. “A DDX6-CNOT1 Complex and W-Binding Pockets in CNOT9 Reveal Direct Links between miRNA Target Recognition and Silencing.” *Molecular Cell* 54 (5): 737–50.

Chicoine, Jarred, Perrine Benoit, Chiara Gamberi, Miltiadis Paliouras, Martine Simonelig, and Paul Lasko. 2007. “Bicaudal-C Recruits CCR4-NOT Deadenylase to Target mRNAs and

Regulates Oogenesis, Cytoskeletal Organization, and Its Own Expression." *Developmental Cell* 13 (5): 691–704.

Chowdhury, Ashis, Kalidindi K Raju, Swathi Kalurupalle, and Sundaresan Tharun. 2012. "Both Sm-Domain and C-Terminal Extension of Lsm1 Are Important for the RNA-Binding Activity of the Lsm1-7-Pat1 Complex." *RNA (New York, N.Y.)* 18 (5): 936–44.

Chritton, Jacqueline J, and Marvin Wickens. 2010. "Translational Repression by PUF Proteins in Vitro", 1217–25.

Chuang, R Y, P L Weaver, Z Liu, and T H Chang. 1997. "Requirement of the DEAD-Box Protein ded1p for Messenger RNA Translation." *Science (New York, N.Y.)* 275 (5305): 1468–71.

Colak, Dilek, Sheng-Jian Ji, Bo T Porse, and Samie R Jaffrey. 2013. "Regulation of Axon Guidance by Compartmentalized Nonsense-Mediated mRNA Decay." *Cell* 153 (6): 1252–65.

Collart, M a, and K Struhl. 1994. "NOT1(CDC39), NOT2(CDC36), NOT3, and NOT4 Encode a Global-Negative Regulator of Transcription That Differentially Affects TATA-Element Utilization." *Genes & Development* 8 (5): 525–37.

Collart, Martine a, and Olesya O Panasenko. 2012. "The Ccr4--Not Complex." *Gene* 492 (1). Elsevier B.V. 42–53.

Collart, Martine a., and H. Th M Timmers. 2004. "The Eukaryotic Ccr4-Not Complex: A Regulatory Platform Integrating mRNA Metabolism with Cellular Signaling Pathways?" *Progress in Nucleic Acid Research and Molecular Biology* 77: 289–322.

Conti, Elena, and Elisa Izaurralde. 2005. "Nonsense-Mediated mRNA Decay: Molecular Insights and Mechanistic Variations across Species." *Current Opinion in Cell Biology* 17 (3): 316–25.

Copeland, P R, and M Wormington. 2001. "The Mechanism and Regulation of Deadenylation: Identification and Characterization of Xenopus PARN." *RNA (New York, N.Y.)* 7 (6): 875–86.

Cougot, Nicolas, Sylvie Babajko, and Bertrand Séraphin. 2004. "Cytoplasmic Foci Are Sites of mRNA Decay in Human Cells." *The Journal of Cell Biology* 165 (1): 31–40.

Cui, Yajun, Deepti B. Ramnarain, Yueh Chin Chiang, Liang Hao Ding, Jeffrey S. McMahon, and Clyde L. Denis. 2008. "Genome Wide Expression Analysis of the CCR4-NOT Complex Indicates That It Consists of Three Modules with the NOT Module Controlling SAGA-Responsive Genes." *Molecular Genetics and Genomics* 279 (4): 323–37.

Daugeron, M C, F Mauxion, and B Séraphin. 2001. "The Yeast POP2 Gene Encodes a Nuclease Involved in mRNA Deadenylation." *Nucleic Acids Research* 29 (12): 2448–55.

De Keersmaecker, Kim, Zeynep Kalender Atak, Ning Li, Carmen Vicente, Stephanie Patchett, Tiziana Girardi, Valentina Gianfelici, et al. 2013. “Exome Sequencing Identifies Mutation in CNOT3 and Ribosomal Genes RPL5 and RPL10 in T-Cell Acute Lymphoblastic Leukemia.” *Nature Genetics* 45 (2): 186–90.

Decker, C J, and R Parker. 1993. “A Turnover Pathway for Both Stable and Unstable mRNAs in Yeast: Evidence for a Requirement for Deadenylation.” *Genes & Development* 7 (8): 1632–43.

Decker, Carolyn J, and Roy Parker. 2012. “P-Bodies and Stress Granules: Possible Roles in the Control of Translation and mRNA Degradation.” *Cold Spring Harbor Perspectives in Biology* 4 (9): a012286.

Decourty, Laurence, Antonia Doyen, Christophe Malabat, Emmanuel Frachon, Delphine Rispal, Bertrand Séraphin, Frank Feuerbach, Alain Jacquier, and Cosmin Saveanu. 2014. “Long Open Reading Frame Transcripts Escape Nonsense-Mediated mRNA Decay in Yeast.” *Cell Reports* 6 (4): 593–98.

Dehlin, E, M Wormington, C G Körner, and E Wahle. 2000. “Cap-Dependent Deadenylation of mRNA.” *The EMBO Journal* 19 (5): 1079–86.

Desrosiers, R C, K H Friderici, and F M Rottman. 1975. “Characterization of Novikoff Hepatoma mRNA Methylation and Heterogeneity in the Methylated 5’ Terminus.” *Biochemistry* 14 (20): 4367–74.

Dever, Thomas E, and Rachel Green. 2012. “The Elongation, Termination, and Recycling Phases of Translation in Eukaryotes.” *Cold Spring Harbor Perspectives in Biology* 4 (7): a013706.

Dever, Thomas E. 1999. “Translation Initiation: Adept at Adapting.” *Trends in Biochemical Sciences* 24 (10): 398–403.

Dimitrova, Lyudmila N, Kazushige Kuroha, Tsuyako Tatematsu, and Toshifumi Inada. 2009. “Nascent Peptide-Dependent Translation Arrest Leads to Not4p-Mediated Protein Degradation by the Proteasome.” *The Journal of Biological Chemistry* 284 (16): 10343–52.

Ding, Yiliang, Yin Tang, Chun Kit Kwok, Yu Zhang, Philip C Bevilacqua, and Sarah M Assmann. 2014. “In Vivo Genome-Wide Profiling of RNA Secondary Structure Reveals Novel Regulatory Features.” *Nature* 505 (7485): 696–700.

Djuranovic, S., a. Nahvi, and R. Green. 2012. “miRNA-Mediated Gene Silencing by Translational Repression Followed by mRNA Deadenylation and Decay.” *Science* 336 (6078): 237–40.

Doma, Meenakshi K, and Roy Parker. 2006. “Endonucleolytic Cleavage of Eukaryotic mRNAs with Stalls in Translation Elongation.” *Nature* 440 (7083): 561–64.

Drummond, Sheona P., John Hildyard, Helena Firczuk, Onrapak Reamtong, Ning Li, Shichina Kannambath, Amy J. Claydon, Robert J. Beynon, Claire E. Eyers, and John E G McCarthy. 2011. “Diauxic Shift-Dependent Relocalization of Decapping Activators Dhh1 and Pat1 to Polysomal Complexes.” *Nucleic Acids Research* 39 (17): 7764–74.

Du, Tingting, and Phillip D Zamore. 2007. “Beginning to Understand microRNA Function.” *Cell Research* 17 (8): 661–63.

Dziembowski, Andrzej, Esben Lorentzen, Elena Conti, and Bertrand Séraphin. 2007. “A Single Subunit, Dis3, Is Essentially Responsible for Yeast Exosome Core Activity.” *Nature Structural & Molecular Biology* 14 (1): 15–22.

Eliyahu, Erez, Lilach Pnueli, Daniel Melamed, Tanja Scherrer, André P Gerber, Ophry Pines, Doron Rapaport, and Yoav Arava. 2010. “Tom20 Mediates Localization of mRNAs to Mitochondria in a Translation-Dependent Manner.” *Molecular and Cellular Biology* 30 (1): 284–94.

Fabian, Marc R, Filipp Frank, Christopher Rouya, Nadeem Siddiqui, Wi S Lai, Alexey Karetnikov, Perry J Blackshear, Bhushan Nagar, and Nahum Sonenberg. 2013. “Structural Basis for the Recruitment of the Human CCR4-NOT Deadenylase Complex by Tristetraprolin.” *Nature Structural & Molecular Biology* 20 (6): 735–39.

Finoux, Anne-Laure, and Bertrand Séraphin. 2006. “In Vivo Targeting of the Yeast Pop2 Deadenylase Subunit to Reporter Transcripts Induces Their Rapid Degradation and Generates New Decay Intermediates.” *The Journal of Biological Chemistry* 281 (36): 25940–47.

Fourati, Zaineb, Olga Kolesnikova, Régis Back, Jenny Keller, Clément Charenton, Valerio Taverniti, Claudine Gaudon Plesse, et al. 2014. “The C-Terminal Domain from S. Cerevisiae Pat1 Displays Two Conserved Regions Involved in Decapping Factor Recruitment.” *PloS One* 9 (5): e96828.

Friend, Kyle, Zachary T Campbell, Amy Cooke, Peggy Kroll-Conner, Marvin P Wickens, and Judith Kimble. 2012. “A Conserved PUF-Ago-eEF1A Complex Attenuates Translation Elongation.” *Nature Structural & Molecular Biology* 19 (2): 176–83.

Frischmeyer, Pamela A, Ambro van Hoof, Kathryn O’Donnell, Anthony L Guerrerio, Roy Parker, and Harry C Dietz. 2002. “An mRNA Surveillance Mechanism That Eliminates Transcripts Lacking Termination Codons.” *Science (New York, N.Y.)* 295 (5563): 2258–61.

Fromm, Simon A, Vincent Truffault, Julia Kamenz, Joerg E Braun, Niklas A Hoffmann, Elisa Izaurralde, and Remco Sprangers. 2012. “The Structural Basis of Edc3- and Scd6-Mediated Activation of the Dcp1:Dcp2 mRNA Decapping Complex.” *The EMBO Journal* 31 (2): 279–90.

Funakoshi, Yuji, Yusuke Doi, Nao Hosoda, Naoyuki Uchida, Masanori Osawa, Ichio Shimada, Masafumi Tsujimoto, Tsutomu Suzuki, Toshiaki Katada, and Shin-ichi Hoshino. 2007. “Mechanism of mRNA Deadenylation: Evidence for a Molecular Interplay between

Translation Termination Factor eRF3 and mRNA Deadenylases." *Genes & Development* 21 (23): 3135–48.

Gadir, Noga, Liora Haim-Vilmovsky, Judith Kraut-Cohen, and Jeffrey E Gerst. 2011. "Localization of mRNAs Coding for Mitochondrial Proteins in the Yeast Saccharomyces Cerevisiae." *RNA (New York, N.Y.)* 17 (8): 1551–65.

Galgano, Alessia, Michael Forrer, Lukasz Jaskiewicz, Alexander Kanitz, Mihaela Zavolan, and André P Gerber. 2008. "Comparative Analysis of mRNA Targets for Human PUF-Family Proteins Suggests Extensive Interaction with the miRNA Regulatory System." *PloS One* 3 (9): e3164.

Garapaty, Shivani, Muktar A Mahajan, and Herbert H Samuels. 2008. "Components of the CCR4-NOT Complex Function as Nuclear Hormone Receptor Coactivators via Association with the NRC-Interacting Factor NIF-1." *The Journal of Biological Chemistry* 283 (11): 6806–16.

Garces, Robert G, Wanda Gillon, and Emil F Pai. 2007. "Atomic Model of Human Rcd-1 Reveals an Armadillo-like-Repeat Protein with in Vitro Nucleic Acid Binding Properties." *Protein Science : A Publication of the Protein Society* 16 (2): 176–88.

Garneau, Nicole L, Jeffrey Wilusz, and Carol J Wilusz. 2007. "The Highways and Byways of mRNA Decay." *Nature Reviews. Molecular Cell Biology* 8 (2): 113–26.

Gebauer, Fátima, and Matthias W Hentze. 2004. "Molecular Mechanisms of Translational Control." *Nature Reviews. Molecular Cell Biology* 5 (10): 827–35.

Gerber, André P, Daniel Herschlag, and Patrick O Brown. 2004. "Extensive Association of Functionally and Cytotopically Related mRNAs with Puf Family RNA-Binding Proteins in Yeast." *PLoS Biology* 2 (3): E79.

Ghildiyal, Megha, and Phillip D Zamore. 2009. "Small Silencing RNAs: An Expanding Universe." *Nature Reviews. Genetics* 10 (2): 94–108.

Ghosh, Sanjay, Virginie Marchand, Imre Gáspár, and Anne Ephrussi. 2012. "Control of RNP Motility and Localization by a Splicing-Dependent Structure in Oskar mRNA." *Nature Structural & Molecular Biology* 19 (4): 441–49.

Gingras, A C, S P Gygi, B Raught, R D Polakiewicz, R T Abraham, M F Hoekstra, R Aebersold, and N Sonenberg. 1999. "Regulation of 4E-BP1 Phosphorylation: A Novel Two-Step Mechanism." *Genes & Development* 13 (11): 1422–37.

Gingras, A C, B Raught, S P Gygi, A Niedzwiecka, M Miron, S K Burley, R D Polakiewicz, A Wyslouch-Cieszynska, R Aebersold, and N Sonenberg. 2001. "Hierarchical Phosphorylation of the Translation Inhibitor 4E-BP1." *Genes & Development* 15 (21): 2852–64.

Giorgi, Corinna, Gene W Yeo, Martha E Stone, Donald B Katz, Christopher Burge, Gina Turrigiano, and Melissa J Moore. 2007. “The EJC Factor eIF4AIII Modulates Synaptic Strength and Neuronal Protein Expression.” *Cell* 130 (1): 179–91.

Godwin, Alan R, Shihoko Kojima, Carla B Green, and Jeffrey Wilusz. 2014. “Kiss Your Tail Goodbye: The Role of PARN, Nocturnin, and Angel Deadenylases in mRNA Biology.” *Biochimica et Biophysica Acta* 1829 (6-7): 571–79.

Goldstrohm, Aaron C, Brad a Hook, Daniel J Seay, and Marvin Wickens. 2006. “PUF Proteins Bind Pop2p to Regulate Messenger RNAs.” *Nature Structural & Molecular Biology* 13 (6): 533–39.

Goldstrohm, Aaron C, Daniel J Seay, Brad a Hook, and Marvin Wickens. 2007. “PUF Protein-Mediated Deadenylation Is Catalyzed by Ccr4p.” *The Journal of Biological Chemistry* 282 (1): 109–14.

Graille, Marc, and Bertrand Séraphin. 2012. “Surveillance Pathways Rescuing Eukaryotic Ribosomes Lost in Translation.” *Nature Reviews. Molecular Cell Biology* 13 (11): 727–35.

Groppo, Rachel, and Joel D. Richter. 2009. “Translational Control from Head to Tail.” *Current Opinion in Cell Biology* 21 (3): 444–51.

Gu, Wei, Yingfeng Deng, Daniel Zenklusen, and Robert H Singer. 2004. “A New Yeast PUF Family Protein, Puf6p, Represses ASH1 mRNA Translation and Is Required for Its Localization.” *Genes & Development* 18 (12): 1452–65.

Haas, Gabrielle, Joerg E Braun, Cátia Igreja, Felix Tritschler, Tadashi Nishihara, and Elisa Izaurralde. 2010. “HPat Provides a Link between Deadenylation and Decapping in Metazoa.” *The Journal of Cell Biology* 189 (2): 289–302.

Halbach, Felix, Peter Reichelt, Michaela Rode, and Elena Conti. 2013. “The Yeast Ski Complex: Crystal Structure and RNA Channeling to the Exosome Complex.” *Cell* 154 (4): 814–26.

Harigaya, Yuriko, and Roy Parker. 2014. “No-Go Decay: A Quality Control Mechanism for RNA in Translation.” *Wiley Interdisciplinary Reviews. RNA* 1 (1): 132–41.

Hata, Hiroaki, Hisayuki Mitsui, Hong Liu, Yongli Bai, Clyde L Denis, and Yuki Shimizu. 1998. “Factors Pop2p and Ccr4p from Saccharomyces Cerevisiae.” *Yeast*.

He, Feng, Chunfang Li, Bijoyita Roy, and Allan Jacobson. 2014. “Yeast Edc3 Targets RPS28B mRNA for Decapping by Binding to a 3’ Untranslated Region Decay-Inducing Regulatory Element.” *Molecular and Cellular Biology* 34 (8): 1438–51.

Heiman, Myriam, Ruth Kulicke, Robert J Fenster, Paul Greengard, and Nathaniel Heintz. 2014. “Cell Type-Specific mRNA Purification by Translating Ribosome Affinity Purification (TRAP).” *Nature Protocols* 9 (6): 1282–91.

Heiman, Myriam, Anne Schaefer, Shiaoching Gong, Jayms D Peterson, Michelle Day, Keri E Ramsey, Mayte Suárez-Fariñas, et al. 2008. “A Translational Profiling Approach for the Molecular Characterization of CNS Cell Types.” *Cell* 135 (4): 738–48.

Hershey, John W B, Nahum Sonenberg, and Michael B Mathews. 2012. “Principles of Translational Control: An Overview.” *Cold Spring Harbor Perspectives in Biology* 4 (12).

Hilliker, Angela, Zhaofeng Gao, Eckhard Jankowsky, and Roy Parker. 2011. “The DEAD-Box Protein Ded1 Modulates Translation by the Formation and Resolution of an eIF4F-mRNA Complex.” *Molecular Cell* 43 (6): 962–72.

Hinnebusch, Alan G, and Jon R Lorsch. 2012. “The Mechanism of Eukaryotic Translation Initiation: New Insights and Challenges.” *Cold Spring Harbor Perspectives in Biology* 4 (10).

Hinnebusch, Alan G. 2006. “eIF3: A Versatile Scaffold for Translation Initiation Complexes.” *Trends in Biochemical Sciences* 31 (10): 553–62.

Hogan, Daniel J., Daniel P. Riordan, Andr?? P. Gerber, Daniel Herschlag, and Patrick O. Brown. 2008. “Diverse RNA-Binding Proteins Interact with Functionally Related Sets of RNAs, Suggesting an Extensive Regulatory System.” *PLoS Biology* 6 (10): 2297–2313.

Horiuchi, Masataka, Kosei Takeuchi, Nobuo Noda, Nobuyuki Muroya, Toru Suzuki, Takahisa Nakamura, Junko Kawamura-Tsuzuku, Kiyohiro Takahasi, Tadashi Yamamoto, and Fuyuhiko Inagaki. 2009. “Structural Basis for the Antiproliferative Activity of the Tob-hCaf1 Complex.” *The Journal of Biological Chemistry* 284 (19): 13244–55.

Houseley, Jonathan, John LaCava, and David Tollervey. 2006. “RNA-Quality Control by the Exosome.” *Nature Reviews. Molecular Cell Biology* 7 (7): 529–39.

Hu, Wenqian, Christine Petzold, Jeff Coller, and Kristian E Baker. 2010. “Nonsense-Mediated mRNA Decapping Occurs on Polyribosomes in Saccharomyces Cerevisiae.” *Nature Structural & Molecular Biology* 17 (2): 244–47.

Hu, Wenqian, Thomas J Sweet, Sangpen Chamnongpol, Kristian E Baker, and Jeff Coller. 2009. “Co-Translational mRNA Decay in Saccharomyces Cerevisiae.” *Nature* 461 (7261): 225–29.

Igreja, C., and E. Izaurralde. 2011. “CUP Promotes Deadenylation and Inhibits Decapping of mRNA Targets.” *Genes & Development* 25 (18): 1955–67.

Inada, Toshifumi. 2014. “Quality Control Systems for Aberrant mRNAs Induced by Aberrant Translation Elongation and Termination.” *Biochimica et Biophysica Acta* 1829 (6-7): 634–42.

Incarnato, Danny, Francesco Neri, Daniela Diamanti, and Salvatore Oliviero. 2013. “MREdictor: A Two-Step Dynamic Interaction Model That Accounts for mRNA

Accessibility and Pumilio Binding Accurately Predicts microRNA Targets." *Nucleic Acids Research* 41 (18): 8421–33.

Inge-Vechtomov, Sergei, Galina Zhouravleva, and Michel Philippe. 2014. "Eukaryotic Release Factors (eRFs) History." *Biology of the Cell / under the Auspices of the European Cell Biology Organization* 95 (3-4): 195–209. Accessed June 19.

Ingolia, Nicholas T, Gloria A Brar, Silvia Rouskin, Anna M McGeachy, and Jonathan S Weissman. 2012. "The Ribosome Profiling Strategy for Monitoring Translation in Vivo by Deep Sequencing of Ribosome-Protected mRNA Fragments." *Nature Protocols* 7 (8): 1534–50.

———. 2013. "Genome-Wide Annotation and Quantitation of Translation by Ribosome Profiling." *Current Protocols in Molecular Biology / Edited by Frederick M. Ausubel ... [et Al.]* Chapter 4 (July): Unit 4.18.

Ingolia, Nicholas T, Sina Ghaemmaghami, John R S Newman, and Jonathan S Weissman. 2009. "Genome-Wide Analysis in Vivo of Translation with Nucleotide Resolution Using Ribosome Profiling." *Science (New York, N.Y.)* 324 (5924): 218–23.

Isken, Olaf, Yoon Ki Kim, Nao Hosoda, Greg L Mayeur, John W B Hershey, and Lynne E Maquat. 2008. "Upf1 Phosphorylation Triggers Translational Repression during Nonsense-Mediated mRNA Decay." *Cell* 133 (2): 314–27.

Isken, Olaf, and Lynne E Maquat. 2008. "The Multiple Lives of NMD Factors: Balancing Roles in Gene and Genome Regulation." *Nature Reviews. Genetics* 9 (9): 699–712.

Ito, Kentaro, Takeshi Inoue, Kazumasa Yokoyama, Masahiro Morita, Toru Suzuki, and Tadashi Yamamoto. 2011. "CNOT2 Depletion Disrupts and Inhibits the CCR4-NOT Deadenylase Complex and Induces Apoptotic Cell Death." *Genes to Cells* 16 (4): 368–79..

Ito, Kentaro, Akinori Takahashi, Masahiro Morita, Toru Suzuki, and Tadashi Yamamoto. 2011. "The Role of the CNOT1 Subunit of the CCR4-NOT Complex in mRNA Deadenylation and Cell Viability." *Protein & Cell* 2 (9): 755–63.

Jackson, Richard J, Christopher U T Hellen, and Tatyana V Pestova. 2010. "The Mechanism of Eukaryotic Translation Initiation and Principles of Its Regulation." *Nature Reviews. Molecular Cell Biology* 11 (2). Nature Publishing Group: 113–27.

Jambor, Helena, Sandra Mueller, Simon L Bullock, and Anne Ephrussi. 2014. "A Stem-Loop Structure Directs Oskar mRNA to Microtubule Minus Ends." *RNA (New York, N.Y.)* 20 (4): 429–39.

James, Nicole, Emilie Landrieux, and Martine a Collart. 2007. "A SAGA-Independent Function of SPT3 Mediates Transcriptional Deregulation in a Mutant of the Ccr4-Not Complex in Saccharomyces Cerevisiae." *Genetics* 177 (1): 123–35.

Jenkins, Huw T., Rosanna Baker-Wilding, and Thomas a. Edwards. 2009. “Structure and RNA Binding of the Mouse Pumilio-2 Puf Domain.” *Journal of Structural Biology* 167 (3). Elsevier Inc. 271–76.

Jenner, Lasse, Sergey Melnikov, Nicolas Garreau de Loubresse, Adam Ben-Shem, Madina Iskakova, Alexandre Urzhumtsev, Arturas Meskauskas, Jonathan Dinman, Gulnara Yusupova, and Marat Yusupov. 2012. “Crystal Structure of the 80S Yeast Ribosome.” *Current Opinion in Structural Biology* 22 (6): 759–67.

Jiang, Peng, Mona Singh, and Hilary A Coller. 2013. “Computational Assessment of the Cooperativity between RNA Binding Proteins and MicroRNAs in Transcript Decay.” *PLoS Computational Biology* 9 (5): e1003075.

Kedde, Martijn, Marieke van Kouwenhove, Wilbert Zwart, Joachim A F Oude Vrielink, Ran Elkon, and Reuven Agami. 2010. “A Pumilio-Induced RNA Structure Switch in p27-3’ UTR Controls miR-221 and miR-222 Accessibility.” *Nature Cell Biology* 12 (10): 1014–20.

Kempf, Brian J, and David J Barton. 2008. “Poliovirus 2A(Pro) Increases Viral mRNA and Polysome Stability Coordinately in Time with Cleavage of eIF4G.” *Journal of Virology* 82 (12): 5847–59.

Kershner, Aaron M, and Judith Kimble. 2010. “Genome-Wide Analysis of mRNA Targets for Caenorhabditis Elegans FBF, a Conserved Stem Cell Regulator.” *Proceedings of the National Academy of Sciences of the United States of America* 107 (8): 3936–41.

Kertesz, Michael, Yue Wan, Elad Mazor, John L Rinn, Robert C Nutter, Howard Y Chang, and Eran Segal. 2010. “Genome-Wide Measurement of RNA Secondary Structure in Yeast.” *Nature* 467 (7311): 103–7.

Kolesnikova, Olga, Régis Back, Marc Graille, and Bertrand Séraphin. 2013. “Identification of the Rps28 Binding Motif from Yeast Edc3 Involved in the Autoregulatory Feedback Loop Controlling RPS28B mRNA Decay.” *Nucleic Acids Research* 41 (20): 9514–23.

Kshirsagar, Meenakshi, and Roy Parker. 2004. “Identification of Edc3p as an Enhancer of mRNA Decapping in Saccharomyces Cerevisiae.” *Genetics* 166 (2): 729–39.

LaCava, John, Jonathan Houseley, Cosmin Saveanu, Elisabeth Petfalski, Elizabeth Thompson, Alain Jacquier, and David Tollervey. 2005. “RNA Degradation by the Exosome Is Promoted by a Nuclear Polyadenylation Complex.” *Cell* 121 (5): 713–24.

LaGrandeur, T E, and R Parker. 1996. “mRNA Decapping Activities and Their Biological Roles.” *Biochimie* 78 (11-12): 1049–55.

———. 1998. “Isolation and Characterization of Dcp1p, the Yeast mRNA Decapping Enzyme.” *The EMBO Journal* 17 (5): 1487–96.

Lau, Nga-Chi, Annemieke Kolkman, Frederik M A van Schaik, Klaas W Mulder, W W M Pim Pijnappel, Albert J R Heck, and H Th Marc Timmers. 2009. “Human Ccr4-Not Complexes Contain Variable Deadenylase Subunits.” *The Biochemical Journal* 422 (3): 443–53.

Laver, John D, Xiao Li, Kristin Ancevicius, J Timothy Westwood, Craig A Smibert, Quaid D Morris, and Howard D Lipshitz. 2013. “Genome-Wide Analysis of Staufen-Associated mRNAs Identifies Secondary Structures That Confer Target Specificity.” *Nucleic Acids Research* 41 (20): 9438–60.

Lebreton, Alice, Rafal Tomecki, Andrzej Dziembowski, and Bertrand Séraphin. 2008. “Endonucleolytic RNA Cleavage by a Eukaryotic Exosome.” *Nature* 456 (7224): 993–96.

Lejeune, Fabrice, Xiaojie Li, and Lynne E Maquat. 2003. “Nonsense-Mediated mRNA Decay in Mammalian Cells Involves Decapping, Deadenylating, and Exonucleolytic Activities.” *Molecular Cell* 12 (3): 675–87.

Leppek, Kathrin, Johanna Schott, Sonja Reitter, Fabian Poetz, Ming C Hammond, and Georg Stoecklin. 2013. “Roquin Promotes Constitutive mRNA Decay via a Conserved Class of Stem-Loop Recognition Motifs.” *Cell* 153 (4): 869–81.

Lin, Chien-Ling, Veronica Evans, Shihao Shen, Yi Xing, and Joel D Richter. 2010. “The Nuclear Experience of CPEB: Implications for RNA Processing and Translational Control.” *RNA (New York, N.Y.)* 16 (2): 338–48.

Lorentzen, Esben, Jérôme Basquin, and Elena Conti. 2008. “Structural Organization of the RNA-Degrading Exosome.” *Current Opinion in Structural Biology* 18 (6): 709–13.

Madhani, Hiten D. 2013. “The Frustrated Gene: Origins of Eukaryotic Gene Expression.” *Cell* 155 (4): 744–49.

Makino, Debora Lika, Marc Baumgärtner, and Elena Conti. 2013. “Crystal Structure of an RNA-Bound 11-Subunit Eukaryotic Exosome Complex.” *Nature* 495 (7439): 70–75.

Mathonnet, Géraldine, Marc R Fabian, Yuri V Svitkin, Armen Parsyan, Laurent Huck, Takayuki Murata, Stefano Biffo, et al. 2007. “MicroRNA Inhibition of Translation Initiation in Vitro by Targeting the Cap-Binding Complex eIF4F.” *Science (New York, N.Y.)* 317 (5845): 1764–67.

Mathys, Hansruedi, Jérôme Basquin, Sevim Ozgur, Mariusz Czarnocki-Cieciura, Fabien Bonneau, Aafke Aartse, Andrzej Dziembowski, Marcin Nowotny, Elena Conti, and Witold Filipowicz. 2014. “Structural and Biochemical Insights to the Role of the CCR4-NOT Complex and DDX6 ATPase in MicroRNA Repression.” *Molecular Cell* 54 (5): 751–65.

Matsuda, Ryo, Ken Ikeuchi, Sene Nomura, and Toshifumi Inada. 2014. “Protein Quality Control Systems Associated with No-Go and Nonstop mRNA Surveillance in Yeast.” *Genes to Cells : Devoted to Molecular & Cellular Mechanisms* 19 (1): 1–12.

Mauxion, Fabienne, Céline Faux, and Bertrand Séraphin. 2008. “The BTG2 Protein Is a General Activator of mRNA Deadenylation.” *The EMBO Journal* 27 (7): 1039–48.

Mauxion, Fabienne, Brigitte Prève, and Bertrand Séraphin. 2013. “C2ORF29/CNOT11 and CNOT10 Form a New Module of the CCR4-NOT Complex.” *RNA Biology* 10 (2): 267–76.

Melnikov, Sergey, Adam Ben-Shem, Nicolas Garreau de Loubresse, Lasse Jenner, Gulnara Yusupova, and Marat Yusupov. 2012. “One Core, Two Shells: Bacterial and Eukaryotic Ribosomes.” *Nature Structural & Molecular Biology* 19 (6): 560–67.

Miller, Christian, Björn Schwalb, Kerstin Maier, Daniel Schulz, Sebastian Dümcke, Benedikt Zacher, Andreas Mayer, et al. 2011. “Dynamic Transcriptome Analysis Measures Rates of mRNA Synthesis and Decay in Yeast.” *Molecular Systems Biology* 7 (January): 458.

Mitkevich, Vladimir A, Artem V Kononenko, Irina Yu Petrushanko, Dmitry V Yanvarev, Alexander A Makarov, and Lev L Kisselev. 2006. “Termination of Translation in Eukaryotes Is Mediated by the Quaternary eRF1*eRF3*GTP*Mg2+ Complex. The Biological Roles of eRF3 and Prokaryotic RF3 Are Profoundly Distinct.” *Nucleic Acids Research* 34 (14): 3947–54.

Mortimer, Stefanie A, Mary Anne Kidwell, and Jennifer A Doudna. 2014. “Insights into RNA Structure and Function from Genome-Wide Studies.” *Nature Reviews. Genetics* 15 (7): 469–79.

Muhlrad, D, C J Decker, and R Parker. 1994. “Deadenylation of the Unstable mRNA Encoded by the Yeast MFA2 Gene Leads to Decapping Followed by 5’-->3' Digestion of the Transcript.” *Genes & Development* 8 (7): 855–66.

———. 1995. “Turnover Mechanisms of the Stable Yeast PGK1 mRNA.” *Molecular and Cellular Biology* 15 (4): 2145–56.

Muhlrad, Denise, and Roy Parker. 2005. “The Yeast EDC1 mRNA Undergoes Deadenylation-Independent Decapping Stimulated by Not2p, Not4p, and Not5p.” *The EMBO Journal* 24 (5): 1033–45.

Mulder, Klaas W, Akiko Inagaki, Elisabetta Cameroni, Florence Mousson, G Sebastiaan Winkler, Claudio De Virgilio, Martine A Collart, and H Th Marc Timmers. 2007. “Modulation of Ubc4p/Ubc5p-Mediated Stress Responses by the RING-Finger-Dependent Ubiquitin-Protein Ligase Not4p in Saccharomyces Cerevisiae.” *Genetics* 176 (1): 181–92.

Myasnikov, Alexander G, Zhanna A Afonina, and Bruno P Klaholz. 2013. “Single Particle and Molecular Assembly Analysis of Polyribosomes by Single- and Double-Tilt Cryo Electron Tomography.” *Ultramicroscopy* 126 (March): 33–39.

Nolde, Mona J, Nazli Saka, Kristy L Reinert, and Frank J Slack. 2007. “The Caenorhabditis Elegans Pumilio Homolog, Puf-9, Is Required for the 3’UTR-Mediated Repression of the Let-7 microRNA Target Gene, Hbl-1.” *Developmental Biology* 305 (2): 551–63.

Oberstrass, Florian C, Albert Lee, Richard Stefl, Michael Janis, Guillaume Chanfreau, and Frédéric H-T Allain. 2006. “Shape-Specific Recognition in the Structure of the Vts1p SAM Domain with RNA.” *Nature Structural & Molecular Biology* 13 (2): 160–67.

Olivas, W, and R Parker. 2000. “The Puf3 Protein Is a Transcript-Specific Regulator of mRNA Degradation in Yeast.” *The EMBO Journal* 19 (23): 6602–11.

Panasenko, Olesya O, and Martine A Collart. 2011. “Not4 E3 Ligase Contributes to Proteasome Assembly and Functional Integrity in Part through Ecm29.” *Molecular and Cellular Biology* 31 (8): 1610–23.

Parsyan, Armen, Yuri Svitkin, David Shahbazian, Christos Gkogkas, Paul Lasko, William C Merrick, and Nahum Sonenberg. 2011. “mRNA Helicases: The Tacticians of Translational Control.” *Nature Reviews. Molecular Cell Biology* 12 (4): 235–45

Petit, Alain-Pierre, Lara Wohlbold, Praveen Bawankar, Eric Huntzinger, Steffen Schmidt, Elisa Izaurralde, and Oliver Weichenrieder. 2012. “The Structural Basis for the Interaction between the CAF1 Nuclease and the NOT1 Scaffold of the Human CCR4-NOT Deadenylase Complex.” *Nucleic Acids Research* 40 (21): 11058–72.

Petrov, Alexey, Jin Chen, Seán O’Leary, Albert Tsai, and Joseph D Puglisi. 2012. “Single-Molecule Analysis of Translational Dynamics.” *Cold Spring Harbor Perspectives in Biology* 4 (9): a011551.

Pillai, Ramesh S, Suvendra N Bhattacharyya, Caroline G Artus, Tabea Zoller, Nicolas Cougot, Eugenia Basyuk, Edouard Bertrand, and Witold Filipowicz. 2005. “Inhibition of Translational Initiation by Let-7 MicroRNA in Human Cells.” *Science (New York, N.Y.)* 309 (5740): 1573–76.

Quenault, Tara, Trevor Lithgow, and Ana Traven. 2011. “PUF Proteins: Repression, Activation and mRNA Localization.” *Trends in Cell Biology* 21 (2): 104–12.

Rendl, Laura M, Melissa A Bieman, and Craig A Smibert. 2008. “S. Cerevisiae Vts1p Induces Deadenylation-Dependent Transcript Degradation and Interacts with the Ccr4p-Pop2p-Not Deadenylase Complex.” *RNA (New York, N.Y.)* 14 (7): 1328–36.

Rodnina, Marina V, Malte Beringer, and Wolfgang Wintermeyer. 2007. “How Ribosomes Make Peptide Bonds.” *Trends in Biochemical Sciences* 32 (1): 20–26.

Rouskin, Silvi, Meghan Zubradt, Stefan Washietl, Manolis Kellis, and Jonathan S Weissman. 2014. “Genome-Wide Probing of RNA Structure Reveals Active Unfolding of mRNA Structures in Vivo.” *Nature* 505 (7485): 701–5.

Saint-Georges, Yann, Mathilde Garcia, Thierry Delaveau, Laurent Jourdren, Stephane Le Crom, Sophie Lemoine, Veronique Tanty, Frederic Devaux, and Claude Jacq. 2008. “Yeast Mitochondrial Biogenesis: A Role for the PUF RNA-Binding Protein Puf3p in mRNA Localization.” *PloS One* 3 (6): e2293.

Salas-Marco, Joe, and David M Bedwell. 2004. “GTP Hydrolysis by eRF3 Facilitates Stop Codon Decoding during Eukaryotic Translation Termination.” *Molecular and Cellular Biology* 24 (17): 7769–78.

Schneider, Claudia, Eileen Leung, Jeremy Brown, and David Tollervey. 2009. “The N-Terminal PIN Domain of the Exosome Subunit Rrp44 Harbors Endonuclease Activity and Tethers Rrp44 to the Yeast Core Exosome.” *Nucleic Acids Research* 37 (4): 1127–40.

Schoenberg, Daniel R, and Lynne E Maquat. 2012. “Regulation of Cytoplasmic mRNA Decay.” *Nature Reviews. Genetics* 13 (4): 246–59.

Schütz, Patrick, Mario Bumann, Anselm Erich Oberholzer, Christoph Bieniossek, Hans Trachsel, Michael Altmann, and Ulrich Baumann. 2008. “Crystal Structure of the Yeast eIF4A-eIF4G Complex: An RNA-Helicase Controlled by Protein-Protein Interactions.” *Proceedings of the National Academy of Sciences of the United States of America* 105 (28): 9564–69.

Schwartz, D C, and R Parker. 2000. “mRNA Decapping in Yeast Requires Dissociation of the Cap Binding Protein, Eukaryotic Translation Initiation Factor 4E.” *Molecular and Cellular Biology* 20 (21): 7933–42.

Schweingruber, Christoph, Simone C Rufener, David Zünd, Akio Yamashita, and Oliver Mühlemann. 2014. “Nonsense-Mediated mRNA Decay - Mechanisms of Substrate mRNA Recognition and Degradation in Mammalian Cells.” *Biochimica et Biophysica Acta* 1829 (6-7): 612–23.

Sevim, Ozgur, Marina Chekulaeva and Georg Stoecklin. 2010. "Human Pat1b connects Deadenylation with mRNA Decapping and Controls the Assembly of Processing Bodies." *Molecular and Cellular Biology* 30 (17): 4308 - 4323.

Sharif, Humayun, Sevim Ozgur, Kundan Sharma, Claire Basquin, Henning Urlaub, and Elena Conti. 2013. “Structural Analysis of the Yeast Dhh1-Pat1 Complex Reveals How Dhh1 Engages Pat1, Edc3 and RNA in Mutually Exclusive Interactions.” *Nucleic Acids Research* 41 (17): 8377–90.

Sheth, Ujwal, and Roy Parker. 2003. “Decapping and Decay of Messenger RNA Occur in Cytoplasmic Processing Bodies.” *Science (New York, N.Y.)* 300 (5620): 805–8.

Simón, Ernesto, and Bertrand Séraphin. 2007. “A Specific Role for the C-Terminal Region of the Poly(A)-Binding Protein in mRNA Decay.” *Nucleic Acids Research* 35 (18): 6017–28.

Sonenberg, Nahum, and Alan G Hinnebusch. 2009. “Regulation of Translation Initiation in Eukaryotes: Mechanisms and Biological Targets.” *Cell* 136 (4): 731–45.

Steitz, Thomas A. 2008. “A Structural Understanding of the Dynamic Ribosome Machine.” *Nature Reviews. Molecular Cell Biology* 9 (3): 242–53.

Stoecklin, Georg, Brigitte Gross, Xiu-Fen Ming, and Christoph Moroni. 2003. “A Novel Mechanism of Tumor Suppression by Destabilizing AU-Rich Growth Factor mRNA.” *Oncogene* 22 (23): 3554–61.

Stynen, Bram, Hélène Tournu, Jan Tavernier, and Patrick Van Dijck. 2012. “Diversity in Genetic in Vivo Methods for Protein-Protein Interaction Studies: From the Yeast Two-Hybrid System to the Mammalian Split-Luciferase System.” *Microbiology and Molecular Biology Reviews : MMBR* 76 (2): 331–82.

Sun, Mai, Björn Schwalb, Nicole Pirkl, Kerstin C Maier, Arne Schenk, Henrik Failmezger, Achim Tresch, and Patrick Cramer. 2013. “Global Analysis of Eukaryotic mRNA Degradation Reveals Xrn1-Dependent Buffering of Transcript Levels.” *Molecular Cell* 52 (1): 52–62.

Sun, Mai, Björn Schwalb, Daniel Schulz, Nicole Pirkl, Stefanie Etzold, Laurent Larivière, Kerstin C Maier, Martin Seizl, Achim Tresch, and Patrick Cramer. 2012. “Comparative Dynamic Transcriptome Analysis (cDTA) Reveals Mutual Feedback between mRNA Synthesis and Degradation.” *Genome Research* 22 (7): 1350–59.

Synowsky, Silvia A, and Albert J R Heck. 2008. “The Yeast Ski Complex Is a Hetero-Tetramer.” *Protein Science : A Publication of the Protein Society* 17 (1): 119–25.

Tarn, Woan-Yuh, and Tien-Hsien Chang. 2014. “The Current Understanding of Ded1p/DDX3 Homologs from Yeast to Human.” *RNA Biology* 6 (1): 17–20. Accessed June 19.

Tharun, S, W He, A E Mayes, P Lennertz, J D Beggs, and R Parker. 2000. “Yeast Sm-like Proteins Function in mRNA Decapping and Decay.” *Nature* 404 (6777): 515–18.

Tharun, S, and R Parker. 2001. “Targeting an mRNA for Decapping: Displacement of Translation Factors and Association of the Lsm1p-7p Complex on Deadenylated Yeast mRNAs.” *Molecular Cell* 8 (5): 1075–83.

Tharun, Sundaresan. 2014. “Lsm1-7-Pat1 Complex: A Link between 3’ and 5'-Ends in mRNA Decay?” *RNA Biology* 6 (3): 228–32. Accessed June 20.

Thomas, María Gabriela, Mariela Loschi, María Andrea Desbats, and Graciela Lidia Boccaccio. 2011. “RNA Granules: The Good, the Bad and the Ugly.” *Cellular Signalling* 23 (2): 324–34.

Triboulet, Robinson, and Richard I Gregory. 2010. “Pumilio Turns on microRNA Function.” *Nature Cell Biology* 12 (10): 928–29.

Tucker, Morgan, Marco A Valencia-Sanchez, Robin R Staples, Junji Chen, Clyde L Denis, and Roy Parker. 2001. “The Transcription Factor Associated Ccr4 and Caf1 Proteins Are Components of the Major Cytoplasmic mRNA Deadenylase in Saccharomyces Cerevisiae.” *Cell* 104 (3): 377–86.

Udagawa, Tsuyoshi, Sharon A Swanger, Koichi Takeuchi, Jong Heon Kim, Vijayalaxmi Nalavadi, Jihae Shin, Lori J Lorenz, R Suzanne Zukin, Gary J Bassell, and Joel D Richter. 2012. "Bidirectional Control of mRNA Translation and Synaptic Plasticity by the Cytoplasmic Polyadenylation Complex." *Molecular Cell* 47 (2): 253–66.

Van den Elzen, Antonia M G, Julien Henri, Noureddine Lazar, María Eugenia Gas, Dominique Durand, François Lacroute, Magali Nicaise, Herman van Tilbeurgh, Bertrand Séraphin, and Marc Graille. 2010. "Dissection of Dom34-Hbs1 Reveals Independent Functions in Two RNA Quality Control Pathways." *Nature Structural & Molecular Biology* 17 (12): 1446–52.

Van Dijk, Erwin, Nicolas Cougot, Sylke Meyer, Sylvie Babajko, Elmar Wahle, and Bertrand Séraphin. 2002. "Human Dcp2: A Catalytically Active mRNA Decapping Enzyme Located in Specific Cytoplasmic Structures." *The EMBO Journal* 21 (24): 6915–24.

Van Hoof, Ambro, Pamela A Frischmeyer, Harry C Dietz, and Roy Parker. 2002. "Exosome-Mediated Recognition and Degradation of mRNAs Lacking a Termination Codon." *Science (New York, N.Y.)* 295 (5563): 2262–64.

Villalba, Ana, Olga Coll, and Fátima Gebauer. 2011. "Cytoplasmic Polyadenylation and Translational Control." *Current Opinion in Genetics & Development* 21 (4): 452–57.

Wagner, Eileen, Sandra L Clement, and Jens Lykke-Andersen. 2007. "An Unconventional Human Ccr4-Caf1 Deadenylase Complex in Nuclear Cajal Bodies." *Molecular and Cellular Biology* 27 (5): 1686–95.

Wahle, Elmar, and G Sebastiaan Winkler. 2014. "RNA Decay Machines: Deadenylation by the Ccr4-Not and Pan2-Pan3 Complexes." *Biochimica et Biophysica Acta* 1829 (6-7): 561–70.

Walsh, Derek, and Ian Mohr. 2011. "Viral Subversion of the Host Protein Synthesis Machinery." *Nature Reviews. Microbiology* 9 (12): 860–75.

Wang, Hui, Masahiro Morita, Xiuna Yang, Toru Suzuki, Wen Yang, Jiao Wang, Kentaro Ito, et al. 2010. "Crystal Structure of the Human CNOT6L Nuclease Domain Reveals Strict poly(A) Substrate Specificity." *The EMBO Journal* 29 (15): 2566–76.

Wang, Xiaoqiang, Juanita McLachlan, Phillip D. Zamore, and Traci M.Tanaka Hall. 2002. "Modular Recognition of RNA by a Human Pumilio-Homology Domain." *Cell* 110 (4): 501–12.

Wasmuth, Elizabeth V, and Christopher D Lima. 2012. "Exo- and Endoribonucleolytic Activities of Yeast Cytoplasmic and Nuclear RNA Exosomes Are Dependent on the Noncatalytic Core and Central Channel." *Molecular Cell* 48 (1): 133–44.

Wei, C M, A Gershowitz, and B Moss. 1976. "5'-Terminal and Internal Methylated Nucleotide Sequences in HeLa Cell mRNA." *Biochemistry* 15 (2): 397–401.

Winter, Julia, Stephanie Jung, Sarina Keller, Richard I Gregory, and Sven Diederichs. 2009. “Many Roads to Maturity: microRNA Biogenesis Pathways and Their Regulation.” *Nature Cell Biology* 11 (3): 228–34.

Wyers, Françoise, Mathieu Rougemaille, Gwenaël Badis, Jean-Claude Rousselle, Marie-Elisabeth Dufour, Jocelyne Boulay, Béatrice Régnault, et al. 2005. “Cryptic Pol II Transcripts Are Degraded by a Nuclear Quality Control Pathway Involving a New poly(A) Polymerase.” *Cell* 121 (5): 725–37.

Youtani, T, K Tomoo, T Ishida, H Miyoshi, and K Miura. 2000. “Regulation of Human eIF4E by 4E-BP1: Binding Analysis Using Surface Plasmon Resonance.” *IUBMB Life* 49 (1): 27–31.

Zhang, Zuo, and Adrian R Krainer. 2004. “Involvement of SR Proteins in mRNA Surveillance.” *Molecular Cell* 16 (4): 597–607.

Vladimir ROUDKO

Structural and functional characterization of Ccr4-Not deadenylation complex

Résumé

La dégradation des ARN messagers (ARNm) est un processus universel extrêmement complexe. D'une manière semblable aux polymerases pour la transcription et ribosomes pour la traduction, les complexes de protéines effectuant la dégradation des ARNm sont précisément régulés. La dégradation des ARNm eucaryotes s'effectue selon un schéma conservé évolutivement qui est initié par la déadénylation résultant dans la formation de transcrits avec des queues polyA courtes. De tels intermédiaires sont alors dégradés par le clivage de leur coiffe suivi par une digestion exonucléolytique 5'-3' effectuée par Xrn1, ou alternativement par une digestion 3 '-5' catalysée par l'exosome. Dans ma thèse je présente une dissection fonctionnelle du complexe de déadénylation CCR4-NOT basée sur son analyse structurale. Je me suis essentiellement intéressé à cinq questions fondamentales concernant ce complexe : La formation du complexe CCR4-NOT complexe est-elle requise pour la déadénylation ? Quel est le rôle moléculaire de sous-unités Not2/3/5 du complexe ? Pourquoi la protéine Not1 est-elle essentielle chez la levure ? Le complexe CCR4-NOT joue-t-il un rôle dans la répression de la traduction ? Comment le complexe CCR4-NOT est-il ciblé sur ses substrats ARNm ?

Mots-clés: CCR4-NOT, déadénylation, la répression de la traduction, analyse structurale et fonctionalle.

Résumé en anglais

mRNA degradation is a highly complex and versatile process. In a manner similar to polymerase complexes in transcription and ribosomes in translation, protein complexes mediating mRNA decay are tightly regulated. Eukaryotic mRNA decay follows a conserved pathway initiated by deadenylation that generates transcripts with short polyA tails. The latter intermediates are degraded either by decapping followed with 5'-3' trimming mediated by Xrn1, or by exosome-mediated digestion in the 3'-5' direction. In my thesis I present a functional dissection of the Ccr4-Not deadenylase complex based on its structural analysis. Essentially, I addressed five fundamental questions related to this complex: Is CCR4-NOT complex formation required for deadenylation activity? What is the molecular role of associated Not2/3/5 subunits? Why is the Not1 protein essential in yeast? Does the CCR4-NOT complex play role in translation regulation? How is the CCR4-NOT complex targeted to its mRNA substrates?

Keywords: CCR4-NOT, deadenylation, translation repression, structural and functional analysis.